Three-Dimensional Static and Dynamic Analysis of Structures

A Physical Approach
With Emphasis on Earthquake Engineering

Edward L. Wilson

Professor Emeritus of Structural Engineering
University of California at Berkeley

STRUCTURAL ENGINEERING IS

THE ART OF USING MATERIALS

That Have Properties Which Can Only Be Estimated

TO BUILD REAL STRUCTURES

That Can Only Be Approximately Analyzed

TO WITHSTAND FORCES

That Are Not Accurately Known

SO THAT OUR RESPONSIBILITY WITH RESPECT TO

PUBLIC SAFETY IS SATISFIED.

Adapted From An Unknown Author

Preface To Third Edition

This edition of the book contains corrections and additions to the July 1998 edition. Most of the new material that has been added is in response to questions and comments from the users of SAP2000, ETABS and SAFE.

Chapter 22 has been written on the direct use of absolute earthquake displacement loading acting at the base of the structure. Several new types of numerical errors for absolute displacement loading have been identified. First, the fundamental nature of displacement loading is significantly different from the base acceleration loading traditionally used in earthquake engineering. Second, a smaller integration time step is required to define the earthquake displacement and to solve the dynamic equilibrium equations. Third, a large number of modes are required for absolute displacement loading to obtain the same accuracy as produced when base acceleration is used as the loading. Fourth, the 90 percent mass participation rule, intended to assure accuracy of the analysis, does not apply for absolute displacement loading. Finally, the effective modal damping for displacement loading is larger than when acceleration loading is used.

To reduce those errors associated with displacement loading, a higher order integration method based on a cubic variation of loads within a time step is introduced in Chapter 13. In addition, static and dynamic participation factors have been defined that allow the structural engineer to minimize the errors associated with displacement type loading. In addition, Chapter 19 on viscous damping has been expanded to illustrate the physical effects of modal damping on the results of a dynamic analysis.

Appendix H, on the speed of modern personal computers, has been updated. It is now possible to purchase a personal computer for approximately $1,500 that is 25 times faster than a $10,000,000 CRAY computer produced in 1974.

Several other additions and modifications have been made in this printing. Please send your comments and questions *to **ed@csiberkeley.com***.

Edward L. Wilson
April 2000

Personal Remarks

My freshman Physics instructor dogmatically warned the class "do not use an equation you cannot derive." The same instructor once stated that "if a person had five minutes to solve a problem, that their life depended upon, the individual should spend three minutes reading and clearly understanding the problem." For the past forty years these simple, practical remarks have guided my work and I hope that the same philosophy has been passed along to my students. With respect to modern structural engineering, one can restate these remarks as "do not use a structural analysis program unless you fully understand the theory and approximations used within the program" and "do not create a computer model until the loading, material properties and boundary conditions are clearly defined."

Therefore, the major purpose of this book is to present the essential theoretical background so that the users of computer programs for structural analysis can understand the basic approximations used within the program, verify the results of all analyses and assume professional responsibility for the results. It is assumed that the reader has an understanding of statics, mechanics of solids, and elementary structural analysis. The level of knowledge expected is equal to that of an individual with an undergraduate degree in Civil or Mechanical Engineering. Elementary matrix and vector notations are defined in the Appendices and are used extensively. A background in tensor notation and complex variables is not required.

All equations are developed using a physical approach, because this book is written for the student and professional engineer and not for my academic colleagues. Three-dimensional structural analysis is relatively simple because of the high speed of the modern computer. Therefore, all equations are presented in three-dimensional form and anisotropic material properties are automatically included. A computer programming background is not necessary to use a computer program intelligently. However, detailed numerical algorithms are given so that the readers completely understand the computational methods that are summarized in this book. The Appendices contain an elementary summary of the numerical methods used; therefore, it should not be necessary to spend additional time reading theoretical research papers to understand the theory presented in this book.

The author has developed and published many computational techniques for the static and dynamic analysis of structures. It has been personally satisfying that many members

of the engineering profession have found these computational methods useful. Therefore, one reason for compiling this theoretical and application book is to consolidate in one publication this research and development. In addition, the recently developed Fast Nonlinear Analysis (FNA) method and other numerical methods are presented in detail for the first time.

The fundamental physical laws that are the basis of the static and dynamic analysis of structures are over 100 years old. Therefore, anyone who believes they have discovered a new fundamental principle of mechanics is a victim of their own ignorance. This book contains computational tricks that the author has found to be effective for the development of structural analysis programs.

The static and dynamic analysis of structures has been automated to a large degree because of the existence of inexpensive personal computers. However, the field of structural engineering, in my opinion, will never be automated. The idea that an expert-system computer program, with artificial intelligence, will replace a creative human is an insult to all structural engineers.

The material in this book has evolved over the past thirty-five years with the help of my former students and professional colleagues. Their contributions are acknowledged. Ashraf Habibullah, Iqbal Suharwardy, Robert Morris, Syed Hasanain, Dolly Gurrola, Marilyn Wilkes and Randy Corson of Computers and Structures, Inc., deserve special recognition. In addition, I would like to thank the large number of structural engineers who have used the TABS and SAP series of programs. They have provided the motivation for this publication.

The material presented in the first edition of *Three Dimensional Dynamic Analysis of Structures* is included and updated in this book. I am looking forward to additional comments and questions from the readers in order to expand the material in future editions of the book.

Edward L. Wilson
July 1998

CONTENTS

3.   Energy and Work

4.   One-Dimensional Elements

5.   Isoparametric Elements

9.   Membrane Element with Normal Rotations

10.   Shell Elements

14.   Calculation of Stiffness and Mass Orthogonal Vectors

15.   Dynamic Analysis Using Response Spectrum Seismic Loading

16.   Soil Structure Interaction

17.   Seismic Analysis Modeling to Satisfy Building Codes

18.   Fast Nonlinear Analysis

19.   Linear Viscous Damping

20.   Dynamic Analysis Using Numerical Integration

Appendix B Matrix Notation

Appendix C Solution or Inversion of Linear Equations

Appendix D The Eigenvalue Problem

Appendix E Transformation of Material Properties

Appendix F A Displacement-Based Beam Element With Shear Deformations

Appendix G Numerical Integration

Appendix H Speed of Computer Systems

Appendix I Method of Least Square

1.

MATERIAL PROPERTIES

Material Properties Must Be Evaluated
By Laboratory or Field Tests

1.1 INTRODUCTION

The fundamental equations of structural mechanics can be placed in three categories[1]. First, the stress-strain relationship contains the material property information that must be evaluated by laboratory or field experiments. Second, the total structure, each element, and each infinitesimal particle within each element must be in force equilibrium in their deformed position. Third, displacement compatibility conditions must be satisfied.

If all three equations are satisfied at all points in time, other conditions will automatically be satisfied. For example, at any point in time the total work done by the external loads must equal the kinetic and strain energy stored within the structural system plus any energy that has been dissipated by the system. Virtual work and variational principles are of significant value in the mathematical derivation of certain equations; however, they are not fundamental equations of mechanics.

1.2 ANISOTROPIC MATERIALS

The linear stress-strain relationships contain the material property constants, which can only be evaluated by laboratory or field experiments. The mechanical material properties for most common material, such as steel, are well known and are defined in terms of three numbers: modulus of elasticity E, Poisson's ratio

v and coefficient of thermal expansion α. In addition, the unit weight w and the unit mass ρ are considered to be fundamental material properties.

Before the development of the finite element method, most analytical solutions in solid mechanics were restricted to materials that were isotropic (equal properties in all directions) and homogeneous (same properties at all points in the solid). Since the introduction of the finite element method, this limitation no longer exists. Hence, it is reasonable to start with a definition of anisotropic materials, which may be different in every element in a structure.

The positive definition of stresses, in reference to an orthogonal 1-2-3 system, is shown in Figure 1.1.
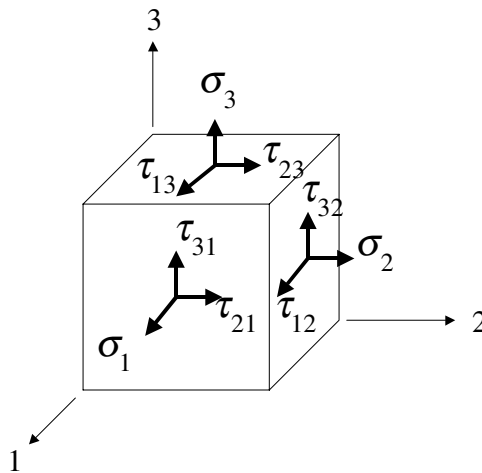
Figure 1.1 Definition of Positive Stresses

All stresses are by definition in units of force-per-unit-area. In matrix notation, the six independent stresses can be defined by:

$$\mathbf{f}^{\mathbf{T}} = \begin{bmatrix} \sigma_1 & \sigma_2 & \sigma_3 & \tau_{21} & \tau_{31} & \tau_{23} \end{bmatrix} \tag{1.1}$$

From equilibrium, $\tau_{12} = \tau_{21}$, $\tau_{31} = \tau_{13}$ and $\tau_{32} = \tau_{23}$. The six corresponding engineering strains are:

$$\mathbf{d}^{\mathrm{T}} = \begin{bmatrix} \varepsilon_1 & \varepsilon_2 & \varepsilon_3 & \gamma_{21} & \gamma_{31} & \gamma_{23} \end{bmatrix} \qquad (1.2)$$

The most general form of the three dimensional strain-stress relationship for linear structural materials subjected to both mechanical stresses and temperature change can be written in the following matrix form[2]:

$$\begin{bmatrix} \varepsilon_1 \\ \varepsilon_2 \\ \varepsilon_3 \\ \gamma_{21} \\ \gamma_{31} \\ \gamma_{23} \end{bmatrix} = \begin{bmatrix} \dfrac{1}{E_1} & -\dfrac{\nu_{12}}{E_2} & -\dfrac{\nu_{13}}{E_3} & -\dfrac{\nu_{14}}{E_4} & -\dfrac{\nu_{15}}{E_5} & -\dfrac{\nu_{16}}{E_6} \\ -\dfrac{\nu_{21}}{E_1} & \dfrac{1}{E_2} & -\dfrac{\nu_{23}}{E_3} & -\dfrac{\nu_{24}}{E_4} & -\dfrac{\nu_{25}}{E_5} & -\dfrac{\nu_{26}}{E_6} \\ -\dfrac{\nu_{31}}{E_1} & -\dfrac{\nu_{32}}{E_2} & \dfrac{1}{E_3} & -\dfrac{\nu_{34}}{E_4} & -\dfrac{\nu_{35}}{E_4} & -\dfrac{\nu_{36}}{E_6} \\ -\dfrac{\nu_{41}}{E_1} & -\dfrac{\nu_{42}}{E_2} & -\dfrac{\nu_{43}}{E_3} & \dfrac{1}{E_4} & -\dfrac{\nu_{45}}{E_5} & -\dfrac{\nu_{46}}{E_6} \\ -\dfrac{\nu_{51}}{E_1} & -\dfrac{\nu_{52}}{E_2} & -\dfrac{\nu_{53}}{E_3} & -\dfrac{\nu_{54}}{E_4} & \dfrac{1}{E_5} & -\dfrac{\nu_{56}}{E_6} \\ -\dfrac{\nu_{61}}{E_1} & -\dfrac{\nu_{62}}{E_2} & -\dfrac{\nu_{63}}{E_3} & -\dfrac{\nu_{64}}{E_4} & -\dfrac{\nu_{65}}{E_5} & \dfrac{1}{E_6} \end{bmatrix} \begin{bmatrix} \sigma_1 \\ \sigma_2 \\ \sigma_3 \\ \tau_{21} \\ \tau_{31} \\ \tau_{23} \end{bmatrix} + \Delta T \begin{bmatrix} \alpha_1 \\ \alpha_2 \\ \alpha_3 \\ \alpha_{21} \\ \alpha_{31} \\ \alpha_{23} \end{bmatrix} \quad (1.3)$$

Or, in symbolic matrix form:

$$\mathbf{d} = \mathbf{C}\mathbf{f} + \Delta T \mathbf{a} \qquad (1.4)$$

The $\mathbf{C}$ matrix is known as the compliance matrix and can be considered to be the most fundamental definition of the material properties because all terms can be evaluated directly from simple laboratory experiments. Each column of the $\mathbf{C}$ matrix represents the strains caused by the application of a unit stress. The temperature increase ΔT is in reference to the temperature at zero stress. The $\mathbf{a}$ matrix indicates the strains caused by a unit temperature increase.

Basic energy principles require that the $\mathbf{C}$ matrix for linear material be symmetrical. Hence,

$$\frac{\nu_{ij}}{E_j} = \frac{\nu_{ji}}{E_i} \qquad\qquad (1.5)$$

However, because of experimental error or small nonlinear behavior of the material, this condition is not identically satisfied for most materials. Therefore, these experimental values are normally averaged so that symmetrical values can be used in the analyses.

1.3   USE OF MATERIAL PROPERTIES WITHIN COMPUTER PROGRAMS

Most of the modern computer programs for finite element analysis require that the stresses be expressed in terms of the strains and temperature change. Therefore, an equation of the following form is required within the program:

$$\mathbf{f} = \mathbf{Ed} + \mathbf{f_0} \qquad\qquad (1.6)$$

in which $\mathbf{E} = \mathbf{C^{-1}}$. Therefore, the zero-strain thermal stresses are defined by:

$$\mathbf{f_0} = -\Delta T\,\mathbf{Ea} \qquad\qquad (1.7)$$

The numerical inversion of the 6 x 6 $\mathbf{C}$ matrix for complex anisotropic materials is performed within the computer program. Therefore, it is not necessary to calculate the $\mathbf{E}$ matrix in analytical form as indicated in many classical books on solid mechanics. In addition, the initial thermal stresses are numerically evaluated within the computer program. Consequently, for the most general anisotropic material, the basic computer input data will be twenty-one elastic constants, plus six coefficients of thermal expansion.

Initial stresses, in addition to thermal stresses, may exist for many different types of structural systems. These initial stresses may be the result of the fabrication or construction history of the structure. If these initial stresses are known, they may be added directly to Equation (1.7).

1.4   ORTHOTROPIC MATERIALS

The most common type of anisotropic material is one in which shear stresses, acting in all three reference planes, cause no normal strains. For this special case, the material is defined as orthotropic and Equation (1.3) can be written as:

$$
\begin{bmatrix} \varepsilon_1 \\ \varepsilon_2 \\ \varepsilon_3 \\ \gamma_{21} \\ \gamma_{31} \\ \gamma_{23} \end{bmatrix} =
\begin{bmatrix}
\dfrac{1}{E_1} & -\dfrac{\nu_{12}}{E_2} & -\dfrac{\nu_{13}}{E_3} & 0 & 0 & 0 \\[8pt]
-\dfrac{\nu_{21}}{E_1} & \dfrac{1}{E_2} & -\dfrac{\nu_{23}}{E_3} & 0 & 0 & 0 \\[8pt]
-\dfrac{\nu_{31}}{E_1} & -\dfrac{\nu_{32}}{E_2} & \dfrac{1}{E_3} & 0 & 0 & 0 \\[8pt]
0 & 0 & 0 & \dfrac{1}{G_4} & 0 & 0 \\[8pt]
0 & 0 & 0 & 0 & \dfrac{1}{G_5} & 0 \\[8pt]
0 & 0 & 0 & 0 & 0 & \dfrac{1}{G_6}
\end{bmatrix}
\begin{bmatrix} \sigma_1 \\ \sigma_2 \\ \sigma_3 \\ \tau_{21} \\ \tau_{31} \\ \tau_{23} \end{bmatrix} + \Delta T
\begin{bmatrix} \alpha_1 \\ \alpha_2 \\ \alpha_3 \\ 0 \\ 0 \\ 0 \end{bmatrix}
\qquad (1.8)
$$

For orthotropic material, the **C** matrix has nine independent material constants, and there are three independent coefficients of thermal expansion. This type of material property is very common. For example, rocks, concrete, wood and many fiber reinforced materials exhibit orthotropic behavior. It should be pointed out, however, that laboratory tests indicate that Equation (1.8) is only an approximation to the behavior of real materials.

1.5   ISOTROPIC MATERIALS

An isotropic material has equal properties in all directions and is the most commonly used approximation to predict the behavior of linear elastic materials. For isotropic materials, Equation (1.3) is of the following form:

$$
\begin{bmatrix} \varepsilon_1 \\ \varepsilon_2 \\ \varepsilon_3 \\ \gamma_{21} \\ \gamma_{31} \\ \gamma_{23} \end{bmatrix} = \begin{bmatrix} \dfrac{1}{E} & -\dfrac{v}{E} & -\dfrac{v}{E} & 0 & 0 & 0 \\ -\dfrac{v}{E} & \dfrac{1}{E} & -\dfrac{v}{E} & 0 & 0 & 0 \\ -\dfrac{v}{E} & -\dfrac{v}{E} & \dfrac{1}{E} & 0 & 0 & 0 \\ 0 & 0 & 0 & \dfrac{1}{G} & 0 & 0 \\ 0 & 0 & 0 & 0 & \dfrac{1}{G} & 0 \\ 0 & 0 & 0 & 0 & 0 & \dfrac{1}{G} \end{bmatrix} \begin{bmatrix} \sigma_1 \\ \sigma_2 \\ \sigma_3 \\ \tau_{21} \\ \tau_{31} \\ \tau_{23} \end{bmatrix} + \alpha\,\Delta T \begin{bmatrix} 1 \\ 1 \\ 1 \\ 0 \\ 0 \\ 0 \end{bmatrix} \qquad (1.9)
$$

It appears that the compliance matrix has three independent material constants. It can easily be shown that the application of a pure shear stress should result in pure tension and compression strains on the element if it is rotated 45 degrees. Using this restriction, it can be shown that:

$$
G = \frac{E}{2(1+v)} \qquad (1.10)
$$

Therefore, for isotropic materials only Young's modulus E and Poisson's ratio v need to be defined. Most computer programs use Equation (1.10) to calculate the shear modulus if it is not specified.

1.6   PLANE STRAIN ISOTROPIC MATERIALS

If $\varepsilon_1, \gamma_{13}, \gamma_{23}, \tau_{13},$ and τ_{23} are zero, the structure is in a state of plane strain. For this case the compliance matrix is reduced to a 3 x 3 array. The cross-sections of many dams, tunnels, and solids with a near infinite dimension along the 3-axis can be considered in a state of plane strain for constant loading in the 1-2 plane. For plane strain and isotropic materials, the stress-strain relationship is:

$$\begin{bmatrix} \sigma_1 \\ \sigma_2 \\ \tau_{12} \end{bmatrix} = \overline{E} \begin{bmatrix} 1-v & v & 0 \\ v & 1-v & 0 \\ 0 & 0 & \dfrac{1-2v}{2} \end{bmatrix} \begin{bmatrix} \varepsilon_1 \\ \varepsilon_2 \\ \gamma_{12} \end{bmatrix} - \alpha\,\Delta T\,\overline{E} \begin{bmatrix} 1 \\ 1 \\ 0 \end{bmatrix} \tag{1.11}$$

where

$$\overline{E} = \frac{E}{(1+v)(1-2v)} \tag{1.12}$$

For the case of plane strain, the displacement and strain in the 3-direction are zero. However, from Equation (1.8) the normal stress in the 3-direction is:

$$\sigma_3 = v\,(\sigma_1 + \sigma_2) - E\alpha\,\Delta T \tag{1.13}$$

It is important to note that as Poisson's ratio, v, approaches 0.5, some terms in the stress-strain relationship approach infinity. These real properties exist for a nearly incompressible material with a relatively low shear modulus.

1.7 PLANE STRESS ISOTROPIC MATERIALS

If σ_3, τ_{13}, and τ_{23} are zero, the structure is in a state of plane stress. For this case the stress-strain matrix is reduced to a 3 x 3 array. The membrane behavior of thin plates and shear wall structures can be considered in a state of plane strain for constant loading in the 1-2 plane. For plane stress and isotropic materials, the stress-strain relationship is:

$$\begin{bmatrix} \sigma_1 \\ \sigma_2 \\ \tau_{12} \end{bmatrix} = \overline{E} \begin{bmatrix} 1 & v & 0 \\ v & 1 & 0 \\ 0 & 0 & \dfrac{1-v}{2} \end{bmatrix} \begin{bmatrix} \varepsilon_1 \\ \varepsilon_2 \\ \gamma_{12} \end{bmatrix} - \alpha\,\Delta T\,\overline{E} \begin{bmatrix} 1 \\ 1 \\ 0 \end{bmatrix} \tag{1.14}$$

where

$$\overline{E} = \frac{E}{(1-v^2)} \tag{1.15}$$

1.8   PROPERTIES OF FLUID-LIKE MATERIALS

Many different isotropic materials, which have a very low shear modulus compared to their bulk modulus, have fluid-like behavior. These materials are often referred to as nearly incompressible solids. The incompressible terminology is very misleading because the compressibility, or bulk modulus, of these materials is normally lower than other solids. The pressure-volume relationship for a solid or a fluid can be written as:

$$\sigma = \lambda \varepsilon \tag{1.16}$$

where λ is the bulk modulus of the material, which must be evaluated by pressure-volume laboratory tests. The volume change ε is equal to $\varepsilon_1 + \varepsilon_2 + \varepsilon_3$, and the hydrostatic pressure σ indicates equal stress in all directions. From Equation (1.9) the bulk modulus can be written in terms of Young's modulus and Poisson's ratio as:

$$\lambda = \frac{E}{3(1-2v)} \tag{1.17}$$

For fluids, the bulk modulus is an independent constant, Poisson's ratio is 0.5, and Young's modulus and the shear modulus are zero. For isotropic materials, the bulk modulus and shear modulus are known as Lame's elastic constants and are considered to be fundamental material properties for both solids and fluids. From Equation (1.10), Poisson's ratio and Young's modulus can be calculated from:

$$v = \frac{3 - 2\dfrac{G}{\lambda}}{6 + 2\dfrac{G}{\lambda}} \quad \text{and} \quad E = 2(1+v)G \tag{1.18a and 1.18b}$$

If the shear modulus becomes small compared to the bulk modulus, $v \approx 0.5$ and $E \approx 3G$. Table 1.1 summarizes approximate material properties for several common materials.

Table 1.1 Approximate Mechanical Properties of Typical Materials

Material	E Young's Modulus ksi	v Poisson's Ratio	G Shear Modulus ksi	λ Bulk Modulus ksi	α Thermal Expansion $\times 10^{-6}$	w Weight Density lb/in^3
Steel	29,000	0.30	11,154	16,730	6.5	0.283
Aluminum	10,000	0.33	3,750	7,300	13.0	0.100
Concrete	4,000	0.20	1,667	1,100	6.0	0.087
Mercury	0	0.50	0	3,300	-	0.540
Water	0	0.50	0	300	-	0.036
Water*	0.9	0.4995	0.3	300	-	0.036

* These are approximate properties that can be used to model water as a solid material.

It is apparent that the major difference between liquids and solids is that liquids have a very small shear modulus compared to the bulk modulus, and *liquids are not incompressible.*

1.9   SHEAR AND COMPRESSION WAVE VELOCITIES

The measurement of compression and shear wave velocities of the material using laboratory or field experiments is another simple method that is often used to define material properties. The compressive wave velocity, V_c, and the shear wave velocity, V_s, are given by:

$$V_c = \sqrt{\frac{\lambda + 2G}{\rho}}$$
(1.19)

$$V_s = \sqrt{\frac{G}{\rho}} \tag{1.20}$$

where ρ is the mass density of the material. Therefore, it is possible to calculate all of the other elastic properties for isotropic materials from these equations. It is apparent that shear waves cannot propagate in fluids since the shear modulus is zero.

1.10 AXISYMMETRIC MATERIAL PROPERTIES

A large number of very common types of structures, such as pipes, pressure vessels, fluid storage tanks, rockets, and other space structures, are included in the category of axisymmetric structures. Many axisymmetric structures have anisotropic materials. For the case of axisymmetric solids subjected to non-axisymmetric loads, the compliance matrix, as defined by Equation (1.3), can be rewritten in terms of the r, z and θ reference system as Equation (1.21). The solution of this special case of a three-dimensional solid can be accomplished by expressing the node point displacements and loads in a series of harmonic functions. The solution is then expressed as a summation of the results of a series of two-dimensional, axisymmetric problems[3].

$$
\begin{bmatrix} \varepsilon_r \\ \varepsilon_z \\ \varepsilon_\theta \\ \gamma_{rz} \\ \gamma_{r\theta} \\ \gamma_{z\theta} \end{bmatrix} =
\begin{bmatrix}
\frac{1}{E_1} & -\frac{v_{12}}{E_2} & -\frac{v_{13}}{E_3} & -\frac{v_{14}}{E_4} & 0 & 0 \\
-\frac{v_{21}}{E_1} & \frac{1}{E_2} & -\frac{v_{23}}{E_3} & -\frac{v_{24}}{E_4} & 0 & 0 \\
-\frac{v_{31}}{E_1} & -\frac{v_{32}}{E_2} & \frac{1}{E_3} & -\frac{v_{34}}{E_4} & 0 & 0 \\
-\frac{v_{41}}{E_1} & -\frac{v_{42}}{E_2} & -\frac{v_{43}}{E_3} & \frac{1}{E_4} & 0 & 0 \\
0 & 0 & 0 & 0 & \frac{1}{E_5} & -\frac{v_{56}}{E_6} \\
0 & 0 & 0 & 0 & -\frac{v_{65}}{E_5} & \frac{1}{E_6}
\end{bmatrix}
\begin{bmatrix} \sigma_r \\ \sigma_z \\ \sigma_\theta \\ \tau_{rz} \\ \tau_{r\theta} \\ \tau_{z\theta} \end{bmatrix}
+ \Delta T
\begin{bmatrix} \alpha_r \\ \alpha_z \\ \alpha_\theta \\ \alpha_{rz} \\ 0 \\ 0 \end{bmatrix}
\tag{1.21}
$$

1.11 FORCE-DEFORMATION RELATIONSHIPS

The stress-strain equations presented in the previous sections are the fundamental *constitutive laws* for linear materials. However, for one-dimensional elements in structural engineering, we often rewrite these equations in terms of forces and deformations. For example, for a one-dimensional axially loaded member of length L and area A, the total axial deformation Δ and axial force P are $\Delta = L\varepsilon$ and $P = A\sigma$. Because $\sigma = E\varepsilon$, the force deformation relationship is:

$$P = k_a\Delta \tag{1.22}$$

where $k_a = \dfrac{AE}{L}$ and is defined as the axial stiffness of the member. Also, Equation (1.22) can be written in the following form:

$$\Delta = f_a P \tag{1.23}$$

where $f_a = \dfrac{L}{AE}$ and is defined as the axial flexibility of the member. It is important to note that the stiffness and flexibility terms are not a function of the load and are only the material and geometric properties of the member.

For a one-dimensional member of constant cross-section, the torsional force T in terms of the relative rotation φ between the ends of the member is given by:

$$T = k_T\varphi \tag{1.24}$$

where $k_T = \dfrac{JG}{L}$ in which J is the torsional moment of inertia. Also, the inverse of the torsional stiffness is the torsional flexibility.

In the case of pure bending of a beam fixed at one end, integration of a stress distribution over the cross-section produces a moment M. The linear strain distribution results in a rotation at the end of the beam of ϕ. For this finite length beam, the moment-rotation relationship is:

$$M = k_b\phi \tag{1.25}$$

where the bending stiffness $k_b = \dfrac{EI}{L}$. For a typical cross-section of the beam of length dx, the moment curvature relationship at location x is:

$$M(x) = EI\,\psi(x) \tag{1.26}$$

These force-deformation relationships are considered fundamental in the traditional fields of structural analysis and design.

1.12 SUMMARY

Material properties must be determined experimentally. Careful examinations of the properties of most structural materials indicate that they are not isotropic or homogeneous. Nonetheless, it is common practice to use the isotropic approximation for most analyses. In the future of structural engineering, however, the use of composite, anisotropic materials will increase significantly. The responsibility of the engineer is to evaluate the errors associated with these approximations by conducting several analyses using different material properties.

Remember the result obtained from a computer model is an estimation of the behavior of the real structure. The behavior of the structure is dictated by the fundamental laws of physics and is not required to satisfy the building code or the computer program's user manual.

1.13 REFERENCES

1. Popov, E. P. 1990. *Engineering Mechanics of Solids*. Prentice-Hall, Inc. ISBN 0-13-279258-3.

2. Boresi, A. P. 1985. *Advanced Mechanics of Materials*. John Wiley & Sons. ISBN 0-471-88392-1.

3. Wilson, E. L. 1965. "Structural Analysis of Axisymmetric Solids." *AIAA Journal*. Vol. 3, pp.2269-2274.

2.

EQUILIBRIUM AND COMPATIBILITY

Equilibrium Is Essential - Compatibility Is Optional

2.1   INTRODUCTION

Equilibrium equations set the externally applied loads equal to the sum of the internal element forces at all joints or node points of a structural system; they are the most fundamental equations in structural analysis and design. The exact solution for a problem in solid mechanics requires that the differential equations of equilibrium for all infinitesimal elements within the solid must be satisfied. *Equilibrium is a fundamental law of physics and cannot be violated within a "real" structural system.* Therefore, it is critical that the mathematical model, which is used to simulate the behavior of a real structure, also satisfies those basic equilibrium equations.

It is important to note that within a finite element, which is based on a formal displacement formulation, the differential stress-equilibrium equations are not always satisfied. However, inter-element force-equilibrium equations are identically satisfied at all node points (joints). The computer program user who does not understand the approximations used to develop a finite element can obtain results that are in significant error if the element mesh is not sufficiently fine in areas of stress concentration[1].

Compatibility requirements should be satisfied. However, if one has a choice between satisfying equilibrium or compatibility, one should use the equilibrium-based solution. For real nonlinear structures, equilibrium is always satisfied in

the deformed position. Many real structures do not satisfy compatibility caused by creep, joint slippage, incremental construction and directional yielding.

2.2   FUNDAMENTAL EQUILIBRIUM EQUATIONS

The three-dimensional equilibrium of an infinitesimal element, shown in Figure 1.1, is given by the following equilibrium equations[2]:

$$\frac{\partial \sigma_1}{\partial x_1} + \frac{\partial \tau_{12}}{\partial x_2} + \frac{\partial \tau_{13}}{\partial x_3} + \beta_1 = 0$$

$$\frac{\partial \tau_{21}}{\partial x_1} + \frac{\partial \sigma_2}{\partial x_2} + \frac{\partial \tau_{23}}{\partial x_3} + \beta_2 = 0 \tag{2.1}$$

$$\frac{\partial \tau_{31}}{\partial x_1} + \frac{\partial \tau_{32}}{\partial x_2} + \frac{\partial \sigma_3}{\partial x_3} + \beta_3 = 0$$

The body force, β_i, is per unit of volume in the i-direction and represents gravitational forces or pore pressure gradients. Because $\tau_{ij} = \tau_{ji}$, the infinitesimal element is automatically in rotational equilibrium. Of course for this equation to be valid for large displacements, it must be satisfied in the deformed position, and all stresses must be defined as force per unit of deformed area.

2.3   STRESS RESULTANTS - FORCES AND MOMENTS

In structural analysis it is standard practice to write equilibrium equations in terms of stress resultants rather than in terms of stresses. Force stress resultants are calculated by the integration of normal or shear stresses acting on a surface. Moment stress resultants are the integration of stresses on a surface times a distance from an axis.

A point load, which is a stress resultant, is by definition an infinite stress times an infinitesimal area and is physically impossible on all real structures. Also, a point moment is a mathematical definition and does not have a unique stress field as a physical interpretation. Clearly, the use of forces and moments is fundamental in structural analysis and design. However, a clear understanding of their use in

finite element analysis is absolutely necessary if stress results are to be physically evaluated.

For a finite size element or joint, a substructure, or a complete structural system *the following six equilibrium equations must be satisfied:*

$$\Sigma\, F_x = 0 \qquad \Sigma\, F_y = 0 \qquad \Sigma\, F_z = 0$$

$$\Sigma\, M_x = 0 \qquad \Sigma\, M_y = 0 \qquad \Sigma\, M_z = 0 \tag{2.2}$$

For two dimensional structures only three of these equations need to be satisfied.

2.4   COMPATIBILITY REQUIREMENTS

For continuous solids we have defined strains as displacements per unit length. To calculate absolute displacements at a point, we must integrate the strains with respect to a fixed boundary condition. This integration can be conducted over many different paths. A solution is compatible if the displacement at all points is not a function of the path. Therefore, a displacement compatible solution involves the existence of a uniquely defined displacement field.

In the analysis of a structural system of discrete elements, all elements connected to a joint or node point must have the same absolute displacement. If the node displacements are given, all element deformations can be calculated from the basic equations of geometry. In a displacement-based finite element analysis, node displacement compatibility is satisfied. However, it is not necessary that the displacements along the sides of the elements be compatible if the element passes the "patch test."

A finite element passes the patch test "if a group (or patch) of elements, of arbitrary shape, is subjected to node displacements associated with constant strain; and the results of a finite element analysis of the patch of elements yield constant strain." In the case of plate bending elements, the application of a constant curvature displacement pattern at the nodes must produce constant curvature within a patch of elements. If an element does not pass the patch test, it may not converge to the exact solution. Also, in the case of a coarse mesh,

elements that do not pass the patch test may produce results with significant errors.

2.5   STRAIN DISPLACEMENT EQUATIONS

If the small displacement fields u_1, u_2 and u_3 are specified, assumed or calculated, the consistent strains can be calculated directly from the following well-known strain-displacement equations[2]:

$$\varepsilon_1 = \frac{\partial u_1}{\partial x_1} \tag{2.3a}$$

$$\varepsilon_2 = \frac{\partial u_2}{\partial x_2} \tag{2.3b}$$

$$\varepsilon_3 = \frac{\partial u_3}{\partial x_3} \tag{2.3c}$$

$$\gamma_{12} = \frac{\partial u_1}{\partial x_2} + \frac{\partial u_2}{\partial x_1} \tag{2.3d}$$

$$\gamma_{13} = \frac{\partial u_1}{\partial x_3} + \frac{\partial u_3}{\partial x_1} \tag{2.3e}$$

$$\gamma_{23} = \frac{\partial u_2}{\partial x_3} + \frac{\partial u_3}{\partial x_2} \tag{2.3f}$$

2.6   DEFINITION OF ROTATION

A unique rotation at a point in a real structure does not exist. A rotation of a horizontal line may be different from the rotation of a vertical line. However, in many theoretical books on continuum mechanics the following mathematical equations are used to define rotation of the three axes:

$$\theta_3 \equiv \frac{1}{2}\left[\frac{\partial u_1}{\partial x_2} - \frac{\partial u_2}{\partial x_1} \right] \tag{2.4a}$$

$$\theta_2 \equiv \frac{1}{2}\left[\frac{\partial u_3}{\partial x_1} - \frac{\partial u_1}{\partial x_3}\right] \tag{2.4b}$$

$$\theta_1 \equiv \frac{1}{2}\left[\frac{\partial u_2}{\partial x_3} - \frac{\partial u_3}{\partial x_2}\right] \tag{2.4c}$$

It is of interest to note that this definition of rotation is the average rotation of two normal lines. It is important to recognize that these definitions are not the same as used in beam theory when shearing deformations are included. When beam sections are connected, the absolute rotation of the end sections must be equal.

2.7   EQUATIONS AT MATERIAL INTERFACES

One can clearly understand the fundamental equilibrium and compatibility requirements from an examination of the stresses and strains at the interface between two materials. A typical interface for a two-dimensional continuum is shown in Figure 2.1. By definition, the displacements at the interface are equal. Or, $u_s(s,n) = \overline{u}_s(s,n)$ and $u_n(s,n) = \overline{u}_n(s,n)$.
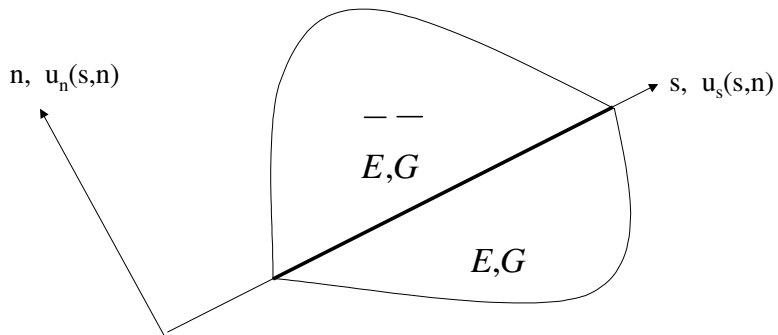
Figure 2.1 Material Interface Properties

Normal equilibrium at the interface requires that the normal stresses be equal. Or:

$$\sigma_n = \overline{\sigma}_n \tag{2.5a}$$

Also, the shear stresses at the interface are equal. Or:

$$\tau_{ns} = \bar{\tau}_{ns} \tag{2.5b}$$

Because displacement u_s and $\bar{u}_s$ must be equal and continuous at the interface:

$$\varepsilon_s = \bar{\varepsilon}_s \tag{2.5c}$$

Because the material properties that relate stress to strain are not equal for the two materials, it can be concluded that:

$$\sigma_s \neq \bar{\sigma}_s \tag{2.5d}$$

$$\varepsilon_n \neq \bar{\varepsilon}_n \tag{2.5e}$$

$$\gamma_{ns} \neq \bar{\gamma}_{ns} \tag{2.5f}$$

For a three-dimensional material interface on a s-t surface, it is apparent that the following 12 equilibrium and compatibility equations exist:

$$\sigma_n = \bar{\sigma}_n \qquad \varepsilon_n \neq \bar{\varepsilon}_n \tag{2.6a}$$

$$\sigma_s \neq \bar{\sigma}_s \qquad \varepsilon_s = \bar{\varepsilon}_s \tag{2.6b}$$

$$\sigma_t \neq \bar{\sigma}_t \qquad \varepsilon_t = \bar{\varepsilon}_t \tag{2.6c}$$

$$\tau_{ns} = \bar{\tau}_{ns} \qquad \gamma_{ns} \neq \bar{\gamma}_{ns} \tag{2.6d}$$

$$\tau_{nt} = \bar{\tau}_{nt} \qquad \gamma_{nt} \neq \bar{\gamma}_{nt} \tag{2.6e}$$

$$\tau_{st} \neq \bar{\tau}_{st} \qquad \gamma_{st} = \bar{\gamma}_{st} \tag{2.6f}$$

These 12 equations cannot be derived because they are fundamental physical laws of equilibrium and compatibility. It is important to note that if a stress is continuous, the corresponding strain, derivative of the displacement, is

discontinuous. Also, if a stress is discontinuous, the corresponding strain, derivative of the displacement, is continuous.

The continuity of displacements between elements and at material interfaces is defined as C_0 displacement fields. Elements with continuities of the derivatives of the displacements are defined by C_1 continuous elements. It is apparent that elements with C_1 displacement compatibility cannot be used at material interfaces.

2.8   INTERFACE EQUATIONS IN FINITE ELEMENT SYSTEMS

In the case of a finite element system in which the equilibrium and compatibility equations are satisfied only at node points along the interface, the fundamental equilibrium equations can be written as:

$$\sum F_n + \sum \overline{F}_n = 0 \tag{2.7a}$$

$$\sum F_s + \sum \overline{F}_s = 0 \tag{2.7b}$$

$$\sum F_t + \sum \overline{F}_t = 0 \tag{2.7c}$$

Each node on the interface between elements has a unique set of displacements; therefore, compatibility at the interface is satisfied at a finite number of points. As the finite element mesh is refined, the element stresses and strains approach the equilibrium and compatibility requirements given by Equations (2.6a) to (2.6f). Therefore, each element in the structure may have different material properties.

2.9   STATICALLY DETERMINATE STRUCTURES

The internal forces of some structures can be determined directly from the equations of equilibrium only. For example, the truss structure shown in Figure 2.2 will be analyzed to illustrate that the classical "method of joints" is nothing more than solving a set of equilibrium equations.
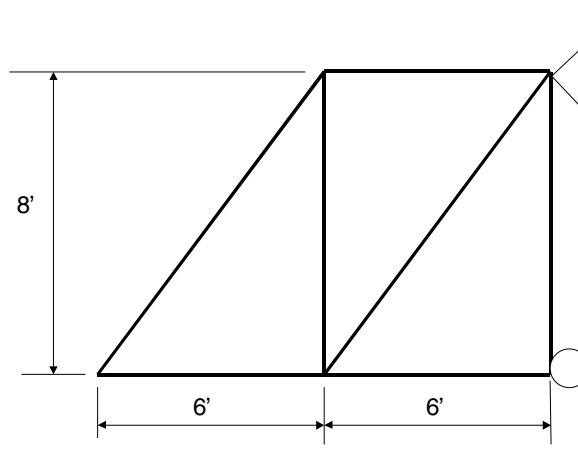
Figure 2.2 Simple Truss Structure

Positive external node loads and node displacements are shown in Figure 2.3. Member forces f_i and deformations d_i are positive in tension.
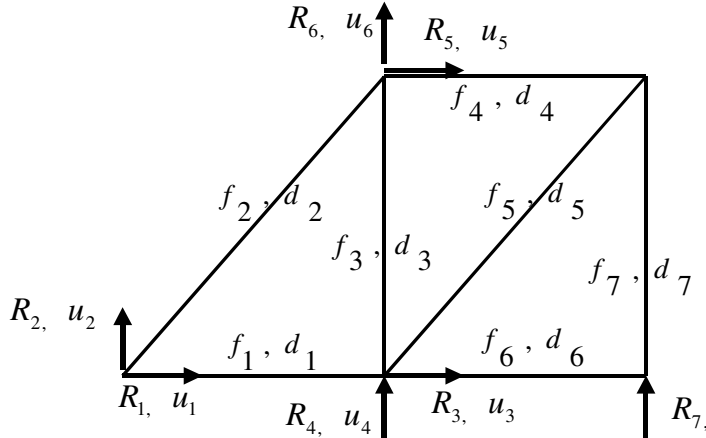
Figure 2.3 Definition of Positive Joint Forces and Node Displacements

Equating two external loads, R_j, at each joint to the sum of the internal member forces, f_i, (see Appendix B for details) yields the following seven equilibrium equations written as one matrix equation:

$$\begin{bmatrix} R_1 \\ R_2 \\ R_3 \\ R_4 \\ R_5 \\ R_6 \\ R_7 \end{bmatrix} = \begin{bmatrix} -1.0 & -0.6 & 0 & 0 & 0 & 0 & 0 \\ 0 & -0.8 & 0 & 0 & 0 & 0 & 0 \\ 1.0 & 0 & 0 & 0 & -0.6 & 0 & 0 \\ 0 & 0 & -1.0 & 0 & -0.8 & -1.0 & 0 \\ 0 & 0.6 & 0 & -1.0 & 0 & 0 & 0 \\ 0 & 0.8 & 1.0 & 0 & 0 & 0 & 0 \\ 0 & 0 & 0 & 0 & 0 & 0 & -1.0 \end{bmatrix} \begin{bmatrix} f_1 \\ f_2 \\ f_3 \\ f_4 \\ f_5 \\ f_6 \\ f_7 \end{bmatrix} \qquad (2.8)$$

Or, symbolically:

$$\mathbf{R} = \mathbf{Af} \qquad (2.9)$$

where **A** is a load-force transformation matrix and is a function of the geometry of the structure only. For this ***statically determinate*** structure, we have seven unknown element forces and seven joint equilibrium equations; therefore, the above set of equations can be solved directly for any number of joint load conditions. If the structure had one additional diagonal member, there would be eight unknown member forces, and a direct solution would not be possible because the structure would be ***statically indeterminate***. The major purpose of this example is to express the well-known traditional method of analysis ("***method of joints***") in matrix notation.

2.10   DISPLACEMENT TRANSFORMATION MATRIX

After the member forces have been calculated, there are many different traditional methods to calculate joint displacements. Again, to illustrate the use of matrix notation, the member deformations d_i will be expressed in terms of joint displacements u_j. Consider a typical truss element as shown in Figure 2.4.
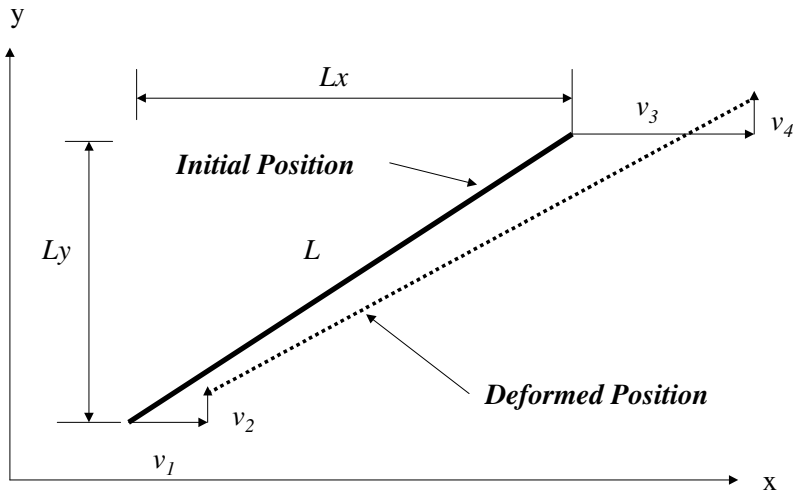
Figure 2.4 Typical Two-Dimension Truss Element

The axial deformation of the element can be expressed as the sum of the axial deformations resulting from the four displacements at the two ends of the element. The total axial deformation written in matrix form is:

$$d = \begin{bmatrix} -\dfrac{L_x}{L} & -\dfrac{L_y}{L} & \dfrac{L_x}{L} & \dfrac{L_y}{L} \end{bmatrix} \begin{bmatrix} v_1 \\ v_2 \\ v_3 \\ v_4 \end{bmatrix} \tag{2.10}$$

Application of Equation (2.10) to all members of the truss shown in Figure 2.3 yields the following matrix equation:

$$\begin{bmatrix} d_1 \\ d_2 \\ d_3 \\ d_4 \\ d_5 \\ d_6 \\ d_7 \end{bmatrix} = \begin{bmatrix} -1.0 & 0 & 1.0 & 0 & 0 & 0 & 0 \\ -0.6 & -0.8 & 0 & 0 & 0.6 & 0.8 & 0 \\ 0 & 0 & 0 & -1.0 & 0 & 1.0 & 0 \\ 0 & 0 & 0 & 0 & -1.0 & 0 & 0 \\ 0 & 0 & -0.6 & -0.8 & 0 & 0 & 0 \\ 0 & 0 & -1.0 & 0 & 0 & 0 & 0 \\ 0 & 0 & 0 & 0 & 0 & 0 & -1.0 \end{bmatrix} \begin{bmatrix} u_1 \\ u_2 \\ u_3 \\ u_4 \\ u_5 \\ u_6 \\ u_7 \end{bmatrix} \tag{2.11}$$

Or, symbolically:

$$\mathbf{d} = \mathbf{B} \, \mathbf{u} \tag{2.12}$$

The element deformation-displacement transformation matrix, **B,** is a function of the geometry of the structure. Of greater significance, however, is the fact that the matrix **B** is the transpose of the matrix **A** defined by the joint equilibrium Equation (2.8). Therefore, given the element deformations within this statically determinate truss structure, we can solve Equation (2.11) for the joint displacements.

2.11   ELEMENT STIFFNESS AND FLEXIBILITY MATRICES

The forces in the elements can be expressed in terms of the deformations in the elements using the following matrix equations:

$$\mathbf{f} = \mathbf{k} \, \mathbf{d} \qquad \text{or,} \qquad \mathbf{d} = \mathbf{k}^{-1} \, \mathbf{f} \tag{2.13}$$

The element stiffness matrix **k** is diagonal for this truss structure, where the diagonal terms are $k_{ii} = \dfrac{A_i E_i}{L_i}$ and all other terms are zero. The element flexibility matrix is the inverse of the stiffness matrix, where the diagonal terms are $\dfrac{L_i}{A_i E_i}$. It is important to note that the element stiffness and flexibility matrices are only a function of the mechanical properties of the elements.

2.12   SOLUTION OF STATICALLY DETERMINATE SYSTEM

The three fundamental equations of structural analysis for this simple truss structure are equilibrium, Equation (2.8); compatibility, Equation (2.11); and force-deformation, Equation (2.13). For each load condition R, the solution steps can be summarized as follows:

1.   Calculate the element forces from Equation (2.8).

2. Calculate element deformations from Equation (2.13).

3. Solve for joint displacements using Equation (2.11).

All traditional methods of structural analysis use these basic equations. However, before the availability of inexpensive digital computers that can solve over 100 equations in less than one second, many special techniques were developed to minimize the number of hand calculations. Therefore, at this point in time, there is little value to summarize those methods in this book on the static and dynamic analysis of structures.

2.13   GENERAL SOLUTION OF STRUCTURAL SYSTEMS

In structural analysis using digital computers, the same equations used in classical structural analysis are applied. The starting point is always joint equilibrium. Or, $\mathbf{R} = \mathbf{A}\,\mathbf{f}$. From the element force-deformation equation, $\mathbf{f} = \mathbf{k}\,\mathbf{d}$, the joint equilibrium equation can be written as $\mathbf{R} = \mathbf{A}\,\mathbf{k}\,\mathbf{d}$. From the compatibility equation, $\mathbf{d} = \mathbf{B}\,\mathbf{u}$, joint equilibrium can be written in terms of joint displacements as $\mathbf{R} = \mathbf{A}\,\mathbf{k}\,\mathbf{B}\,\mathbf{u}$. Therefore, the general joint equilibrium can be written as:

$$\mathbf{R} = \mathbf{K}\,\mathbf{u} \tag{2.14}$$

The global stiffness matrix $\mathbf{K}$ is given by one of the following matrix equations:

$$\mathbf{K} = \mathbf{A}\,\mathbf{k}\,\mathbf{B} \qquad \text{or} \qquad \mathbf{K} = \mathbf{A}\,\mathbf{k}\,\mathbf{A}^{\mathrm{T}} \qquad \text{or} \qquad \mathbf{K} = \mathbf{B}^{\mathrm{T}}\,\mathbf{k}\,\mathbf{B} \tag{2.15}$$

It is of interest to note that the equations of equilibrium or the equations of compatibility can be used to calculate the global stiffness matrix $\mathbf{K}$.

The standard approach is to solve Equation (2.14) for the joint displacements and then calculate the member forces from:

$$\mathbf{f} = \mathbf{k}\,\mathbf{B}\,\mathbf{u} \qquad \text{or} \qquad \mathbf{f} = \mathbf{k}\,\mathbf{A}^{\mathrm{T}}\,\mathbf{u} \tag{2.16}$$

It should be noted that within a computer program, the sparse matrices **A**, **B**, **k** and **K** are never formed because of their large storage requirements. The symmetric global stiffness matrix **K** is formed and solved in condensed form.

2.14 SUMMARY

Internal member forces and stresses must be in equilibrium with the applied loads and displacements. All real structures satisfy this fundamental law of physics. Hence, our computer models must satisfy the same law.

At material interfaces, all stresses and strains are not continuous. Computer programs that average node stresses at material interfaces produce plot stress contours that are continuous; however, the results will not converge and significant errors can be introduced by this approximation.

Compatibility conditions, which require that all elements attached to a rigid joint have the same displacement, are fundamental requirements in structural analysis and can be physically understood. Satisfying displacement compatibility involves the use of simple equations of geometry. However, the compatibility equations have many forms, and most engineering students and many practicing engineers can have difficulty in understanding the displacement compatibility requirement. Some of the reasons we have difficulty in the enforcement of the compatibility equations are the following:

1. The displacements that exist in most linear structural systems are small compared to the dimensions of the structure. Therefore, deflected shape drawing must be grossly exaggerated to write equations of geometry.

2. For structural systems that are statically determinate, the internal member forces and stresses can be calculated exactly without the use of the compatibility equations.

3. Many popular (approximate) methods of analysis exist that do not satisfy the displacement compatibility equations. For example, for rectangular frames, both the cantilever and portal methods of analysis assume the inflection points to exist at a predetermined location within the beams or columns; therefore, the displacement compatibility equations are not satisfied.

4. Many materials, such as soils and fluids, do not satisfy the compatibility equations. Also, locked in construction stresses, creep and slippage within joints are real violations of displacement compatibility. Therefore, approximate methods that satisfy statics may produce more realistic results for the purpose of design.

5. In addition, engineering students are not normally required to take a course in geometry; whereas, all students take a course in statics. Hence, there has not been an emphasis on the application of the equations of geometry.

The relaxation of the displacement compatibility requirement has been justified for hand calculation to minimize computational time. Also, if one must make a choice between satisfying the equations of statics or the equations of geometry, in general, we should satisfy the equations of statics for the reasons previously stated.

However, because of the existence of inexpensive powerful computers and efficient modern computer programs, it is not necessary to approximate the compatibility requirements. For many structures, such approximations can produce significant errors in the force distribution in the structure in addition to incorrect displacements.

2.15   REFERENCES

1. Cook, R. D., D. S. Malkus and M. E. Plesha. 1989. *Concepts and Applications of Finite Element Analysis,* Third Edition. John Wiley & Sons, Inc. ISBN 0-471-84788-7.

2. Boresi, A. P. 1985. *Advanced Mechanics of Materials.* John Wiley & Sons, Inc. ISBN 0-471-88392-1.

3.

ENERGY AND WORK

All External Work Supplied to a Real Structural
System is Stored or Dissipated as Energy

3.1   INTRODUCTION

A large number of energy methods have been presented during the last 150 years for the analysis of both determinate and statically indeterminate structures. However, if all methods are formulated in matrix notation, it can be shown that only two fundamental methods exist. They are generally defined as the force and displacement methods. One can use minimum energy principles or methods of virtual-work to derive the general equations for linear structural analysis. *Energy* is defined as the ability to do *work*. Both have the units of force-distance.

For many types of structural elements, however, there can be many advantages in using both force and displacement methods in approximating the stiffness properties of the element. For example, the classical non-prismatic beam element uses a force approach to define the forces at a typical cross-section within the beam; however, a displacement approximation, such as plane sections remain plane, is used to define the strain distribution over the cross-section.

In recent years, assumed-stress hybrid formulations have been used to produce element stiffness properties. In addition, assumed-stress distributions, virtual work methods and the least-square error approach have been used to calculate accurate stresses in displacement-based finite elements. Therefore, no one method can be used to solve all problems in structural analysis. The only

restriction on the computational techniques used is that the results must converge to the exact values as the elements become smaller.

3.2   VIRTUAL AND REAL WORK

The principles of virtual work are very simple and are clear statements of conservation of energy. The principles apply to structures that are in equilibrium in a real displaced position **u** when subjected to loading **R**. The corresponding real internal deformations and internal forces are **d** and **f** respectively. All terms are illustrated in Figures 3.1 and 3.2.

A.   *External Virtual Work* $\bar{R}\,u$ B. *Internal Virtual Work* $\bar{f}d$
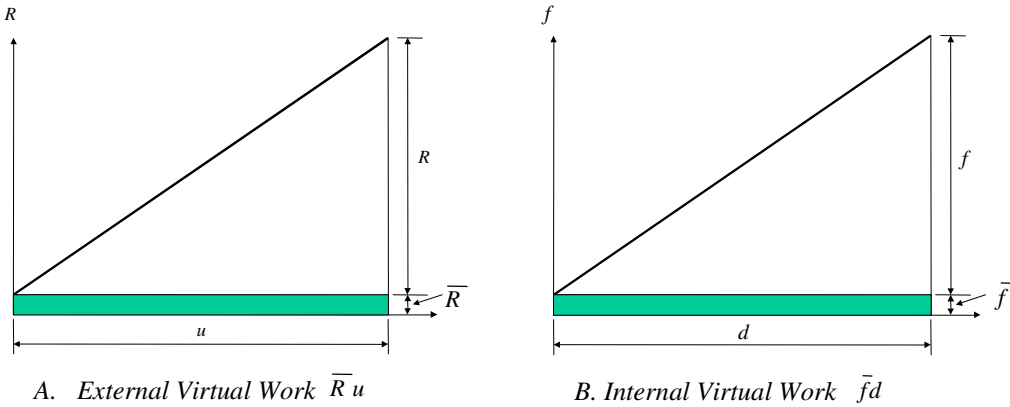
Figure 3.1 Method of Virtual Forces

The principle of virtual forces states (in my words) *if a set of infinitesimal external forces,* $\bar{\mathbf{R}}$*, in equilibrium with a set of infinitesimal internal forces* $\bar{\mathbf{f}}$ *that exist before the application of the real loads and displacements, the external virtual work is equal to the internal virtual work.* Or, in terms of the notation defined previously:

$$\bar{\mathbf{R}}^{\mathrm{T}}\mathbf{u} = \bar{\mathbf{f}}^{\mathrm{T}}\mathbf{d} \tag{3.1}$$

If only one joint displacement u_i is to be calculated, only one external virtual load exists, $\bar{R}_i = 1$. For this case, the equation is the same as the unit load method. It is apparent for nonlinear analysis that the principle of virtual forces

A. *External Virtual Work* $\overline{u}R$ B. *Internal Virtual Work* $\overline{d}f$
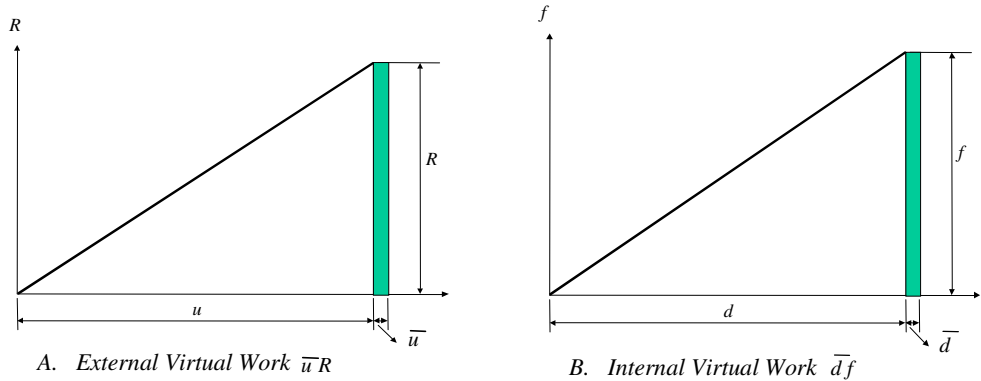
Figure 3.2 Method of Virtual Displacements

cannot be used, because the linear relationship between $\overline{\mathbf{R}}$ and $\overline{\mathbf{f}}$ may not hold after the application of the real loads and displacements.

The principle of virtual displacements states (in my words) *if a set of infinitesimal external displacements,* $\overline{\mathbf{u}}$, *consistent with a set of internal virtual displacements,* $\overline{\mathbf{d}}$, *and boundary conditions are applied* <u>after</u> *the application of the real loads and displacements, the external virtual work is equal to the internal virtual work.* Or, in terms of matrix notation:

$$\overline{\mathbf{u}}^{\mathrm{T}}\mathbf{R} = \overline{\mathbf{d}}^{\mathrm{T}}\mathbf{f} \tag{3.2}$$

It is important to note that the principle of virtual displacements does apply to the solution of nonlinear systems because the virtual displacements are applied to real forces in the deformed structure.

In the case of finite element analysis of continuous solids, the virtual work principles are applied at the level of stresses and strains; therefore, integration over the volume of the element is required to calculate the virtual work terms.

For linear analysis, it is apparent that the real external work, or energy, is given by:

$$W_E = \frac{1}{2}\mathbf{u}^{\mathrm{T}}\mathbf{R} = \frac{1}{2}\mathbf{R}^{\mathrm{T}}\mathbf{u} \tag{3.3}$$

The real internal work, or strain energy, is given by:

$$W_I = \frac{1}{2}\mathbf{d}^T\mathbf{f} = \frac{1}{2}\mathbf{f}^T\mathbf{d} \qquad (3.4)$$

3.3   POTENTIAL ENERGY AND KINETIC ENERGY

One of the most fundamental forms of energy is the position of a mass within a gravitational field near the earth's surface. The gravitational potential energy V_g is defined as the constant weight w moved against a constant gravitational field of distance h. Or:

$$V_g = mgh \quad \text{or} \quad V_g = Wh \qquad (3.5)$$

A mass that is moving with velocity v has kinetic energy given by the following equation:

$$V_k = \frac{1}{2}mv^2 \qquad (3.6)$$

One of the most common examples that illustrates the physical significance of both the potential and kinetic energy is the behavior of a pendulum shown in Figure 3.3.

If the mass of the pendulum has an initial position of h_{max}, the kinetic energy is zero and the potential energy is $h_{max}W$. When h equals zero, the potential energy is zero; therefore, from conservation of energy, the kinetic energy is:

$$V_k = h_{max}\ W = \frac{W\,v^2}{2g} \qquad (3.7)$$

Hence, the maximum horizontal velocity is:

$$v_{max} = \sqrt{2\,g\,h_{max}} \qquad (3.8)$$
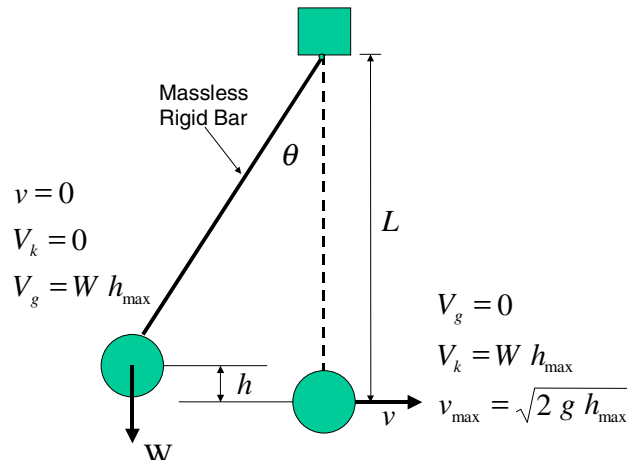
Figure 3.3 Oscillation of Pendulum

It is important to note that the total energy in the oscillating system is always constant; therefore, the following energy equation, at any time t, must be satisfied:

$$V_g(t) + V_k(t) = W\,h_{max} = \text{constant} \tag{3.9}$$

The physical behavior of the oscillating pendulum can be considered to be an *energy pump*, where there is an interchange between potential and kinetic energy.

The tangential force accelerating the mass is $W\sin\theta$. From Newton's Second Law, the following nonlinear, differential equation of equilibrium can be written:

$$mL\ddot{\theta} + W\sin\theta = 0 \quad \text{or,} \quad \ddot{\theta} + \frac{g}{L}\sin\theta = 0 \tag{3.10}$$

For very small angles, $\sin\theta \approx \theta$, the approximate linear differential equation is:

$$\ddot{\theta} + \frac{g}{L}\theta = 0 \tag{3.11}$$

Hence, the *small displacement* period of oscillation of a pendulum is:

$$T = 2\pi \sqrt{\frac{L}{g}} \tag{3.12}$$

3.4   STRAIN ENERGY

The strain energy stored in an element "i" within a general structural system is the area under the stress-strain diagram integrated over the volume of the element. For linear systems, the stress-strain matrix $\mathbf{E}^{(i)}$, including initial thermal stresses $\mathbf{f}_t^{(i)}$, can be written in matrix form as:

$$\mathbf{f}^{(i)} = \mathbf{E}^{(i)}\mathbf{d}^{(i)} + \mathbf{f}_t^{(i)} \tag{3.13}$$

The column matrices $\mathbf{f}^{(i)}$ and $\mathbf{d}^{(i)}$ are the stresses and strain respectively. Therefore, the strain energy within one element is given by:

$$W_I^{(i)} = \frac{1}{2}\int \mathbf{d}^{(i)\mathbf{T}} \mathbf{E}^{(i)} \mathbf{d}^{(i)} \, dV \quad + \quad \int \mathbf{d}^{(i)\mathbf{T}} \mathbf{f}_t^{(i)} \, dV \tag{3.14}$$

Within each element, an approximation can be made on the displacements. Or:

$$u_x^{(i)} = \mathbf{N}^{(i)} \mathbf{u}_x \;, \quad u_y^{(i)} = \mathbf{N}^{(i)} \mathbf{u}_y \quad \text{and} \quad u_z^{(i)} = \mathbf{N}^{(i)} \mathbf{u}_z \tag{3.15}$$

Hence, after the application of the strain-displacement equations, the element strains can be expressed in terms of nodal displacements. Or:

$$\mathbf{d}^{(i)} = \mathbf{B}^{(i)} \mathbf{u} \quad \text{or} \quad \mathbf{d}^{(i)\mathbf{T}} = \mathbf{u}^{\mathbf{T}} \mathbf{B}^{(i)\mathbf{T}} \tag{3.16}$$

The column matrix $\mathbf{u}$ contains all of the node, or joint, displacements of the complete structural system. In addition, it may contain displacement patterns within the element. When equation (3.16) is written in this form, it is apparent that the $\mathbf{B}^{(i)}$ matrix can be very large; however, it only has non-zero terms associated with the displacements at the nodes connected to nodes adjacent to the element. Therefore, the $\mathbf{B}^{(i)}$ matrix is always formed and used in compacted form within a computer program, and an ***integer location array***, $\mathbf{L}_a^{(i)}$, is formed for

each element that is used to relate the local node displacements $\mathbf{u}^{(i)}$ to the **global** node displacements $\mathbf{u}$.

After integration over the volume of the element, the strain energy, in terms of the global node displacements, can be written as:

$$W_I^{(i)} = \frac{1}{2}\mathbf{u}^{\mathbf{T}}\ \mathbf{k}^{(i)}\ \mathbf{u} + \mathbf{u}^{\mathbf{T}}\ \mathbf{F_t}^{(i)} \tag{3.17}$$

Therefore, the element stiffness matrix is by definition:

$$\mathbf{k}^{(i)} = \int \mathbf{B}^{(i)\mathbf{T}}\mathbf{E}^{(i)}\mathbf{B}^{(i)}\ dV \tag{3.18}$$

And the element thermal force matrix is:

$$\mathbf{F}^{(i)} = \int \mathbf{B}^{(i)\mathbf{T}}\mathbf{f_t}^{(i)}\ dV \tag{3.19}$$

The total internal strain energy is the sum of the element strain energies. Or:

$$W_I = \frac{1}{2}\mathbf{u}^{\mathbf{T}}\ \mathbf{K}\ \mathbf{u} + \mathbf{u}^{\mathbf{T}}\ \mathbf{F_t} \tag{3.20}$$

The global stiffness matrix $\mathbf{K}$ is the sum of the element stiffness matrices $\mathbf{k}^{(i)}$. Or:

$$\mathbf{K} = \sum \mathbf{k}^{(i)} \tag{3.21}$$

The summation of element stiffness matrices to form the global stiffness matrix is termed the **direct stiffness method**. The global thermal load vector $\mathbf{F_t}$ is the sum of the element thermal load matrices:

$$\mathbf{F_t} = \sum \mathbf{F}_t^{(t)} \tag{3.22}$$

3.5   EXTERNAL WORK

The external work W_c performed by a system of concentrated node, or joint, loads $\mathbf{F}_c$ is:

$$W_c = \frac{1}{2} \mathbf{u}^\mathrm{T} \mathbf{F}_c \tag{3.23}$$

Within each element "i", the external work $W_g^{(i)}$ performed by the body forces because of gravitational loads is:

$$W_g^{(i)} = \frac{1}{2} \int (m_x^{(i)} g_x u_x^{(i)} + \rho_y g_y u_y + \rho_z g_z u_z)\, dV \tag{3.24}$$

Application of the displacement assumptions given by Equation (3.15), integration over the volume of the element, and summation over all elements produces the following equation for the energy because of body forces:

$$W_g = \frac{1}{2} \mathbf{u}^\mathrm{T} \mathbf{F}_g \tag{3.25}$$

The external work W_s^j performed because of element surface stresses (tractions) $\mathbf{t}_s^{(j)}$, for a typical surface "j" is of the form:

$$W_s^{(j)} = \frac{1}{2} \mathbf{u}^\mathrm{T} \int \mathbf{B}_s^{(j)\mathrm{T}} \mathbf{t}_s^{(j)}\, dS \tag{3.26}$$

Application of the displacement assumptions given by Equation (3.15), integration over the surface of the element, and summation over all surface elements produces the following equation for the energy because of surface tractions:

$$W_s = \frac{1}{2} \mathbf{u}^\mathrm{T} \mathbf{F}_s \tag{3.27}$$

Therefore, the total external work performed on any system of structural elements is:

$$W_E = \frac{1}{2} \mathbf{u}^\mathrm{T} \left[\mathbf{F}_c + \mathbf{F}_g + \mathbf{F}_s \right] \tag{3.28}$$

3.6   STATIONARY ENERGY PRINCIPLE

It is a fact for linear systems that the internal strain energy must equal the external work performed on the structure. For a single degree-of-freedom system, we can use this principle to solve for the displacement. However, for a multi degree-of-freedom system, a different approach is required. The energy plots, shown in Figure 3.4, illustrate that a new energy function Ω can be defined.

$$W_I = \frac{1}{2}\mathbf{u}^T\mathbf{K}\mathbf{u} + \mathbf{u}^T\mathbf{F_t}$$

$$W_E = \frac{1}{2}\mathbf{u}^T\left[\mathbf{F}_c + \mathbf{F}_g + \mathbf{F}_s\right]$$

$$\Omega = W_I - 2W_E$$

$$\frac{\partial\Omega}{\partial u_n} = 0 \text{ at } \Omega_{\text{MIN}}$$
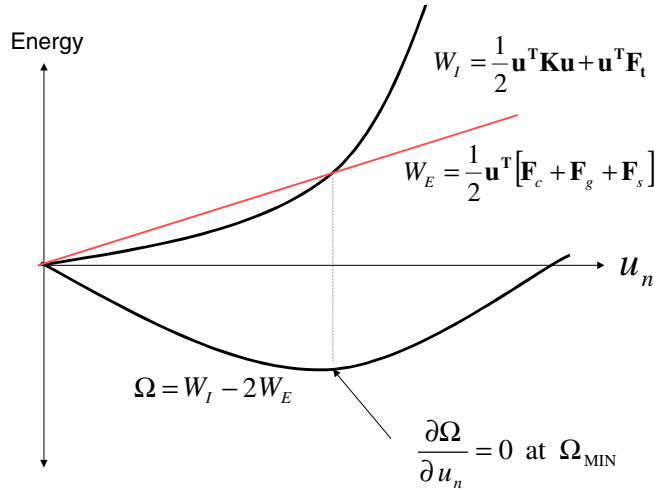
Figure 3.4 Energy as a Function of a Typical Displacement

It is apparent that the solution at the point of minimum potential energy is where the internal energy equals the external energy. Therefore, the major advantage of the use of the potential energy function is that the solution must satisfy the following equation for all displacement degrees-of-freedom u_n:

$$\frac{\partial\Omega}{\partial u_n} = 0 \tag{3.29}$$

The energy function written in matrix form is:

$$\Omega = \frac{1}{2}\mathbf{u}^T\mathbf{K}\mathbf{u} - \mathbf{u}^T\mathbf{R} \tag{3.30}$$

The resultant load vector $\mathbf{R}$ associated with the four types of loading is:

$$\mathbf{R} = \mathbf{F}_c + \mathbf{F}_g + \mathbf{F}_s - \mathbf{F}_t \tag{3.31}$$

Application of Equation (3.29) to all displacements yields:

$$
\begin{bmatrix}
\dfrac{\partial \Omega}{\partial \mathbf{u}_1} \\
- \\
\dfrac{\partial \Omega}{\partial \mathbf{u}_2} \\
- \\
\dfrac{\partial \Omega}{\partial \mathbf{u}_n} \\
- \\
\dfrac{\partial \Omega}{\partial \mathbf{u}_N}
\end{bmatrix}
=
\begin{bmatrix}
1 & 0 & - & 0 & - & 0 \\
0 & 1 & - & 0 & - & 0 \\
- & - & - & - & - & - \\
0 & 0 & - & 1 & - & 0 \\
- & - & - & - & - & - \\
0 & 0 & - & 0 & - & 1
\end{bmatrix}
[\mathbf{Ku} - \mathbf{R}] = [0] \tag{3.32}
$$

Therefore, the node equilibrium equation for all types of structural systems can be written as the following matrix equation:

$$\mathbf{K u = R} \tag{3.33}$$

The only approximation involved in the development of this equation is the assumption of the displacement patterns within each element. If the same displacement approximation is used to calculate the kinetic energy, the resulting mass matrix is termed a ***consistent mass matrix***.

Another important fact concerning compatible displacement-based finite elements is that they converge from below, to the exact solution, as the mesh is refined. Therefore, the displacements and stresses tend to be lower than the exact values. From a practical structural engineering viewpoint, this can produce very dangerous results. To minimize this problem, the structural engineer must check statics and conduct parameter studies using different meshes.

3.7   THE FORCE METHOD

The traditional method of *cutting* a statically indeterminate structure, applying redundant forces, and solving for the redundant forces by setting the relative

displacements at the cuts to zero has been the most popular method of structural analysis, if hand calculations are used. The author has developed structural analysis programs based on both the force and displacement methods of analysis. At this point in time, there appears to be no compelling reason for using the force method within a computer program for solving large structural systems. In fact, programs based on the displacement approach are simple to program and, in general, require less computer time to execute. Another significant advantage of a displacement approach is that the method is easily extended to the dynamic response of structures.

To develop the stiffness of one-dimensional elements, however, the force method should be used because the internal forces can be expressed exactly in terms of the forces at the two ends of the element. Therefore, the force method will be presented here for a single-element system.

Neglecting thermal strains, the energy function can be written as:

$$\Omega = \frac{1}{2} \int \mathbf{f}^T \mathbf{d} \; dV - \mathbf{R}^T \mathbf{u} \tag{3.34}$$

The internal forces can be expressed in terms of the node forces using the following equation:

$$\mathbf{f} = \mathbf{P} \, \mathbf{R} \tag{3.35}$$

For linear material $\mathbf{d} = \mathbf{Cf}$ and the energy function can be written as:

$$\Omega = \frac{1}{2} \mathbf{R}^T \mathbf{F} \mathbf{R} - \mathbf{R}^T \mathbf{u} \tag{3.36}$$

Where the element flexibility matrix is:

$$\mathbf{F} = \int \mathbf{P}^T \mathbf{C} \mathbf{P} \, dV \tag{3.37}$$

We can now minimize the ***complementary energy function*** by requiring that:

$$\frac{\partial \Omega}{\partial R_n} = 0 \tag{3.38}$$

The node displacements can now be expressed in terms of node forces by:

$$\mathbf{u} = \mathbf{FR} \qquad (3.39)$$

The element stiffness can now be numerically evaluated from:

$$\mathbf{K} = \mathbf{F}^{-1} \qquad (3.40)$$

The element stiffness can be used in the direct stiffness approach where the basic unknowns are the node displacements. One can also derive the element flexibility by applying the virtual force method.

3.8   LAGRANGE'S EQUATION OF MOTION

In the case of dynamic analysis of structures, the direct application of the well-known Lagrange's equation of motion can be used to develop the dynamic equilibrium of a complex structural system[1]. Lagrange's minimization equation, written in terms of the previously defined notation, is given by:

$$\frac{\partial}{\partial t}\left(\frac{\partial V_k}{\partial \dot{u}_n}\right) - \frac{\partial V_k}{\partial u_n} + \frac{\partial \Omega}{\partial u_n} = 0 \qquad (3.41)$$

The node point velocity is defined as $\dot{u}_n$. The most general form for the kinetic energy $V_k^{(i)}$ stored within a three-dimensional element i of mass density ρ is:

$$V_k^{(i)} = \int \frac{1}{2}\begin{bmatrix} \dot{u}_x & \dot{u}_y & \dot{u}_z \end{bmatrix}\begin{bmatrix} \rho & 0 & 0 \\ 0 & \rho & 0 \\ 0 & 0 & \rho \end{bmatrix}\begin{bmatrix} \dot{u}_x \\ \dot{u}_y \\ \dot{u}_z \end{bmatrix} dV \qquad (3.42)$$

The same shape functions used to calculate the strain energy within the element allow the velocities within the element to be expressed in terms of the node point velocities. Or:

$$\dot{u}_x^{(i)} = \mathbf{N}^{(i)}\,\dot{\mathbf{u}}_x \ , \quad \dot{u}_y^{(i)} = \mathbf{N}^{(i)}\,\dot{\mathbf{u}}_y \quad \text{and} \quad \dot{u}_z^{(i)} = \mathbf{N}^{(i)}\,\dot{\mathbf{u}}_z \qquad (3.43)$$

Therefore, the velocity transformation equations can be written in the following form:

$$\begin{bmatrix} \dot{u}_x^{(i)} \\ \dot{u}_y^{(i)} \\ \dot{u}_z^{(i)} \end{bmatrix} = \overline{\mathbf{N}}^{(i)} \dot{\mathbf{u}} \tag{3.44}$$

Using exact or numerical integration, it is now possible to write the total kinetic energy within a structure as:

$$V_k = \sum_i V_k^{(i)} = \frac{1}{2} \dot{\mathbf{u}}^{\mathbf{T}} \mathbf{M} \dot{\mathbf{u}} \tag{3.45}$$

The total mass matrix $\mathbf{M}$ is the sum of the element mass matrices $\mathbf{M}^{(i)}$. The element consistent mass matrices are calculated from:

$$\mathbf{M}^{(\mathbf{i})} = \int \overline{\mathbf{N}}^{(i)T} \mathbf{m} \, \overline{\mathbf{N}}^{(i)} dV \tag{3.46}$$

where $\mathbf{m}$ is the 3 by 3 diagonal mass density matrix shown in Equation (3.42). Equation (3.46) is very general and can be used to develop the ***consistent mass matrix*** for any displacement-based finite element. The term "consistent" is used because the same shape functions are used to develop both the stiffness and mass matrices.

Direct application of Equation (3.41) will yield the dynamic equilibrium equations:

$$\mathbf{M}\ddot{\mathbf{u}} + \mathbf{K}\mathbf{u} = \mathbf{R} \tag{3.47}$$

Later in the book the more general dynamic equilibrium equations with damping will be developed using a physical equilibrium approach.

3.9   CONSERVATION OF MOMENTUM

The conservation of momentum is often presented as a fundamental principle of physics. However, it can be easily derived from the basic equilibrium equations. Consider the two rigid bodies shown in Figure 3.5.

$$M_1 \dot{u}_1 + M_2 \dot{u}_2 = M_1 \bar{u}_1 + M_2 \bar{u}_2$$
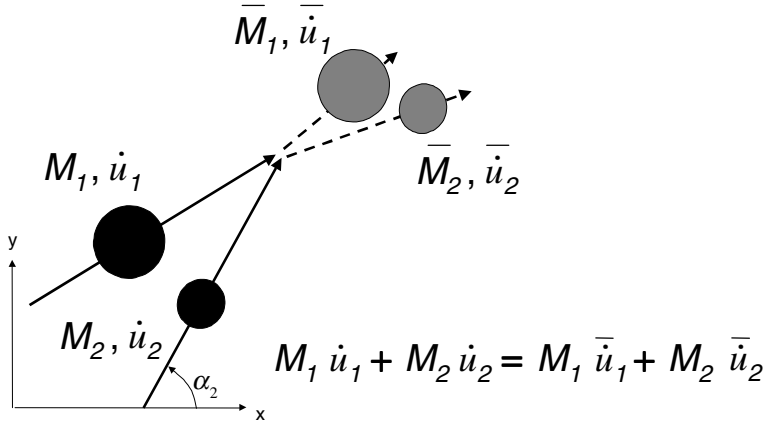
Figure 3.5 Conservation of Linear Momentum

From Newton's Second Law, the equal and opposite forces acting on the rigid bodies during impact will be:

$$F = M\ddot{u} \approx M \frac{\dot{u} - \bar{u}}{\delta t} \tag{3.48}$$

If the duration of contact between the two bodies is δt, the contact force can be approximated by a change in the velocity before and after impact. During contact, equilibrium must be satisfied in both the x and y directions. Therefore:

$$F_x \, \delta t = M_1(\dot{u}_{1x} - \bar{\bar{u}}_{1x}) + M_2(\dot{u}_{2x} - \bar{\bar{u}}_{2x}) = 0$$
$$F_y \, \delta t = M_1(\dot{u}_{1y} - \bar{\bar{u}}_{1y}) + M_2(\dot{u}_{2y} - \bar{\bar{u}}_{2y}) = 0 \tag{3.49}$$

Momentum is defined as mass times the velocity of the mass and has the properties of a vector. From Equation (3.49), momentum has the direction of the velocity and its components can be plus or minus in reference to the x-y system. Or:

$$M_1\dot{u}_{1x} + M_2\dot{u}_{2x} = M_1\bar{\bar{u}}_{1x} + M_2\bar{\bar{u}}_{2x}$$
$$M_1\dot{u}_{1y} + M_2\dot{u}_{2y} = M_1\bar{\bar{u}}_{1y} + M_2\bar{\bar{u}}_{2y} \tag{3.50}$$

In addition, the resultant momentum vector must be the same before and after impact. Or:

$$M_1 \dot{u}_1 + M_2 \dot{u}_2 = M_1 \bar{\dot{u}}_1 + M_2 \bar{\dot{u}}_2 \tag{3.51}$$

It is apparent that three equations, given by Equations (3.50) and (3.51), do not have a unique solution because there are four unknowns. The following principle of conservation of kinetic energy must be enforced as an additional condition:

$$M_1 \dot{u}_1^2 + M_2 \dot{u}_2^2 = M_1 \bar{\dot{u}}_1^2 + M_2 \bar{\dot{u}}_2^2 \tag{3.52}$$

Consider a direct collision, with no energy dissipation, of a mass M_1 at a known velocity $\dot{u}_1$ with a mass of M_2 that is at rest. Conservation of momentum (equilibrium) and conservation of kinetic energy requires that:

$$\begin{aligned} M_1 \dot{u}_1 &= M_1 \bar{\dot{u}}_1 + M_2 \bar{\dot{u}}_2 \\ M_1 \dot{u}_1^2 &= M_1 \bar{\dot{u}}_1^2 + M_2 \bar{\dot{u}}_2^2 \end{aligned} \tag{3.53}$$

After impact, the new velocities are:

$$\bar{\dot{u}}_1 = \frac{M_1 - M_2}{M_1 + M_2} \dot{u}_1 \quad \text{and} \quad \bar{\dot{u}}_2 = \frac{2M_1}{M_1 + M_2} \dot{u}_1 \tag{3.54}$$

If the two masses are equal, the velocity of the first is reduced to zero. If the first mass is less than the second mass, the first will bounce back and the large mass will move forward with a small velocity.

These simple equations can be extended to model the impact between different parts of a structural system. These equations also may apply to the closing of gaps between different elastic structures.

3.10 SUMMARY

Several energy methods have been presented that can be used to derive the basic equations used for the static and dynamic analysis of structures. The fundamental equations of structural analysis are equilibrium, force-deformation and compatibility. If the same sign convention is used for element and joint

displacements and forces, the compatibility and equilibrium equations are directly related. If the joint equilibrium equations are written in the same order as the joint forces, the resulting stiffness and flexibility matrices will always be symmetrical.

By assuming displacement shape functions within structural elements, consistent mass and stiffness matrices can be developed. In most cases, however, a physical mass lumping will not produce significant errors.

In dynamic analysis, the independent time integration of the various components of energy, including energy dissipation, can be used to evaluate the accuracy of the solution. By comparing the strain energy stored in the structure resulting from a given load condition, one can modify and improve a structural design to minimize the energy absorbed by the structure

After the structural model has been selected and the loading has been assumed, the structural analysis procedure can be automated. However, the selection of the structural model and the interpretation and verification of the results is the major responsibility of the professional structural engineer.

3.11   REFERENCES

1. Clough, R., and J. Penzien. 1993. *Dynamics of Structures*, Second Edition. McGraw-Hill, Inc. ISBN 0-07-011394-7.

4.

ONE-DIMENSIONAL ELEMENTS

*Before 1960, the Field of Structural Analysis
Was Restricted to One-Dimensional Elements*

4.1   INTRODUCTION

Most structural engineers have the impression that two- and three-dimensional finite elements are very sophisticated and accurate compared to the one-dimensional frame element. After more than forty years of research in the development of practical structural analysis programs, it is my opinion that ***the non-prismatic frame element, used in an arbitrary location in three-dimensional space, is definitely the most complex and useful element compared to all other types of finite elements.***

The fundamental theory for frame elements has existed for over a century. However, only during the past forty years have we had the ability to solve large three-dimensional systems of frame elements. In addition, we now routinely include torsion and shear deformations in all elements. In addition, the finite size of connections is now considered in most analyses. Since the introduction of computer analysis, the use of non-prismatic sections and arbitrary member loading in three-dimensions has made the programming of the element very tedious. In addition, the post processing of the frame forces to satisfy the many different building codes is complex and not clearly defined.

4.2 ANALYSIS OF AN AXIAL ELEMENT

To illustrate the application of the basic equations presented in the previous chapter, the 2 x 2 element stiffness matrix will be developed for the truss element shown in Figure 4.1.
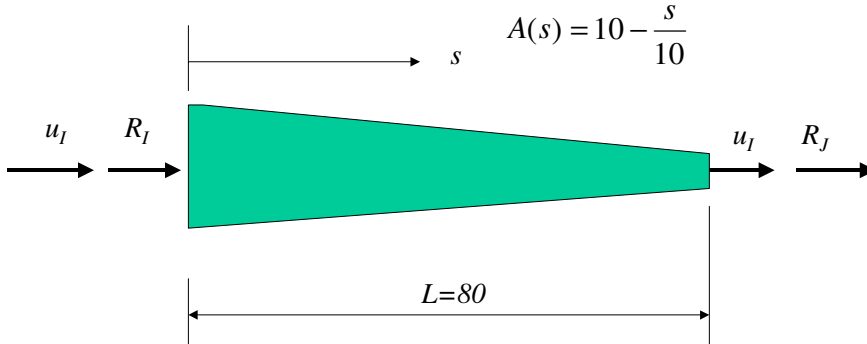
Figure 4.1 Tapered Bar Example

The axial displacements at position *s* can be expressed in terms of the axial displacements at points I and J at the ends of the element. Or:

$$u(s) = u_I + \frac{s}{L}(u_J - u_I) \tag{4.1}$$

The axial strain is by definition $\varepsilon_s = \dfrac{\partial u}{\partial s}$. Hence, the strain-displacement relationship will be:

$$\varepsilon = \frac{1}{L}(u_J - u_I) = \begin{bmatrix} -\dfrac{1}{L} & \dfrac{1}{L} \end{bmatrix} \begin{bmatrix} u_I \\ u_J \end{bmatrix} = \mathbf{B}\,\mathbf{u} \tag{4.2}$$

The stress-strain relationship is $\sigma = E\varepsilon$. Therefore, the element stiffness matrix is:

$$\mathbf{k}^{(i)} = \int \mathbf{B}^{(i)\mathbf{T}} \mathbf{E}^{(i)} \mathbf{B}^{(i)} \, dV = \frac{AE}{L} \begin{bmatrix} 1 & -1 \\ -1 & 1 \end{bmatrix} \tag{4.3}$$

Because the strain is constant, integration over the element produces the volume $A_a L$ where A_a is the average cross-sectional area of the element. If the cross-sectional area is constant, the stiffness matrix is exact and the force and displacement methods will produce identical results. However, if the area is not constant, significant errors may be introduced by the formal application of the displacement method.

To illustrate the errors involved in the application of the displacement method, let us assume the following properties:

$E=1,000$ ksi $\qquad A_a = 6.0\,\text{in}^2 \qquad L = 80\,\text{in.} \qquad u_I = 0 \qquad R_J = 10\,\text{kips}$

Hence, the displacement at point J is given by:

$$u_J = \frac{L}{A_a E} R_J = 0.1333\,\text{in.} \tag{4.4}$$

From equation (4.2), the corresponding constant strain is 0.0016666. Therefore, the constant axial stress is given by:

$$\sigma = E\varepsilon = 1.667\,\text{ksi} \tag{4.5}$$

However, if a force approach is used for the solution of this problem, significant and more accurate results are obtained. From simple statics, the axial stress distribution is:

$$\sigma = \frac{R_J}{A(s)} = \frac{10}{100-s} R_J = \mathbf{P}\,\mathbf{R} \tag{4.6}$$

From the force method, the displacement at the end of the member is given by:

$$u_J = \left[\int \mathbf{P}^\mathrm{T}\mathbf{C}\mathbf{P}\,dV\right]\mathbf{R} = \frac{1}{E}\int_0^{80} \frac{10}{100-s}\,ds\,\mathbf{R} = 0.1607\,\text{in.} \tag{4.7}$$

Note that the end displacement obtained by the displacement method is approximately 17 percent less than the exact displacement produced by the force method.

Of greater significance, however, is the comparison of the axial stress distribution summarized in Figure 4.2, using both the force and displacement methods of analysis.
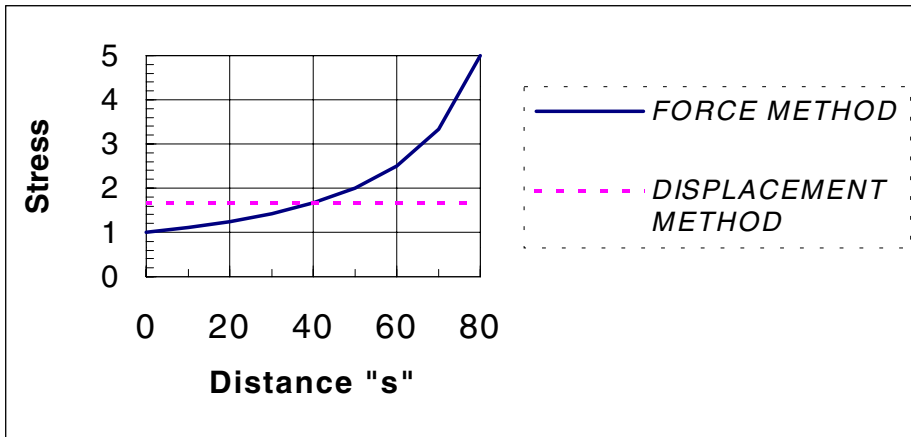
Figure 4.2 Comparison of Stresses for Force and Displacement Method

At the end of the tampered rod, the displacement method produces only 33 percent of the maximum stress of 5.0 ksi. Of course, if a fine mesh is used, the results will be closer. Also, if higher order elements are used, with interior points, the displacement method results can be improved significantly. Nevertheless, this example clearly illustrates that *the force approach should be used to predict the behavior of one-dimensional elements*.

4.3   TWO-DIMENSIONAL FRAME ELEMENT

A non-prismatic frame element with axial, bending and shearing deformations will be developed to illustrate the power of the force method. The displacement method has the ability to calculate a stiffness matrix of any element directly in terms of all displacement degrees-of-freedom associated with the elements; and the element automatically includes the rigid body displacement modes of the element. The force method only allows for the development of the element flexibility matrix in terms of displacements relative to a stable support system.

The general frame element is composed of any number of non-prismatic frame segments. Each segment can have independent axial, shear or bending properties. Therefore, at the ends of the element, rigid bending segments are possible, with or without shearing and axial deformations. Hence, it is possible to approximate the behavior of the finite connection area. A typical frame member is shown in Figure 4.3.
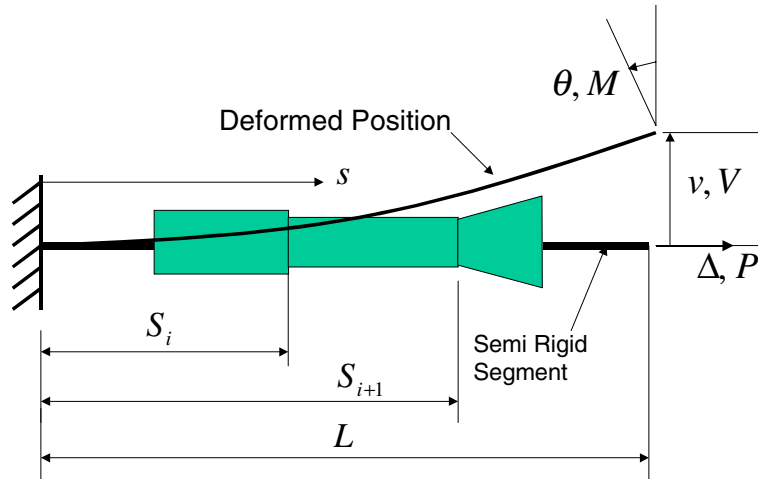
Figure 4.3 Arbitrary, Two-Dimensional Frame Element

The relative displacements are the axial displacement Δ, vertical displacement v, and the end rotation θ. The corresponding loads are the axial load P, vertical load V, and the end moment M. At a typical cross-section at location s, the force-deformation relationship is:

$$\mathbf{d}(s) = \mathbf{C}(s)\,\mathbf{f}(s)\,, \text{ or } \begin{bmatrix} \varepsilon(s) \\ \gamma(s) \\ \psi(s) \end{bmatrix} = \begin{bmatrix} \dfrac{1}{E(s)\,A(s)} & 0 & 0 \\ 0 & \dfrac{1}{G(s)\,A_S(s)} & 0 \\ 0 & 0 & \dfrac{1}{E(s)\,I(s)} \end{bmatrix} \begin{bmatrix} P(s) \\ V(s) \\ M(s) \end{bmatrix} \qquad (4.8)$$

All cross-sectional properties, including the effective shear area A_s, can vary within each segment of the frame element.

The section forces within a typical segment at location s can be expressed directly from statics in terms of the arbitrary end forces $\mathbf{R}$. Or:

$$\mathbf{f}(s) = \mathbf{P}(s)\mathbf{R}, \quad \text{or} \quad \begin{bmatrix} P(s) \\ V(s) \\ M(s) \end{bmatrix} = \begin{bmatrix} 1 & 0 & 0 \\ 0 & 1 & 0 \\ 0 & L-s & 1 \end{bmatrix} \begin{bmatrix} P \\ V \\ M \end{bmatrix} \tag{4.9}$$

The 3 x 3 flexibility matrix as defined by the force method is calculated from:

$$\mathbf{F} = \int_0^L \mathbf{P}(s)^{\mathrm{T}} \mathbf{C}(s)\mathbf{P}(\mathbf{s})\, ds = \sum_i^{I_{MAX}} \int_{S_i}^{S_{i+1}} \mathbf{P}(s)^{\mathrm{T}} \mathbf{C}(s)\mathbf{P}(\mathbf{s})\ ds \tag{4.10}$$

It is of interest to note that because of the discontinuity of the properties of the segments, each segment produces a separate 3 by 3 flexibility matrix. Therefore, Equation (4.10) can be written in the following form:

$$\mathbf{F} = \sum_i^{I_{MAX}} \mathbf{F^{(i)}}, \quad \text{where} \quad \mathbf{F}^{(i)} = \int_{S_i}^{S_{i+1}} \mathbf{P}(s)^{\mathrm{T}} \mathbf{C}(s)\mathbf{P}(\mathbf{s})\ ds \tag{4.11}$$

Equation (4.11) can be termed the ***direct flexibility method***, because the segment flexibility terms are directly added. It should be pointed out that if any cross-sectional stiffness properties are infinite, as defined in Equation (4.9), the contribution to the flexibility at the end of the element is zero.

The $\mathbf{C}$ and $\mathbf{P}$ matrices contain a significant number of zero terms. Therefore, the element flexibility matrix for a straight member contains only four independent terms, which are illustrated by:

$$\mathbf{F} = \begin{bmatrix} F_P & 0 & 0 \\ 0 & F_{VV} & F_{VM} \\ 0 & F_{VM} & F_{MM} \end{bmatrix}, \tag{4.12}$$

It can easily be shown that the individual flexibility terms are given by the following simple equations:

$$F_P = \sum_i^{I_{MAX}} \int_{S_i}^{S_{I+1}} \frac{1}{E(s)A(s)} ds \qquad (4.13a)$$

$$F_{VV} = \sum_i^{I_{MAX}} \int_{S_i}^{S_{I+1}} \left[\frac{(L-s)^2}{E(s)\,I(s)} + \frac{1}{G(s)A_s(s)} \right] ds \qquad (4.13b)$$

$$F_{VM} = \sum_i^{I_{MAX}} \int_{S_i}^{S_{I+1}} \frac{(L-s)}{E(s)\,I(s)} ds \qquad (4.13c)$$

$$F_{MM} = \sum_i^{I_{MAX}} \int_{S_i}^{S_{I+1}} \frac{1}{E(s)\,I(s)} ds \qquad (4.13d)$$

For frame segments with constant or linear variation of element properties, those equations can be evaluated in closed form. For the case of more complex segment properties, numerical integration may be required. For a prismatic element without rigid end offsets, those flexibility constants are well-known and reduce to:

$$F_P = \frac{L}{EA} \qquad (4.14a)$$

$$F_{VV} = \frac{L^3}{3EI} + \frac{L}{GA_s} \qquad (4.14b)$$

$$F_{VM} = \frac{L^2}{2EI} \qquad (4.14c)$$

$$F_{MM} = \frac{L}{EI} \qquad (4.14d)$$

For rectangular cross-sections, the shear area is $A_s = \frac{5}{6}A$.

One can easily consider loading within the segment by calculating the additional relative displacements at the end of the element using simple virtual work

methods. For this more general case, the total relative displacement will be of the following form:

$$\begin{bmatrix} \Delta \\ v \\ \theta \end{bmatrix} = \begin{bmatrix} F_P & 0 & 0 \\ 0 & F_{VV} & F_{VM} \\ 0 & F_{VM} & F_{MM} \end{bmatrix} \begin{bmatrix} P \\ V \\ M \end{bmatrix} + \begin{bmatrix} \Delta_L \\ v_L \\ \theta_L \end{bmatrix} \quad \text{or,} \quad \mathbf{v} = \mathbf{FR} + \mathbf{v_L} \qquad (4.15)$$

The displacements caused by span loading are designated by $\mathbf{v_L}$. Equation (4.15) can be rewritten in terms of the element stiffness as:

$$\mathbf{r} = \mathbf{Kv} \text{ - } \mathbf{Kv_L} = \mathbf{Kv} \text{ - } \mathbf{r_L} \qquad (4.16)$$

The element stiffness is the inverse of the element flexibility, $\mathbf{K} = \mathbf{F}^{-1}$, and the fixed-end forces caused by span loading are $\mathbf{r_L} = \mathbf{Kv_L}$. Within a computer program, those equations are evaluated numerically for each element; therefore, it is not necessary to develop the element stiffness in closed form.

4.4   THREE-DIMENSIONAL FRAME ELEMENT

The development of the three-dimensional frame element stiffness is a simple extension of the equations presented for the two-dimensional element. Bending and shearing deformations can be included in the normal direction using the same equations. In addition, it is apparent that the uncoupled torsional flexibility is given by:

$$F_T = \sum_{i}^{I_{MAX}} \int_{S_i}^{S_{I+1}} \frac{1}{G(s)J(s)} ds \qquad (4.17)$$

The torsional stiffness term, $G(s)J(s)$, can be difficult to calculate for many cross-sections. The use of a finite element mesh may be necessary for complex sections.

An arbitrary, three-dimensional frame element is shown in Figure 4.4. Note that only the six forces at the J end are shown. The six relative displacements at node J have the same positive sign convention as the forces at node J.
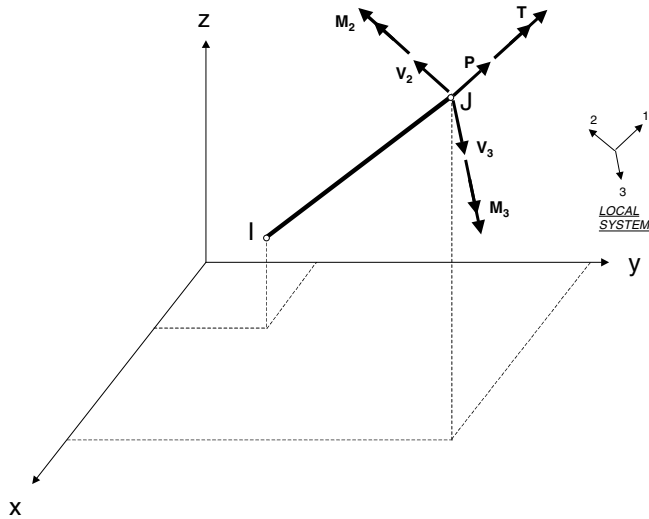
Figure 4.4 Member Forces in Local Reference Systems

The 6 by 6 stiffness matrix is formed in the local 1-2-3 coordinate system, as shown in Figure 4.4. The order of the forces and relative deformations are given by:

$$\begin{bmatrix} P \\ V_2 \\ V_3 \\ T \\ M_2 \\ M_3 \end{bmatrix} = \begin{bmatrix} k_{11} & 0 & 0 & 0 & 0 & 0 \\ 0 & \mathbf{k_{22}} & 0 & 0 & 0 & \mathbf{k_{26}} \\ 0 & 0 & k_{33} & 0 & k_{35} & 0 \\ 0 & 0 & 0 & k_{44} & 0 & 0 \\ 0 & 0 & k_{53} & 0 & k_{55} & 0 \\ 0 & \mathbf{k_{62}} & 0 & 0 & 0 & \mathbf{k_{66}} \end{bmatrix} \begin{bmatrix} \Delta \\ v_2 \\ v_3 \\ \phi_T \\ \theta_2 \\ \theta_3 \end{bmatrix} \quad \text{or,} \quad \mathbf{f_J} = \mathbf{k_J d_J} \qquad (4.18)$$

The bold terms indicate the shear and bending contributions in the 1-2 plane. For a curved member in three dimensions, the 6 by 6 **k** matrix may be full without the existence of any zero terms. Note that the 6 by 6 stiffness matrix formed in the local system does not have the six rigid body modes.

The forces acting at node **I** are not independent and can be expressed in terms of the forces acting at node **J** by the application of the basic equations of statics. Therefore:

$$
\begin{bmatrix} P \\ V_2 \\ V_3 \\ T \\ M_2 \\ M_3 \end{bmatrix}_I
=
\begin{bmatrix}
-1 & 0 & 0 & 0 & 0 & 0 \\
0 & -1 & 0 & 0 & 0 & \dfrac{1}{L} \\
0 & 0 & -1 & 0 & \dfrac{1}{L} & 0 \\
0 & 0 & 0 & -1 & 0 & 0 \\
0 & 0 & L & 0 & -1 & 0 \\
0 & L & 0 & 0 & 0 & -1
\end{bmatrix}
\begin{bmatrix} P \\ V_2 \\ V_3 \\ T \\ M_2 \\ M_3 \end{bmatrix}_J
\quad \text{or,} \quad \mathbf{f}_I = \mathbf{b}_{IJ}^T \mathbf{f}_J
\qquad (4.19)
$$

The twelve forces at both ends of the beam can now be expressed in terms of the six forces at the **J** end of the beam by the following submatrix equations:

$$
\begin{bmatrix} \mathbf{f}_I \\ \mathbf{f}_J \end{bmatrix}
=
\begin{bmatrix} \mathbf{b}_{IJ}^T \\ \mathbf{I} \end{bmatrix} \mathbf{f}_J
\quad \text{or,} \quad \mathbf{f}_{IJ} = \mathbf{b}^T \mathbf{f}_J
\qquad (4.20)
$$

Also, from the relationship between the equations of statics and compatibility, the following displacement transformation equation exists:

$$
\mathbf{d}_I = \mathbf{b}\,\mathbf{d}_{IJ}
\qquad (4.21)
$$

Therefore, the 12 by 12 frame element stiffness, $\mathbf{k}_{IJ}$, with respect to the local 1-2-3 reference system, is:

$$
\mathbf{k}_{IJ} = \mathbf{b}^T \mathbf{k}_J \mathbf{b}
\qquad (4.22)
$$

Hence, the force-displacement equations in the local 1-2-3 system can be written as:

$$
\mathbf{f}_{IJ} = \mathbf{k}_{IJ}\,\mathbf{u}_{IJ}
\qquad (4.23)
$$

To use the direct stiffness formulation, it is necessary to transform the local element stiffness into the global x-y-z reference system. The global 12 by 12 stiffness matrix must be formed with respect to the node forces shown in Figure 4.5. All twelve node forces **R** and twelve node displacements **u** have the same sign convention.
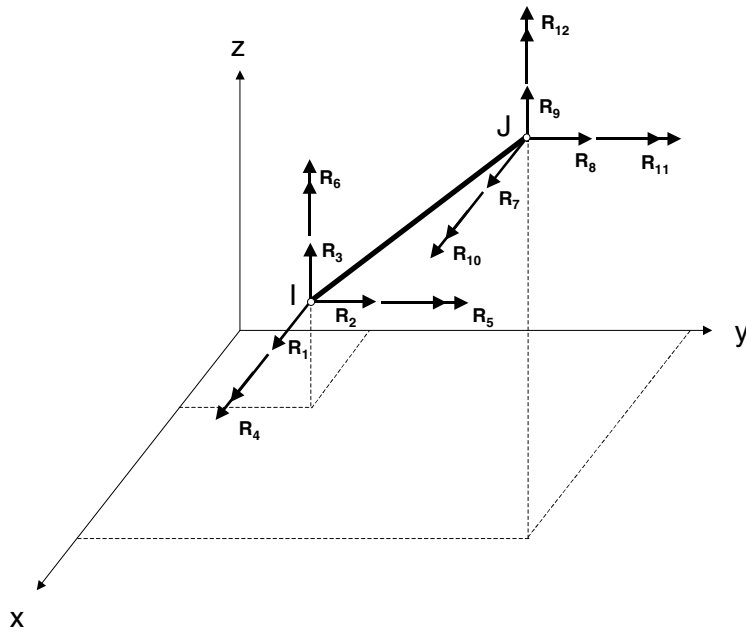
Figure 4.5 Frame Member Forces in Absolute Reference System

The local displacements and forces can be expressed using the elementary direction cosine matrix given in Appendix A. Or:

$$\begin{bmatrix} u_1 \\ u_2 \\ u_3 \end{bmatrix} = \mathbf{V} \begin{bmatrix} u_x \\ u_y \\ u_z \end{bmatrix} \quad \text{and} \quad \begin{bmatrix} f_x \\ f_y \\ f_x \end{bmatrix} = \mathbf{V}^{\mathsf{T}} \begin{bmatrix} f_1 \\ f_2 \\ f_2 \end{bmatrix} \tag{4.24}$$

Therefore, the final twelve transformation equations are in the following simple 4 by 4 submatrix form:

$$\mathbf{u}_{IJ} = \begin{bmatrix} \mathbf{V} & \mathbf{0} & \mathbf{0} & \mathbf{0} \\ \mathbf{0} & \mathbf{V} & \mathbf{0} & \mathbf{0} \\ \mathbf{0} & \mathbf{0} & \mathbf{V} & \mathbf{0} \\ \mathbf{0} & \mathbf{0} & \mathbf{0} & \mathbf{V} \end{bmatrix} \mathbf{u} \quad \text{or,} \quad \mathbf{u}_{IJ} = \mathbf{T}\mathbf{u} \tag{4.25}$$

The twelve global equilibrium equations in x-y-z reference system are now given by:

$$\mathbf{R} = \mathbf{Ku} + \mathbf{R}_\mathbf{L} \tag{4.26}$$

The frame element stiffness matrix is:

$$\mathbf{K} = \mathbf{T}^\mathbf{T}\mathbf{k}_\mathbf{IJ}\mathbf{T} \tag{4.27}$$

It can be shown that the six fixed-end forces $\mathbf{r}_\mathbf{J}$ caused by member loads, which are defined in the local 1-2-3 system, can be transformed to twelve global loads by:

$$\mathbf{R}_\mathbf{L} = \mathbf{T}^\mathbf{T}\mathbf{b}^\mathbf{T}\mathbf{r}_\mathbf{J} \tag{4.28}$$

It should be pointed out that within most efficient computer programs, formal matrix multiplication is not used to form the matrices. Programming methods are used to skip most multiplication by zero terms.

4.5   MEMBER END-RELEASES

Including member loading in Equation (4.23), the twelve equilibrium equations in the local IJ reference system can be written as

$$\mathbf{f}_\mathbf{IJ} = \mathbf{k}_\mathbf{IJ}\mathbf{u}_\mathbf{IJ} + \mathbf{r}_\mathbf{IJ} \quad \text{or, without subscripts} \quad \mathbf{f} = \mathbf{ku} + \mathbf{r} \tag{4.29}$$

If one end of the member has a hinge, or other type of release that causes the corresponding force to be equal to zero, Equation (4.29) requires modification. A typical equation is of the following form:

$$f_n = \sum_{j=1}^{12} k_{nj}u_j + r_n \tag{4.30}$$

If we know a specific value of f_n is zero because of a release, the corresponding displacement u_n can be written as:

$$u_n = \sum_{j=1}^{n-1} \frac{k_{nj}}{k_{nn}} u_j + \sum_{j=n+1}^{12} \frac{k_{nj}}{k_{nn}} u_j + r_n \tag{4.31}$$

Therefore, by substitution of equation (4.31) into the other eleven equilibrium equations, the unknown u_n can be eliminated and the corresponding row and column set to zero. Or:

$$\bar{\mathbf{f}}_{IJ} = \bar{\mathbf{k}}_{IJ} \mathbf{u}_{IJ} + \bar{\mathbf{r}}_{IJ} \tag{4.32}$$

The terms $f_n = r_n = 0$ and the new stiffness and load terms are equal to:

$$\begin{aligned} \bar{k}_{ij} &= k_{ij} - k_{in} \frac{k_{nj}}{k_{nn}} \\ \bar{r}_i &= r_i - r_n \frac{k_{ni}}{k_{nn}} \end{aligned} \tag{4.33}$$

This procedure can be repeatedly applied to the element equilibrium equations for all releases. After the other displacements associated with the element have been found from a solution of the global equilibrium equations, the displacements associated with the releases can be calculated from Equation (4.31) in reverse order from the order in which the displacements were eliminated. The repeated application of these simple numerical equations is defined in Appendix C as *static condensation* or *partial Gauss elimination*.

4.6   SUMMARY

The force method should be used to develop the stiffness matrices for one-dimensional elements where the internal section stress-resultants can be expressed, by satisfying equilibrium, in terms of the forces acting on the ends of the element. First, the flexibility matrix, with respect to a stable support system, is developed in the element local reference system. Second, this flexibility matrix is inverted to form the element stiffness matrix. Third, the local stiffness matrix is expanded to include the rigid-body displacements and is modified because of end releases. Finally, the stiffness and load matrices are transformed into the global reference system.

5.

ISOPARAMETRIC ELEMENTS

Bruce Irons, in 1968, Revolutionized the Finite Element Method by Introducing a Natural Coordinate Reference System

5.1   INTRODUCTION

Before development of the Finite Element Method, researchers in the field of structural engineering and structural mechanics found "closed form" solutions in terms of known mathematical functions of many problems in continuum mechanics. However, practical structures of arbitrary geometry, non-homogeneous materials or structures made of several different materials are difficult to solve by this classical approach.

Professor Ray Clough coined the terminology "Finite Element Method" in a paper presented in 1960 [1]. This paper proposed to use the method as an alternative to the finite difference method for the numerical solution of stress concentration problems in continuum mechanics. The major purpose of the earlier work at the Boeing Airplane Company published in 1956 [2] was to include the skin stiffness in the analysis of wing structures and was not intended to accurately calculate stresses in continuous structures. The first, fully automated, finite element computer program was developed during the period of 1961 - 1962 [3].

It is the author's opinion that the introduction of the isoparametric element formulation in 1968 by Bruce Irons [4] was the single most significant

contribution to the field of finite element analysis during the past 40 years. It allowed very accurate, higher-order elements of arbitrary shape to be developed and programmed with a minimum of effort. The addition of incompatible displacement modes to isoparametric elements in 1971 was an important, but minor, extension to the formulation [5].

5.2   A SIMPLE ONE-DIMENSIONAL EXAMPLE

To illustrate the fundamentals of the isoparametric approach, the one-dimensional, three-node element shown in Figure 5.1 is formulated in a natural coordinate reference system.
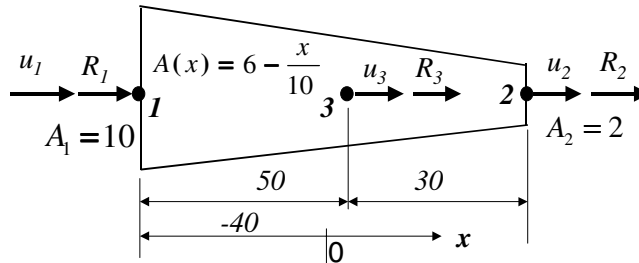
A. GLOBAL REFERENCE SYSTEM "x"
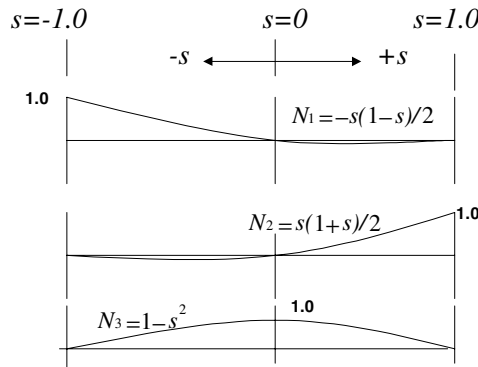
B. ISOPARAMETRIC REFERENCE SYSTEM "s"

Figure 5.1 A Simple Example of an Isoparametric Element

The shape functions N_i are written in terms of the element isoparametric reference system. The "natural" coordinate s has a range of $s = \pm 1.0$. The isoparametric and global reference systems are related by the following elementary equation:

$$x(s) \equiv N_1(s)\, x_1 + N_2(s)\, x_2 + N_3(s)\, x_3 = \mathbf{N}(s)\, \mathbf{x} \tag{5.1}$$

The validity of this equation can be verified at values of $s = -1$, $s = 0$ and $s = 1$. No additional mathematical references are required to understand Equation (5.1).

The global displacement can now be expressed in terms of the fundamental isoparametric shape functions. Or:

$$u(s) = N_1(s)\, u_1 + N_2(s)\, u_2 + N_3(s)\, u_3 = \mathbf{N}(s)\, \mathbf{u} \tag{5.2}$$

Note that the sum of the shape functions is equal to 1.0 for all values of s; therefore, rigid-body displacement of the element is possible. This is a fundamental requirement of all displacement approximations for all types of finite elements.

The strain-displacement equation for this one-dimensional element is:

$$\varepsilon_x = \frac{\partial u(s)}{\partial x} = \frac{du(s)}{dx} = \frac{du(s)}{ds}\frac{ds}{dx} \tag{5.3}$$

You may recall from sophomore calculus that this is a form of the *chain rule*. For any value of s the following equations can be written:

$$\frac{du(s)}{ds} = \mathbf{N(s)}_{,\mathbf{s}}\, \mathbf{u} \tag{5.4a}$$

$$\frac{dx}{ds} = \mathbf{N(s)}_{,\mathbf{s}}\, \mathbf{x} = J\,(s) \tag{5.4b}$$

Therefore:

$$\varepsilon_x = \frac{du(s)}{ds}\frac{ds}{dx} = \frac{1}{J(s)}\mathbf{N}(s)_{,\mathbf{s}}\, \mathbf{u} = \mathbf{B}(s)\, \mathbf{u} \tag{5.5}$$

From Equation (5.1), the derivatives with respect to the global and isoparametric reference systems are related by:

$$dx = \mathbf{N}(s),_s \, \mathbf{x} \, ds = J(s) \, ds \tag{5.6}$$

The 3 by 3 element stiffness can now be expressed in terms of the natural system:

$$\mathbf{K} = \int_{-1}^{+1} \mathbf{B}(s)^T \mathbf{E} \, \mathbf{B}(s) \, J(s) \, ds \tag{5.7}$$

In general, Equation (5.7) cannot be evaluated in closed form. However, it can be accurately evaluated by numerical integration.

5.3   ONE-DIMENSIONAL INTEGRATION FORMULAS

Most engineers have used Simpson's rule or the trapezoidal rule to integrate a function evaluated at equal intervals. However, those traditional methods are not as accurate, for the same computational effort, as the Gauss numerical integration method presented in Appendix G. The Gauss integration formulas are of the following form:

$$I = \int_{-1}^{+1} f(s) \, ds = \sum_{i=1}^{n} W_i \, f(s_i) \tag{5.8}$$

The Gauss points and weight factors for three different formulas are summarized in Table 5.1.

Table 5.1 Gauss Points and Weight Factors for Numerical Integration

n	s_1	W_1	s_2	W_2	s_3	W_3
1	0	2				
2	$-1/\sqrt{3}$	1	$1/\sqrt{3}$	1		
3	$-\sqrt{0.6}$	5/9	0	8/9	$\sqrt{0.6}$	5/9

Note that the sum of the weight factors is always equal to 2. Higher order numerical integration formulas are possible. However, for most displacement-based finite element analysis higher order integration is not required. In fact, for many elements, lower order integration produces more accurate results than higher order integration.

For the analysis of the tapered beam, shown in Figure 5.1, the same material properties, loading and boundary conditions are used as were used for the example presented in Section 4.2. The results are summarized in Table 5.2.

Table 5.2 Summary of Results of Tapered Rod Analyses

ELEMENT TYPE	Integration Order	u_3 (%error)	σ_1 (%error)	σ_2 (%error)	σ_3 (%error)
EXACT		0.1607	1.00	5.00	2.00
Constant Strain	Exact	0.1333 (-17.1 %)	1.67 (+67 %)	1.67 (-66 %)	1.67 (-16.5 %)
3-node isoparametric	2 point	0.1615 (+0.5 %)	0.58 (-42 %)	4.04 (-19 %)	2.31 (+15.5 %)
3-node isoparametric	3 point	0.1609 (+0.12 %)	0.83 (-17 %)	4.67 (-6.7 %)	2.76 (+34 %)

From this simple example, the following conclusions and remarks can be made:

1. Small errors in displacement do not indicate small errors in stresses.

2. Lower order integration produces a more flexible structure than the use of higher order numerical integration.

3. If this isoparametric element is integrated exactly, the tip displacement would be less than the exact displacement.

4. The stresses were calculated at the integration point and extrapolated to the nodes. Every computer program uses a different method to evaluate the stresses within an element. Those methods will be discussed later.

5.4   RESTRICTION ON LOCATIONS OF MID-SIDE NODES

The previous example illustrates that the location of the mid-side node need not be at the geometric center of the element. However, its location is not completely arbitrary.

Equation (5.4b) can be rewritten, with $x_1 = -\dfrac{L}{2}$, $x_2 = \dfrac{L}{2}$ and $x_3 = r\dfrac{L}{2}$, as

$$J(s) = (2 - sr)\frac{L}{2} \tag{5.9}$$

where r is the relative location of node 3, with respect to the center of the element. Equation (5.5) indicates that the strains can be infinite if $J(s)$ is zero. Also, if $J(s)$ is negative, it implies that the coordinate transformation between x and s is very distorted. For infinite strains at locations $s = \pm 1$, the zero singularity can be found from:

$$2 \pm r = 0 \text{, or } r = \pm\frac{1}{2} \tag{5.10}$$

Hence, the mid-side node location must be within the middle one-half of the element. In the case of two- and three-dimensional elements, ***mid-side nodes should be located within the middle one -half of each edge or side***.

At a crack tip, where the physical strains can be very large, it has been proposed that the elements adjacent to the crack have the mid-side node located at one-fourth the length of the element side. The stresses at the integration points will then be realistic; and element strain energy can be estimated, which may be used to predict crack propagation or stability [5].

5.5   TWO-DIMENSIONAL SHAPE FUNCTIONS

Two-dimensional shape functions can be written for different elements with an arbitrary number of nodes. The formulation presented here will be for a general four-sided element with four to nine nodes. Therefore, one formulation will cover all element types shown in Figure 5.2.
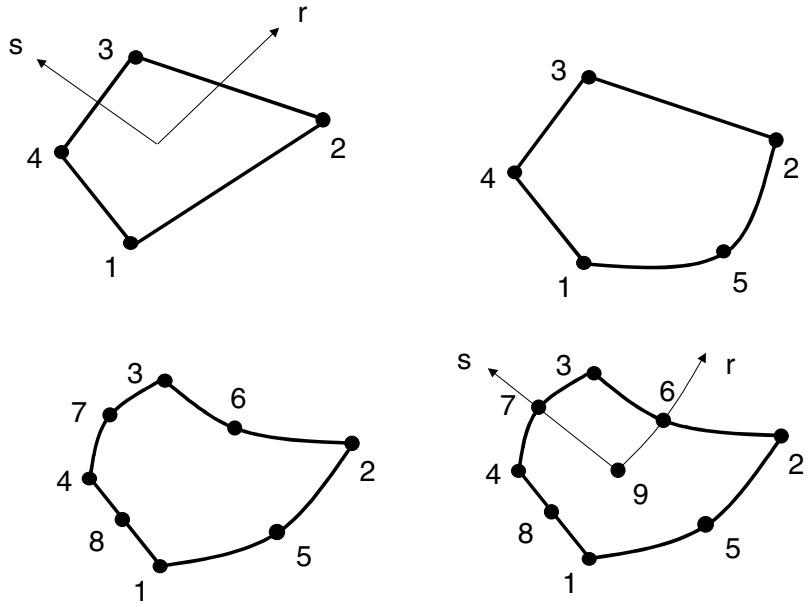
Figure 5.2 Four- to Nine-Node Two-Dimensional Isoparametric Elements

The shape functions, in the natural r-s system, are a product of the one-dimensional functions shown in Figure 5.1. The range of both r and s is ± 1. All functions must equal 1.0 at the node and equal zero at all other nodes associated with the element. The shape functions shown in Table 5.3 are for the basic four-node element. The table indicates how the functions are modified if nodes 5, 6, 7, 8 or 9 exist.

Table 5.3 Shape Functions for a Four- to Nine-Node 2D Element

NODE			SHAPE FUNCTION	OPTIONAL NODES				
i	r_i	s_i	$N_1(r,s)$	5	6	7	8	9
1	-1	-1	$N_1 = (1-r)(1-s)/4$	$-\dfrac{N_5}{2}$			$-\dfrac{N_8}{2}$	$-\dfrac{N_9}{4}$
2	1	-1	$N_2 = (1+r)(1-s)/4$	$-\dfrac{N_5}{2}$	$-\dfrac{N_6}{2}$			$-\dfrac{N_9}{4}$

Table 5.3 Shape Functions for a Four- to Nine-Node 2D Element

NODE i	r_i	s_i	SHAPE FUNCTION $N_1(r,s)$	OPTIONAL NODES 5	6	7	8	9
3	1	1	$N_3 = (1+r)(1+s)/4$		$-\dfrac{N_6}{2}$	$-\dfrac{N_7}{2}$		$-\dfrac{N_9}{4}$
4	-1	1	$N_4 = (1-r)(1+s)/4$			$-\dfrac{N_7}{2}$	$-\dfrac{N_8}{2}$	$-\dfrac{N_9}{4}$
5	0	-1	$N_5 = (1-r^2)(1-s)/2$					$-\dfrac{N_9}{2}$
6	1	0	$N_6 = (1+r)(1-s^2)/2$					$-\dfrac{N_9}{2}$
7	0	1	$N_7 = (1-r^2)(1+s)/2$					$-\dfrac{N_9}{2}$
8	-1	0	$N_8 = (1-r)(1-s^2)/2$					$-\dfrac{N_9}{2}$
9	0	0	$N_9 = (1-r^2)(1-s^2)$					

If any node from 5 to 9 does not exist, the functions associated with that node are zero and need not be calculated. Note the sum of all shape functions is always equal to 1.0 for all points within the element. Tables with the same format can be created for the derivatives of the shape functions $N_{i,r}$ and $N_{i,s}$. The shape functions and their derivatives are numerically evaluated at the integration points.

The relationship between the natural *r-s* and local orthogonal *x-y* systems are by definition:

$$x(r,s) = \sum N_i x_i \tag{5.11a}$$

$$y(r,s) = \sum N_i y_i \tag{5.11b}$$

Also, the local x and y displacements are assumed to be of the following form:

$$u_x(r,s) = \sum N_i u_{xi} \qquad\qquad (5.12a)$$

$$u_y(r,s) = \sum N_i u_{yi} \qquad\qquad (5.12b)$$

To calculate strains it is necessary to take the derivatives of the displacements with respect to x and y. Therefore, it is necessary to use the classical chain rule, which can be written as:

$$\frac{\partial u}{\partial r} = \frac{\partial u}{\partial x}\frac{\partial x}{\partial r} + \frac{\partial u}{\partial y}\frac{\partial y}{\partial r}$$
$$\text{or} \quad \begin{bmatrix} \dfrac{\partial u}{\partial r} \\ \dfrac{\partial u}{\partial s} \end{bmatrix} = \mathbf{J} \begin{bmatrix} \dfrac{\partial u}{\partial x} \\ \dfrac{\partial u}{\partial y} \end{bmatrix} \qquad (5.13)$$
$$\frac{\partial u}{\partial s} = \frac{\partial u}{\partial x}\frac{\partial x}{\partial s} + \frac{\partial u}{\partial y}\frac{\partial y}{\partial s}$$

The matrix $\mathbf{J}$ is known in mathematics as the **Jacobian matrix** and can be numerically evaluated from:

$$\mathbf{J} = \begin{bmatrix} \dfrac{\partial x}{\partial r} & \dfrac{\partial y}{\partial r} \\ \dfrac{\partial x}{\partial s} & \dfrac{\partial y}{\partial s} \end{bmatrix} = \begin{bmatrix} \sum N_{i,r}\, x_i & \sum N_{i,r}\, y_i \\ \sum N_{i,s}\, x_i & \sum N_{i,s}\, y_i \end{bmatrix} = \begin{bmatrix} J_{11} & J_{12} \\ J_{21} & J_{22} \end{bmatrix} \qquad (5.14)$$

At the integration points the $\mathbf{J}$ matrix can be numerically inverted. Or:

$$\mathbf{J}^{-1} = \frac{1}{J}\begin{bmatrix} J_{22} & -J_{21} \\ -J_{12} & J_{11} \end{bmatrix} \qquad (5.15)$$

The term J is the determinate of the Jacobian matrix and is:

$$J = J_{11} J_{22} - J_{12} J_{21} = \frac{\partial x}{\partial r}\frac{\partial y}{\partial s} - \frac{\partial x}{\partial s}\frac{\partial y}{\partial r} \qquad (5.16)$$

Figure 5.3 illustrates the physical significance of this term at any point r and s within the element. Simple geometry calculations will illustrate that J relates the area in the x-y system to the natural reference system. Or:

$$dA = dx\, dy = J\, dr\, ds \qquad\qquad (5.17)$$

Hence, all the basic finite element equations can be transformed into the natural reference system and standard numerical integration formulas can be used to evaluate the integrals.
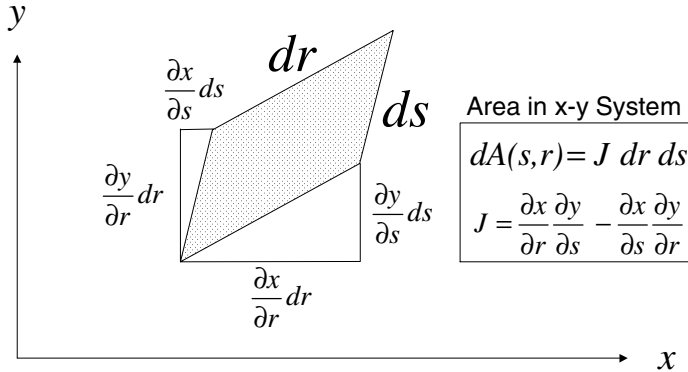
Figure 5.3 True Area in Natural Reference System

5.6 NUMERICAL INTEGRATION IN TWO DIMENSIONS

Numerical integration in two dimensions can be performed using the one-dimensional formulas summarized in Table 5.1. Or:

$$I = \int_{-1}^{1}\int_{-1}^{1} f(r,s)\,J(r,s)\,dr\,ds = \sum_{i}\sum_{j} W_i\, W_j\, f(r_i,s_j)\,J(r_i,s_j) \qquad (5.18)$$

Note that the sum of the weighting factors, $W_i W_j$, equals four, the natural area of the element. Most computer programs use 2 by 2 or 3 by 3 numerical integration formulas. The fundamental problem with this approach is that for certain elements, the 3 by 3 produces elements that are too stiff and the 2 by 2 produces stiffness matrices that are unstable, or, *rank deficient* using matrix analysis terminology. Using a 2 by 2 formula for a nine-node element produces three zero energy displacement modes in addition to the three zero energy rigid body modes. One of these zero energy modes is shown in Figure 5.4.

9 Node Element
2 by 2 Integration   Zero Energy Mode
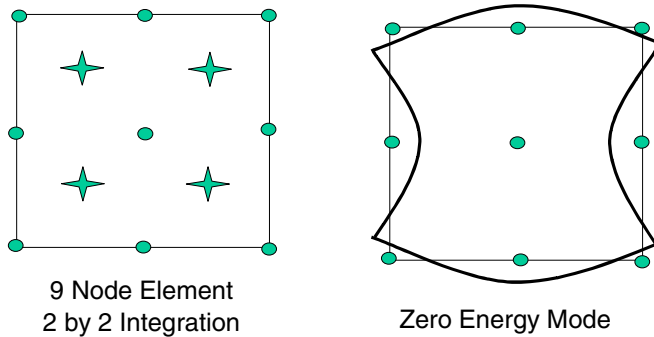
Figure 5.4 A Zero Energy Hourglass Displacement Mode

For certain finite element meshes, these zero energy modes may not exist after the element stiffness matrices have been added and boundary conditions applied. In many cases, however, inaccurate results may be produced if reduced integration is used for solid elements. Because of those potential problems, the author recommends the use of true two-dimensional numerical integration methods that are accurate and are always more numerically efficient. Therefore, Equation (5.18) can be written as

$$I = \int_{-1}^{1}\int_{-1}^{1} f(r,s)\, J(r,s)\, dr\, ds = \sum_i W_i\ f(r_i,s_i)\ J(r_i,s_i) \tag{5.19}$$

Eight- and five-point formulas exist and are summarized in Figure 5.5.

If $W_\alpha = 9/49$, the eight-point formula gives the same accuracy as the 3 by 3 Gauss product rule, with less numerical effort. On the other hand, if $W_\alpha = 1.0$ the eight-point formula reduces to the 2 by 2 Gauss product rule. If one wants to have the benefits of reduced integration, without the introduction of zero energy modes, it is possible to let $W_\alpha = 0.99$. Note that the sum of the weight factors equals four.

$$W_\alpha = ?$$
$$W_\beta = 1.0 - W_\alpha$$
$$\alpha = \sqrt{\frac{1.0}{3\sqrt{W_\alpha}}}$$
$$\beta = \sqrt{\frac{2 - 2\sqrt{W_\alpha}}{3 W_\beta}}$$

$$W_0 = ?$$
$$W_\alpha = 1.0 - W_0 / 4$$
$$\alpha = \sqrt{\frac{1.0}{3 W_\alpha}}$$
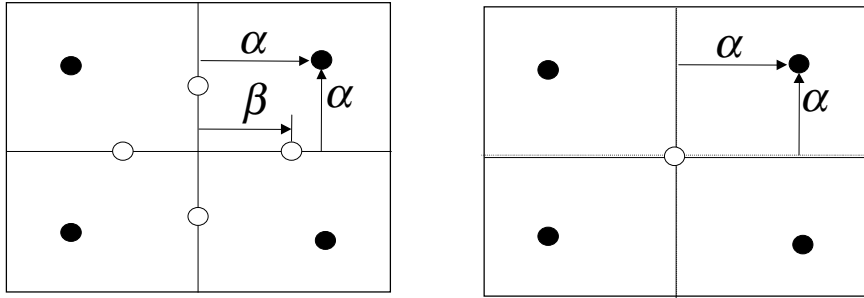
Figure 5.5 Eight- and Five-Point Integration Rules

The five point formula is very effective for certain types of elements. It has the advantage that the center point, which in my opinion is the most important location in the element, can be assigned a large weight factor. For example, if W_0 is set to 224/81, the other four integration points are located at $\alpha = \pm\sqrt{0.6}$, with weights of $W_i = 5/9$, which are the same corner points as the 3 by 3 Gauss rule. If W_0 is set to zero, the five-point formula reduces to the 2 by 2 Gauss rule.

5.7   THREE-DIMENSIONAL SHAPE FUNCTIONS

One can easily extend the two-dimensional approach, used to develop the 4- to 9-node element, to three dimensions and create an 8- to 27-node solid element, as shown in Figure 5.6.
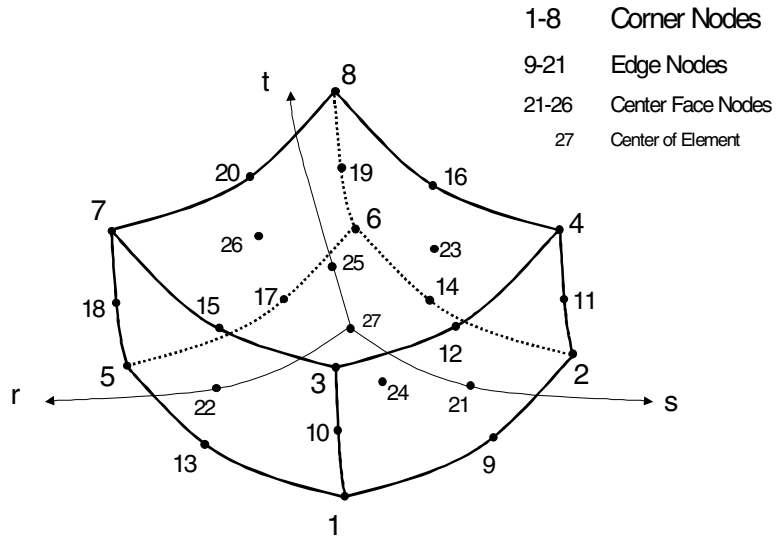
Figure 5.6 Eight- to 27-Node Solid Element

Three-dimensional shape functions are products of the three basic one-dimensional functions and can be written in the following form:

$$G(r_i, s_i, t_i) = g(r, r_i) g(s, s_i) g(t, t_i) \tag{5.20}$$

The terms r_i, s_i and t_i are the natural coordinates of node "*i*." The one-dimensional functions in the *r*, *s* and *t* direction are defined as:

$$g_i = g(r, r_i) = \frac{1}{2}(1 + r_i r) \text{ if } r_i = \pm 1$$

$$g_i = g(r, r_i) = (1 + r^2) \quad \text{if } r_i = 0 \tag{5.21}$$

$$g_i = 0 \qquad \text{if node } i \text{ does not exist}$$

Using this notation, it is possible to program a shape function subroutine directly without any additional algebraic manipulations. The fundamental requirement of a shape function is that it has a value of 1.0 at the node and is zero at all other nodes. The node shape function is the basic node shape function g_i corrected to be zero at all nodes by a fraction of the basic shape functions at adjacent nodes.

The shape functions N_1 and N_8 for the 8-corner nodes are:

$$N_i = g_i - g_E / 2 - g_F / 4 - g_{27} / 8 \qquad\qquad (5.22a)$$

The shape functions N_9 and N_{20} for the 12-edge nodes are:

$$N_i = g_i - g_F / 2 - g_{27} / 4 \qquad\qquad (5.22b)$$

The shape functions N_{21} and N_{26} for the 6 center nodes of each face are:

$$N_i = g_i - g_{27} / 2 \qquad\qquad (5.22c)$$

The shape function for the node at the center of the element is:

$$N_{27} = g_{27} \qquad\qquad (5.22d)$$

The term g_E is the sum of the g values at the three adjacent edges. The term g_F is the sum of the g values at the center of the three adjacent faces.

The 27-node solid element is not used extensively in the structural engineering profession. The major reason for its lack of practical value is that almost the same accuracy can be obtained with the 8-node solid element, with the addition of corrected incompatible displacement modes, as presented in the next chapter. The numerical integration can be 3 by 3 by 3 or 2 by 2 by 2 as previously discussed. A nine-point, third-order, numerical integration formula can be used for the eight-node solid element with incompatible modes and, is given by:

$$W_0 = ?, \quad W_\alpha = 1 - W_0 / 8 \text{ and } \alpha = \sqrt{\frac{1}{3W_\alpha}} \qquad\qquad (5.23)$$

The eight integration points are located at $r = \pm\alpha$, $s = \pm\alpha$ and $t = \pm\alpha$ and the center point is located at the center of the element. If $W_0 = 0$ the formula reduces to the 2 by 2 by 2. If $W_0 = 16/3$ the other eight integration points are located at eight nodes of the element, $\alpha = \pm 1$ and $W_\alpha = 1/3$.

5.8   TRIANGULAR AND TETRAHEDRAL ELEMENTS

The constant strain plane triangular element and the constant strain solid tetrahedral element should never be used to model structures. They are

numerically inefficient, compared to the computational requirements of higher order elements, and do not produce accurate displacements and stresses. However, the six-node plane triangular element and the ten-node solid tetrahedral element, shown in Figure 5.7, are accurate and numerically efficient. The reason for their success is that their shape functions are complete second order polynomials.
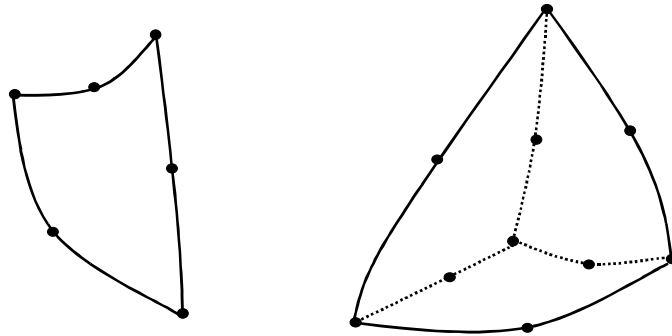
A. SIX-NODE TRIANGLE   B. TEN-NODE TETRAHEDRAL

Figure 5.7 Six-Node Plane Triangle and Ten-Node Solid Tetrahedral Elements

They are used extensively for computer programs with special mesh generation or automatic adaptive mesh refinement. They are best formulated in area and volume coordinate systems. For the details and basic formulation of these elements see Cook [5].

5.9   SUMMARY

The use of isoparametric, or natural, reference systems allows the development of curved, higher-order elements. Numerical integration must be used to evaluate element matrices because closed form solutions are not possible for non-rectangular shapes. Elements must have the appropriate number of rigid-body displacement modes. Additional zero energy modes may cause instabilities and oscillations in the displacements and stresses. Constant strain triangular and tetrahedral elements should not be used because of their inability to capture stress gradients. The six-node triangle and ten-node tetrahedral elements produce excellent results.

5.10 REFERENCES

1. Clough, R. W. 1960. "The Finite Element Method in Plane Stress Analysis," *Proc. ASCE Conf. On Electronic Computations.* Pittsburg, PA. September.

2. Turner, M. J., R. W. Clough, H. C. Martin and L. J. Topp. 1956. "Stiffness and Deflection Analysis of Complex Structures," *J. Aeronaut. Sc*. V.23, N. 6. pp. 805-823. Sept. 1.

3. Wilson, E.L. 1963 "Finite Element Analysis of Two-Dimensional Structures," D. Eng. Thesis. University of California at Berkeley.

4. Irons, B. M. and O. C. Zienkiewicz. 1968. "The Isoparametric Finite Element System – A New Concept in Finite Element Analysis," *Proc. Conf. Recent Advances in Stress Analysis.* Royal Aeronautical Society. London.

5. Wilson, E. L., R. L. Taylor, W. Doherty, and J. Ghaboussi. 1971. "Incompatible Displacement Models," *Proceedings, ONR Symposium on Numerical and Computer Methods in Structural Mechanics.* University of Illinois, Urbana. September.

6. Cook, R. D., D. S. Malkus and M. E. Plesha. 1989. *Concepts and Applications of Finite Element Analysis.* Third Edition. John Wiley & Sons, Inc. ISBN 0-471-84788-7.

6.

INCOMPATIBLE ELEMENTS

When Incompatible Elements Were Introduced in 1971,
Mathematics Professor Strang of MIT Stated
"In Berkeley, Two Wrongs Make a Right"

6.1   INTRODUCTION

In the early years of the development of the Finite Element Method, researchers in the fields of Mathematics, Structural Engineering and Structural Mechanics considered that displacement compatibility between finite elements was absolutely mandatory. Therefore, when the author first introduced incompatible displacements into rectangular isoparametric finite elements at a conference in 1971 [1], the method was received with great skepticism by fellow researchers. The results for both displacements and stresses for rectangular elements were very close to the results from the nine-node isoparametric element. The two ***theoretical crimes*** committed were ***displacement compatibility was violated*** and ***the method was not verified with examples using non-rectangular elements*** [2]. As a consequence of these crimes, Bruce Irons introduced the patch test restriction and the displacement compatible requirement was eliminated [3].

In 1976 a method was presented by Taylor to correct the incompatible displacement mode; he proposed using a constant Jacobian during the integration of the incompatible modes so that the incompatibility elements passed the patch test [4]. However, the results produced by the non-rectangular isoparametric element were not impressive.

In 1986 Simo and Rafai introduced the B bar method to correct the strains produced by incompatible displacements, achieving excellent results for non-rectangular elements [5]. Since that time the use of incompatible lower-order elements has reduced the need for reduced integration and the use of very high-order isoparametric elements. Many of these new elements, based on corrected incompatible displacement modes, are summarized in this book.

6.2   ELEMENTS WITH SHEAR LOCKING

The simple four-node isoparametric element does not produce accurate results for many applications. To illustrate this deficiency, consider the rectangular element, shown in Figure 6.1, subjected to pure bending loading.
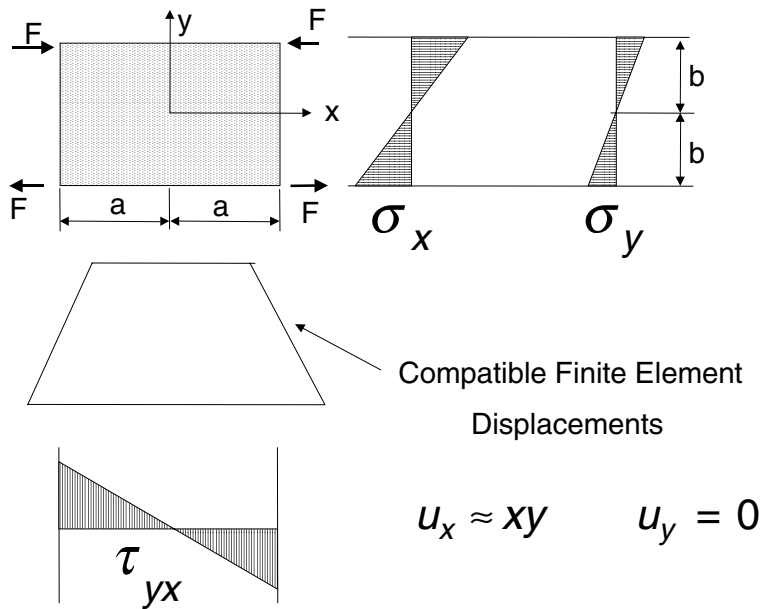
Figure 6.1 Basic Equilibrium Errors in Four-Node Plane Element

It is apparent that the compatible four-point rectangular element produces significant errors in both displacements and stresses when subjected to simple stress gradients. Shear-locking is the term used to describe the development of shear stresses when the element is subjected to pure bending. In addition to the shear stress problem, an error in the vertical stress is developed because of the Poisson's ratio effect. The exact displacements, which allow the element to satisfy internal equilibrium, are of the form:

$$u_x = c_1 xy \quad \text{and} \quad u_y = c_2 \left(1 - \left(\frac{x}{a}\right)^2\right) + c_3 \left(1 - \left(\frac{y}{b}\right)^2\right) \tag{6.1}$$

These displacements allow the shear strain to be zero at all points within the element. Also, the neutral axis must move vertically, thereby reducing the vertical stresses to zero.

6.3 ADDITION OF INCOMPATIBLE MODES

The motivation for the addition of incompatible displacement modes, of magnitude α_j, is to cancel the stresses associated with the error terms defined in Equation (6.1). Or, in terms of the r-s natural reference system, the new displacement shape functions for the four-node isoparametric element are:

$$u_x = \sum_{i=1}^{4} N_i u_{xi} + \alpha_1 (1 - r^2) + \alpha_2 (1 - s^2)$$

$$u_y = \sum_{i=1}^{4} N_i u_{xy} + \alpha_3 (1 - r^2) + \alpha_4 (1 - s^2) \tag{6.2}$$

Hence, the strain-displacement equation for an incompatible element can be written as:

$$\mathbf{d} = \begin{bmatrix} \mathbf{B_C} & \mathbf{B_I} \end{bmatrix} \begin{bmatrix} \mathbf{u} \\ \boldsymbol{\alpha} \end{bmatrix} \tag{6.3}$$

If we let $\mathbf{d}^\mathrm{T} = \begin{bmatrix} \varepsilon_x & \varepsilon_y & \gamma_{xy} \end{bmatrix}$ and $\mathbf{f}^\mathrm{T} = \begin{bmatrix} \sigma_x & \sigma_y & \tau_{xy} \end{bmatrix}$, the strain energy within the incompatible element is given as:

$$W = \frac{1}{2} \int \mathbf{f}^T \mathbf{d} \, dV = \frac{1}{2} \int \mathbf{f}^T \mathbf{B}_C \mathbf{u} \, dV + \frac{1}{2} \int \mathbf{f}^T \mathbf{B}_I \, \boldsymbol{\alpha} \, dV \qquad (6.4)$$

To pass the patch test, the strain energy associated with the incompatible modes must be zero for a state of constant element stress. Hence, for a state of constant stress, the following equation must be satisfied:

$$\frac{1}{2} \mathbf{f}^T \int \mathbf{B}_I \, \boldsymbol{\alpha} \, dV = 0 \quad \text{or} \quad \int \mathbf{B}_I \, dV = 0 \qquad (6.5)$$

This can be satisfied if we add a constant *correction matrix* $\mathbf{B}_{IC}$ to the $\mathbf{B}_I$ matrix and to form a new strain-displacement, $\overline{\mathbf{B}}_I = \mathbf{B}_I + \mathbf{B}_{IC}$, so that the following equation is satisfied:

$$\int (\mathbf{B}_I + \mathbf{B}_{IC}) \, dV = 0 \quad \text{or,} \quad \int \mathbf{B}_I \, dV + V \, \mathbf{B}_{IC} = 0 \qquad (6.6)$$

The volume of the element is V. Hence, the correction matrix can be calculated from:

$$\mathbf{B}_{IC} = -\frac{1}{V} \int \mathbf{B}_I \, dV \qquad (6.7)$$

This is a very general approach and can be used to add any number of incompatible displacement modes, or strain patterns, to all types of isoparametric elements. The same numerical integration formula should be used to evaluate Equation (6.7) as is used in calculating the element stiffness matrix.

6.4   FORMATION OF ELEMENT STIFFNESS MATRIX

In the minimization of the potential energy the forces associated with the incompatible displacement modes $\boldsymbol{\alpha}$ are zero. Therefore, the element equilibrium equations are given by:

$$\begin{bmatrix} \mathbf{f}_c \\ \mathbf{0} \end{bmatrix} = \begin{bmatrix} \mathbf{k}_{CC} & \mathbf{k}_{CI} \\ \mathbf{k}_{IC} & \mathbf{k}_{II} \end{bmatrix} \begin{bmatrix} \mathbf{u} \\ \boldsymbol{\alpha} \end{bmatrix} \qquad (6.8)$$

The individual sub-matrices within the element stiffness matrix are given by:

$$\mathbf{k_{CC}} = \int \mathbf{B_C^T} \mathbf{E} \mathbf{B}_C \, dV \qquad (6.9a)$$

$$\mathbf{k_{CI}} = \int \mathbf{B_C^T} \mathbf{E} \overline{\mathbf{B}}_I \, dV \qquad (6.9b)$$

$$\mathbf{k_{IC}} = \int \overline{\mathbf{B}}_I^T \mathbf{E} \mathbf{B}_C \, dV \qquad (6.9c)$$

$$\mathbf{k_{II}} = \int \overline{\mathbf{B}}_I^T \mathbf{E} \overline{\mathbf{B}}_I \, dV \qquad (6.9d)$$

Using *static condensation* [6] the incompatible displacement modes are eliminated before assembly of the element stiffness matrices. Or:

$$\mathbf{f_C} = \mathbf{k_C} \mathbf{u} \qquad (6.10)$$

Therefore, the element stiffness matrix is given by:

$$\mathbf{k_C} = \mathbf{k_{CC}} - \mathbf{k_{CI}} \, \mathbf{k_{II}^{-1}} \, \mathbf{k_{IC}} \qquad (6.11)$$

Symbolically, Equation (6.11) is correct; however, it should be pointed out that matrix inversion and matrix multiplication are not used in the static condensation algorithm as presented in Section 4.5 for the modification of frame element stiffness because of moment end releases.

6.5   INCOMPATIBLE TWO-DIMENSIONAL ELEMENTS

The addition of the incompatible shape functions, $(1-s^2)$ and $(1-r^2)$, to u_x and u_y displacement approximations is very effective for plane rectangular elements. Therefore, for quadrilaterals of arbitrary shape, the following displacement approximation has been found to be effective:

$$
\begin{aligned}
u_x &= \sum_{i=1}^{4} N_i u_{xi} + \sum_{i=5}^{6} N_i \alpha_{xi} \\
u_y &= \sum_{i=1}^{4} N_i u_{xy} + \sum_{i=5}^{6} N_i \alpha_{yi}
\end{aligned}
\qquad (6.12)
$$

The incompatible shape functions are:

$$N_5 = 1 - r^2$$
$$N_6 = 1 - s^2$$

(6.13)

The four incompatible modes increase computational time required to form the element stiffness matrix; however, the improvement in accuracy is worth the additional calculations.

6.6   EXAMPLE USING INCOMPATIBLE DISPLACEMENTS

To illustrate the accuracy of both compatible and incompatible elements in two dimensions, the cantilever beam shown in Figure 6.2 is analyzed assuming a moment and concentrated forces acting at the end of the cantilever.
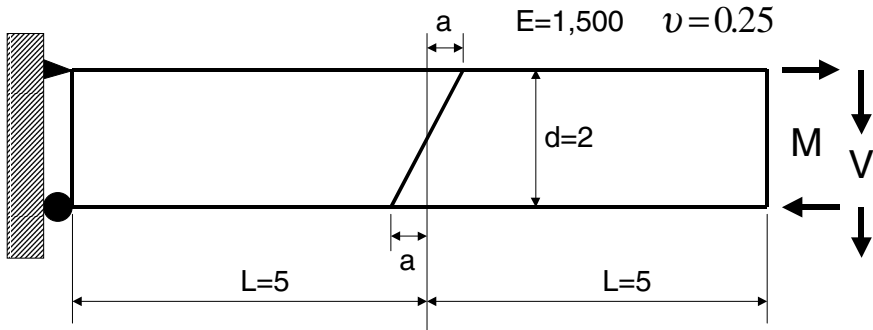
Figure 6.2 Beam Modeled with Distorted Mesh

An element shape sensitivity study can be accomplished using different distortion factors. Table 6.1 presents a summary of the results.

Table 6.1 Results of Analysis of Cantilever Beam

Mesh Distortion Factor "a"	Number of Incompatible Modes	TIP MOMENT LOADING		TIP SHEAR LOADING	
		Normalized Tip Displacement	Normalized Maximum Stress At Support	Normalized Tip Displacement	Normalized Maximum Stress At Support
EXACT	-	1.000	1.000	1.000	1.000
0	0	0.280	0.299	0.280	0.149

Table 6.1 Results of Analysis of Cantilever Beam

Mesh Distortion Factor "a"	Number of Incompatible Modes	TIP MOMENT LOADING		TIP SHEAR LOADING	
		Normalized Tip Displacement	Normalized Maximum Stress At Support	Normalized Tip Displacement	Normalized Maximum Stress At Support
0	4	1.000	1.000	0.932	0.750
1	4	0.658	0.638	0.706	0.600
2	4	0.608	0.657	0.688	0.614

It is apparent that the classical four-node, rectangular, compatible isoparametric element, without incompatible modes, produces very poor results. The use of this *classical element* can produce significant errors that may have serious practical engineering consequences. One notes that the stresses may be less than 20 percent of the correct value.

The addition of four parabolic shape functions produces the exact values of displacements and stresses for rectangular elements resulting from constant moment loading. However, because of tip shear loading, the maximum stress has a 25 percent error. In addition, as the element is distorted, the accuracy of both displacements and stresses is reduced by 30 to 40 percent.

It should be noted that all elements pass the patch test and will converge to the exact solution, as the mesh is refined. It appears that the plane quadrilateral elements, with eight incompatible displacement modes, will converge faster than the lower-order elements.

6.7   THREE-DIMENSIONAL INCOMPATIBLE ELEMENTS

The classical eight-node, hexahedral displacement compatible element has the same shear-locking problem as the classical, four-node plane element. The addition of nine incompatible shape functions has proven effective for three dimensional, eight-node, hexahedral elements. Or:

$$u_x = \sum_{i=1}^{8} N_i u_{xi} + \sum_{9}^{11} N_i a_{xi}$$

$$u_y = \sum_{i=1}^{8} N_i u_{yi} + \sum_{9}^{11} N_i a_{yi} \qquad (6.14)$$

$$u_z = \sum_{i=1}^{8} N_i u_{xi} + \sum_{9}^{11} N_i a_{yi}$$

The three additional incompatible shape functions are:

$$N_9 = 1 - r^2$$
$$N_{10} = 1 - s^2 \qquad (6.15)$$
$$N_{11} = 1 - t^2$$

The 2 by 2 by 2 integration formula previously presented for three-dimensional isoparametric elements has been found to be effective for the eight-node hexahedral element with nine additional incompatible modes.

6.8   SUMMARY

Because of the serious problem associated with shear-locking, the classical compatible four-node quadrilateral and eight-node hexahedral elements should not be used to simulate the behavior of real structures. It has been demonstrated that the addition of incompatible displacement modes, corrected to pass the patch test, significantly enhances the performance of quadrilateral and hexahedral isoparametric elements.

The nine-node quadrilateral and the 27-node hexahedral elements are accurate and can be improved by adding corrected incompatible modes. For example, cubic modes can be added to the nine-node plane element in which the exact results can be calculated, for tip shear loading, using only one element to model a cantilever beam [7].

6.9   REFERENCES

1.   Wilson, E. L., R. L. Taylor, W. P. Doherty and J. Ghaboussi. 1973. "Incompatible Displacement Models," Proceedings, *ONR Symposium on Numerical and Computer Method in Structural Mechanics*. University of Illinois, Urbana. September. 1971. Also published in *Numerical and Computational Mechanics* (ed. S. T. Fenves). Academic Press.

2.   Strang, G. 1972. "Variational Crimes in the Finite Element Method," in *The Mathematical Foundations of the Finite Element Method*. pp.689-710 (ed. A. K. Aziz). Academic Press.

3.   Irons, B. M., and A. Razzaque. 1972. "Experience with the Patch Test," in *The Mathematical Foundations of the Finite Element Method.* pp. 557-87 (ed. A. K. Aziz). Academic Press.

4.   Taylor, R. L., P. J. Beresford and E. L. Wilson. 1976. "A Non-Conforming Element for Stress Analysis," *Int. J. Num. Meth. Eng*. pp. 1211-20.

5.   Simo, J. C., and M. S. Rafai. 1990. "A Class of Assumed Strain Method and Incompatible Modes,*" J. Numerical Methods in Engineering*. Vol. 29. pp. 1595-1638.

6.   Wilson, E. L. 1974. "The Static Condensation Algorithm,*" Int. J. Num. Meth. Eng.* Vol. 8. pp. 199-203.

7.   Wilson, E. L. and A. Ibrahimbegovic. 1990. "Use of Incompatible Displacement Modes for the Calculation of Element Stiffnesses and Stresses," *Finite Elements in Analysis and Design.* Vol. 7. pp. 229-241.

<div align="right">

7.

</div>

BOUNDARY CONDITIONS AND
GENERAL CONSTRAINTS

The Specification of Known Joint Displacements
Reduces the Number of Equations to be Solved

7.1 INTRODUCTION

The fundamentals of structural analysis and mechanics as applied to the linear
static analysis have been summarized in the first several chapters of this book.
However, additional computational and modeling techniques used to solve
special problems remain to be presented.

It has been established that the displacement method, where the joint
displacements and rotations are the unknowns, generates a system of joint
equilibrium equations. Both statically determinate and statically indeterminate
structures are solved by the displacement method. The global stiffness matrix is
the sum of element stiffness matrices and can be formed with respect to all
possible joint displacement degrees of freedom. The minimum number of
supports required for a stable system is that which will prevent rigid body
movement of the structure.

There are several reasons that the general displacement method is not used for
non-computer calculations. For most problems, the solution of a large number of
equations is required. Also, to avoid numerical problems, a large number of

significant figures is required if both bending and axial deformations are included in the analysis of frame structures. One notes that the two traditional displacement analysis methods, moment distribution and slope-deflection, involve only moments and rotations. When those traditional displacement methods are extended to more general frame-type structures, it is necessary to set the axial deformations to zero; which, in modern terminology, is the application of a displacement constraint.

It has been shown that for the development of finite element stiffness matrices it is necessary to introduce approximate displacement shape functions. Based on the same shape functions, it is possible to develop constraints between different coarse and fine finite element meshes in two and three dimensions.

7.2   DISPLACEMENT BOUNDARY CONDITIONS

One of the significant advantages of the displacement method is the ease in specifying displacement boundary conditions. Consider the following set of N equilibrium equations formed including the displacements associated with the supports:

$$\mathbf{Ku} = \mathbf{R} \quad \text{Or, in subscript notation} \sum_{j=1}^{N} K_{ij} u_j = R_i \quad i = 1,...N \qquad (7.1)$$

If a particular displacement u_n is known and is specified, the corresponding load, or reaction R_n, is unknown. Hence, the N-1 equilibrium equations are written as:

$$\sum_{j=1}^{n-1} K_{ij} u_j = R_i - K_{in} u_n \quad i = 1,...n-1$$
$$\sum_{j=n+1}^{N} K_{ij} u_j = R_i - K_{in} u_n \quad i = n+1,...N \qquad \text{or,} \quad \overline{\mathbf{K}}\overline{\mathbf{u}} = \overline{\mathbf{R}} \qquad (7.2)$$

This simple modification to the stiffness and load matrices is applied to each specified displacement and the *nth* row and column are discarded. For a fixed support, where the displacement is zero, the load vectors are not modified. Those modifications, resulting from applied displacements, can be applied at the

element level, before formation of the global stiffness matrix. After all displacements have been calculated, the load associated with the specified displacements can be calculated from the discarded equilibrium equation. This same basic approach can be used where the displacements are specified as a function of time.

It should be apparent that *it is not possible to specify both* u_n *and* R_n at the same degree of freedom. One can design a structure so that a specified displacement will result from a specified load; therefore, *this is a structural design problem* and not a problem in structural analysis.

7.3   NUMERICAL PROBLEMS IN STRUCTURAL ANALYSIS

Many engineers use large values for element properties when modeling rigid parts of structures. This can cause large errors in the results for static and dynamic analysis problems. In the case of nonlinear analysis the practice of using unrealistically large numbers can cause slow convergence and result in long computer execution times. Therefore, the purpose of this section is to explain the physical reasons for those problems and to present some guidelines for the selection of properties for stiff elements.

Elements with infinite stiffness and rigid supports do not exist in real structures. We can only say that an element, or a support, is stiff relative to other parts of the structure. In many cases, the relative stiffness of what we call a rigid element is 10 to 1,000 times the stiffness of the adjacent flexible elements. The use of these realistic values will not normally cause numerical problems in the analysis of the computer model of a structure. However, if a relative value of 10^{20} is used, a solution may not be possible, because of what is known as *truncation errors*.

To illustrate truncation errors, consider the simple three-element model shown in Figure 7.1.
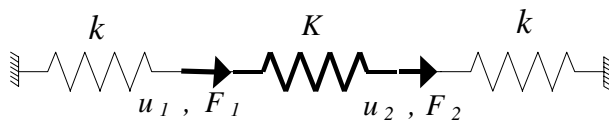
Figure 7.1 Example to Illustrate Numerical Problems

The equilibrium equations for this simple structure, written in matrix form, are the following:

$$\begin{bmatrix} K+k & -K \\ -K & K+k \end{bmatrix} \begin{bmatrix} u_1 \\ u_2 \end{bmatrix} = \begin{bmatrix} F_1 \\ F_2 \end{bmatrix} \tag{7.3}$$

Most structural analysis programs are written in double precision, and the stiffness terms have approximately 15 significant figures and can be in the range of 10^{-308} to 10^{+308}. Therefore, if the stiff element has a stiffness of $K=10^{20}\,k$, the term $K+k$ is truncated to K and the equilibrium equations are singular and cannot be solved. If $K=10^{12}\,k$, approximately 12 significant figures are lost and the solution is accurate to approximately three significant figures. The equation solvers used in the well-written structural analysis programs can sometimes detect this type of error and warn the user. However, for large systems, this type of error can be cumulative and is not always detected by the computer program.

This problem can be avoided by using realistic stiffness values, or by using constraints in the place of very stiff elements. This is one reason the rigid floor diaphragm constraint is often used in the solution of multistory buildings, because the in-plane stiffness of the floor system is often several orders-of-magnitude greater than the bending stiffness of the columns that connect the stiff floor slabs.

In nonlinear dynamic analysis, iteration is often used to satisfy equilibrium at the end of each time step. If elements have a large stiffness change during the time step, the solution can oscillate about the converged solution for alternate iterations. To avoid this convergence problem, it is necessary to select realistic stiffness values; or displacement constraints can be activated and deactivated during the incremental solution.

7.4   GENERAL THEORY ASSOCIATED WITH CONSTRAINTS

Structural engineers have used displacement constraints in structural analysis for over a century. For example, the two dimensional portal frame shown in Figure 7.2 has six *displacement* degrees of freedom (DOF). Therefore, six independent joint loads are possible.
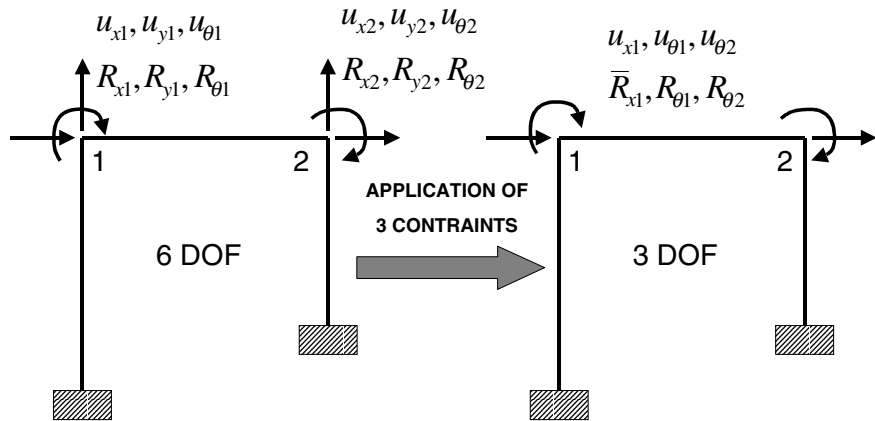
Figure 7.2 Utilization of Displacement Constraints in Portal Frame Analysis

Using hand calculations and the slope-deflection method, it is common practice to neglect axial deformations within the three members of the portal frame. In mathematical notation, those three constraint equations can be written as:

$$u_{y1} = 0$$
$$u_{y2} = 0 \qquad\qquad (7.4)$$
$$u_{x2} = u_{x1}$$

As a result of these constraints, the following load assumptions must be made:

$$R_{y1} = 0$$
$$R_{y2} = 0 \qquad\qquad (7.5)$$
$$\overline{R}_{x1} = R_{x1} + R_{x2}$$

Note the similarities between the displacement compatibility conditions, Equation (7.4), and the force equilibrium requirements, Equation (7.5).

From this simple example, the following general comments can be made:

1. The application of a constraint equation must be justified by a physical understanding of structural behavior. In this case, we can say that the axial deformations are small compared to lateral deformation u_{x1}. Also, the axial deformations in the columns do not cause significant bending forces within the other members of the structure. In addition, vertical loads cannot be applied that can cause horizontal displacements in the real structure.

2. In general, for each application of a constraint equation, one global joint displacement degree of freedom is eliminated.

3. The force association with each axial deformation, which has been set to zero, cannot be calculated directly. Because the axial deformation has been set to zero, a computer program based on a displacement method will produce a zero axial force. This approximation can have serious consequences if "automatic code design checks" are conducted by the computer program.

4. The constraint equations should be applied at the element stiffness level before addition of element stiffness matrices to the global joint equilibrium equations.

7.5   FLOOR DIAPHRAGM CONSTRAINTS

Many automated structural analysis computer programs use master-slave constraint options. However, in many cases the user's manual does not clearly define the mathematical constraint equations that are used within the program. To illustrate the various forms that this constraint option can take, let us consider the floor diaphragm system shown in Figure 7.3.

The diaphragm, or the physical floor system in the real structure, can have any number of columns and beams connected to it. At the end of each member, at the diaphragm level, six degrees of freedom exist for a three-dimensional structure before introduction of constraints.

A. Typical Joint "I" on Floor System in x-y Plane   **B. Master-Slave Constraints**
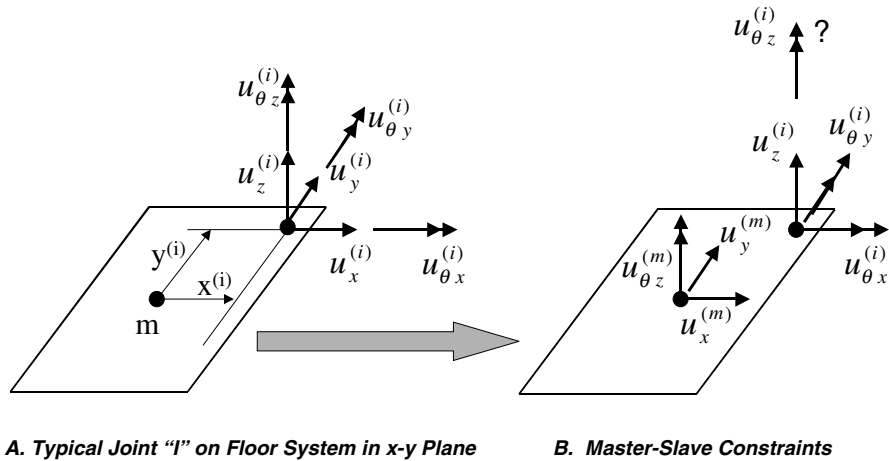
Figure 7.3 Rigid Diaphragm Approximation

Field measurements have verified for a large number of building-type structures that the in-plane deformations in the floor systems are small compared to the inter-story horizontal displacements. Hence, it has become common practice to assume that the in-plane motion of all points on the floor diaphragm move as a rigid body. Therefore, the in-plane displacements of the diaphragm can be expressed in terms of two displacements, $u_x^{(m)}$ and $u_y^{(m)}$, and a rotation about the z-axis, $u_{z\theta}^{(m)}$.

In the case of static loading, the location of the master node (m) can be at any location on the diaphragm. However, for the case of dynamic earthquake loading, *the master node must be located at the center of mass* of each floor if a diagonal mass matrix is to be used. The SAP2000 program automatically calculates the location of the master node based on the center of mass of the constraint nodes.

As a result of this rigid diaphragm approximation, the following compatibility equations must be satisfied for joints attached to the diaphragm:

$$u_x^{(i)} = u_x^{(m)} - y^{(i)} u_{\theta z}^{(m)}$$
$$u_y^{(i)} = u_y^{(m)} + x^{(i)} u_{\theta z}^{(m)}$$

(7.6)

The rotation $u_{\theta z}^{(i)}$ may or may not be constrained to the rigid body rotation of the diaphragm. This decision must be based on how the beams and columns are physically connected to the floor system. In the case of a steel structure, the structural designer may specify that the floor slab is released in the vicinity of the joint, which would allow the joint to rotate independently of the diaphragm. On the other hand, in the case of a poured-in-place concrete structure, where columns and beams are an intricate part of the floor system, the following additional constraint must be satisfied:

$$u_{\theta z}^{(i)} = u_{\theta z}^{(m)}$$

(7.7)

Or in matrix form, the displacement transformation is:

$$\begin{bmatrix} u_x^{(i)} \\ u_y^{(i)} \\ u_{\theta z}^{(i)} \end{bmatrix} = \begin{bmatrix} 1 & 0 & -y^{(i)} \\ 0 & 1 & x^{(i)} \\ 0 & 0 & u_{\theta z}^{(i)} \end{bmatrix} \begin{bmatrix} u_x^{(m)} \\ u_y^{(m)} \\ u_{\theta z}^{(m)} \end{bmatrix} \text{ or, } \mathbf{u}^{(i)} = \mathbf{T}^{(i)} \mathbf{u}^{(m)}$$

(7.8)

If displacements are eliminated by the application of constraint equations, the loads associated with those displacements must also be transformed to the master node. From simple statics the loads applied at joint "i" can be moved to the master node "m" by the following equilibrium equations:

$$R_x^{(mi)} = R_x^{(i)}$$
$$R_y^{(mi)} = R_y^{(i)}$$
$$R_{\theta z}^{(mi)} = R_{\theta z}^{(i)} - y^{(i)} R_x^{(i)} + x^{(i)} R_y^{(i)}$$

(7.9)

Or in matrix form. the load transformation is:

$$\begin{bmatrix} R_x^{(mi)} \\ R_y^{(mi)} \\ R_{\theta z}^{(mi)} \end{bmatrix} = \begin{bmatrix} 1 & 0 & 0 \\ 0 & 1 & 0 \\ -y^{(i)} & x^{(i)} & 1 \end{bmatrix} \begin{bmatrix} R_x^{(i)} \\ R_y^{(i)} \\ R_{\theta z}^{(i)} \end{bmatrix} \text{ Or, } \mathbf{R}^{(mi)} = \mathbf{T}^{(i)^T} \mathbf{R}^{(i)}$$

(7.10)

Again, one notes that the force transformation matrix is the transpose of the displacement transformation matrix.

The total load applied at the master point will be the sum of the contributions from all slave nodes. Or:

$$\mathbf{R}^{(m)} = \sum_i \mathbf{R}^{(mi)} = \sum \mathbf{T}^{(i)^T} \mathbf{R}^{(i)} \qquad (7.11)$$

Now, consider a vertical column connected between joint i at level m and joint j at level m+1, as shown in Figure 7.4. Note that the location of the master node can be different for each level.
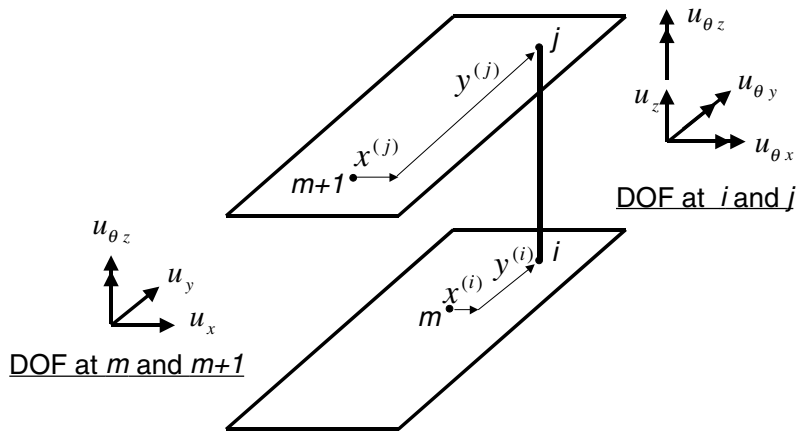
Figure 7.4 Column Connected Between Horizontal Diaphragms

From Equation (7.6) it is apparent that the displacement transformation matrix for the column is given by

$$
\begin{bmatrix}
u_x^{(i)} \\
u_y^{(i)} \\
u_z^{(i)} \\
u_{\theta x}^{(i)} \\
u_{\theta y}^{(i)} \\
u_{\theta z}^{(i)} \\
u_x^{(j)} \\
u_y^{(j)} \\
u_z^{(j)} \\
u_{\theta x}^{(j)} \\
u_{\theta y}^{(j)} \\
u_{\theta z}^{(j)}
\end{bmatrix}
=
\begin{bmatrix}
1 & 0 & 0 & 0 & 0 & 0 & -y^{(i)} & 0 & 0 & 0 & 0 & 0 & 0 & 0 \\
0 & 1 & 0 & 0 & 0 & 0 & x^{(i)} & 0 & 0 & 0 & 0 & 0 & 0 & 0 \\
0 & 0 & 1 & 0 & 0 & 0 & 0 & 0 & 0 & 0 & 0 & 0 & 0 & 0 \\
0 & 0 & 0 & 1 & 0 & 0 & 0 & 0 & 0 & 0 & 0 & 0 & 0 & 0 \\
0 & 0 & 0 & 0 & 1 & 0 & 0 & 0 & 0 & 0 & 0 & 0 & 0 & 0 \\
0 & 0 & 0 & 0 & 0 & 1 & 0 & 0 & 0 & 0 & 0 & 0 & 0 & 0 \\
0 & 0 & 0 & 0 & 0 & 0 & 0 & 1 & 0 & 0 & 0 & 0 & 0 & -y^{(j)} \\
0 & 0 & 0 & 0 & 0 & 0 & 0 & 0 & 1 & 0 & 0 & 0 & 0 & x^{(j)} \\
0 & 0 & 0 & 0 & 0 & 0 & 0 & 0 & 0 & 1 & 0 & 0 & 0 & 0 \\
0 & 0 & 0 & 0 & 0 & 0 & 0 & 0 & 0 & 0 & 1 & 0 & 0 & 0 \\
0 & 0 & 0 & 0 & 0 & 0 & 0 & 0 & 0 & 0 & 0 & 1 & 0 & 0 \\
0 & 0 & 0 & 0 & 0 & 0 & 0 & 0 & 0 & 0 & 0 & 0 & 1 & 0
\end{bmatrix}
\begin{bmatrix}
u_x^{(m)} \\
u_y^{(m)} \\
u_z^{(i)} \\
u_{\theta x}^{(i)} \\
u_{\theta y}^{(i)} \\
u_{\theta z}^{(i)} \\
u_{\theta z}^{(m)} \\
u_x^{(m+1)} \\
u_y^{(m+1)} \\
u_z^{(i)} \\
u_{\theta x}^{(i)} \\
u_{\theta y}^{(i)} \\
u_{\theta z}^{(i)} \\
u_{\theta z}^{(m+1)}
\end{bmatrix}
\quad (7.12)
$$

Or in symbolic form:

$$\mathbf{d} = \mathbf{B}\mathbf{u} \tag{7.13}$$

The displacement transformation matrix is 12 by 14 if the z-rotations are retained as independent displacements. The new 14 by 14 stiffness matrix, with respect to the master and slave reference systems at both levels, is given by:

$$\mathbf{K} = \mathbf{B}^{\mathrm{T}}\mathbf{k}\mathbf{B} \tag{7.14}$$

where $\mathbf{k}$ is the initial 12 by 12 global stiffness matrix for the column. It should be pointed out that the formal matrix multiplication, suggested by Equation (7.14), need not be conducted within a computer program. Sparse matrix operations reduce the numerical effort significantly.

In the case of a beam at a diaphragm level, the axial deformation will be set to zero by the constraints, and the resulting 8 by 8 stiffness matrix will be in

reference to six rotations and two vertical displacements. Therefore, the force in the beam element will be zero.

7.6   RIGID CONSTRAINTS

There are several different types of constraints that require displacements at one point to be related to displacements at another point. The most general form of a three-dimensional rigid constraint is illustrated in Figure 7.5.
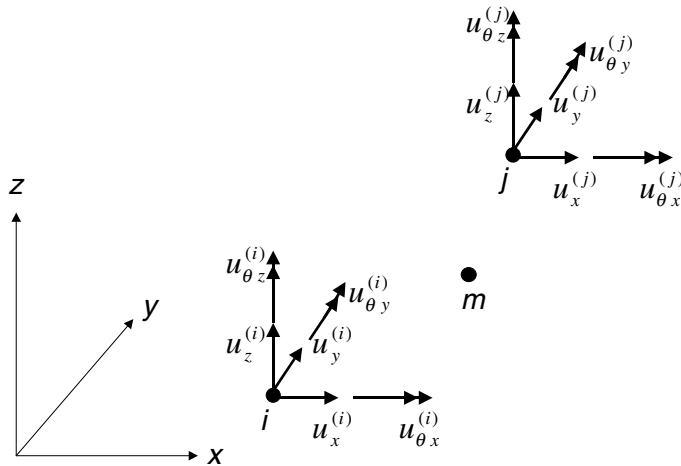
Figure 7.5 Rigid Body Constraints

The points i, j and m are all points on a body that can be considered to move with six rigid body displacements. Any point in space can be considered as the master node for static loading; however, for dynamic analysis, the master node must be at the center of the mass if we wish to restrict our formulation to a diagonal mass matrix.

It is apparent from the fundamental equations of geometry that all points connected to the rigid body are related to the displacements of the master node by the following equations:

$$u_x^{(i)} = u_x^{(m)} + (z^{(i)} - z^{(m)})u_{\theta y}^{(m)} - (y^{(i)} - y^{(m)})u_{\theta z}^{(m)}$$
$$u_y^{(i)} = u_y^{(m)} - (z^{(i)} - z^{(m)})u_{\theta x}^{(m)} + (x^{(i)} - x^{(m)})u_{\theta z}^{(m)}$$
$$u_z^{(i)} = u_z^{(m)} + (y^{(i)} - y^{(m)})u_{\theta x}^{(m)} - (x^{(i)} - x^{(m)})u_{\theta y}^{(m)}$$
$$u_{\theta x}^{(i)} = u_{\theta x}^{(m)}$$
$$u_{\theta y}^{(i)} = u_{\theta y}^{(m)}$$
$$u_{\theta z}^{(i)} = u_{\theta z}^{(m)}$$

$$(7.15)$$

The constraint equations for point j are identical to matrix Equation (7.15) with i replaced with j.

7.7   USE OF CONSTRAINTS IN BEAM-SHELL ANALYSIS

An example that illustrates the practical use of a three-dimensional rigid constraint is the beam-slab system shown in Figure 7.6.
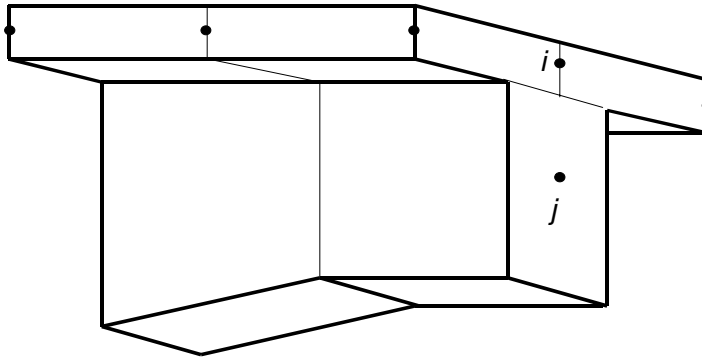
Figure 7.6 Connection of Beam to Slab by Constraints

It is realistic to use four-node shell elements to model the slab and two-node beam elements to model the beam. Both elements have six DOF per node. However, there are no common nodes in space to directly connect the two element types. Therefore, it is logical to connect node i, at the mid-surface of the slab, with point j at the neutral axis of the beam with a rigid constraint. If these constraints are enforced at the shell nodes along the axis of the beam, it will allow the natural interaction of the two element types. In addition to reducing the

number of unknowns, it avoids the problem of selecting an effective width of the slab. Also, it allows non-prismatic beams, where the neutral axis in not on a straight line, to be realistically modeled. To maintain compatibility between the beam and slab, it may be necessary to apply the rigid-body constraint at several sections along the axis of the beam.

7.8 USE OF CONSTRAINTS IN SHEAR WALL ANALYSIS

Another area in which the use of constraints has proven useful is in the analysis of perforated concrete shear walls. Consider the two-dimensional shear wall shown in Figure 7.7a.

A. SHEAR WALL WITH LINE LOADS   B. FINITE ELEMENT MODEL

COLUMNS
BEAMS
RIGID ZONES

3 DOF PER
RIGID ZONE

C. DEFINE BEAMS & COLUMNS   D. BEAM-COLUMN MODEL
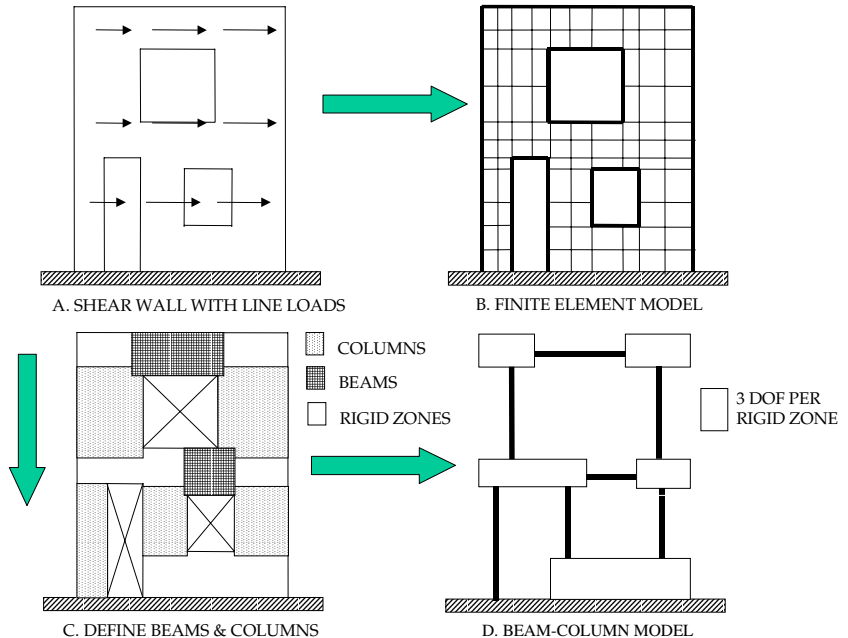
Figure 7.7 Beam-Column Model of Shear Wall

Many engineers believe that the creation of a two-dimensional finite element mesh, as shown in Figure 7.7b, is the best approach to evaluate the displacements and stresses within the shear wall. In the author's opinion, this approach may not be the best for the following reasons:

1. As previously illustrated, the use of four-node plane elements for frame analysis does not accurately model linear bending. The approximation of constant shear stress within each element makes it very difficult to capture the parabolic shear distribution that exists in the classical frame element.

2. If a very fine mesh is used, the linear finite element solution will produce near infinite stresses at the corners of the openings. Because the basic philosophy of reinforced concrete design is based on cracked sections, it is not possible to use the finite element results directly for design.

3. Using common sense and a physical insight into the behavior of the structure, it is possible to use frame elements to create a very simple model that accurately captures the behavior of the structure and directly produces results that can be used to design the concrete elements.

Figure 7.7c illustrates how the shear wall is reduced to a frame element model interconnected with rigid zones. The columns are first defined by identifying regions of the structure that have two stress-free vertical sides. The beams are then defined by identifying areas that have two stress-free horizontal sides. The length of each beam and column should be increased by approximately 20 percent of the depth of the element to allow for deformations near the ends of the elements. The remaining areas of the structure are assumed to be rigid in-plane.

Based on these physical approximations, the simple model, shown in Figure 7.7d, is produced. Each rigid area will have three DOF, two translations and two rotations. The end of the frame elements must be constrained to move with these rigid areas. Therefore, this model has only 12 DOF. Additional nodes within the frame elements may be required to accurately model the lateral loading.

7.9   USE OF CONSTRAINTS FOR MESH TRANSITIONS

It is a fact that rectangular elements are more accurate than arbitrary quadrilateral elements. Also, regular eight-node prisms are more accurate than hexahedral elements of arbitrary shape. Therefore, there is a motivation to use constraints to connect a fine mesh with coarse mesh.
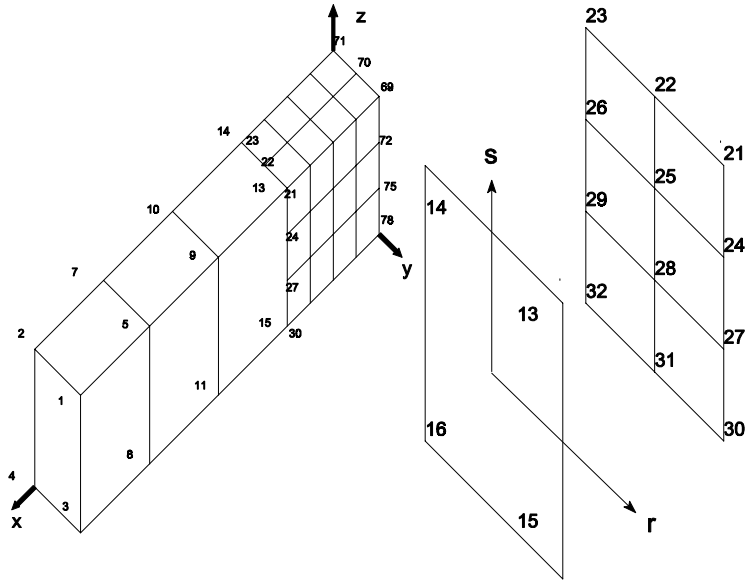
Figure 7.8 Use of Constraints to Merge Different Finite Element Meshes

To illustrate the use of constraints to merge different sized elements, consider the three-dimensional finite element shown in Figure 7.8.

The easiest method to generate the mesh shown in Figure 7.8 is to use completely different numbering systems to generate the coarse and fine mesh areas of the finite element model. The two sections can then be connected by displacement constraints. To satisfy compatibility, it is necessary that *the fine mesh be constrained to the coarse mesh*. Therefore, the shape functions of the surface of the coarse mesh must be used to evaluate the displacements at the nodes of the fine mesh. In this case, the 36 DOF of the 12 fine mesh nodes, numbers 21 to 32, are related to the displacements at nodes 13 to 16 by 36 equations of the following form:

$$u_c = N_{13}u_{13} + N_{14}u_{14} + N_{15}u_{15} + N_{16}u_{16} \qquad (7.16)$$

The equation is applied to the x, y and z displacements at the 12 points. The bilinear shape functions, N_i, are evaluated at the natural coordinates of the 12 points. For example, the natural coordinates for node 25 are $r = 0$ and $s = 1/3$. It is apparent that these displacement transformations can automatically be formed

and applied within a computer program. This approach has been used in computer programs that use adaptive mesh refinement.

7.10   LAGRANGE MULTIPLIERS AND PENALTY FUNCTIONS

In rigid-body mechanics the classical approach to specify displacement constraints is by using Lagrange multipliers. A more recent approach used in computational mechanics is to use penalty functions, within the variational formulation of the problem, to enforce constraint conditions.

The penalty method can be explained using a simple physical approach in which the constraint is enforced using a ***semi-rigid element***. To illustrate this approach Equation (7.17) can be written as:

$$N_{13}u_{13} + N_{14}u_{14} + N_{15}u_{15} + N_{16}u_{16} - u_c = 0 \approx e \text{ or, } e = \mathbf{B}_c \mathbf{u} \qquad (7.17)$$

An equation of this form can be written for all degrees of freedom at the constraint node. The displacement transformation matrix $\mathbf{B}_c$ is a 1 by 5 matrix for each constraint displacement. For the constraint equation to be satisfied, the error e must be zero, or a very small number compared to the other displacements in the equation. This can be accomplished by assigning a large stiffness k_c, or ***penalty term***, to the error in the constraint equation. Hence, the force associated with the constraint is $f_c = k_c e$ and the 5 by 5 constraint element stiffness matrix can be written as:

$$\mathbf{k}_c = \mathbf{B}_c^T k_c \mathbf{B}_c \qquad (7.18)$$

As the value of k_c is increased, the error is reduced and the strain energy within the constraint element will approach zero. Therefore, the energy associated with the constraint element can be added directly to the potential energy of the system before application of the principle of minimum potential energy.

It should be pointed out that the penalty term should not be too large, or numerical problems may be introduced, as illustrated in Figure 7.1. This can be avoided if the penalty term is three to four orders-of-magnitude greater than the stiffness of the adjacent elements.

The Lagrange multiplier approach adds the constraint equations to the potential energy. Or:

$$\Omega = \frac{1}{2}\mathbf{u}^T\mathbf{Ku} - \mathbf{u}^T\mathbf{R} + \sum_{j=1}^{J}\lambda_j\mathbf{B}_j\mathbf{u} \tag{7.19}$$

where λ_j is defined as the Lagrange multiplier for the constraint j. After the potential energy is minimized with respect to each displacement and each Lagrange multiplier, the following set of equations is produced:

$$\begin{bmatrix} \mathbf{K} & \mathbf{B} \\ \mathbf{B}^T & \mathbf{0} \end{bmatrix}\begin{bmatrix} \mathbf{u} \\ \lambda \end{bmatrix} = \begin{bmatrix} \mathbf{R} \\ \mathbf{0} \end{bmatrix} \tag{7.20}$$

The number of equations to be solved is increased by "J" additional equations. Equation (7.20) has both equilibrium equations and equations of geometry. Also, the symmetric matrix is not positive-definite. Therefore, pivoting may be required during the solution process. Hence, the penalty method is the preferable approach.

7.11   SUMMARY

Traditionally, constraints were used to reduce the number of equations to be solved. At the present time, however, the high speed of the current generation of inexpensive personal computers allows for the double-precision solution of several thousand equations within a few minutes. Hence, constraints should be used to avoid numerical problems and to create a realistic model that accurately predicts the behavior of the real structure.

Constraint equations are necessary to connect different element types together. In addition, they can be very useful in areas of mesh transitions and adaptive mesh refinement.

Care must be exercised to avoid numerical problems if penalty functions are used to enforce constraints. The use of Lagrange multipliers avoids numerical problems; however, additional numerical effort is required to solve the mixed set of equations.

8.

PLATE BENDING ELEMENTS

Plate Bending is a Simple Extension of Beam Theory

8.1 INTRODUCTION

Before 1960, plates and slabs were modeled using a grid of beam elements for many civil engineering structures. Only a small number of "closed form" solutions existed for plates of simple geometry and isotropic materials. Even at the present time many slab designs are based on grid models. This classical approximate approach, in general, produces conservative results because it satisfies statics and violates compatibility. However, the internal moment and shear distribution may be incorrect. The use of a converged finite element solution will produce a more consistent design. The fundamental difference between a grid of beam elements and a plate-bending finite element solution is that a twisting moment exists in the finite element model; whereas, the grid model can only produce one-dimensional torsional moments and will not converge to the theoretical solution as the mesh is refined.

The following approximations are used to reduce the three-dimensional theory of elasticity to govern the behavior of ***thin plates and beams***:

1. It is assumed that a *line normal to the reference surface* (neutral axis) of the plate (beam) *remains straight* in the loaded position. This displacement constraint is the same as stating that the in-plane strains are a linear function in the thickness direction. This assumption does not require that the rotation

of the normal line to be equal to the rotation of the reference surface; hence, transverse shear deformations are possible.

2. In addition, the normal stress in the thickness direction, which is normally very small compared to the bending stresses, is assumed to be zero for both beams and plates. This is accomplished by using **plate stress material properties** in-plane as defined in Chapter 1. Note that this approximation allows Poisson's ratio strains to exist in the thickness direction.

3. If the transverse shearing strains are assumed to be zero, an additional displacement constraint is introduced that states that **lines normal to the reference surface remain normal to the reference surface after loading**. This approximation is attributed to Kirchhoff and bears his name.

Classical thin plate theory is based on all three approximations and leads to the development of a fourth order partial differential equation in terms of the normal displacement of the plate. This approach is only possible for plates of constant thickness. Many books and papers, using complicated mathematics, have been written based on this approach. However, the Kirchhoff approximation is not required to develop plate bending finite elements that are accurate, robust and easy to program. At the present time, it is possible to include transverse shearing deformations for thick plates without a loss of accuracy for thin plates.

In this chapter, plate bending theory is presented as an extension of beam theory (see Appendix F) and the equations of three-dimensional elasticity. Hence, no previous background in plate theory is required by the engineer to fully understand the approximations used. Several hundred plate-bending finite elements have been proposed during the past 30 years. However, only one element will be presented here. The element is a three-node triangle or a four-node quadrilateral and is formulated with and without transverse shearing deformations. The formulation is restricted to small displacements and elastic materials. Numerical examples are presented to illustrate the accuracy of the element. The theory presented here is an expanded version of the plate bending element first presented in reference [1] using a variational formulation.

8.2   THE QUADRILATERAL ELEMENT

First, the formulation for the quadrilateral element will be considered. The same approach applies to the triangular element. A quadrilateral of arbitrary geometry, in a local x-y plane, is shown in Figure 8.1. Note that the parent four-node element, Figure 8.1a, has 16 rotations at the four node points and at the mid-point of each side. The mid-side rotations are then rotated to be normal and tangential to each side. The tangential rotations are then set to zero, reducing the number of degrees-of-freedom to 12, Figure 8.1b. The sides of the element are constrained to be a cubic function in u_z and four displacements are introduced at the corner nodes of the element, Figure 8.1c. Finally, the mid-side rotations are eliminated by static condensation, Figure 8.1d, and a 12 DOF element is produced.
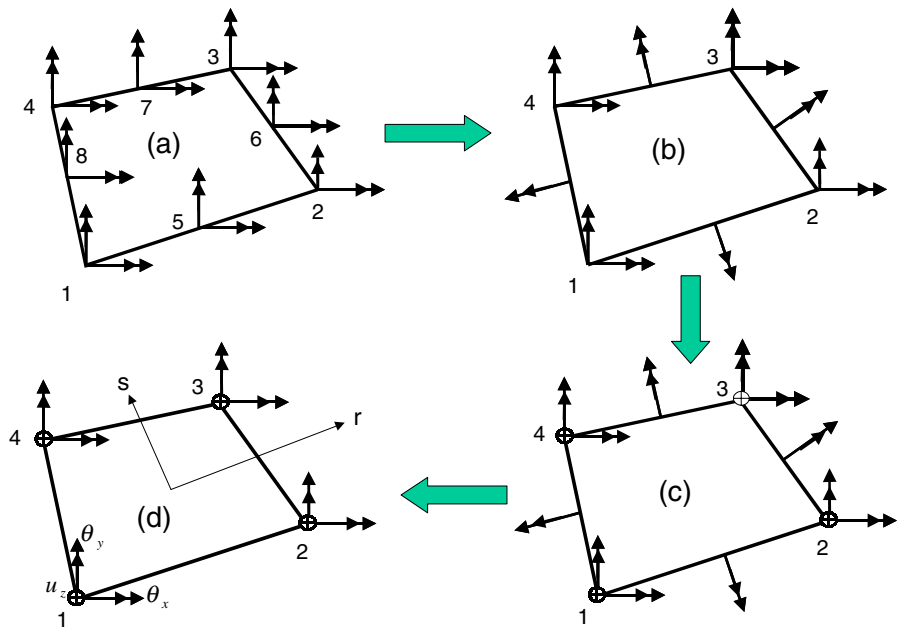
Figure 8.1 Quadrilateral Plate Bending Element

The basic displacement assumption is that the rotation of lines normal to the reference plane of the plate is defined by the following equations:

$$\theta_x(r,s) = \sum_{i=1}^{4} N_i(r,s)\theta_{xi} + \sum_{i=5}^{8} N_i(r,s)\,\Delta\theta_{xi}$$

$$\theta_y(r,s) = \sum_{i=1}^{8} N_i(r,s)\theta_{yi} + \sum_{i=5}^{8} N_i(r,s)\,\Delta\theta_{yi}$$

(8.1)

The eight-node shape functions are given by:

$$N_1 = (1-r)(1-s)/4 \qquad N_2 = (1+r)(1-s)/4$$

$$N_3 = (1+r)(1+s)/4 \qquad N_4 = (1-r)(1+s)/4$$

$$N_5 = (1-r^2)(1-s)/2 \qquad N_6 = (1+r)(1-s^2)/2$$

(8.2)

$$N_7 = (1-r^2)(1+s)/2 \qquad N_8 = (1-r)(1-s^2)/2$$

Note that the first four shape functions are the natural bilinear shape functions for a four-node quadrilateral. The four shape functions for the mid-side nodes are an addition to the bilinear functions and are often referred to as *hierarchical* functions. A typical element side *ij* is shown in Figure 8.2.
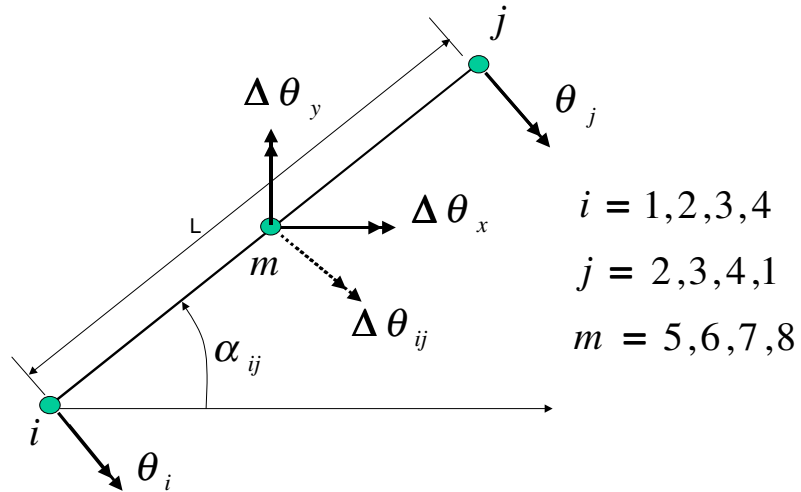
Figure 8.2 Typical Element Side

The tangential rotations are set to zero and only the normal rotations exist. Therefore, the x and y components of the normal rotation are given by:

$$\Delta\theta_x = \sin\alpha_{ij}\ \Delta\theta_{ij}$$
$$\Delta\theta_y = -\cos\alpha_{ij}\ \Delta\theta_{ij}$$

(8.3)

Hence, Equation (8.1) can be rewritten as:

$$\theta_x(r,s) = \sum_{i=1}^{4} N_i(r,s)\theta_{xi} + \sum_{i=5}^{8} M_{xi}(r,s)\ \Delta\theta_i$$
$$\theta_y(r,s) = \sum_{i=1}^{8} N_i(r,s)\theta_{yi} + \sum_{i=5}^{8} M_{yi}(r,s)\ \Delta\theta_i$$

(8.4)

The number of displacement degrees-of-freedom has now been reduced from 16 to 12, as indicated in Figure 8.1b. The three-dimensional displacements, as defined in Figure 8.3 with respect to the x-y reference plane, are:
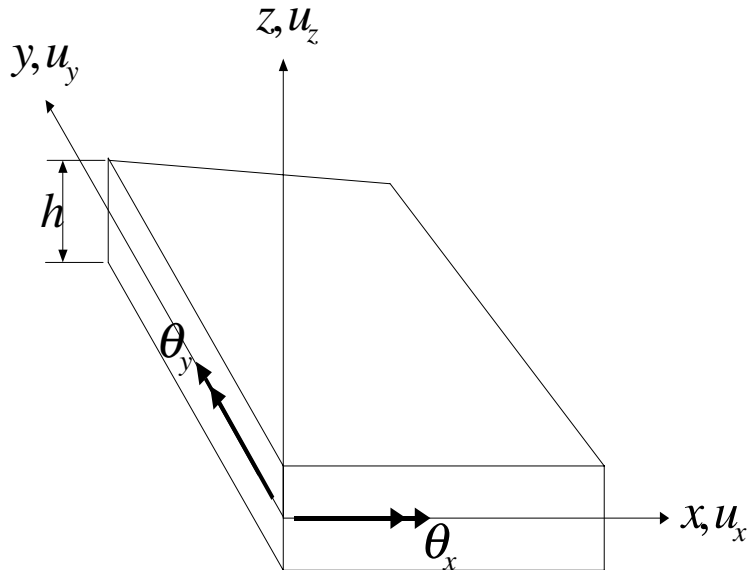
Figure 8.3 Positive Displacements in Plate Bending Element

$$u_x(r,s) = z\,\theta_y(r,s)$$
$$u_y(r,s) = -z\,\theta_x(r,s)$$

$$(8.5)$$

Note that the normal displacement of the reference plane $u_z(r,s)$ has not been defined as a function of space. Now, it is assumed that the normal displacement along each side is a cubic function. From Appendix F, the transverse shear strain along the side is given by:

$$\gamma_{ij} = \frac{1}{L}(u_{zj} - u_{zi}) - \frac{1}{2}(\theta_i + \theta_j) - \frac{2}{3}\Delta\theta_{ij}$$

$$(8.6)$$

From Figure 8.2, the normal rotations at nodes i and j are expressed in terms of the x and y rotations. Or, Equation (8.6) can be written as:

$$\gamma_{ij} = \frac{1}{L}(u_{zj} - u_{zi}) - \frac{\sin\alpha_{ij}}{2}(\theta_{xi} + \theta_{xj}) + \frac{\cos\alpha_{ij}}{2}(\theta_{yi} + \theta_{yj}) - \frac{2}{3}\Delta\theta_{ij}$$

$$(8.7)$$

This equation can be written for all four sides of the element.

It is now possible to express the node shears in terms of the side shears. A typical node is shown in Figure 8.4.

Figure 8.4 Node Point Transverse Shears

The two mid-side shears are related to the shears at node i by the following strain transformation:

$$\begin{bmatrix} \gamma_{ij} \\ \gamma_{ki} \end{bmatrix} = \begin{bmatrix} \cos\alpha_{ij} & \sin\alpha_{ij} \\ \cos\alpha_{ki} & \sin\alpha_{ki} \end{bmatrix} \begin{bmatrix} \gamma_{xz} \\ \gamma_{yz} \end{bmatrix}_i \qquad (8.8)$$

Or, in inverse form:

$$\begin{bmatrix} \gamma_{xz} \\ \gamma_{yz} \end{bmatrix}_i = \frac{1}{\det} \begin{bmatrix} \sin\alpha_{ki} & -\cos\alpha_{ki} \\ -\sin\alpha_{ij} & \cos\alpha_{ij} \end{bmatrix} \begin{bmatrix} \gamma_{ij} \\ \gamma_{ki} \end{bmatrix} \qquad (8.9)$$

where $\det = \cos\alpha_{ij}\,\sin\alpha_{ki} - \cos\alpha_{ki}\,\sin\alpha_{ij}$.

The final step in determining the transverse shears is to use the standard four-node bilinear functions to evaluate the shears at the integration point.

8.3   STRAIN-DISPLACEMENT EQUATIONS

Using the three-dimensional strain-displacement equations, the strains within the plate can be expressed in terms of the node rotations. Or:

$$\varepsilon_x = \frac{\partial u_x}{\partial x} = z\,\theta_y(r,s)_{,x}$$

$$\varepsilon_y = \frac{\partial u_y}{\partial y} = -z\,\theta_x(r,s)_{,y} \qquad (8.10)$$

$$\gamma_{xy} = \frac{\partial u_x}{\partial y} + \frac{\partial u_y}{\partial x} = z[\theta_y(r,s)_{,y} - \theta_x(r,s)]$$

Therefore, at each integration point the five components of strain can be expressed in terms of the 16 displacements, shown in Figure 8.2c, by an equation of the following form:

$$
\begin{bmatrix} \varepsilon_x \\ \varepsilon_y \\ \gamma_{xy} \\ \gamma_{xz} \\ \gamma_{yz} \end{bmatrix} = \begin{bmatrix} z & 0 & 0 & 0 & 0 \\ 0 & z & 0 & 0 & 0 \\ 0 & 0 & z & 0 & 0 \\ 0 & 0 & 0 & 1 & 0 \\ 0 & 0 & 0 & 0 & 1 \end{bmatrix} \mathbf{b} \begin{bmatrix} \theta_X \\ \theta_Y \\ u_Z \\ \Delta\theta \end{bmatrix} \text{ or } \mathbf{d} = \mathbf{B}\mathbf{u} = \mathbf{a}(z)\,\mathbf{b}(r,s)\mathbf{u} \qquad (8.11)
$$

Hence, the strain-displacement transformation matrix is a product of two matrices in which one is a function of z only.

8.4   THE QUADRILATERAL ELEMENT STIFFNESS

From Equation (8.11), the element stiffness matrix can be written as:

$$
\mathbf{k} = \int \mathbf{B}^{\mathbf{T}}\mathbf{E}\mathbf{B}\,dV = \int \mathbf{b}^T D\mathbf{b}\,dA \qquad (8.12)
$$

where

$$
D = \int \mathbf{a}^T \mathbf{E}\mathbf{a}\,dz \qquad (8.13)
$$

After integration in the z-direction, the 5 by 5 force-deformation relationship for orthotropic materials is of the following form:

$$
\begin{bmatrix} M_{xx} \\ M_{yy} \\ M_{xy} \\ V_{xz} \\ V_{yz} \end{bmatrix} = \begin{bmatrix} D_{11} & D_{12} & D_{13} & D_{14} & D_{15} \\ D_{21} & D_{22} & D_{23} & D_{24} & D_{25} \\ D_{31} & D_{31} & D_{33} & D_{34} & D_{35} \\ D_{41} & D_{42} & D_{43} & D_{44} & D_{45} \\ D_{51} & D_{52} & D_{53} & D_{54} & D_{55} \end{bmatrix} \begin{bmatrix} \psi_{xx} \\ \psi_{yy} \\ \psi_{xy} \\ \gamma_{xz} \\ \gamma_{yz} \end{bmatrix} \qquad (8.14)
$$

The moments M and shears resultant V are forces per unit length. As in the case of beam elements, the deformations associated with the moment are the curvature ψ. For isotropic plane stress materials, the non-zero terms are given by:

$$D_{11} = D_{22} = \frac{Eh^3}{12(1-v^2)}$$

$$D_{12} = D_{21} = \frac{vEh^3}{12(1-v^2)} \tag{8.15}$$

$$D_{44} = D_{55} = \frac{5Eh}{12(1+v)}$$

8.5   SATISFYING THE PATCH TEST

For the element to satisfy the patch test, it is necessary that constant curvatures be produced if the node displacements associated with constant curvature are applied. Equation (8.11) can be written in the following form:

$$\begin{bmatrix} \psi_{xx} \\ \psi_{yy} \\ \psi_{xy} \\ \gamma_{xz} \\ \gamma_{yz} \end{bmatrix} = \begin{bmatrix} \mathbf{b}_{11} & \mathbf{b}_{12} \\ \mathbf{b}_{21} & \mathbf{b}_{22} \end{bmatrix} \begin{bmatrix} \theta_x \\ \theta_y \\ w \\ \Delta\theta \end{bmatrix} \tag{8.16}$$

where, for a quadrilateral element, $\mathbf{b}_{11}$ is a 3 by 12 matrix associated with the 12 node displacements (θ_x, θ_y, w) and $\mathbf{b}_{12}$ is a 3 by 4 matrix associated with the incompatible 4 normal side rotations ($\Delta\theta$). In order that the element satisfies the constant moment patch test, the following modification to $\mathbf{b}_{12}$ must be made:

$$\bar{\mathbf{b}}_{12} = \mathbf{b}_{12} - \frac{1}{A}\int \mathbf{b}_{12}\, dA \tag{8.17}$$

The development of this equation is presented in the chapter on incompatible elements, Equation (6.4).

8.6   STATIC CONDENSATION

The element 16 by 16 stiffness matrix for the plate bending element with shearing deformations is obtained by numerical integration. Or:

$$\overline{\mathbf{K}} = \int \mathbf{B}^{\mathrm{T}}\mathbf{D}\mathbf{B}\,dA = \begin{bmatrix} \mathbf{K}_{11} & \mathbf{K}_{12} \\ \mathbf{K}_{21} & \mathbf{K}_{22} \end{bmatrix} \tag{8.18}$$

where $\mathbf{K}_{22}$ is the 4 by 4 matrix associated with the incompatible normal rotations.

The element equilibrium equations are of the following form:

$$\begin{bmatrix} \mathbf{K}_{11} & \mathbf{K}_{12} \\ \mathbf{K}_{21} & \mathbf{K}_{22} \end{bmatrix} \begin{bmatrix} \mathbf{u} \\ \Delta\theta \end{bmatrix} = \begin{bmatrix} \mathbf{F} \\ \mathbf{0} \end{bmatrix} \tag{8.19}$$

where $\mathbf{F}$ is the 12 node forces. Because the forces associated with $\Delta\theta$ must be zero, those deformation degrees-of-freedom can be eliminated, by static condensation, before assembly of the global stiffness matrix. Therefore, the 12 by 12 element stiffness matrix is not increased in size if shearing deformations are included. This quadrilateral (or triangular) plate bending element, including shear deformations, is defined in this book as the Discrete Shear Element, or DSE.

8.7   TRIANGULAR PLATE BENDING ELEMENT

The same approximations used to develop the quadrilateral element are applied to the triangular plate bending element with three mid-side nodes. The resulting stiffness matrix is 9 by 9. Approximately 90 percent of the computer program for the quadrilateral element is the same as for the triangular element. Only different shape functions are used and the constraint associated with the fourth side is skipped. In general, the triangle is stiffer than the quadrilateral.

8.8   OTHER PLATE BENDING ELEMENTS

The fundamental equation for the discrete shear along the sides of an element is given by Equation (8.6). Or:

$$\gamma_{ij} = \frac{1}{L}(u_{zj} - u_{zi}) - \frac{1}{2}(\theta_i + \theta_j) - \frac{2}{3}\Delta\theta \tag{8.20}$$

If $\Delta\theta$ is set to zero at the mid-point of each side, shearing deformations are still included in the element. However, the internal moments within the element are constrained to a constant value for a thin plate. This is the same as the PQ2 element given in reference [1], which is based on a second order polynomial approximation of the normal displacement. The displacements produced by this element tend to have a small error; however, the internal moments for a coarse mesh tend to have a significant error. Therefore, this author does not recommend the use of this element.

If the shear is set to zero along each side of the element, the following equation is obtained:

$$\Delta\theta = \frac{3}{2L}(w_j - w_i) - \frac{3}{4}(\theta_i + \theta_j) \tag{8.21}$$

Hence, it is possible to directly eliminate the mid-side relative rotations directly without using static condensation. This approximation produces the Discrete Kirchhoff Element, DKE, in which transverse shearing deformations are set to zero. It should be noted that the DSE and the DKE for thin plates converge at approximately the same rate for both displacements and moments. For many problems, the DSE and the DKE tend to be more flexible than the exact solution.

8.9   NUMERICAL EXAMPLES

Several examples are presented to demonstrate the accuracy and convergence properties of quadrilateral and triangular plate bending elements with and without transverse shear deformations. A four-point numerical integration formula is used for the quadrilateral element. A three-point integration formula is used for the triangular element.

8.9.1   One Element Beam

To illustrate that the plate element reduces to the same behavior as classical beam theory, the cantilever beam shown in Figure 8.5 is modeled as one element that is 2 inches thick. The narrow element is 6 inches by 0.2 inch in plan.
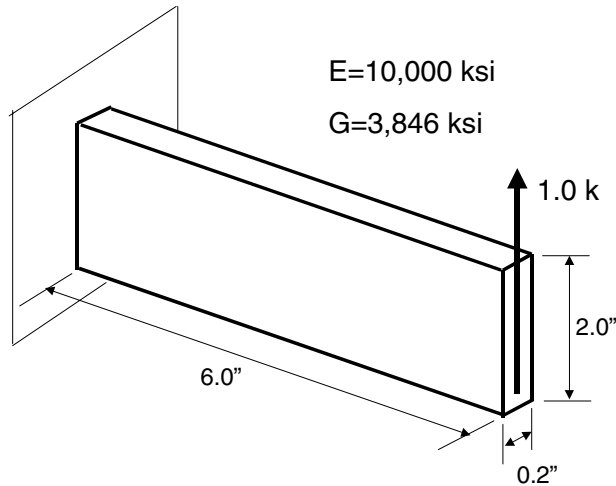
Figure 8.5 Cantilever Beam Modeled using One Plate Element

The end displacements and base moments are summarized in Table 8.1 for various theories.

Table 8.1 Displacement and Moment for Cantilever Beam

THEORY and ELEMENT	Tip Displacement (inches)	Maximum Moment (kip-in.)
Beam Theory	0.0000540	6.00
Beam Theory with Shear Deformation	0.0000587	6.00
DSE Plate Element	0.0000587	6.00
DKE Plate Element	0.0000540	6.00
PK2 Plate Element – Ref. [1]	0.0000452	3.00

This example clearly indicates that one plate element can model a one-dimensional beam without the loss of accuracy. It is worth noting that many plate elements with shear deformations, which are currently used within computer programs, have the same accuracy as the PQ2 element. Hence, the user must verify the theory and accuracy of all elements within a computer program by checking the results with simple examples.

8.9.2   Point Load On Simply Supported Square Plate

To compare the accuracy of the DSE and DKE as the elements become very thin, a 4 by 4 mesh, as shown in Figure 8.6, models one quadrant of a square plate. Note that the normal rotation along the pinned edge is set to zero. This "hard" boundary condition is required for the DSE. The DKE yields the same results for both hard and soft boundary conditions at the pinned edge.
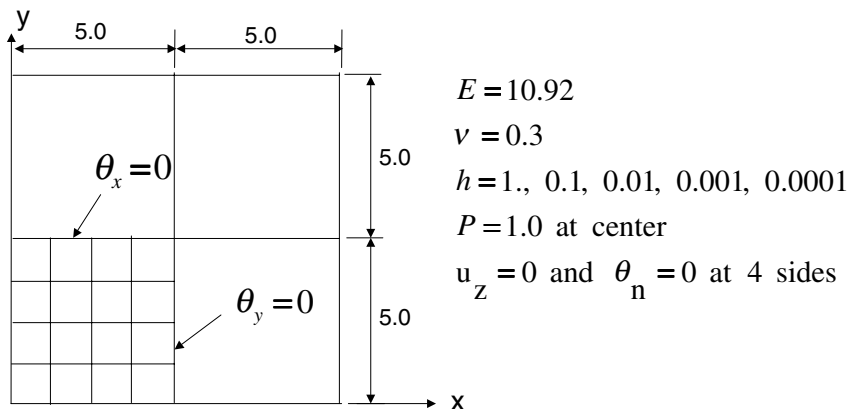
Figure 8.6 Point Load at Center of Simply Supported Square Plate

The maximum displacement and moment at the center of the plate are summarized in Table 8.2. For a thin plate without shear displacements, the displacement is proportional to $1/h^3$. Therefore, to compare results, the displacement is normalized by the factor h^3. The maximum moment is not a function of thickness for a thin plate. For this example, shearing deformations are only significant for a thickness of 1.0. The exact thin-plate displacement for this problem is 1.160, which is very close to the average of the DKE and the DSE

results. Hence, one can conclude that DSE converges to an approximate thin plate solution as the plate becomes thin. However, DSE does not converge for a coarse mesh to the same approximate value as the DKE.

Table 8.2 Convergence of Plate Elements – 4 by 4 Mesh – Point Load

Thickness, h	Displacement times h^3		Maximum Moment	
	DKE	DSE	DKE	DSE
1	1.195	1.383	0.3545	0.4273
0.1	1.195	1.219	0.3545	0.4269
0.01	1.195	1.218	0.3545	0.4269
0.001	1.195	1.218	0.3545	0.4269
0.0001	1.195	1.218	0.3545	0.4269

To demonstrate that the two approximations converge for a fine mesh, a 16 by 16 mesh is used for one quadrant of the plate. The results obtained are summarized in Table 8.3.

Table 8.3 Convergence of Plate Element –16 by 16 Mesh – Point Load

Thickness h	Displacement times h^3		Maximum Moment	
	DKE	DSE	DKE	DSE
1	1.163	1.393	0.5187	0.5704
0.01	1.163	1.164	0.5187	0.5295
0.0001	1.163	1.164	0.5187	0.5295

One notes that the DKE and DSE displacements converge to the approximately same value for a point load at the center of the plate. However, because of stress singularity, the maximum moments are not equal, which is to be expected.

8.9.3   Uniform Load On Simply Supported Square Plate

To eliminate the problem associated with the point load, the same plate is subjected to a uniform load of 1.0 per unit area. The results are summarized in

Table 8.4. For thin plates, the quadrilateral DKE and DSE displacements and moments agree to three significant figures.

Table 8.4 Convergence of Quad Plate Elements –16 by 16 Mesh - Uniform Load

Thickness h	Displacement times h^3		Maximum Moment	
	DKE	DSE	DKE	DSE
1	9.807	10.32	1.142	1.144
0.01	9.807	9.815	1.142	1.144
0.0001	9.807	9.815	1.142	1.144

8.9.4 Evaluation of Triangular Plate Bending Elements

The accuracy of the triangular plate bending element can be demonstrated by analyzing the same square plate subjected to a uniform load. The plate is modeled using 512 triangular elements, which produces a 16 by 16 mesh, with each quadrilateral divided into two triangles. The results are summarized in Table 8.5. For thin plates, the quadrilateral DKE and DSE displacements and moments agree to four significant figures. The fact that both moments and displacements converge to the same value for thin plates indicates that the triangular elements may be more accurate than the quadrilateral elements for both thin and thick plates. However, if the triangular mesh is changed by dividing the quadrilateral on the other diagonal the results are not as impressive.

Table 8.5 Convergence of Triangular Plate Elements –- Uniform Load

Thickness h	Displacement times h^3		Maximum Moment	
	DKE	DSE	DKE	DSE
1	9.807	10.308	1.145	1.145
0.01	9.807	9.807	1.145	1.145
0.0001	9.807	9.807	1.145	1.145
0.0001*	9.800	9.807	1.142	1.145

 * Quadrilateral divided on other diagonal

It should be noted, however, that if the triangular element is used in shell analysis, the membrane behavior of the triangular shell element is very poor and inaccurate results will be obtained for many problems.

8.9.5   Use of Plate Element to Model Torsion in Beams

For one-dimensional beam elements, the plate element can be used to model the shear and bending behavior. However, plate elements should not be used to model the torsional behavior of beams. To illustrate the errors introduced by this approximation, consider the cantilever beam structure shown in Figure 8.7 subjected to a unit end torque.
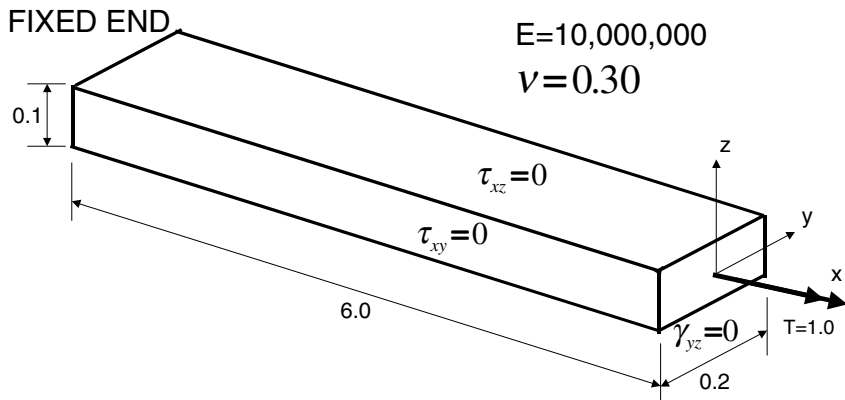
Figure 8.7 Beam Subjected to Torsion Modeled by Plate Elements

The results for the rotation at the end of the beam are shown in Table 8.6.

Table 8.6 Rotation at End of Beam Modeled using Plate Elements

Y-ROTATION	DKE		DSE	
	1 x 6	9 x 9	1 x 6	9 x 9
free	0.0284	0.0233	0.2368	0.1249
fixed	0.0227	0.0218	0.0849	0.0756

The exact solution, based on an elasticity theory that includes warpage of the rectangular cross section, is 0.034 radians. Note that the shear stress and strain

boundary conditions shown in Figure 8.6 cannot be satisfied exactly by plate elements regardless of the fineness of the mesh. Also, it is not apparent if the y-rotation boundary condition should be free or set to zero

For this example, the DKE element does give a rotation that is approximately 68 percent of the elasticity solution; however, as the mesh is refined, the results are not improved significantly. The DSE element is very flexible for the coarse mesh. The results for the fine mesh are stiffer. Because neither element is capable of converging to the exact results, the torsion of the beam should not be used as a test problem to verify the accuracy of plate bending elements. Triangular elements produce almost the same results as the quadrilateral elements.

8.10   SUMMARY

A relatively new and robust plate bending element has been summarized in this chapter. The element can be used for both thin and thick plates, with or without shearing deformations. It has been extended to triangular elements and orthotropic materials. The plate bending theory was presented as an extension of beam theory and three-dimensional elasticity theory. The DKE and DSE are currently used in the SAFE, FLOOR and SAP2000 programs.

In the next chapter, a membrane element will be presented with three DOF per node, two translations and one rotation normal to the plane. Based on the bending element presented in this chapter and membrane element presented in the next chapter, a general thin or thick shell element is presented in the following chapter.

8.11   REFERENCES

1.   Ibrahimbegovic, Adnan. 1993. "Quadrilateral Elements for Analysis of Thick and Thin Plates," *Computer Methods in Applied Mechanics and Engineering*. Vol. 110 (1993). 195-209.

9.

MEMBRANE ELEMENT WITH NORMAL ROTATIONS

Rotations Must Be Compatible Between Beam,
Membrane and Shell Elements

9.1   INTRODUCTION

The complex nature of most buildings and other civil engineering structures requires that frame, plate bending and membrane elements exist in the same computer model. The three-dimensional beam element normally has six degrees-of-freedom per node—three displacements and three rotations per node. The plate bending element, presented in the previous chapter, has two rotations in the plane of the element and one displacement normal to the element at each node. The standard plane stress element, used to model the membrane behavior in shell elements, has only two in-plane displacements at each node and cannot carry moments applied normal to the plane of the element.

A frame element embedded normal to a shear wall or slab is very common in the modeling of buildings and many other types of structural systems. It is possible to use a constraint to transfer the frame element moment to a force-couple applied in the plane of the element. However, for shells connected to edge beams and many other common types of structural systems, there is a need for a membrane element that has a normal rotation as a basic DOF at each node.

The search for a membrane element with normal rotations was a fruitless endeavor for the first 30 years of the development of finite element technology. Within the last 15 years, however, a practical quadrilateral element has evolved. Rather than refer to the many research papers (summarized in reference [1]) that led to the development of the element currently used in the general structural analysis program SAP2000, the fundamental equations will be developed in this chapter. In addition, numerical examples will be presented to illustrate the accuracy of the element.

9.2   BASIC ASSUMPTIONS

The development of the membrane element is very similar to the plate bending element presented in the previous chapter. The quadrilateral element is shown in Figure 9.1.
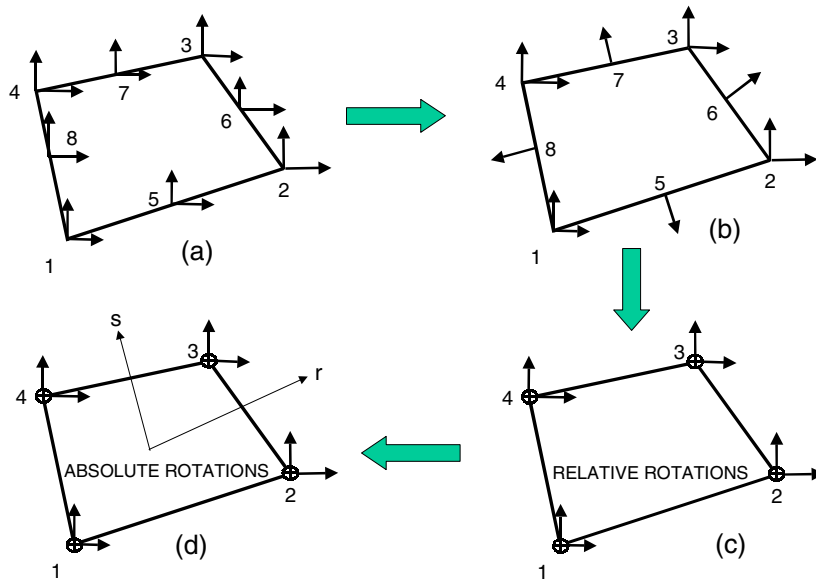
Figure 9.1 Quadrilateral Membrane Element with Normal Rotations

Development of the element can be divided into the following four steps:

1. The starting point is the nine-node quadrilateral element, 16 DOF, shown in Figure 9.1a.

2. The next step is to rotate the mid-side relative displacements to be normal and tangential to each side and to set the relative tangential displacement to zero, reducing the element to the 12 DOF shown in Figure 9.1b.

3. The third step is to introduce parabolic normal displacement constraints to eliminate the four mid-side normal displacements and to introduce four relative normal rotations at the nodes shown in Figure 9.1c.

4. The final step is to convert the relative normal rotations to absolute values and to modify the shape functions to pass the patch test. This results in the 12 by 12 element stiffness with respect to the 12 DOF shown in Figure 9.1d.

9.3   DISPLACEMENT APPROXIMATION

The basic assumption is that in-plane x and y displacements are defined by the following equations:

$$u_x(r,s) = \sum_{i=1}^{4} N_i(r,s) u_{xi} + \sum_{i=5}^{8} N_i(r,s)\,\Delta u_{xi}$$

$$u_y(r,s) = \sum_{i=1}^{4} N_i(r,s) u_{yi} + \sum_{i=5}^{8} N_i(r,s)\,\Delta u_{yi}$$

(9.1)

The eight shape functions are given by:

$$N_1 = (1-r)(1-s)/4 \qquad N_2 = (1+r)(1-s)/4$$

$$N_3 = (1+r)(1+s)/4 \qquad N_4 = (1-r)(1+s)/4$$

$$N_5 = (1-r^2)(1-s)/2 \qquad N_6 = (1+r)(1-s^2)/2$$

(9.2)

$$N_7 = (1-r^2)(1+s)/2 \qquad N_8 = (1-r)(1-s^2)/2$$

The first four shape functions are the natural bilinear shape functions for a four-node quadrilateral and are not zero at nodes 5 to 8. The last four shape functions for the mid-side nodes and center node are an addition to the bilinear functions and are referred to as *hierarchical* functions.

9.4   INTRODUCTION OF NODE ROTATION

A typical element side *ij* is shown in Figure 9.2.

$$L_{ij} = \sqrt{(x_j - x_i)^2 + (y_j - y_i)^2}$$

$i = 1,2,3,4$

$j = 2,3,4,1$

$m = 5,6,7,8$
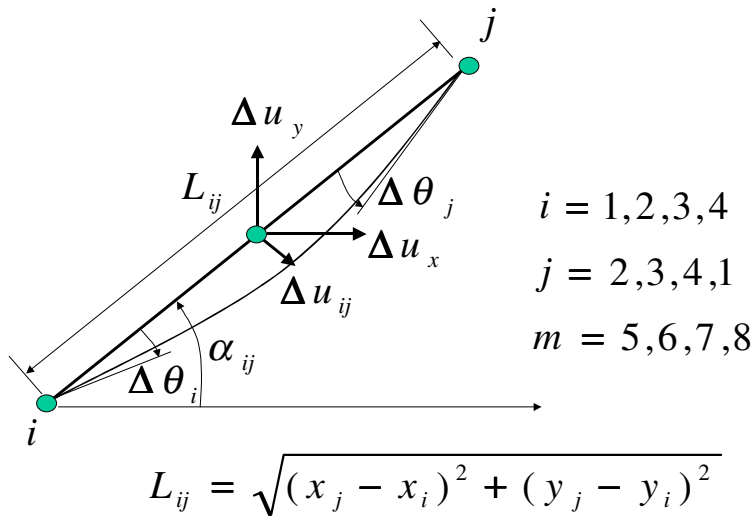
Figure 9.2 Typical Side of Quadrilateral Element

If it is assumed that the relative normal displacement of the side is parabolic, the following equation must be satisfied:

$$\Delta u_{ij} = \frac{L_{ij}}{8}(\Delta \theta_j - \Delta \theta_i) \tag{9.3}$$

Because the tangential mid-side displacement is zero, the global relative mid-side displacements are given by:

$$\Delta u_x = \cos\alpha_{ij}\Delta u_{ij} = \cos\alpha_{ij}\frac{L_{ij}}{8}(\Delta\theta_j - \Delta\theta_i)$$

$$\Delta u_y = -\sin\alpha_{ij}\Delta u_{ij} = -\sin\alpha_{ij}\frac{L_{ij}}{8}(\Delta\theta_j - \Delta\theta_i)$$

$$(9.4)$$

Equation (9.4) can be applied to all four sides and the global displacements, Equation (9.1), can be written as:

$$u_x(r,s) = \sum_{i=1}^{4} N_i(r,s)u_{xi} + \sum_{i=5}^{8} M_{xi}(r,s)\,\Delta\theta_i$$

$$u_y(r,s) = \sum_{i=1}^{4} N_i(r,s)u_{yi} + \sum_{i=5}^{8} M_{yi}(r,s)\,\Delta\theta_i$$

$$(9.5)$$

Therefore, the system has been reduced to 12 DOF.

9.5   STRAIN-DISPLACEMENT EQUATIONS

The strain-displacement equations can now be constructed from the following fundamental equations:

$$\varepsilon_x = \frac{\partial u_x}{\partial x}, \quad \varepsilon_y = \frac{\partial u_y}{\partial y} \quad \text{and} \quad \gamma_{xy} = \frac{\partial u_x}{\partial y} + \frac{\partial u_y}{\partial x}$$

$$(9.6)$$

Alternatively, the 3 by 12 strain-displacement equations written in sub matrix form are the following:

$$\begin{bmatrix} \varepsilon_x \\ \varepsilon_y \\ \gamma_{xy} \end{bmatrix} = \begin{bmatrix} \mathbf{B}_{11} & \mathbf{B}_{12} \end{bmatrix} \begin{bmatrix} \mathbf{u} \\ \Delta\theta \end{bmatrix}$$

$$(9.7)$$

In order that the element satisfies the constant stress patch test, the following modification to the 3 by 4 $\mathbf{B}_{12}$ matrix must be made:

$$\overline{\mathbf{B}}_{12} = \mathbf{B}_{12} - \frac{1}{A}\int \mathbf{B}_{12}\,dA$$

$$(9.8)$$

The development of this equation is presented in the chapter on incompatible elements, Equation (6.4).

9.6 STRESS-STRAIN RELATIONSHIP

The stress-strain relationship for orthotropic plane stress materials can be written as:

$$\begin{bmatrix} \sigma_x \\ \sigma_y \\ \tau_{xy} \end{bmatrix} = \begin{bmatrix} D_{11} & D_{12} & D_{13} \\ D_{21} & D_{22} & D_{23} \\ D_{31} & D_{32} & D_{33} \end{bmatrix} \begin{bmatrix} \varepsilon_x \\ \varepsilon_y \\ \gamma_{xy} \end{bmatrix} \tag{9.9}$$

The only restriction on the stress-strain matrix is that it must be symmetric and positive definite.

9.7 TRANSFORM RELATIVE TO ABSOLUTE ROTATIONS

The element 12 by 12 stiffness matrix for a quadrilateral element with normal rotations is obtained using four-point numerical integration. Or:

$$\overline{\mathbf{K}} = \int \mathbf{B}^{\mathrm{T}} D \mathbf{B} \, dV \tag{9.10}$$

The stiffness matrix for the membrane element, as calculated from Equation (9.9), has four unknown relative rotations at the nodes. An examination of the properties of the stiffness matrix indicates that it has a zero energy mode in addition to the three rigid body modes. This spurious deformation mode, relative to the rigid-body rotation of the element, is shown in Figure 9.3.
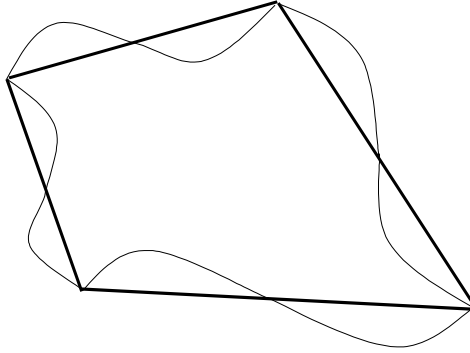
Figure 9.3 Zero Energy Displacement Mode

The zero energy displacement mode has equal rotations at all nodes and zero mid-side displacements. To eliminate this mode, it is only necessary to add a rank one matrix to the element stiffness matrix that has stiffness associated with the mode. From the elasticity definition of rotation, the absolute rotation at the center of the element, or an estimation of the rigid-body rotation of the element, can be calculated from:

$$\theta_0 = \frac{1}{2}\left[\frac{\partial u_x}{\partial y} - \frac{\partial u_y}{\partial x}\right] = \mathbf{b}_0 \mathbf{u} \tag{9.11}$$

where $\mathbf{b}_0$ is a 1 by 12 matrix. The difference between the absolute rotation and the average relative rotation at the center of the element is:

$$d = \theta_0 - \sum_{i=1}^{4} N_i(0,0)\Delta\theta_i = \overline{\mathbf{b}}_0 \mathbf{u} \tag{9.12}$$

A stiffness k_0 (or a penalty term) can now be assigned to this deformation to create, using one point integration, the following rank one stiffness matrix:

$$\mathbf{K}_0 = \int \overline{\mathbf{b}}_0^T k_0 \, \overline{\mathbf{b}}_0 \, dV = k_0 \, Vol \, \overline{\mathbf{b}}_0^T \, \overline{\mathbf{b}}_0 \tag{9.13}$$

Experience with the solution of a large number of problems indicates that the following value for rotational stiffness is effective:

$$k_0 = 0.025 D_{33}$$
(9.14)

where D_{33} is the shear modulus for isotropic materials. When this rank one matrix is added to the 12 by 12 stiffness matrix, the zero energy mode is removed and the node rotation is converted to an absolute rotation.

9.8   TRIANGULAR MEMBRANE ELEMENT

The same approximations used to develop the quadrilateral element are applied to the triangular element with three mid-side nodes. The resulting stiffness matrix is 9 by 9. Approximately 90 percent of the computer program for the quadrilateral element is the same as for the triangular element. Only different shape functions are used and the constraint associated with the fourth side is skipped. However, the triangle is significantly more stiff than the quadrilateral. In fact, the accuracy of the membrane behavior of the triangle with the drilling degrees of freedom is nearly the same as the constant strain triangle.

9.9   NUMERICAL EXAMPLE

The beam shown in Figure 9.4 is modeled with two membrane elements with drilling degrees-of-freedom.
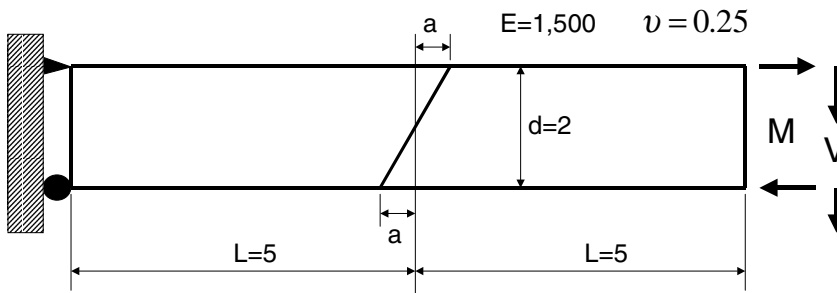
Figure 9.4 Beam Modeled with Distorted Elements

Results for both displacements and stresses are summarized in Table 9.1.

Table 9.1. Results of Analysis of Cantilever Beam

Mesh Distortion Factor "a"	TIP MOMENT LOADING		TIP SHEAR LOADING	
	Normalized Tip Displacement	Normalized Maximum Stress At Support	Normalized Tip Displacement	Normalized Maximum Stress At Support
Exact	1.000	1.000	1.000	1.000
0	1.000	1.000	0.958	0.750
1	0.502	0.675	0.510	0.601
2	0.280	0.627	0.303	0.557

For rectangular elements subjected to end moment, the exact results are obtained and "shear locking" does not exist. For a tip shear loading, the displacements are in error by only 4 percent; however, the bending stresses are in error by 25 percent. This behavior is almost identical to the behavior of plane elements with incompatible modes. As the element is distorted, the displacements and stresses deteriorate. All results were obtained using four-point integration.

The end moment can be applied as two equal and opposite horizontal forces at the end of the beam. Or, one half of the end moment can be applied directly as two concentrated moments at the two end nodes. The results for the two different methods of loading are almost identical. Therefore, standard beam elements can be attached directly to the nodes of the membrane elements with normal rotational DOF.

9.10   SUMMARY

The membrane plane stress element presented in this chapter can be used to accurately model many complex structural systems where frame, membrane and plate elements interconnect. The quadrilateral element produces excellent results. However, the performance of the triangular membrane element is very poor.

9.11   REFERENCES

1. Ibrahimbegovic, Adnan, R. Taylor, and E. Wilson. 1990. "A Robust
    Membrane Quadrilateral Element with Drilling Degrees of Freedom," *Int. J.
    of Num. Meth.*

10.

SHELL ELEMENTS

All Shell Elements Are Approximate and
a Special Case of Three-Dimensional Elasticity

10.1 INTRODUCTION

The use of classical thin shell theory for problems of arbitrary geometry leads to the development of higher order differential equations that, in general, can only be solved approximately using the numerical evaluation of infinite series. Therefore, a limited number of solutions exist only for shell structures with simple geometric shapes. Those solutions provide an important function in the evaluation of the numerical accuracy of modern finite element computer programs. However, for the static and dynamic analysis of shell structures of arbitrary geometry, which interact with edge beams and supports, the finite element method provides the only practical approach at this time.

Application of the finite element method for the analysis of shell structures requires that the user have an understanding of the approximations involved in the development of the elements. In the previous two chapters, the basic theory of plate and membrane elements has been presented. In this book, both the plate and membrane elements were derived as a special case of three-dimensional elasticity theory, in which the approximations are clearly stated. Therefore, using those elements for the analysis of shell structures involves the introduction of very few new approximations.

Before analyzing a structure using a shell element, one should always consider the direct application of three-dimensional solids to model the structure. For

example, consider the case of a three-dimensional arch dam. The arch dam may be thin enough to use shell elements to model the arch section with six degrees-of-freedom per node; however, modeling the foundation requires the use of solid elements. One can introduce constraints to connect the two element types together. However, it is simpler and more accurate to use solid elements, with incompatible modes, for both the dam and foundation. For that case, only one element in the thickness direction is required, and the size of the element used should not be greater than two times the thickness. Because one can now solve systems of over one thousand elements within a few minutes on a personal computer, this is a practical approach for many problems.

10.2   A SIMPLE QUADRILATERAL SHELL ELEMENT

The two-dimensional plate bending and membrane elements presented in the previous two chapters can be combined to form a four-node shell element as shown in Figure 10.1.

PLATE BENDING ELEMENT   +   MEMBRANE ELEMENT   =   SHELL ELEMENT

LOCAL REFERENCE *xyz* SYSTEM   GLOBAL X YZ REFERENCE SYSTEM
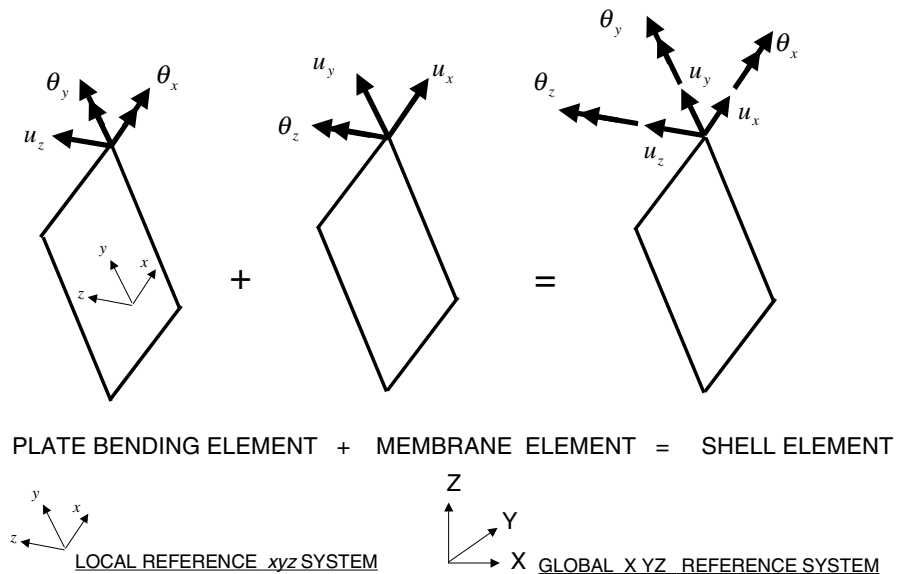
Figure 10.1 Formation of Flat Shell Element

It is only necessary to form the two element stiffness matrices in the local *xyz* system. The 24 by 24 local element stiffness matrix, Figure 10.1, is then transformed to the global XYZ reference system. The shell element stiffness and loads are then added using the direct stiffness method to form the global equilibrium equations.

Because plate bending (DSE) and membrane elements, in any plane, are special cases of the three-dimensional shell element, only the shell element needs to be programmed. This is the approach used in the SAP2000 program. As in the case of plate bending, the shell element has the option to include transverse shearing deformations.

10.3   MODELING CURVED SHELLS WITH FLAT ELEMENTS

Flat quadrilateral shell elements can be used to model most shell structures if all four nodes can be placed at the mid-thickness of the shell. However, for some shells with double curvature this may not be possible. Consider the shell structure shown in Figure 10.2.

Shell Structure With Double Curvature   Typical Flat Shell Element
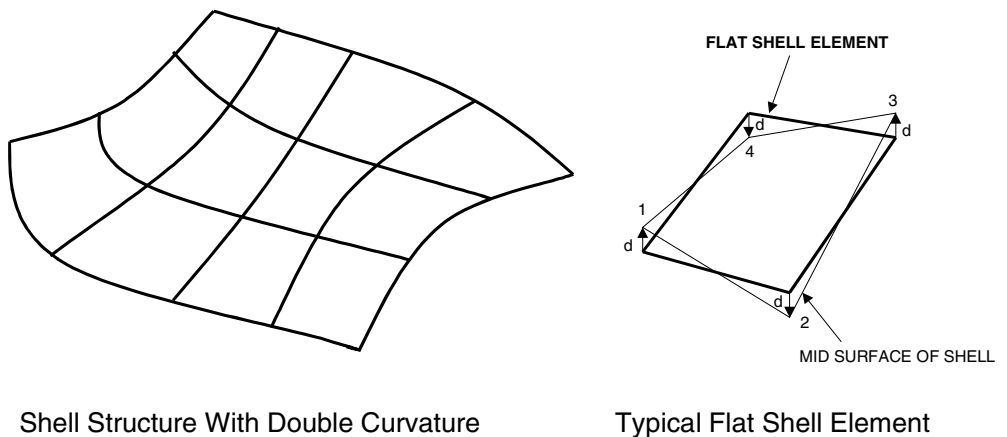
Figure 10.2 Use of Flat Elements to Model Arbitrary Shells

The four input points 1, 2 3 and 4 that define the element are located on the mid-surface of the shell, as shown in Figure 10.2. The local xyz coordinate system is defined by taking the cross product of the diagonal vectors. Or, $V_z = V_{1-3} \, V_{2-4}$. The distance vector d is normal to the flat element and is between the flat element node points and input node points at the mid-surface of the shell and is calculated from:

$$d = \pm \frac{z_1 + z_3 - z_2 - z_4}{2} \tag{10.1}$$

For most shells, this offset distance is zero and the finite element nodes are located at the mid-surface nodes. However, if the distance d is not zero, the flat element stiffness must be modified before transformation to the global XYZ reference system. It is very important to satisfy force equilibrium at the mid-surface of the shell structure. This can be accomplished by a transformation of the flat element stiffness matrix to the mid-surface locations by applying the following displacement transformation equation at each node:

$$
\begin{bmatrix} u_x \\ u_y \\ u_z \\ \theta_x \\ \theta_y \\ \theta_z \end{bmatrix}_n
=
\begin{bmatrix}
1 & 0 & 0 & 0 & -d & 0 \\
0 & 1 & 0 & d & 0 & 0 \\
0 & 0 & 1 & 0 & 0 & 0 \\
0 & 0 & 0 & 1 & 0 & 0 \\
0 & 0 & 0 & 0 & 1 & 0 \\
0 & 0 & 0 & 0 & 0 & 1
\end{bmatrix}
\begin{bmatrix} u_x \\ u_y \\ u_z \\ \theta_x \\ \theta_y \\ \theta_z \end{bmatrix}_s
\tag{10.2}
$$

Physically, this is stating that the flat element nodes are rigidly attached to the mid-surface nodes. It is apparent that as the elements become smaller, the distance d approaches zero and the flat element results will converge to the shell solution.

10.4 TRIANGULAR SHELL ELEMENTS

It has been previously demonstrated that the triangular plate-bending element, with shearing deformations, produces excellent results. However, the triangular membrane element with drilling rotations tends to lock, and great care must be

practiced in its application. Because any geometry can be modeled using quadrilateral elements, the use of the triangular element presented in this book can always be avoided.

10.5 USE OF SOLID ELEMENTS FOR SHELL ANALYSIS

The eight-node solid element with incompatible modes can be used for thick shell analysis. The cross-section of a shell structure modeled with eight-node solid elements is shown in Figure 10.3.
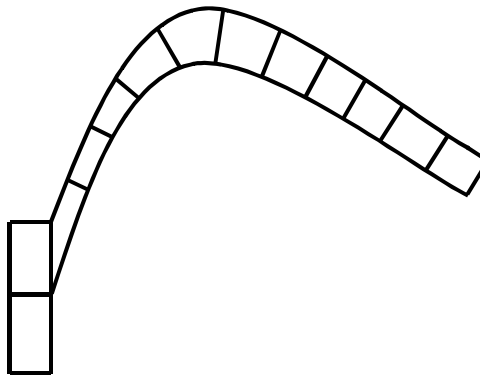
Figure 10.3 Cross-Section of Thick Shell Structure
Modeled with Solid Elements

Note that there is no need to create a reference surface when solid elements are used. As in the case of any finite element analysis, more than one mesh must be used, and statics must be checked to verify the model, the theory and the computer program.

10.6 ANALYSIS OF THE SCORDELIS-LO BARREL VAULT

The Scordelis-Lo barrel vault is a classical test problem for shell structures [1,2]. The structure is shown in Figure 10.4, with one quadrant modeled with a 4 by 4 shell element mesh. The structure is subjected to a factored gravity load in the

negative z-direction. The maximum vertical displacement is 0.3086 ft. and mid-span moment is 2,090 lb. ft.
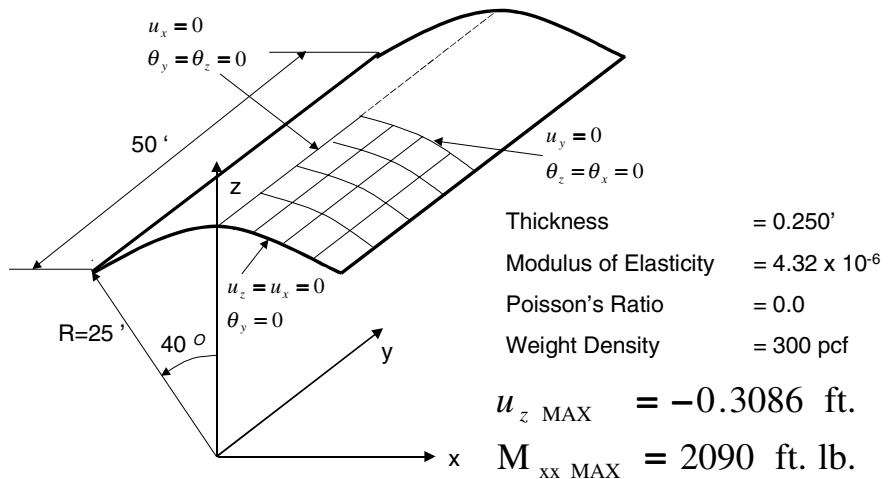
Figure 10.4 Scordelis-Lo Barrel Vault Example

To illustrate the convergence and accuracy of the shell element presented in this chapter, two meshes, with and without shearing deformations, will be presented. The results are summarized in Table 10.1.

Table 10.1 Result of Barrel Shell Analysis

	Theoretical	4 x4 DKE	4 x4 DSE	8 x 8 DKE	8 x 8 DSE
Displacement	0.3086	0.3173	0.3319	0.3044	0.3104
Moment	2090	2166	2252	2087	2113

One notes that the DSE tends to be more flexible than the DKE formulation. From a practical viewpoint, both elements yield excellent results. It appears that both will converge to almost the same result for a very fine mesh. Because of local shear deformation at the curved pinned edge, one would expect DSE displacement to converge to a slightly larger, and more correct, value.

10.7   HEMISPHERICAL SHELL EXAMPLE

The hemispherical shell shown in Figure 10.5 was proposed as a standard test problem for elements based on the Kirchhoff thin shell theory [1].

Radius	= 10.0
Thickness	= 0.4
Modulus of Elasticity	= 68,250,000
Poisson's Ratio	= 0.30

Loads as shown on one quadrant
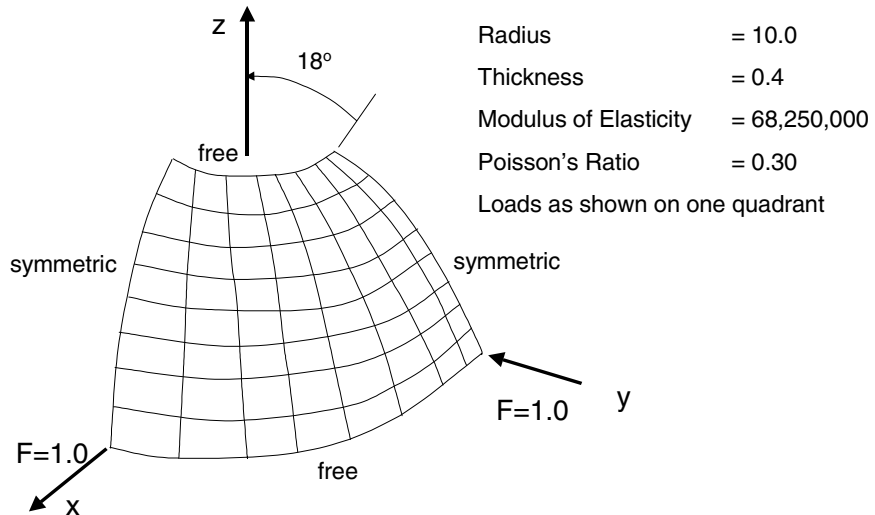
Figure 10.5 Hemispherical Shell Example

The results of the analyses using the DKE and DSE are summarized in Table 10.2. Because the theoretical results are based on the Kichhoff approximation, the DKE element produces excellent agreement with the theoretical solution. The DSE results are different. Because the theoretical solution under a point load does not exist, the results using the DSE approximation are not necessarily incorrect.

Table 10.2 Result of Hemispherical Shell Analysis

	Theoretical	8 x 8 DKE	8 x 8 DSE
Displacement	0.094	0.0939	0.0978
Moment	----------	1.884	2.363

It should be emphasized that it is physically impossible to apply a point load to a real structure. All real loads act on a finite area and produce finite stresses. The point load, which produces infinite stress, is a mathematical definition only and cannot exist in a real structure.

10.8   SUMMARY

It has been demonstrated that the shell element presented in this book is accurate for both thin and thick shells. It appears that one can use the DSE approximation for all shell structures. The results for both displacements and moment appear to be conservative when compared to the DKE approximation.

10.9   REFERENCES

1.   MacNeal, R. H. and R. C. Harder. 1985. "A Proposed Standard Set to Test Element Accuracy, Finite Elements in Analysis and Design." Vol. 1 (1985). pp. 3-20.

2.   Scordelis, A. C. and K. S. Lo. 1964. "Computer Analysis of Cylinder Shells," *Journal of American Concrete Institute*. Vol. 61. May.

<div align="right">

11.

</div>

GEOMETRIC STIFFNESS AND P-DELTA EFFECTS

P-Delta Effects, Due To Dead Load, Can Be Considered Without Iteration for Both Static and Dynamic Analysis

11.1 DEFINITION OF GEOMETRIC STIFFNESS

We are all aware that a cable has an increased lateral stiffness when subjected to a large tension force. If a long rod is subjected to a large compressive force and is on the verge of buckling, we know that the lateral stiffness of the rod has been reduced significantly and a small lateral load may cause the rod to buckle. This general type of behavior is caused by a change in the "geometric stiffness" of the structure. It is apparent that this stiffness is a function of the load in the structural member and can be either positive or negative.

The fundamental equations for the geometric stiffness for a rod or a cable are very simple to derive. Consider the horizontal cable shown in Figure 11.1 of length L with an initial tension T. If the cable is subjected to lateral displacements, v_i and v_j, at both ends, as shown, then additional forces, F_i and F_i , must be developed for the cable element to be in equilibrium in its displaced position. Note that we have assumed all forces and displacements are positive in the up direction. We have also made the assumption that the displacements are small and do not change the tension in the cable.
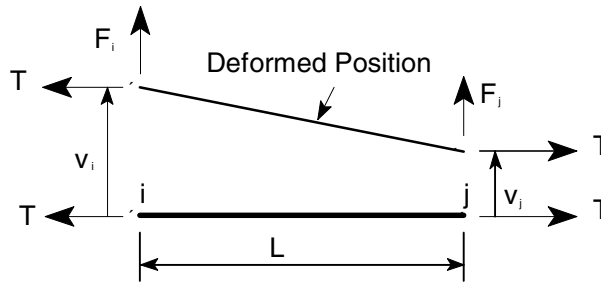
Figure 11.1 Forces Acting on a Cable Element

Taking moments about point j in the deformed position, the following equilibrium equation can be written:

$$F_i = \frac{T}{L}(v_i - v_j) \tag{11.1}$$

And from vertical equilibrium the following equation is apparent:

$$F_j = -F_i \tag{11.2}$$

Combining Equations 11.1 and 11.2, the lateral forces can be expressed in terms of the lateral displacements by the following matrix equation:

$$\begin{bmatrix} F_i \\ F_j \end{bmatrix} = \frac{T}{L} \begin{bmatrix} 1 & -1 \\ -1 & 1 \end{bmatrix} \begin{bmatrix} v_i \\ v_j \end{bmatrix} \qquad \text{or symbolically,} \qquad \mathbf{F_g} = \mathbf{k_g v} \tag{11.3}$$

Note that the 2 by 2 geometric stiffness matrix, $\mathbf{k_g}$, is not a function of the mechanical properties of the cable and is only a function of the element's length and the force in the element. Hence, the term "geometric" or "stress" stiffness matrix is introduced so that the matrix has a different name from the "mechanical" stiffness matrix, which is based on the physical properties of the element. The geometric stiffness exists in all structures; however, it becomes important only if it is large compared to the mechanical stiffness of the structural system.

In the case of a beam element with bending properties in which the deformed shape is assumed to be a cubic function caused by the rotations ϕ_i and ϕ_j at the ends, additional moments M_i and M_j are developed. From Reference [1] the force-displacement relationship is given by the following equation:

$$
\begin{bmatrix} F_i \\ M_i \\ F_j \\ M_j \end{bmatrix} = \frac{T}{30L} \begin{bmatrix} 36 & 3L & -36 & 3L \\ 3L & 4L^2 & -3L & -L^2 \\ -36 & -3L & 36 & -3L \\ 3L & -L^2 & -3L & 4L^2 \end{bmatrix} \begin{bmatrix} v_i \\ \phi_i \\ v_j \\ \phi_j \end{bmatrix} \qquad \text{or, } \mathbf{F}_G = \mathbf{k}_G \mathbf{v} \qquad (11.4)
$$

The well-known elastic force deformation relationship for a prismatic beam without shearing deformations is:

$$
\begin{bmatrix} F_i \\ M_i \\ F_j \\ M_j \end{bmatrix} = \frac{EI}{L^3} \begin{bmatrix} 12 & 6L & -12 & 6L \\ 6L & 4L^2 & -6L & -2L^2 \\ -12 & -6L & 12 & -6L \\ -6L & -2L^2 & -6L & 4L^2 \end{bmatrix} \begin{bmatrix} v_i \\ \phi_i \\ v_j \\ \phi_j \end{bmatrix} \qquad \text{or, } \mathbf{F}_E = \mathbf{k}_E \mathbf{v} \qquad (11.5)
$$

Therefore, the total forces acting on the beam element will be:

$$
\mathbf{F}_T = \mathbf{F}_E + \mathbf{F}_G = [\mathbf{k}_E + \mathbf{k}_G]\mathbf{v} = \mathbf{k}_T \mathbf{v} \qquad (11.6)
$$

Hence, if the large axial force in the member remains constant, it is only necessary to form the total stiffness matrix, $\mathbf{k}_T$, to account for this stress stiffening or softening effect.

11.2 APPROXIMATE BUCKLING ANALYSIS

In the case when the axial compressive force is large, $T = -P$, the total stiffness matrix of the beam can become singular. To illustrate this instability, consider the beam shown in Figure 11.2 with the displacements at point j set to zero.
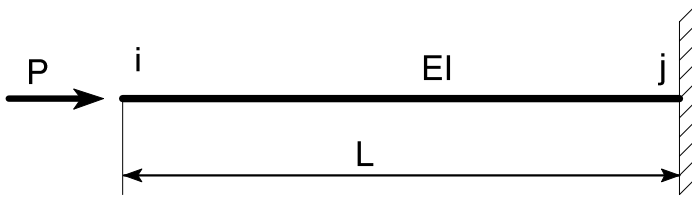
Figure 11.2 Cantilever Beam Subjected to Buckling Load

From Equation (11.6) the equilibrium equations for the beam shown in Figure 11.2 are in matrix form:

$$\begin{bmatrix} 12+36\lambda & 6L+3L\lambda \\ 6L+3L\lambda & 4L^2+4L^2\lambda \end{bmatrix} \begin{bmatrix} v_i \\ \phi_i \end{bmatrix} = \begin{bmatrix} 0 \\ 0 \end{bmatrix} \tag{11.7}$$

Where $\lambda = -\dfrac{PL^2}{30EI}$. This eigenvalue problem can be solved for the lowest root, which is:

$$\lambda_1 = -0.0858 \qquad \text{or} \qquad P_{cr} = 2.57\frac{EI}{L^2} \tag{11.8}$$

The well-known exact Euler buckling load for the cantilever beam is given by:

$$P_{cr} = \frac{\pi^2 EI}{4L^2} = 2.47\frac{EI}{L^2} \tag{11.9}$$

Therefore, the approximate solution Equation (11.8), which is based on a cubic shape, is within five percent of the exact solution.

If the straight line approximation is used, given by Equation (11.3), an approximate buckling load of $3.0\dfrac{EI}{L^2}$ is obtained. This is still a reasonable approximation.

11.3   P-DELTA ANALYSIS OF BUILDINGS

The use of the geometric stiffness matrix is a general approach to include secondary effects in the static and dynamic analysis of all types of structural systems. However, in Civil Structural Engineering it is commonly referred to as P-Delta Analysis that is based on a more physical approach. For example, in building analysis, the lateral movement of a story mass to a deformed position generates second-order overturning moments. This second-order behavior has been termed the P-Delta effect because the additional overturning moments on the building are equal to the sum of story weights "P" times the lateral displacements "Delta."

Many techniques have been proposed for evaluating this second-order behavior. Rutenberg [2] summarized the publications on this topic and presents a simplified method to include those second-order effects. Some methods consider the problem as one of geometric non-linearity and propose iterative solution techniques that can be numerically inefficient. Also, those iterative methods are not appropriate for dynamic analysis where the P-Delta effect causes lengthening of the periods of vibration. The equations presented in this section are not new. However, the simple approach used in their derivation should add physical insight to the understanding of P-Delta behavior in buildings [3].

The P-Delta problem can be linearized and the solution to the problem obtained *directly* and *exactly*, without iteration, in building type structures where the weight of the structure is constant during lateral motions and the overall structural displacements can be assumed to be small compared to the structural dimensions. Furthermore, the additional numerical effort required is negligible.

The method does not require iteration because the total axial force at a story level is equal to the weight of the building above that level and does not change during the application of lateral loads. Therefore, the sum of the column of geometric stiffness terms associated with the lateral loads is zero, and only the axial forces caused by the weight of the structure need to be included in the evaluation of the geometric stiffness terms for the complete building.

The effects of P-Delta are implemented in the basic analytical formulation thus causing the effects to be consistently included in both static and dynamic

analyses. The resulting structural displacements, mode shapes and frequencies include the effect of structural softening automatically. Member forces satisfy both static and dynamic equilibrium and reflect the additional P-Delta moments consistent with the calculated displacements.

(a) Displaced position
of story weights

(b) Additional overturning
moments or lateral loads
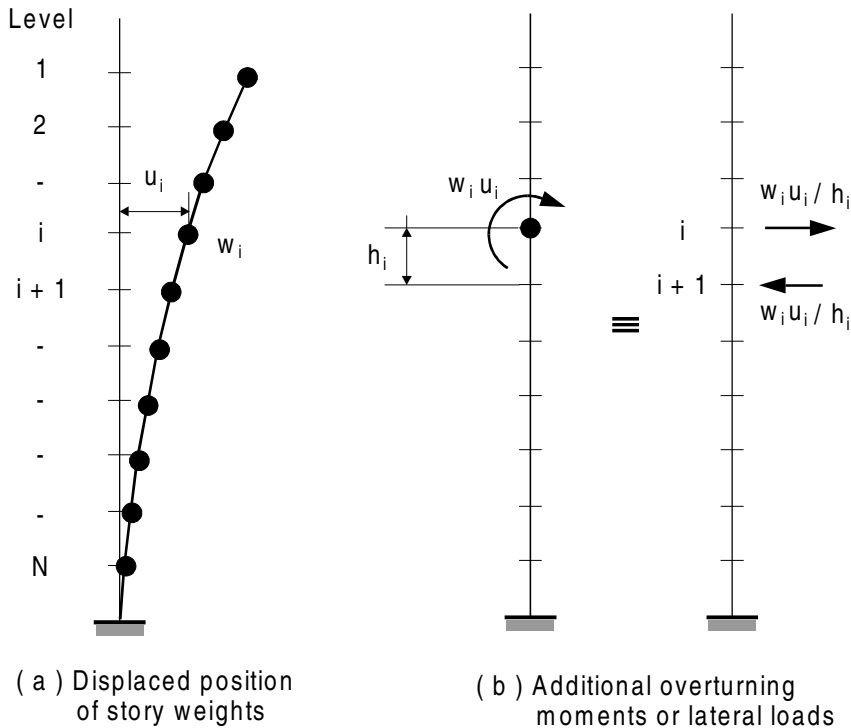
Figure 11.3 Overturning Loads Due to Translation of Story Weights

The vertical "cantilever type" structure shown in Figure 11.3 (a) is considered to illustrate the basic problem. Under lateral displacements, let us consider the additional overturning moments related to one mass, or story weight, at level i. The total overturning effects will be the sum of all story weight contributions. Figure 11.3 (b) indicates statically equivalent force systems that produce the same overturning moments. Or, in terms of matrix notation:

$$\begin{bmatrix} f_i \\ f_{i+1} \end{bmatrix} = \frac{w_i}{h_i} \begin{bmatrix} 1.0 \\ -1.0 \end{bmatrix} \begin{bmatrix} u_i \end{bmatrix} \tag{11.10}$$

The lateral forces shown in Figure 11.3 (b) can be evaluated for all stories and added to the external loads on the structure. The resulting lateral equilibrium equation of the structure is:

$$\mathbf{Ku} = \mathbf{F} + \mathbf{Lu} \tag{11.11}$$

where $\mathbf{K}$ is the lateral stiffness matrix with respect to the lateral story displacements $\mathbf{u}$. The vector $\mathbf{F}$ represents the known lateral loads and $\mathbf{L}$ is a matrix that contains w_i/h_i factors. Equation (11.11) can be rewritten in the form:

$$\mathbf{K}^* \mathbf{u} = \mathbf{F} \tag{11.12}$$

where $\mathbf{K}^* = \mathbf{K} - \mathbf{L}$

Equation (11.12) can be solved directly for the lateral displacements. If internal member forces are evaluated from these displacements, consistent with the linear theory used, it will be found that equilibrium with respect to the deformed position has been obtained. One minor problem exists with the solution of Equation (11.12); the matrix $\mathbf{K}^*$ is not symmetric. However, it can be made symmetric by replacing the lateral loads shown in Figure 11.3 (b) with another statically equivalent load system.

From simple statics the total contribution to overturning associated with the relative story displacement " u_i - u_{i+1} ," can be written as:

$$\begin{bmatrix} f_i \\ f_{i+1} \end{bmatrix} = \frac{W_i}{h_i} \begin{bmatrix} 1.0 & -1.0 \\ -1.0 & 1.0 \end{bmatrix} \begin{bmatrix} u_i \\ u_{i+1} \end{bmatrix} \tag{11.13}$$

where W_i is the total dead load weight above story i. The $\mathbf{L}$ matrix is now symmetrical and no special non-symmetric equation solver is required.

It is of significant interest to note that Equation (11.13) is the exact form of the "geometric stiffness," Equation (11.3), for a column, including axial force effects only. Therefore, the physical development given here is completely equivalent to the more theoretical approach normally used to formulate the incremental stiffness in nonlinear structural analysis.

The equilibrium of a complete building can be formulated in terms of the lateral displacement of the floor level. Then, one can evaluate the contribution to the total geometric stiffness for each column at a particular story level in which the effects of the external lateral loads **F** are included in the evaluation of the axial forces in all columns. If this approach is used, the total geometric stiffness at the lateral equilibrium level is identical to Equation (11.13) because the lateral axial forces **F** do not produce a net increase in the total of all axial forces that exist in the columns at any level. Such a refined analysis must be iterative in nature; however, it does not produce more exact results.

It is clear that the beam-column stiffness effects as defined by Equation (11.4) have been neglected. The errors associated with those cubic shape effects can be estimated at the time member forces are calculated. However, the method presented here does include the overall large displacement side-sway behavior of the complete structure that is associated with the global stability of the building.
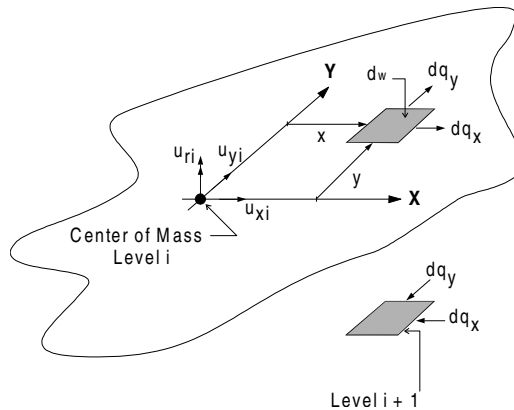
Figure 11.4 Mass Distribution at Typical Floor Level

11.4   EQUATIONS FOR THREE-DIMENSIONAL BUILDINGS

Equation (11.13) can be applied directly in both directions for buildings in which the centroids are the same for all story levels. However, for the more general building, the equations for the story couples are more complicated. A general three-dimensional building system is shown schematically in Figure 11.4.

It is assumed that the three-dimensional building stiffness of the system has been formulated with respect to the two lateral displacements, u_{xi}, u_{yi}, and rotation, u_{ri}, at the center of mass at each story level. In addition to the overturning forces given by Equation (11.13), secondary forces exist because of the distribution of the story mass over a finite floor size.

The first step before developing the 6 by 6 geometric stiffness matrix for each story is to calculate the location of the center of mass and the rotational moment of inertia for all story levels. For a typical story i, it is then necessary to calculate the total weight and centroid of the structure above that level. Because of the relative displacements between story i and story i + 1, from Equation 11.13, forces must be developed to maintain equilibrium. Those forces and displacements must then be transformed to the center of mass at both level i and i + 1.

11.5   THE MAGNITUDE OF P-DELTA EFFECTS

The comparison of the results of two analyses with and without P-Delta will illustrate the magnitude of the P-Delta effects. A well-designed building usually has well-conditioned level-by-level stiffness/weight ratios. For such structures, P-Delta effects are usually not very significant. The changes in displacements and member forces are less than 10%.

However, if the weight of the structure is high in proportion to the lateral stiffness of the structure, the contributions from the P-Delta effects are highly amplified and, under certain circumstances, can change the displacements and member forces by 25 percent or more. Excessive P-Delta effects will eventually introduce singularities into the solution, indicating physical structure instability. Such behavior is clearly indicative of a poorly designed structure that is in need of additional stiffness.

An analysis of a 41-story steel building was conducted with and without P-Delta effects. The basic construction was braced frame and welded steel shear wall. The building was constructed in a region where the principal lateral loading is wind. The results are summarized in Table 11.1.

Table 11.1 P-Delta Effects on Typical Building

	Without P-Delta	With P-Delta
First Mode Period (seconds)	5.33	5.52
Second Mode Period (seconds)	4.21	4.30
Third Mode Period (seconds)	4.01	4.10
Fourth Mode Period (seconds)	1.71	1.75
Wind Displacement (inches)	7.99	8.33

Because the building is relatively stiff, the P-Delta effects are minimal. Also, it is apparent that P-Delta effects are less important for higher frequencies.

11.6 P-DELTA ANALYSIS WITHOUT COMPUTER PROGRAM MODIFICATION

Many engineers are using general purpose, structural analysis programs for buildings that cannot be easily modified to include the equations presented here. Equation 11.4 presents the form of the lateral force-displacement equations for story i. We note that the form of this 2 x 2 geometric stiffness matrix is the same as the stiffness matrix for a prismatic column that has zero rotations at the top and bottom. Therefore, it is possible to add "dummy columns" between story levels of the building and assign appropriate properties to achieve the same effects as the use of geometric stiffness [2]. The force-displacement equations of the "dummy column" are:

$$\begin{bmatrix} f_i \\ f_{i+1} \end{bmatrix} = \frac{12EI}{h_i^3} \begin{bmatrix} 1 & -1 \\ -1 & 1 \end{bmatrix} \begin{bmatrix} u_i \\ u_{i+1} \end{bmatrix} \tag{11.14}$$

Therefore, if the moment of inertia of the column is selected as:

$$I = -\frac{W_i h_i^2}{12E} \tag{11.15}$$

The dummy column will have the same negative stiffness values as the linear geometric stiffness.

11.7   EFFECTIVE LENGTH - K FACTORS

The solution procedure for the P-Delta effects described in this chapter has been implemented and verified in the ETABS program. The application of the method of analysis presented in this chapter should lead to the elimination of the column effective length (K-) factors, since the P-Delta effects automatically produce the required design moment amplifications. Also, the K-factors are approximate, complicated, and time-consuming to calculate. Building codes for concrete [4] and steel [5] now allow explicit accounting of P-Delta effects as an alternative to the more involved and approximate methods of calculating moment magnification factors for most column designs.

11.8   GENERAL FORMULATION OF GEOMETRY STIFFNESS

It is relatively simple to develop the geometric stiffness matrix for any type of displacement-based finite element [1]. It is only necessary to add to the linear strain-displacement equations, Equations (2.3a-f), the higher order nonlinear terms. These large strain equations, in a local x-y-z reference system, are:

$$\varepsilon_x = \frac{\partial u_x}{\partial x} + \frac{1}{2}\overline{\mathbf{u}}_{,x}^T\overline{\mathbf{u}}_{,x}$$

$$\varepsilon_y = \frac{\partial u_y}{\partial y} + \frac{1}{2}\overline{\mathbf{u}}_{,y}^T\overline{\mathbf{u}}_{,y}$$

$$\varepsilon_z = \frac{\partial u_z}{\partial z} + \frac{1}{2}\overline{\mathbf{u}}_{,z}^T\overline{\mathbf{u}}_{,z}$$

$$\gamma_{xy} = \frac{\partial u_x}{\partial y} + \frac{\partial u_y}{\partial x} + \frac{1}{2}\overline{\mathbf{u}}_{,x}^T\overline{\mathbf{u}}_{,y} + \frac{1}{2}\overline{\mathbf{u}}_{,y}^T\overline{\mathbf{u}}_{,x}$$

$$\gamma_{xz} = \frac{\partial u_x}{\partial z} + \frac{\partial u_z}{\partial x} + \frac{1}{2}\overline{\mathbf{u}}_{,x}^T\overline{\mathbf{u}}_{,z} + \frac{1}{2}\overline{\mathbf{u}}_{,z}^T\overline{\mathbf{u}}_{,x}$$

$$\gamma_{yz} = \frac{\partial u_y}{\partial z} + \frac{\partial u_z}{\partial x} + \frac{1}{2}\overline{\mathbf{u}}_{,y}^T\overline{\mathbf{u}}_{,z} + \frac{1}{2}\overline{\mathbf{u}}_{,z}^T\overline{\mathbf{u}}_{,y}$$

(11.16)

The nonlinear terms are the product of matrices that are defined as:

$$\overline{\mathbf{u}}_{,x} = \begin{bmatrix} u_{x,x} \\ u_{y,x} \\ u_{z,x} \end{bmatrix}, \quad \overline{\mathbf{u}}_{,y} = \begin{bmatrix} u_{x,y} \\ u_{y,y} \\ u_{z,y} \end{bmatrix}, \quad \overline{\mathbf{u}}_{,z} = \begin{bmatrix} u_{x,z} \\ u_{y,z} \\ u_{z,z} \end{bmatrix} \qquad (11.17)$$

Equation (11.16) can be expressed in terms of the following sum of linear and nonlinear components:

$$\mathbf{d} = \mathbf{d}_L + \mathbf{d}_N \qquad (11.18)$$

These strain-displacement equations, written in terms of engineering strains and in matrix notation, are identical to the classical Green-Lagrange strains. This is often referred to as the total Lagrangian approach in which the strains are computed with respect to the original reference system and the large rigid-body rotation is exact.

Using the same shape functions as used to form the element stiffness matrix, the derivatives of the displacements can be written as:

$$\mathbf{g} = \mathbf{G}\mathbf{u} \qquad (11.19)$$

If the initial stresses are large, the potential energy of the structure must be modified by the addition of the following term:

$$\Omega_\sigma = \frac{1}{2} \int \begin{bmatrix} \overline{\mathbf{u}}_{,x}^T & \overline{\mathbf{u}}_{,y}^T & \overline{\mathbf{u}}_{,z}^T \end{bmatrix} \begin{bmatrix} \mathbf{s}_{xx} & \mathbf{s}_{xy} & \mathbf{s}_{xz} \\ \mathbf{s}_{yx} & \mathbf{s}_{yy} & \mathbf{s}_{yz} \\ \mathbf{s}_{zx} & \mathbf{s}_{zy} & \mathbf{s}_{zz} \end{bmatrix} \begin{bmatrix} \overline{\mathbf{u}}_{,x} \\ \overline{\mathbf{u}}_{,y} \\ \overline{\mathbf{u}}_{,z} \end{bmatrix} dV = \frac{1}{2} \int \mathbf{g}^T \mathbf{S} \mathbf{g} \, dV \quad (11.20)$$

The 3 by 3 initial stress matrices are of the following form:

$$\mathbf{s}_{ij} = \begin{bmatrix} \sigma_{ij} & 0 & 0 \\ & \sigma_{ij} & 0 \\ 0 & 0 & \sigma_{ij} \end{bmatrix}_0 \qquad (11.21)$$

where the initial stresses are defined as:

$$\mathbf{s}_0^T = \begin{bmatrix} \sigma_{xx} & \sigma_{yy} & \sigma_{zz} & \sigma_{xy} & \sigma_{xz} & \sigma_{yz} \end{bmatrix}_0 \qquad (11.22)$$

Therefore, the geometric stiffness for any element can be calculated from:

$$\mathbf{k}_g = \int \mathbf{G}^T \mathbf{S} \mathbf{G} dV \tag{11.23}$$

For most finite elements the geometric stiffness is evaluated by numerical integration.

11.9 SUMMARY

The SAP2000 program has the option to add a three-dimensional geometric stiffness matrix to each frame element. Therefore, guyed towers, cable stay and suspension bridges can be modeled if the tension in the cable is not modified by the application of the load. If the initial axial forces in the elements are significantly changed by the addition of loads, iteration may be required. However, in the case of dynamic analysis, the evaluation of the eigen or LDR vectors must be based on one set of axial forces.

Most traditional methods for incorporating P-Delta effects in analysis of buildings are based on iterative techniques. Those techniques are time-consuming and are, in general, used for static analysis only. For building structures, the mass that causes the P-Delta effect is constant irrespective of the lateral loads and displacements. This information is used to linearize the P-Delta effect for buildings and solve the problem "exactly," satisfying equilibrium in the deformed position without iterations. An algorithm is developed that incorporates P-Delta effects into the basic formulation of the structural stiffness matrix as a geometric stiffness correction. This procedure can be used for static and dynamic analysis and will account for the lengthening of the periods and changes in mode shapes caused by P-Delta effects.

A well designed building should not have significant P-Delta effects. Analyses *with and without the P-Delta effects* will yield the magnitude of the P-Delta effects separately. If those lateral displacements differ by more than 5% *for the same lateral load*, the basic design may be too flexible and a redesign should be considered.

The current SEAOC Blue Book states "the drift ratio of $0.02/R_w$ serves to define the threshold of deformation beyond which there may be significant P-Delta effects." Clearly, if one includes P-Delta effects in all analyses, one can

disregard this statement. If the loads acting on the structure have been reduced by a ductility factor R_w, however, the P-Delta effects should be amplified by R_w to reflect ultimate load behavior. This can be automatically included in a computer program using a multiplication factor for the geometric stiffness terms.

It is possible to calculate geometric stiffness matrices for all types of finite elements. The same shape functions used in developing the elastic stiffness matrices are used in calculating the geometric stiffness matrix.

11.10   REFERENCES

1. Cook, R. D., D. S. Malkus and M. E. Plesha. 1989. *Concepts and Applications of Finite Element Analysis*, Third Edition. John Wiley & Sons, Inc. ISBN 0-471-84788-7.

2. Rutenberg, A. 1982. "Simplified P-Delta Analysis for Asymmetric Structures," *ASCE Journal of the Structural Division*. Vol. 108, No. 9. September.

3. Wilson, E. L. and A. Habibullah. 1987. "Static and Dynamic Analysis of Multi-Story Buildings Including P-Delta Effects," *Earthquake Spectra.* Vol. 3, No.3. Earthquake Engineering Research Institute. May.

4. American Concrete Institute. 1995. *Building Code Requirements for Reinforced Concrete (ACI 318-95) and Commentary (ACI 318R-95).* Farmington Hills, Michigan.

5. American Institute of Steel Construction, Inc. 1993. *Load and Resistance Factor Design Specification for Structural Steel Buildings.* Chicago, Illinois. December.

12.

DYNAMIC ANALYSIS

Force Equilibrium is Fundamental in
the Dynamic Analysis of Structures

12.1 INTRODUCTION

All real physical structures behave dynamically when subjected to loads or displacements. The additional inertia forces, *from Newton's second law*, are equal to the mass times the acceleration. If the loads or displacements are applied very slowly, the inertia forces can be neglected and a static load analysis can be justified. Hence, dynamic analysis is a simple extension of static analysis.

In addition, all real structures potentially have an infinite number of displacements. Therefore, the most critical phase of a structural analysis is to create a computer model with a finite number of massless members and a finite number of node (joint) displacements that will simulate the behavior of the real structure. The mass of a structural system, which can be accurately estimated, is lumped at the nodes. Also, for linear elastic structures, the stiffness properties of the members can be approximated with a high degree of confidence with the aid of experimental data. However, the dynamic loading, energy dissipation properties and boundary (foundation) conditions for many structures are difficult to estimate. This is always true for the cases of seismic input or wind loads.

To reduce the errors that may be caused by the approximations summarized in the previous paragraph, it is necessary to conduct many different dynamic analyses using different computer models, loading and boundary conditions. It is

not unrealistic to conduct 20 or more computer runs to design a new structure or to investigate retrofit options for an existing structure.

Because of the large number of computer runs required for a typical dynamic analysis, it is very important that accurate and numerically efficient methods be used within computer programs. Some of those methods have been developed by the author and are relatively new. Therefore, one of the purposes of this book is to summarize those numerical algorithms, their advantages and limitations.

12.2 DYNAMIC EQUILIBRIUM

The force equilibrium of a multi-degree-of-freedom lumped mass system as a function of time can be expressed by the following relationship:

$$\mathbf{F}(t)_I + \mathbf{F}(t)_D + \mathbf{F}(t)_S = \mathbf{F}(t) \tag{12.1}$$

in which the force vectors at time t are:

$\mathbf{F}(t)_I$ is a vector of inertia forces acting on the node masses

$\mathbf{F}(t)_D$ is a vector of viscous damping, or energy dissipation, forces

$\mathbf{F}(t)_S$ is a vector of internal forces carried by the structure

$\mathbf{F}(t)$ is a vector of externally applied loads

Equation (12.1) is based on physical laws and is valid for both linear and nonlinear systems if equilibrium is formulated with respect to the deformed geometry of the structure.

For many structural systems, the approximation of linear structural behavior is made to convert the physical equilibrium statement, Equation (12.1), to the following set of second-order, linear, differential equations:

$$\mathbf{M}\ddot{\mathbf{u}}(t)_a + \mathbf{C}\dot{\mathbf{u}}(t)_a + \mathbf{K}\mathbf{u}(t)_a = \mathbf{F}(t) \tag{12.2}$$

in which $\mathbf{M}$ is the mass matrix (lumped or consistent), $\mathbf{C}$ is a viscous damping matrix (which is normally selected to approximate energy dissipation in the real

structure) and $\mathbf{K}$ is the static stiffness matrix for the system of structural elements. The time-dependent vectors $\mathbf{u}(t)_a$, $\dot{\mathbf{u}}(t)_a$ and $\ddot{\mathbf{u}}(t)_a$ are the absolute node displacements, velocities and accelerations, respectively.

Many books on structural dynamics present several different methods of applied mathematics to obtain the exact solution of Equation (12.2). Within the past several years, however, with the general availability of inexpensive, high-speed personal computers (see Appendix H), the exact solution of Equation (12.2) can be obtained without the use of complex mathematical techniques. Therefore, the modern structural engineer who has a physical understanding of dynamic equilibrium and energy dissipation can perform dynamic analysis of complex structural systems. A strong engineering mathematical background is desirable; however, in my opinion, it is no longer mandatory.

For seismic loading, the external loading $\mathbf{F}(t)$ is equal to zero. The basic seismic motions are the three components of free-field ground displacements $u(t)_{ig}$ that are known at some point below the foundation level of the structure. Therefore, we can write Equation (12.2) in terms of the displacements $\mathbf{u}(t)$, velocities $\dot{\mathbf{u}}(t)$ and accelerations $\ddot{\mathbf{u}}(t)$ that are relative to the three components of free-field ground displacements.

Therefore, the absolute displacements, velocities and accelerations can be eliminated from Equation (12.2) by writing the following simple equations:

$$\mathbf{u}(t)_a = \mathbf{u}(t) + \mathbf{I}_x u(t)_{xg} + \mathbf{I}_y u(t)_{yg} + \mathbf{I}_z u(t)_{zg}$$

$$\dot{\mathbf{u}}(t)_a = \dot{\mathbf{u}}(t) + \mathbf{I}_x \dot{u}(t)_{xg} + \mathbf{I}_y \dot{u}(t)_{yg} + \mathbf{I}_z \dot{u}(t)_{zg} \qquad (12.3)$$

$$\ddot{\mathbf{u}}(t)_a = \ddot{\mathbf{u}}(t) + \mathbf{I}_x \ddot{u}(t)_{xg} + \mathbf{I}_y \ddot{u}(t)_{yg} + \mathbf{I}_z \ddot{u}(t)_{zg}$$

where $\mathbf{I}_i$ is a vector with ones in the "i" directional degrees-of-freedom and zero in all other positions. The substitution of Equation (12.3) into Equation (12.2) allows the node point equilibrium equations to be rewritten as:

$$\mathbf{M}\ddot{\mathbf{u}}(t) + \mathbf{C}\dot{\mathbf{u}}(t) + \mathbf{K}\mathbf{u}(t) = -\mathbf{M}_x \ddot{u}(t)_{xg} - \mathbf{M}_y \ddot{u}(t)_{yg} - \mathbf{M}_z \ddot{u}(t)_{zg} \qquad (12.4)$$

where $\mathbf{M}_i = \mathbf{M}\mathbf{I}_i$.

The simplified form of Equation (12.4) is possible since the rigid body velocities and displacements associated with the base motions cause no additional damping or structural forces to be developed.

It is important for engineers to realize that the displacements, which are normally printed by a computer program, are relative displacements and that the fundamental loading on the structure is foundation displacements and not externally applied loads at the joints of the structure. For example, the static pushover analysis of a structure is a poor approximation of the dynamic behavior of a three-dimensional structure subjected to complex time-dependent base motions. Also, one must calculate absolute displacements to properly evaluate base isolation systems.

There are several different classical methods that can be used for the solution of Equation (12.4). Each method has advantages and disadvantages that depend on the type of structure and loading. To provide a general background for the various topics presented in this book, the different numerical solution methods are summarized below.

12.3   STEP-BY-STEP SOLUTION METHOD

The most general solution method for dynamic analysis is an incremental method in which the equilibrium equations are solved at times $\Delta t, 2\Delta t, 3\Delta t$, etc. There are a large number of different incremental solution methods. In general, they involve a solution of the complete set of equilibrium equations at each time increment. In the case of nonlinear analysis, it may be necessary to reform the stiffness matrix for the complete structural system for each time step. Also, iteration may be required within each time increment to satisfy equilibrium. As a result of the large computational requirements, it can take a significant amount of time to solve structural systems with just a few hundred degrees-of-freedom.

In addition, artificial or numerical damping must be added to most incremental solution methods to obtain stable solutions. For this reason, engineers must be very careful in the interpretation of the results. For some nonlinear structures subjected to seismic motions, incremental solution methods are necessary.

For very large structural systems, a combination of mode superposition and incremental methods has been found to be efficient for systems with a small number of nonlinear members. This method has been incorporated into the new versions of SAP and ETABS and will be presented in detail later in this book.

12.4   MODE SUPERPOSITION METHOD

The most common and effective approach for seismic analysis of linear structural systems is the mode superposition method. After a set of orthogonal vectors have been evaluated, this method reduces the large set of global equilibrium equations to a relatively small number of uncoupled second order differential equations. The numerical solution of those equations involves greatly reduced computational time.

It has been shown that seismic motions excite only the lower frequencies of the structure. Typically, earthquake ground accelerations are recorded at increments of 200 points per second. Therefore, the basic loading data does not contain information over 50 cycles per second. Hence, neglecting the higher frequencies and mode shapes of the system normally does not introduce errors.

12.5   RESPONSE SPECTRA ANALYSIS

The basic mode superposition method, which is restricted to linearly elastic analysis, produces the complete time history response of joint displacements and member forces because of a specific ground motion loading [1, 2]. There are two major disadvantages of using this approach. First, the method produces a large amount of output information that can require an enormous amount of computational effort to conduct all possible design checks as a function of time. Second, the analysis must be repeated for several different earthquake motions to ensure that all the significant modes are excited, because a response spectrum for one earthquake, in a specified direction, is not a smooth function.

There are significant computational advantages in using the response spectra method of seismic analysis for prediction of displacements and member forces in structural systems. The method involves the calculation of only the maximum

values of the displacements and member forces in each mode using smooth design spectra that are the average of several earthquake motions. In this book, we will recommend the CQC method to combine these maximum modal response values to obtain the most probable peak value of displacement or force. In addition, it will be shown that the SRSS and CQC3 methods of combining results from orthogonal earthquake motions will allow one dynamic analysis to produce design forces for all members in the structure.

12.6 SOLUTION IN THE FREQUENCY DOMAIN

The basic approach used to solve the dynamic equilibrium equations in the frequency domain is to expand the external loads $\mathbf{F}(t)$ in terms of Fourier series or Fourier integrals. The solution is in terms of complex numbers that cover the time span from $-\infty$ to ∞. Therefore, it is very effective for periodic types of loads such as mechanical vibrations, acoustics, sea-waves and wind [1]. However, the use of the frequency domain solution method for solving structures subjected to earthquake motions has the following disadvantages:

1. The mathematics for most structural engineers, including myself, is difficult to understand. Also, the solutions are difficult to verify.

2. Earthquake loading is not periodic; therefore, it is necessary to select a long time period so that the solution from a finite length earthquake is completely damped out before application of the same earthquake at the start of the next period of loading.

3. For seismic type loading, the method is not numerically efficient. The transformation of the result from the frequency domain to the time domain, even with the use of Fast Fourier Transformation methods, requires a significant amount of computational effort.

4. The method is restricted to the solution of linear structural systems.

5. The method has been used, without sufficient theoretical justification, for the approximate nonlinear solution of site response problems and soil/structure interaction problems. Typically, it is used in an iterative manner to create linear equations. The linear damping terms are changed after each iteration to

approximate the energy dissipation in the soil. Hence, dynamic equilibrium within the soil is not satisfied.

12.7 SOLUTION OF LINEAR EQUATIONS

The step-by-step solution of the dynamic equilibrium equations, the solution in the frequency domain, and the evaluation of eigenvectors and Ritz vectors all require the solution of linear equations of the following form:

$$\mathbf{AX} = \mathbf{B} \tag{12.5}$$

Where $\mathbf{A}$ is an 'N by N' symmetric matrix that contains a large number of zero terms. The 'N by M' $\mathbf{X}$ displacement and $\mathbf{B}$ load matrices indicate that more than one load condition can be solved at the same time.

The method used in many computer programs, including SAP2000 [5] and ETABS [6], is based on the profile or active column method of compact storage. Because the matrix is symmetric, it is only necessary to form and store the first non-zero term in each column down to the diagonal term in that column. Therefore, the sparse square matrix can be stored as a one-dimensional array along with a *N by 1* integer array that indicates the location of each diagonal term. If the stiffness matrix exceeds the high-speed memory capacity of the computer, a block storage form of the algorithm exists. Therefore, the capacity of the solution method is governed by the low speed disk capacity of the computer. This solution method is presented in detail in Appendix C of this book.

12.8 UNDAMPED HARMONIC RESPONSE

The most common and very simple type of dynamic loading is the application of steady-state harmonic loads of the following form:

$$\mathbf{F}(t) = \mathbf{f} \sin(\overline{\omega}t) \tag{12.6}$$

The node point distribution of all static load patterns, $\mathbf{f}$, which are not a function of time, and the frequency of the applied loading, $\overline{\omega}$, are user

specified. Therefore, for the case of zero damping, the exact node point equilibrium equations for the structural system are:

$$\mathbf{M\ddot{u}}(t) + \mathbf{Ku}(t) = \mathbf{f}\sin(\overline{\omega}t) \qquad (12.7)$$

The exact steady-state solution of this equation requires that the node point displacements and accelerations are given by:

$$\mathbf{u}(t) = \mathbf{v}\sin(\overline{\omega}t), \qquad \mathbf{\ddot{u}}(t) = -\mathbf{v}\,\overline{\omega}^2\sin(\overline{\omega}t) \qquad (12.8)$$

Therefore, the harmonic node point response amplitude is given by the solution of the following set of linear equations:

$$[\mathbf{K} - \overline{\omega}^2\mathbf{M}]\mathbf{v} = \mathbf{f} \qquad \text{or} \quad \overline{\mathbf{K}}\mathbf{v} = \mathbf{f} \qquad (12.9)$$

It is of interest to note that the normal solution for static loads is nothing more than a solution of this equation for zero frequency for all loads. It is apparent that the computational effort required for the calculation of undamped steady-state response is almost identical to that required by a static load analysis. Note that it is not necessary to evaluate mode shapes or frequencies to solve for this very common type of loading. The resulting node point displacements and member forces vary as $\sin(\overline{\omega}t)$. However, other types of loads that do not vary with time, such as dead loads, must be evaluated in a separate computer run.

12.9   UNDAMPED FREE VIBRATIONS

Most structures are in a continuous state of dynamic motion because of random loading such as wind, vibrating equipment, or human loads. These small ambient vibrations are normally near the natural frequencies of the structure and are terminated by energy dissipation in the real structure. However, special instruments attached to the structure can easily measure the motion. Ambient vibration field tests are often used to calibrate computer models of structures and their foundations.

After all external loads have been removed from the structure, the equilibrium equation, which governs the undamped free vibration of a typical displaced shape **v,** is:

$$\mathbf{M\ddot{v} + Kv = 0} \tag{12.10}$$

At any time, the displaced shape **v** may be a natural mode shape of the system, or any combination of the natural mode shapes. However, it is apparent the total energy within an undamped free vibrating system is a constant with respect to time. The sum of the kinetic energy and strain energy at all points in time is a constant that is defined as the ***mechanical energy*** of the dynamic system and calculated from:

$$E_M = \frac{1}{2}\mathbf{\dot{v}^T M \dot{v}} + \frac{1}{2}\mathbf{v^T Kv} \tag{12.11}$$

12.10 SUMMARY

Dynamic analysis of three-dimensional structural systems is a direct extension of static analysis. The elastic stiffness matrices are the same for both dynamic and static analysis. It is only necessary to lump the mass of the structure at the joints. The addition of inertia forces and energy dissipation forces will satisfy dynamic equilibrium. The dynamic solution for steady state harmonic loading, without damping, involves the same numerical effort as a static solution. Classically, there are many different mathematical methods to solve the dynamic equilibrium equations. However, it will later be shown in this book that the majority of both linear and nonlinear systems can be solved with one numerical method.

Energy is fundamental in dynamic analysis. At any point in time, the external work supplied to the system must be equal to the sum of the kinetic and strain energy plus the energy dissipated in the system.

It is my opinion, with respect to earthquake resistant design, that we should try to minimize the mechanical energy in the structure. It is apparent that a rigid structure will have only kinetic energy and zero strain energy. On the other hand, a completely base isolated structure will have zero kinetic energy and zero strain energy. A structure cannot fail if it has zero strain energy.

12.11 REFERENCES

1. Clough, R., and J. Penzien. 1993. *Dynamics of Structures*, Second Edition. McGraw-Hill, Inc. ISBN 0-07-011394-7.

2. Chopra, A. 1995. *Dynamics of Structures*. Prentice-Hall, Inc. Englewood Cliffs, New Jersey, 07632. ISBN 0-13-855214-2.

3. Bathe, K. 1982. *Finite Element Procedures in Engineering Analysis*. Prentice-Hall, Inc. Englewood Cliffs, New Jersey 07632. ISBN 0-13-317305-4.

4. Wilson, E. L., and K. Bathe. 1973. "Stability and Accuracy Analysis of Direct Integration Methods," *Earthquake Engineering and Structural Dynamics.* Vol. 1. pp. 283-291.

5. Computers and Structures, Inc. 1997. *SAP2000 - Integrated Structural Analysis & Design Software.* Berkeley, California.

6. Habibullah, A. 1997. *ETABS - Three Dimensional Analysis of Building Systems, User's Manual*. Computers and Structures Inc. Berkeley, California.

DYNAMIC ANALYSIS USING MODE SUPERPOSITION

The Mode Shapes used to Uncouple the Dynamic Equilibrium Equations Need Not Be the Exact Free-Vibration Mode Shapes

13.1 EQUATIONS TO BE SOLVED

The dynamic force equilibrium Equation (12.4) can be rewritten in the following form as a set of N_d second order differential equations:

$$\mathbf{M\ddot{u}}(t) + \mathbf{C\dot{u}}(t) + \mathbf{Ku}(t) = \mathbf{F}(t) = \sum_{j=1}^{J} \mathbf{f}_j \mathbf{g}(t)_j \qquad (13.1)$$

All possible types of time-dependent loading, including wind, wave and seismic, can be represented by a sum of "J" space vectors $\mathbf{f}_j$, which are not a function of time, and J time functions $\mathbf{g}(t)_j$.

The number of dynamic degrees of freedom is equal to the number of lumped masses in the system. Many publications advocate the elimination of all massless displacements by static condensation before solution of Equation (13.1). The static condensation method reduces the number of dynamic equilibrium equations to solve; however, it can significantly increase the density and the bandwidth of the condensed stiffness matrix. In building type structures, in which each diaphragm has only three lumped masses, this approach is effective and is automatically used in building analysis programs.

For the dynamic solution of arbitrary structural systems, however, the elimination of the massless displacement is, in general, not numerically efficient. Therefore, the modern versions of the SAP program do not use static condensation to retain the sparseness of the stiffness matrix.

13.2   TRANSFORMATION TO MODAL EQUATIONS

The fundamental mathematical method that is used to solve Equation (13.1) is the separation of variables. This approach assumes the solution can be expressed in the following form:

$$\mathbf{u}(t) = \mathbf{\Phi}\mathbf{Y}(t) \tag{13.2a}$$

Where $\mathbf{\Phi}$ is an "N_d by N" matrix containing N spatial vectors that are not a function of time, and $\mathbf{Y}(t)$ is a vector containing N functions of time.

From Equation (13.2a), it follows that:

$$\dot{\mathbf{u}}(t) = \mathbf{\Phi}\dot{\mathbf{Y}}(t) \quad \text{and} \quad \ddot{\mathbf{u}}(t) = \mathbf{\Phi}\ddot{\mathbf{Y}}(t) \tag{13.2b and 13.2c}$$

Before solution, we require that the space functions satisfy the following mass and stiffness orthogonality conditions:

$$\mathbf{\Phi}^T\mathbf{M}\mathbf{\Phi} = \mathbf{I} \quad \text{and} \quad \mathbf{\Phi}^T\mathbf{K}\mathbf{\Phi} = \mathbf{\Omega}^2 \tag{13.3}$$

where $\mathbf{I}$ is a diagonal unit matrix and Ω^2 is a diagonal matrix in which the diagonal terms are ω_n^2. The term ω_n has the units of radians per second and may or may not be a free vibration frequencies. It should be noted that the fundamentals of mathematics place no restrictions on those vectors, other than the orthogonality properties. In this book each space function vector, ϕ_n, is always normalized so that the ***Generalized Mass*** is equal to one, or $\phi_n^T\mathbf{M}\phi_n = 1.0$.

After substitution of Equations (13.2) into Equation (13.1) and the pre-multiplication by $\mathbf{\Phi}^T$, the following matrix of N equations is produced:

$$\mathbf{I}\ddot{\mathbf{Y}}(t) + \mathbf{d}\dot{\mathbf{Y}}(t) + \Omega^2 \mathbf{Y}(t) = \sum_{j=1}^{J} \mathbf{p}_j \mathbf{g}(t)_j \tag{13.4}$$

where $\mathbf{p}_j = \Phi^T \mathbf{f}_j$ and are defined as the *modal participation factors* for load function j. The term p_{nj} is associated with the nth mode. Note that there is one set of "N" modal participation factors for each spatial load condition $\mathbf{f}_j$.

For all real structures, the "N by N" matrix $\mathbf{d}$ is not diagonal; however, to uncouple the modal equations, it is necessary to assume *classical damping* where there is no coupling between modes. Therefore, the diagonal terms of the modal damping are defined by:

$$d_{nn} = 2\zeta_n \omega_n \tag{13.5}$$

where ζ_n is defined as the ratio of the damping in mode n to the critical damping of the mode [1].

A typical uncoupled modal equation for linear structural systems is of the following form:

$$\ddot{y}(t)_n + 2\zeta_n \omega_n \dot{y}(t)_n + \omega_n^2 y(t)_n = \sum_{j=1}^{J} p_{nj} g(t)_j \tag{13.6}$$

For three-dimensional seismic motion, this equation can be written as:

$$\ddot{y}(t)_n + 2\zeta_n \omega_n \dot{y}(t)_n + \omega_n^2 y(t)_n = p_{nx} \ddot{u}(t)_{gx} + p_{ny} \ddot{u}(t)_{gy} + p_{nz} \ddot{u}(t)_{gz} \tag{13.7}$$

where the three-directional modal participation factors, or in this case *earthquake excitation factors*, are defined by $p_{nj} = -\phi_n^{\,\cdot} \mathbf{M}_j$ in which j is equal to x, y or z and n is the mode number. Note that all mode shapes in this book are normalized so that $\phi_n^T \mathbf{M}\phi_n = 1$.

13.3   RESPONSE DUE TO INITIAL CONDITIONS ONLY

Before presenting the solution of Equation (13.6) for various types of loading, it is convenient to define additional constants and functions that are summarized in

Table 13.1. This will allow many of the equations presented in other parts of this book to be written in a compact form. Also, the notation reduces the tedium involved in the algebraic derivation and verification of various equations. In addition, it will allow the equations to be in a form that can be easily programmed and verified.

If the "n" subscript is dropped, Equation (13.6) can be written for a typical mode as:

$$\ddot{y}(t) + 2\xi\omega\dot{y}(t) + \omega^2 y(t) = 0 \tag{13.8}$$

in which the initial modal displacement y_0 and velocity $\dot{y}_0$ are specified as a result of previous loading acting on the structure. Note that the functions $S(t)$ and $C(t)$ given in Table 13.1 are solutions to Equation (13.8).

Table 13.1 Summary of Notation used in Dynamic Response Equations

---

CONSTANTS

$$\omega_D = \omega\sqrt{1-\xi^2} \qquad\qquad \overline{\omega} = \omega\xi \qquad\qquad \overline{\xi} = \frac{\xi}{\sqrt{1-\xi^2}}$$

$$a_0 = 2\xi\omega \qquad\qquad a_1 = \omega_D^2 - \overline{\omega}^2 \qquad\qquad a_2 = 2\overline{\omega}\omega_D$$

FUNCTIONS

$$S(t) = e^{-\xi\omega t}\sin(\omega_D t) \qquad\qquad C(t) = e^{-\xi\omega t}\cos(\omega_D t)$$

$$\dot{S}(t) = -\overline{\omega}S(t) + \omega_D C(t) \qquad\qquad \dot{C}(t) = -\overline{\omega}C(t) - \omega_D S(t)$$

$$\ddot{S}(t) = -a_1 S(t) - a_2 C(t) \qquad\qquad \ddot{C}(t) = -a_1 C(t) + a_2 S(t)$$

$$A_1(t) = C(t) + \overline{\xi}S(t) \qquad\qquad A_2(t) = \frac{1}{\omega_D}S(t)$$

The solution of Equation (13.8) can now be written in the following compact form:

$$y(t) = A_1(t)y_0 + A_2(t)\dot{y}_0 \tag{13.9}$$

This solution can be easily verified because it satisfies Equation (13.8) and the initial conditions.

13.4   GENERAL SOLUTION DUE TO ARBITRARY LOADING

There are many different methods available to solve the typical modal equations. However, the use of the exact solution for a load, approximated by a polynomial within a small time increment, has been found to be the most economical and accurate method to numerically solve this equation within computer programs. It does not have problems with stability, and it does not introduce numerical damping. Because most seismic ground accelerations are defined as linear within 0.005 second intervals, the method is exact for this type of loading for all frequencies. Also, if displacements are used as the basic input, the load function derived from linear accelerations are cubic functions within each time interval, as shown in Appendix J.

To simplify the notation, all loads are added together to form a typical modal equation of the following form:

$$\ddot{y}(t) + 2\zeta\omega\dot{y}(t) + \omega^2 y(t) = R(t) \tag{13.10}$$

where the modal loading $R(t)$ is a piece-wise polynomial function as shown in Figure 13.1. Note that the higher derivatives required by the cubic load function can be calculated using the numerical method summarized in Appendix J. Therefore, the differential equation to be solved, within the interval $i-1$ to i, is of the following form for both linear and cubic load functions:

$$\ddot{y}(t) + 2\zeta\omega\dot{y}(t) + \omega^2 y(t) = R_{i-1} + t\,\dot{R}_{i-1} + \frac{t^2}{2}\ddot{R}_{i-1} + \frac{t^3}{6}\dddot{R}_{i-1} \tag{13.11}$$

$$R(t) = R_{i-1} + t\,\dot{R}_{i-1} + \frac{t^2}{2}\ddot{R}_{i-1} + \frac{t^3}{6}\dddot{R} \quad in \ interval \ i\text{-}1 \ to \ i$$

For linear loading within interval

$$\dddot{R}_i = 0$$

$$\ddot{R}_i = 0$$

$$\dot{R}_{i-1} = \frac{(R_i - R_{i-1})}{\Delta t}$$

For cubic loading within interval where R_i and $\dot{R}_i$ are specified

$$\ddot{R}_i = \frac{6}{\Delta t^2}(R_i - R_{i+1}) + \frac{2}{\Delta t}(\dot{R}_{i+1} + 2\dot{R}_i)$$

$$\dddot{R} = \frac{\ddot{R}_i - \ddot{R}_{i-1}}{\Delta t}$$

Figure 13.1 Modal Load Functions

From the basic theory of linear differential equations, the general solution of Equation (13.11) is the sum of a homogeneous solution and a particular solution and is of the following form:

$$y(t) = b_1 S(t) + b_2 C(t) + b_3 + b_4 t + b_5 t^2 + b_6 t^3 \tag{13.12a}$$

The velocity and acceleration associated with this solution are:

$$\dot{y}(t) = b_1 \dot{S}(t) + b_2 \dot{C}(t) + b_4 + 2b_5 t + 3b_6 t^2 \tag{13.12b}$$

$$\ddot{y}(t) = b_1 \ddot{S}(t) + b_2 \ddot{C}(t) + 2b_5 + 6b_6 t \tag{13.12c}$$

These equations are summarized in the following matrix equation:

$$\overline{\mathbf{y}}_i = \begin{bmatrix} y_i \\ \dot{y}_i \\ \ddot{y}_i \end{bmatrix} = \begin{bmatrix} S(t) & C(t) & 1.0 & t & t^2 & t^3 \\ \dot{S}(t) & \dot{C}(t) & 0 & 1.0 & 2t & 3t^2 \\ \ddot{S}(t) & \ddot{C}(t) & 0 & 0 & 2.0 & 6t \end{bmatrix} \begin{bmatrix} b_1 \\ b_2 \\ b_3 \\ b_4 \\ b_5 \\ b_6 \end{bmatrix} = \mathbf{B}(t)\mathbf{b} \qquad (13.13)$$

It is now possible to solve for the constants b_i. The initial conditions at $t = 0$ are $\dot{y}(0) = \dot{y}_{i-1}$ and $y(0) = y_{i-1}$. Therefore, from Equations (13.12a and 13.12b)

$$\dot{y}_{i-1} = \omega_D b_1 - \varpi b_2 + b_4$$
$$y_{i-1} = b_2 + b_3 \qquad\qquad\qquad (13.13a)$$

The substitution of Equations (13.12a, 13.12b and 13.12c) into Equation (13.11) and setting the coefficients of each polynomial term to be equal produce the following four equations:

$$\begin{aligned} 1: \quad & R_{i-1} = \omega^2 b_3 + a_0 b_4 + 2b_5 \\ t: \quad & \dot{R}_{i-1} = \omega^2 b_4 + 2a_0 b_5 + 6b_6 \\ t^2: \quad & \ddot{R}_{i-1} = 2\omega^2 b_5 + 6a_0 b_6 \\ t^3: \quad & \dddot{R}_{i-1} = 6\omega^2 b_6 \end{aligned} \qquad (13.13b)$$

These six equations, given by Equations (13.13a and 13.13b), can be written as the following matrix equation:

$$\begin{bmatrix} \dot{y}_{i-1} \\ y_{i-1} \\ R_{i-1} \\ \dot{R}_{i-1} \\ \ddot{R}_{i-1} \\ \dddot{R}_{i-1} \end{bmatrix} = \begin{bmatrix} \omega_D & -\varpi & 0 & 1.0 & 0 & 0 \\ 0 & 1.0 & 1.0 & 0 & 0 & 0 \\ 0 & 0 & \omega^2 & a_0 & 2.0 & 0 \\ 0 & 0 & 0 & \omega^2 & 2a_0 & 6.0 \\ 0 & 0 & 0 & 0 & 2\omega^2 & 6a_0 \\ 0 & 0 & 0 & 0 & 0 & 6\omega^2 \end{bmatrix} \begin{bmatrix} b_1 \\ b_2 \\ b_3 \\ b_4 \\ b_5 \\ b_6 \end{bmatrix} \quad \text{or,} \ \ \overline{\mathbf{R}}_{i-1} = \mathbf{C}^{-1}\mathbf{b} \ \ (13.14)$$

Therefore,

$$\mathbf{b} = \mathbf{C}\overline{\mathbf{R}}_{i-1} \qquad\qquad (13.15)$$

The inversion of the upper-triangular matrix $\mathbf{C}$ can be formed analytically; or it can easily be numerically inverted within the computer program. Hence, the exact solution at time point *i* of a modal equation because of a cubic load within the time step is the following:

$$\overline{\mathbf{y}}_i = \mathbf{B}(\Delta t)\mathbf{C}\overline{\mathbf{R}}_{i-1} = \mathbf{A}\overline{\mathbf{R}}_{i-1} \qquad\qquad (13.16)$$

Equation (13.16) is a very simple and powerful recursive relationship. The complete algorithm for linear or cubic loading is summarized in Table 13.2. Note that the 3 by 6 $\mathbf{A}$ matrix is computed only once for each mode. Therefore, for each time increment, approximately 20 multiplications and 16 additions are required. Modern, inexpensive personal computers can complete one multiplication and one addition in approximately 10^{-6} seconds. Hence, the computer time required to solve 200 steps per second for a 50 second duration earthquake is approximately 0.01 seconds. Or 100 modal equations can be solved in one second of computer time. Therefore, there is no need to consider other numerical methods, such as the approximate Fast Fourier Transformation Method or the numerical evaluation of the Duhamel integral, to solve these equations. Because of the speed of this exact piece-wise polynomial technique, it can also be used to develop accurate earthquake response spectra using a very small amount of computer time.

Table 13.2 Higher-Order Recursive Algorithm for Solution of Modal Equation

I. EQUATION TO BE SOLVED:

$$\ddot{y}(t) + 2\xi\omega\dot{y}(t) + \omega^2 y(t) = R_{i-1} + t\dot{R}_{i-1} + \frac{t^2}{2}\ddot{R}_{i-1} + \frac{t^3}{6}\dddot{R}_{i-1}$$
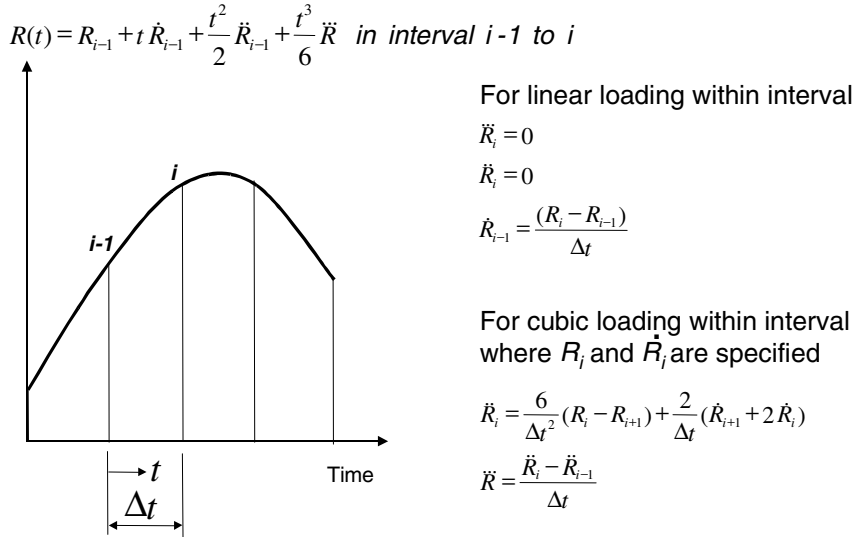
II. INITIAL CALCULATIONS

$$\omega_D = \omega\sqrt{1-\xi^2} \qquad \overline{\omega} = \omega\xi \qquad \overline{\xi} = \frac{\xi}{\sqrt{1-\xi^2}}$$

$$a_0 = 2\overline{\xi}\,\omega \qquad\qquad a_1 = \omega_D^2 - \overline{\omega}^2 \qquad a_2 = 2\overline{\omega}\omega_D$$

$$S(\Delta t) = e^{-\overline{\xi}\omega\Delta t}\sin(\omega_D\Delta t) \qquad\qquad C(\Delta t) = e^{-\overline{\xi}\omega\Delta t}\cos(\omega_D\Delta t)$$

$$\dot{S}(\Delta t) = -\overline{\omega}S(\Delta t) + \omega_D C(\Delta t) \qquad\qquad \dot{C}(\Delta t) = -\overline{\omega}C(\Delta t) - \omega_D S(\Delta t)$$

$$\ddot{S}(\Delta t) = -a_1 S(\Delta t) - a_2 C(\Delta t) \qquad\qquad \ddot{C}(\Delta t) = -a_1 C(\Delta t) + a_2 S(\Delta t)$$

$$\mathbf{B}(\Delta t) = \begin{bmatrix} S(\Delta t) & C(\Delta t) & 1.0 & \Delta t & \Delta t^2 & \Delta t^3 \\ \dot{S}(\Delta t) & \dot{C}(\Delta t) & 0 & 1.0 & 2\Delta t & 3\Delta t^2 \\ \ddot{S}(\Delta t) & \ddot{C}(\Delta t) & 0 & 0 & 2.0 & 6\Delta t \end{bmatrix}$$

$$\mathbf{C} = \begin{bmatrix} \omega_D & -\overline{\omega} & 0 & 1.0 & 0 & 0 \\ 0 & 1.0 & 1.0 & 0 & 0 & 0 \\ 0 & 0 & \omega^2 & a_0 & 2.0 & 0 \\ 0 & 0 & 0 & \omega^2 & 2a_0 & 6.0 \\ 0 & 0 & 0 & 0 & 2\omega^2 & 6a_0 \\ 0 & 0 & 0 & 0 & 0 & 6\omega^2 \end{bmatrix}^{-1} \quad \text{and } \mathbf{A} = \mathbf{B}(\Delta t)\mathbf{C}$$

III. RECURSIVE SOLUTION *i=1,2*

a. $\quad \dddot{R}_i = \dfrac{6}{\Delta t^2}(R_i - R_{i+1}) + \dfrac{2}{\Delta t}(\dot{R}_{i+1} + 2\dot{R}_i)$

b. $\quad \dddot{R}_{i-1} = \dfrac{\ddot{R}_i - \ddot{R}_{i-1}}{\Delta t}$

c. $\quad \overline{\mathbf{y}}_i = \mathbf{A}\overline{\mathbf{R}}_{i-1}$

d. $\quad$ *i=i+1* and return to III.a

13.5   SOLUTION FOR PERIODIC LOADING

The recurrence solution algorithm summarized by Equation 13.16 is a very efficient computational method for arbitrary, transient, dynamic loads with initial conditions. It is possible to use this same simple solution method for arbitrary periodic loading as shown in Figure 13.2. Note that the total duration of the loading is from $-\infty$ to $+\infty$ and the loading function has the same amplitude and shape for each typical period T_p. Wind, sea wave and acoustic forces can produce this type of periodic loading. Also, dynamic live loads on bridges may be of periodic form.
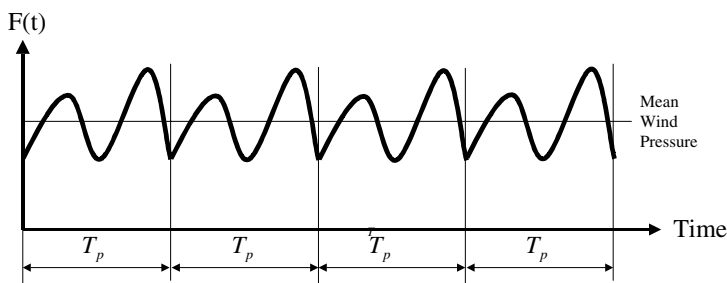
Figure 13.2 Example of Periodic Loading

For a typical duration T_p of loading, a numerical solution for each mode can be evaluated by applying Equation (13.11) without initial conditions. This solution is incorrect because it does not have the correct initial conditions. Therefore, it is necessary for this solution $y(t)$ to be corrected so that the exact solution $z(t)$ has the same displacement and velocity at the beginning and end of each loading period. To satisfy the basic dynamic equilibrium equation, the corrective solution $x(t)$ must have the following form:

$$x(t) = x_0 A_1(t) + \dot{x}_0 A_2(t) \tag{13.17}$$

where the functions are defined in Table 13.1.

The total exact solution for displacement and velocity for each mode can now be written as:

$$z(t) = y(t) + x(t) \tag{13.18a}$$

$$\dot{z}(t) = \dot{y}(t) + \dot{x}(t) \tag{13.18b}$$

So that the exact solution is periodic, the following conditions must be satisfied:

$$z(T_p) = z(0) \tag{13.19a}$$

$$\dot{z}(T_p) = \dot{z}(0) \tag{13.19b}$$

The numerical evaluation of Equation (13.14) produces the following matrix equation, which must be solved for the unknown initial conditions:

$$\begin{bmatrix} 1 - A_1(T_p) & -A_2(T_p) \\ -\dot{A}_1(T_p) & 1 - \dot{A}_2(T_p) \end{bmatrix} \begin{bmatrix} x_0 \\ \dot{x}_0 \end{bmatrix} = \begin{bmatrix} -y(T_p) \\ -\dot{y}(T_p) \end{bmatrix} \tag{13.20}$$

The exact periodic solution for modal displacements and velocities can now be calculated from Equations (13.18a and 13.18b). Hence, it in not necessary to use a frequency domain solution approach for periodic loading as suggested in most text books on structural dynamics.

13.6 PARTICIPATING MASS RATIOS

Several Building Codes require that at least 90 percent of the *participating mass* is included in the calculation of response for each principal direction. This requirement is based on a unit base acceleration in a particular direction and calculating the base shear due to that load. The steady state solution for this case involves no damping or elastic forces; therefore, the modal response equations for a unit base acceleration in the x-direction can be written as:

$$\ddot{y}_n = p_{nx} \tag{13.21}$$

The node point inertia forces in the x-direction for that mode are by definition:

$$f_{xn} = M\ddot{u}(t) = M\phi_n \ddot{y}_n = p_{nx} M\phi_n \tag{13.22}$$

The resisting base shear in the x-direction for mode n is the sum of all node point x forces. Or:

$$V_{nx} = - p_{nx} \, \mathbf{I}_x^T \mathbf{M} \phi_n = p_{nx}^2 \tag{13.23}$$

The total base shear in the x-direction, including N modes, will be:

$$V_x = \sum_{n=1}^{N} p_{nx}^2 \tag{13.24}$$

For a unit base acceleration in any direction, the exact base shear must be equal to the sum of all mass components in that direction. Therefore, the ***participating mass ratio*** is defined as the participating mass divided by the total mass in that direction. Or:

$$X_{mass} = \frac{\displaystyle\sum_{n=1}^{N} p_{nx}^2}{\displaystyle\sum m_x} \tag{13.25a}$$

$$Y_{mass} = \frac{\displaystyle\sum_{n=1}^{N} p_{ny}^2}{\displaystyle\sum m_y} \tag{13.25b}$$

$$Z_{mass} = \frac{\displaystyle\sum_{n=1}^{N} p_{nz}^2}{\displaystyle\sum m_z} \tag{13.25c}$$

If all modes are used, these ratios will all be equal to 1.0. It is clear that the 90 percent participation rule is intended to estimate the accuracy of a solution for base motion only. ***It cannot be used as an error estimator for other types of loading, such as point loads or base displacements acting on the structure***.

Most computer programs produce the contribution of each mode to those ratios. In addition, an examination of those factors gives the engineer an indication of the direction of the base shear associated with each mode. For example, the angle with respect to the x-axis of the base shear associated with the first mode is given by:

$$\theta_1 = \tan^{-1}\left(\frac{p_{1x}}{p_{1y}}\right) \tag{13.26}$$

13.7   STATIC LOAD PARTICIPATION RATIOS

For arbitrary loading, it is useful to determine if the number of vectors used is adequate to approximate the true response of the structural system. One method, which the author has proposed, is to evaluate the static displacements using a truncated set of vectors to solve for the response resulting from static load patterns. As indicated by Equation (13.1), the loads can be written as:

$$\mathbf{F}(t) = \sum_{j=1}^{J} \mathbf{f}_j \mathbf{g}(t)_j \tag{13.27}$$

First, one solves the statics problem for the exact displacement $\mathbf{u}_j$ associated with the load pattern $\mathbf{f}_j$. Then, the total external work associated with load condition j is:

$$E_j = \frac{1}{2} \mathbf{f}_j^T \mathbf{u}_j \tag{13.28}$$

From Equation (13.6), the modal response, neglecting inertia and damping forces, is given by:

$$y_n = \frac{1}{\omega_n^2} \phi_n^T \mathbf{f}_j \tag{13.29}$$

From the fundamental definition of the mode superposition method, a truncated set of vectors defines the approximate displacement v_j as:

$$v_j = \sum_{n=1}^{N} y_n \phi_n = \sum_{n=1}^{N} \frac{1}{\omega_n^2} \phi_n^T \mathbf{f}_j \phi_n \tag{13.30}$$

The total external work associated with the truncated mode shape solution is:

$$\overline{E}_j = \frac{1}{2} \mathbf{f}_j^T \mathbf{v}_j = \sum_{n=1}^{N} \left(\frac{\phi_n^T \mathbf{f}_j}{\omega_n} \right)^2 = \sum_{n=1}^{N} \left(\frac{p_{nj}}{\omega_n} \right)^2 \tag{13.31}$$

A *static load participation ratio* r_j can now be defined for load condition j as the ratio of the sum of the work done by the truncated set of modes to the external total work done by the load pattern. Or:

$$r_j = \frac{\overline{E}_j}{E_j} = \frac{\displaystyle\sum_{n=1}^{L}\left(\frac{p_{nj}}{\omega_n}\right)^2}{\mathbf{f}_j^T \mathbf{u}_j} \tag{13.32}$$

If this ratio is close to 1.0, the errors introduced by vector truncation will be very small. However, if this ratio is less than 90 percent, additional vectors should be used in the analysis to capture the *static load response.*

It has been the experience of the author that the use of exact eigenvectors is not an accurate vector basis for the dynamic analysis of structures subjected to point loads. Whereas, load-dependent vectors, which are defined in the following chapter, always produce a static load participation ratio of 1.0.

13.8   DYNAMIC LOAD PARTICIPATION RATIOS

In addition to participating mass ratios and static load participation ratios, it is possible to calculate a *dynamic load participation ratio* for each load pattern. All three of these ratios are automatically produced by the SAP2000 program.

The dynamic load participation ratio is based on the physical assumption that only inertia forces resist the load pattern. Considering only mass degrees of freedom, the exact acceleration $\ddot{\mathbf{u}}_j$ because of the load pattern $\mathbf{f}_j$ is:

$$\ddot{\mathbf{u}}_j = \mathbf{M}^{-1}\mathbf{f}_j \tag{13.33}$$

The velocity of the mass points at time $t = 1$ is:

$$\dot{\mathbf{u}}_j = t\mathbf{M}^{-1}\mathbf{f}_j = \mathbf{M}^{-1}\mathbf{f}_j \tag{13.34}$$

Hence, the total kinetic energy associated with load pattern *j* is:

$$E_j = \frac{1}{2}\dot{\mathbf{u}}^T\mathbf{M}\dot{\mathbf{u}} = \frac{1}{2}\mathbf{f}_j^T\mathbf{M}^{-1}\mathbf{f}_j \tag{13.35}$$

From Equation 13.6, the modal acceleration and velocity, neglecting the massless degrees of freedom, is given by:

$$\ddot{y}_n = \phi_n^T\mathbf{f}_j \quad \text{and} \quad \dot{y}_n = t\phi_n^T\mathbf{f}_j = \phi_n^T\mathbf{f}_j \quad \text{at} \quad t = 1 \tag{13.36}$$

From the fundamental definition of the mode superposition method, a truncated set of vectors defines the approximate velocity $\dot{\mathbf{v}}_j$ as:

$$\dot{\mathbf{v}}_j = \sum_{n=1}^{N}\dot{y}_n\phi_n = \sum_{n=1}^{N}\phi_n^T\mathbf{f}_j\phi_n = \sum_{n=1}^{N}p_{nj}\phi_n = \sum_{n=1}^{N}\phi_n\, p_{nj} \tag{13.37}$$

The total kinetic energy associated with the truncated mode shape solution is:

$$\overline{E}_j = \frac{1}{2}\dot{\mathbf{v}}_j^T\mathbf{M}\dot{\mathbf{v}}_j = \frac{1}{2}\sum_{n=1}^{N}p_{nj}\phi_n^T\,\mathbf{M}\sum_{n=1}^{N}\phi_n\, p_{nj} = \frac{1}{2}\sum_{n=1}^{N}(p_{nj})^2 \tag{13.38}$$

A *dynamic load participation ratio* r_j can now be defined for load condition j as the ratio of the sum of the kinetic energy associated with the truncated set of modes to the total kinetic energy associated with the load pattern. Or:

$$r_j = \frac{\overline{E}_j}{E_j} = \frac{\displaystyle\sum_{n=1}^{N}(p_{nj})^2}{\mathbf{f}_j^T\mathbf{M}^{-1}\mathbf{f}_j} \tag{13.39}$$

The dynamic load participation ratio includes only loads that are associated with mass degrees of freedom. However, the static load participation factor includes the effects of the loads acting at the massless degrees of freedom.

A 100 percent dynamic load participation indicates that the high frequency response of the structure is captured. In addition, for the cases of mass proportional loading in the three global directions, the dynamic load participation ratios are identical to the mass participation factors.

13.9 SUMMARY

The mode superposition method is a very powerful method used to reduce the number of unknowns in a dynamic response analysis. All types of loading can be accurately approximated by piece-wise linear or cubic functions within a small time increment. Exact solutions exist for these types of loading and can be computed with a trivial amount of computer time for equal time increments. Therefore, there is no need to present other methods for the numerical evaluation of modal equations.

To solve for the linear dynamic response of structures subjected to periodic loading, it is only necessary to add a corrective solution to the transient solution for a typical time period of loading. The corrective solution forces the initial conditions of a typical time period to be equal to the final conditions at the end of the time period. Hence, the same time-domain solution method can be used to solve wind or wave dynamic response problems in structural engineering.

Participating mass factors can be used to estimate the number of vectors required in an elastic seismic analysis where base accelerations are used as the fundamental loading. The use of mass participation factors to estimate the accuracy of a nonlinear seismic analysis can introduce significant errors. Internal nonlinear concentrated forces that are in equal and opposite directions do not produce a base shear. In addition, for the case of specified base displacements, the participating mass ratios do not have a physical meaning.

Static and dynamic participation ratios are defined and can be used to estimate the number of vectors required. It will later be shown that the use of Ritz vectors, rather than the exact eigenvectors, will produce vectors that have static and dynamic participation ratios at or near 100 percent.

<div align="right">

14.

</div>

CALCULATION OF STIFFNESS AND MASS ORTHOGONAL VECTORS

LDR Vectors are Always More Accurate than Using the Exact Eigenvectors in a Mode Superposition Analysis

14.1 INTRODUCTION

The major reason to calculate mode shapes (or eigenvectors and eigenvalues) is that they are used to uncouple the dynamic equilibrium equations for mode superposition and/or response spectra analyses. The main purpose of a dynamic response analysis of a structure is ***to accurately estimate displacements and member forces*** in the real structure. In general, there is no direct relationship between the accuracy of the eigenvalues and eigenvectors and the accuracy of node point displacements and member forces.

In the early days of earthquake engineering, the Rayleigh-Ritz method of dynamic analysis was used extensively to calculate approximate solutions. With the development of high-speed computers, the use of exact eigenvectors replaced the use of Ritz vectors as the basis for seismic analysis. It will be illustrated in this book that **L**oad-**D**ependent **R**itz, LDR, vectors can be used for the dynamic analysis of both linear and nonlinear structures. The new modified Ritz method produces more accurate results, with less computational effort, than the use of exact eigenvectors.

There are several different numerical methods available for the evaluation of the eigenvalue problem. However, for large structural systems, only a few methods have proven to be both accurate and robust.

14.2   DETERMINATE SEARCH METHOD

The equilibrium equation, which governs the undamped free vibration of a typical mode, is given by:

$$[\mathbf{K} - \omega_i^2 \mathbf{M}]\mathbf{v}_i = \mathbf{0} \quad \text{or} \quad \overline{\mathbf{K}}_i \mathbf{v}_i = \mathbf{0} \tag{14.1}$$

Equation 14.1 can be solved directly for the natural frequencies of the structure by assuming values for ω_i and factoring the following equation:

$$\overline{\mathbf{K}}_i = \mathbf{L}_i \mathbf{D}_i \mathbf{L}_i^T \tag{14.2}$$

From Appendix C the determinant of the factored matrix is defined by:

$$\text{Det}(\omega_i) = D_{11} D_{22} ---- D_{NN} \tag{14.3}$$

It is possible, by repeated factorization, to develop a plot of the determinant vs. λ, as shown in Figure 14.1. This classical method for evaluating the natural frequencies of a structure is called the ***determinant search method*** [1]. It should be noted that for matrices with small bandwidths the numerical effort to factor the matrices is very small. For this class of problem the determinant search method, along with inverse iteration, is an effective method of evaluating the undamped frequencies and mode shapes for small structural systems. However, because of the increase in computer speeds, small problems can be solved by any method in a few seconds. Therefore, the determinant search method is no longer used in modern dynamic analysis programs.
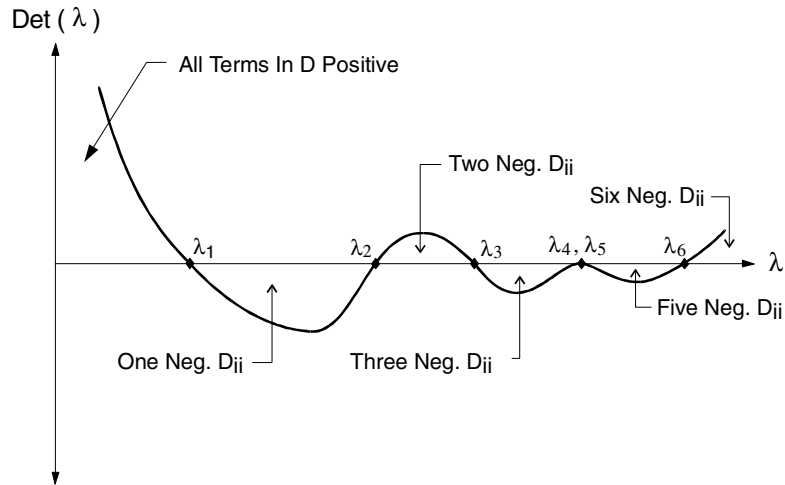
Figure 14.1 Determinant vs. Frequency for Typical System

14.3 STURM SEQUENCE CHECK

Figure 14.1 illustrates a very important property of the sequence of diagonal terms of the factored matrix. One notes that for a specified value of ω_i, one can count the number of negative terms in the diagonal matrix and it is always equal to the number of frequencies below that value. Therefore, it can be used to check a method of solution that fails to calculate all frequencies below a specified value. Also, another important application of the Sturm Sequence Technique is to evaluate the number of frequencies within a frequency range. It is only necessary to factor the matrix at both the maximum and minimum frequency points, and the difference in the number of negative diagonal terms is equal to the number of frequencies in the range. This numerical technique is useful in machine vibration problems.

14.4 INVERSE ITERATION

Equation (14.1) can be written in an iterative solution form as:

$$K \overline{V}_n^{(i)} = \lambda_n^{(i-1)} M V_n^{(i-1)} \quad \text{or} \quad LDL^T \overline{V}_n^{(i)} = R^{(i)} \tag{14.4}$$

The computational steps required for the solution of one eigenvalue and eigenvector can be summarized as follows:

1. Factor stiffness matrix into triangularized LDL^T form during static load solution phase.

2. For the first iteration, assume $R^{(1)}$ to be a vector of random numbers and solve for initial vector $\overline{V}_n^{(1)}$.

3. Iterate with i = 1, 2 . . .

    a. Normalize vector so that $V_n^{T(i)} M V_n^{(i)} = I$

    b. Estimate eigenvalue $\lambda_n^{(i)} = V_n^{T(i)} R^{(i)}$

    c. Check $\lambda_n^{(i)}$ for convergence - if converged, terminate

    d. $i = i + 1$ and calculate $R^{(i)} = \lambda_n^{(i-1)} M V^{(i-1)}$

    e. Solve for new vector $LDL^T \overline{V}_n^{(i)} = R^{(i)}$

    f. Repeat Step 3

It can easily be shown that this method will converge to the smallest unique eigenvalue.

14.5 GRAM-SCHMIDT ORTHOGONALIZATION

Additional eigenvectors can be calculated using the inverse iteration method if, after each iteration cycle, the iteration vector is made orthogonal to all previously calculated vectors. To illustrate the method, let us assume that we have an approximate vector $\overline{V}$ that needs to be made orthogonal to the previously calculated vector V_n. Or, the new vector can be calculated from:

$$V = \overline{V} - \alpha V_n \qquad\qquad (14.5)$$

Multiplying Equation (14.3) by $V_n^T M$, we obtain:

$$V_n^T M V = V_n^T M \overline{V} - \alpha V_n^T M V_n = 0 \tag{14.6}$$

Therefore, the orthogonality requirement is satisfied if:

$$\alpha = \frac{V_n^T M \overline{V}}{V_n^T M V_n} = V_n^T M \overline{V} \tag{14.7}$$

If the orthogonalization step is inserted after Step 3.e in the inverse iteration method, additional eigenvalues and vectors can be calculated.

14.6 BLOCK SUBSPACE ITERATION

Inverse iteration with one vector may not converge if eigenvalues are identical and the eigenvectors are not unique. This case exists for many real three-dimensional structures, such as buildings with equal stiffness and mass in the principle directions. This problem can be avoided by iterating with a block of orthogonal vectors [2]. The block subspace iteration algorithm is summarized in Table 14.1 and is the method used in the modern versions of the SAP program.

Experience has indicated that the subspace block size "b" should be set equal to the square root of the *average bandwidth of the stiffness matrix*, but, not less than six. The block subspace iteration algorithm is relatively slow; however, it is very accurate and robust. In general, after a vector is added to a block, it requires five to ten forward reductions and back-substitutions before the iteration vector converges to the exact eigenvector.

Table 14.1 Subspace Algorithm for the Generation of Eigenvectors

---

I. INITIAL CALCULATIONS

    A. Triangularize Stiffness Matrix.

    B. Use random numbers to form a block of "b" vectors $V^{(0)}$.

II. GENERATE L EIGENVECTORS BY ITERATION   i = 1,2...

    A. Solve for block of vectors, $X^{(i)}$ in, $K\,X^{(i)} = M\,V^{(i-1)}$.

    B. Make block of vectors, $X^{(i)}$, stiffness and mass orthogonal, $\overline{V}^{(i)}$. Order
        eigenvalues and corresponding vectors in ascending order.

    C. Use Gram-Schmidt method to make $\overline{V}^{(i)}$ orthogonal to all previously
        calculated vectors and normalized so that $V^{T(i)} M V^{(i)} = I$.

    D. Perform the following checks and operations:

        1. If first vector in block is not converged, go to Step A with **i = i + 1** .

        2. Save Vector ϕ_n on Disk.

        3. If n equals L , terminate iteration.

        4. Compact block of vectors.

        5. Add random number vector to last column of block.

        Return to Step D.1 with **n = n + 1**

14.7   SOLUTION OF SINGULAR SYSTEMS

For a few types of structures, such as aerospace vehicles, it is not possible to use inverse or subspace iteration directly to solve for mode shapes and frequencies. This is because there is a minimum of six rigid-body modes with zero frequencies and the stiffness matrix is singular and cannot be triangularized. To

solve this problem, it is only necessary to introduce the following eigenvalue *shift,* or change of variable:

$$\lambda_n = \overline{\lambda}_n - \rho \tag{14.8}$$

Hence, the iterative eigenvalue problem can be written as:

$$\overline{\mathbf{K}}\,\overline{\mathbf{V}}_n^{(i)} = \overline{\lambda}_n^{(i-1)}\mathbf{M}\,\mathbf{V}_n^{(i-1)} \quad \text{or} \quad \mathbf{L}\mathbf{D}\mathbf{L}^{\mathrm{T}}\,\overline{\mathbf{V}}_n^{(i)} = \mathbf{R}^{(i)} \tag{14.9}$$

The shifted stiffness matrix is now non-singular and is defined by:

$$\overline{\mathbf{K}} = \mathbf{K} + \rho\,\mathbf{M} \tag{14.10}$$

The eigenvectors are not modified by the arbitrary shift ρ. The correct eigenvalues are calculated from Equation (14.8).

14.8 GENERATION OF LOAD-DEPENDENT RITZ VECTORS

The numerical effort required to calculate the exact eigen solution can be enormous for a structural system if a large number of modes are required. However, many engineers believe that this computational effort is justifiable if accurate results are to be obtained. One of the purposes of this section is to clearly illustrate that this assumption is not true for the dynamic response analyses of all structural systems.

It is possible to use the exact free-vibration mode shapes to reduce the size of both linear and nonlinear problems. However, this is not the best approach for the following reasons:

1. For large structural systems, the solution of the eigenvalue problem for the free-vibration mode shapes and frequencies can require a significant amount of computational effort.

2. In the calculation of the free-vibration mode shapes, the spatial distribution of the loading is completely disregarded. Therefore, many of the mode shapes that are calculated are orthogonal to the loading and do not participate in the dynamic response.

3. If dynamic loads are applied at massless degrees-of-freedom, the use of all the exact mode shapes in a mode superposition analysis will not converge to the exact solution. In addition, displacements and stresses near the application of the loads can be in significant error. Therefore, there is no need to apply the "static correction method" as would be required if exact eigenvectors are used for such problems.

4. It is possible to calculate a set of stiffness and mass orthogonal Ritz vectors, with a minimum of computational effort, which will converge to the exact solution for any spatial distribution of loading [2].

It can be demonstrated that a dynamic analysis based on a unique set of Load Dependent Vectors yields a more accurate result than the use of the same number of exact mode shapes. The efficiency of this technique has been illustrated by solving many problems in structural response and in wave propagation types of problems [4]. Several different algorithms for the generation of Load Dependent Ritz Vectors have been published since the method was first introduced in 1982 [3]. Therefore, it is necessary to present in Table 14.2 the latest version of the method for multiple load conditions.

Table 14.2 Algorithm for Generation of Load Dependent Ritz Vectors

---

I. INITIAL CALCULATIONS

    A. Triangularize Stiffness Matrix $\mathbf{K} = \mathbf{L}^\mathrm{T}\mathbf{D}\mathbf{L}$.

    B. Solve for block of "b" static displacement vectors $\mathbf{u}_\mathrm{s}$ resulting from spatial load patterns $\mathbf{F}$; or, $\mathbf{K}\mathbf{u}_\mathrm{s} = \mathbf{F}$.

    C. Make block of vectors $\mathbf{u}_\mathrm{s}$, stiffness and mass orthogonal, $\mathbf{V}_1$.

II. GENERATE BLOCKS OF RITZ VECTORS   i = 2,....N

    A. Solve for block of vectors, $\mathbf{X}_\mathrm{i}$, $\mathbf{K}\mathbf{X}_\mathrm{i} = \mathbf{M}\mathbf{V}_{\mathrm{i}\text{-}1}$.

    B. Make block of vectors, $\mathbf{X}_\mathrm{i}$, stiffness and mass orthogonal, $\overline{\mathbf{V}}_\mathrm{i}$.

Table 14.2 Algorithm for Generation of Load Dependent Ritz Vectors

C. Use Modified Gram-Schmidt method (two times) to make $\overline{\mathbf{V}}_i$ orthogonal to all previously calculated vectors and normalized so that $\mathbf{V}_i^T \mathbf{M} \mathbf{V}_i = \mathbf{I}$.

III. MAKE VECTORS STIFFNESS ORTHOGONAL

A. Solve Nb by Nb eigenvalue problem $[\overline{\mathbf{K}} - \Omega^2 \mathbf{I}]\mathbf{Z} = 0$ where $\overline{\mathbf{K}} = \mathbf{V}^T \mathbf{K} \mathbf{V}$.

B. Calculate stiffness orthogonal Ritz vectors, $\mathbf{\Phi} = \mathbf{V}\mathbf{Z}$.

14.9   A PHYSICAL EXPLANATION OF THE LDR ALGORITHM

The physical foundation for the method is the recognition that the dynamic response of a structure will be a function of the spatial load distribution. The undamped, dynamic equilibrium equations of an elastic structure can be written in the following form:

$$\mathbf{M\ddot{u}}(t) + \mathbf{Ku}(t) = \mathbf{R}(t) \tag{14.11}$$

In the case of earthquake or wind, the time-dependent loading acting on the structure, $\mathbf{R}(t)$, Equation (13.1), can be written as:

$$\mathbf{R}(t) = \sum_{j=1}^{J} \mathbf{f}_j \mathbf{g}(t)_j = \mathbf{F}\mathbf{G}(t) \tag{14.12}$$

Note that the independent load patterns $\mathbf{F}$ are not a function of time. For constant earthquake ground motions at the base of the structure three independent load patterns are possible. These load patterns are a function of the directional mass distribution of the structure. In case of wind loading, the downwind mean wind pressure is one of those vectors. The time functions $\mathbf{G}(t)$ can always be expanded into a Fourier series of sine and cosine functions. Hence, neglecting

damping, a typical dynamic equilibrium equation to be solved is of the following form:

$$\mathbf{M\ddot{u}}(t) + \mathbf{Ku}(t) = \mathbf{F}\sin\varpi t \qquad (14.13)$$

Therefore, the exact dynamic response for a typical loading frequency ϖ is of the following form:

$$\mathbf{Ku} = \mathbf{F} + \varpi^2 \mathbf{Mu} \qquad (14.14)$$

This equation cannot be solved directly because of the unknown frequency of the loading. However, a series of stiffness and mass orthogonal vectors can be calculated that will satisfy this equation using a perturbation algorithm. The first block of vectors is calculated by neglecting the mass and solving for the static response of the structure. Or:

$$\mathbf{Ku}_0 = \mathbf{F} \qquad (14.15)$$

From Equation (14.14) it is apparent that the distribution of the error in the solution, due to neglecting the inertia forces, can be approximated by:

$$\mathbf{F}_1 \approx \mathbf{Mu}_0 \qquad (14.16)$$

Therefore, an additional block of displacement error, or correction, vectors can be calculated from:

$$\mathbf{Ku}_1 = \mathbf{F}_1 \qquad (14.17)$$

In calculating $\mathbf{u}_1$ the additional inertia forces are neglected. Hence, in continuing this thought process, it is apparent the following recurrence equation exists:

$$\mathbf{Ku}_i = \mathbf{Mu}_{i-1} \qquad (14.18)$$

A large number of blocks of vectors can be generated by Equation (14.18). However, to avoid numerical problems, the vectors must be stiffness and mass orthogonal after each step. In addition, care should be taken to make sure that all vectors are linearly independent. The complete numerical algorithm is summarized in Table 14.2. After careful examination of the LDR vectors, one

can conclude that *dynamic analysis is a simple extension of static analysis* because the first block of vectors is the static response from all load patterns acting on the structure. For the case where loads are applied at only the mass degrees-of-freedom, the LDR vectors are always a linear combination of the exact eigenvectors.

It is of interest to note that the recursive equation, used to generate the LDR vectors, is similar to the Lanczos algorithm for calculating exact eigenvalues and vectors, except that the starting vectors are the static displacements caused by the spatial load distributions. Also, *there is no iteration involved in the generation of Load Dependent Ritz vectors*.

14.10 COMPARISON OF SOLUTIONS USING EIGEN AND RITZ VECTORS

The fixed-end beam shown in Figure 14.1 is subjected to a point load at the center of the beam. The load varies in time as a constant unit step function.
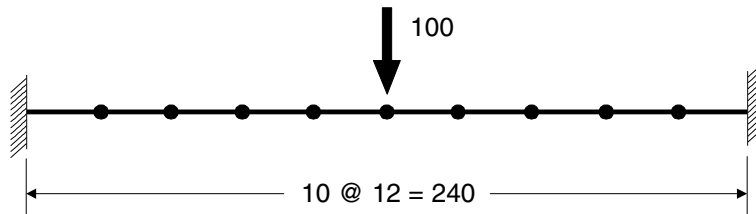
Modulus of Elasticity = 30,000,000
Moment of Inertia = 100
Mass per Unit Length = 0.1
Damping Ratio = 0.01

All units in Pounds and Inches

Figure 14.1 Dimensions, Stiffness and Mass for Beam Structure

The damping ratio for each mode was set at one percent and the maximum displacement and moment occur at 0.046 second, as shown in Table 14.3.

The results clearly indicate the advantages of using load-dependent vectors. One notes that the free-vibration modes 2, 4, 6 and 8 are not excited by the loading because they are nonsymmetrical. However, the load dependent algorithm

generates only the symmetrical modes. In fact, the algorithm will fail for this case, if more than five vectors are requested.

Table 14.3 Results from Dynamic Analyses of Beam Structure

Number of Vectors	Free-Vibration Mode Shapes		Load-Dependent Ritz Vectors	
	Displacement	Moment	Displacement	Moment
1	0.004572 (-2.41)	4178 (-22.8)	0.004726 (+0.88)	5907 (+9.2)
2	0.004572 (-2.41)	4178 (-22.8)	0.004591 (-2.00)	5563 (+2.8)
3	0.004664 (-0.46)	4946 (-8.5)	0.004689 (+0.08)	5603 (+3.5)
4	0.004664 (-0.46)	4946 (-8.5)	0.004688 (+0.06)	5507 (+1.8)
5	0.004681 (-0.08)	5188 (-4.1)	0.004685 (0.00)	5411 (0.0)
7	0.004683 (-0.04)	5304 (-2.0)		
9	0.004685 (0.00)	5411 (0.0)		

Note: Numbers is parentheses are percentage errors.

Both methods give good results for the maximum displacement. The results for maximum moment, however, indicate that the load-dependent vectors give significantly better results and converge from above the exact solution. It is clear that free-vibration mode shapes are not necessarily the best vectors to be used in mode-superposition dynamic response analysis. Not only is the calculation of the exact free-vibration mode shapes computationally expensive, it requires more vectors, which increases the number of modal equations to be integrated and stored within the computer.

14.11 CORRECTION FOR HIGHER MODE TRUNCATION

In the analysis of many types of structures, the response of higher modes can be significant. In the use of exact eigenvectors for mode superposition or response spectra analyses, approximate methods of analysis have been developed to improve the results. The purpose of those approximate methods is "to account for missing mass" or "to add static response" associated with "higher mode truncation." Those methods are used to reduce the number of exact eigenvectors to be calculated, which reduces computation time and computer storage requirements.

The use of Load Dependent Ritz, LDR, vectors, on the other hand, does not require the use of those approximate methods because the "static response" is included in the initial set of vectors. This is illustrated by the time history analysis of a simple cantilever structure subjected to earthquake motions shown in Figure 14.2. This is a model of a light-weight superstructure built on a massive foundation supported on stiff piles that are modeled using a spring.
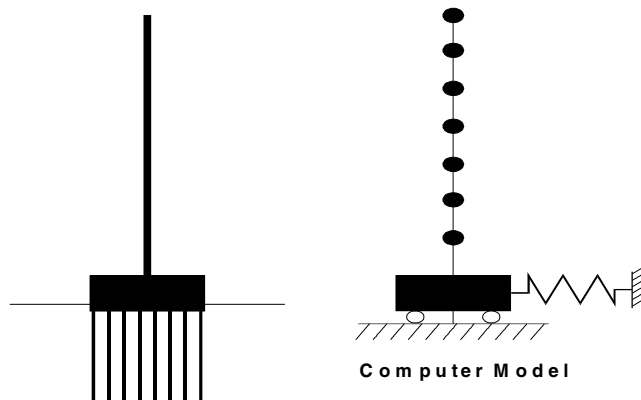
Computer Model

Figure 14.2 Cantilever Structure on Massive Stiff Foundation

Only eight eigen or Ritz vectors can be used because the model has only eight masses. The computed periods, using the exact eigen or Ritz method, are summarized in Table 14.4. It is apparent that the eighth mode is associated with the vibration of the foundation mass and the period is very short: 0.00517 seconds.

Table 14.4 Periods and Mass Participation Factors

MODE NUMBER	PERIOD (Seconds)	MASS PARTICIPATION (Percentage)
1	1.27321	11.706
2	0.43128	01.660
3	0.24205	00.613
4	0.16018	00.310
5	0.11899	00.208
6	0.09506	00.100
7	0.07951	00.046
8	0.00517	85.375

The maximum foundation force using different numbers of eigen and LDR vectors is summarized in Table 14.5. In addition, the total mass participation associated with each analysis is shown. The integration time step is the same as the earthquake motion input; therefore, no errors are introduced other than those resulting from mode truncation. Five percent damping is used in all cases.

Table 14.5 Foundation Forces and Total Mass Participation

NUMBER OF VECTORS	FOUNDATION FORCE (Kips)		MASS PARTICIPATION (Total Percentage)	
	EIGEN	RITZ	EIGEN	RITZ
8	1,635	1,635	100.0	100.0
7	260	1,636	14.6	83.3
5	259	1,671	14.5	16.2
3	258	1,756	14.0	14.5
2	257	3,188	13.4	13.9

The solution for eight eigen or LDR vectors produces the exact solution for the foundation force and 100 percent of the participating mass. For seven

eigenvectors, the solution for the foundation force is only 16 percent of the exact value—a significant error; whereas, the LDR solution is almost identical to the exact foundation force. It is of interest to note that the LDR method overestimates the force as the number of vectors is reduced—a conservative engineering result.

Also, it is apparent that the mass participation factors associated with the LDR solutions are not an accurate estimate the error in the foundation force. In this case, 90 percent mass participation is not a requirement if LDR vectors are used. If only five LDR vectors are used, the total mass participation factor is only 16.2 percent; however, the foundation force is over-estimated by 2.2 percent.

14.12 VERTICAL DIRECTION SEISMIC RESPONSE

Structural engineers are required for certain types of structures, to calculate the vertical dynamic response. During the past several years, many engineers have told me that it was necessary to calculate several hundred mode shapes for a large structure to obtain the 90 percent mass participation in the vertical direction. In all cases, the "exact" free vibration frequencies and mode shapes were used in the analysis.

To illustrate this problem and to propose a solution, a vertical dynamic analysis is conducted of the two dimensional frame shown in Figure 14.3. The mass is lumped at the 35 locations shown; therefore, the system has 70 possible mode shapes.

Using the exact eigenvalue solution for frequencies and mode shapes, the mass participation percentages are summarized in Table 14.6.

One notes that the lateral and vertical modes are uncoupled for this very simple structure. Only two of the first ten modes are in the vertical direction. Hence, the total vertical mass participation is only 63.3 percent.
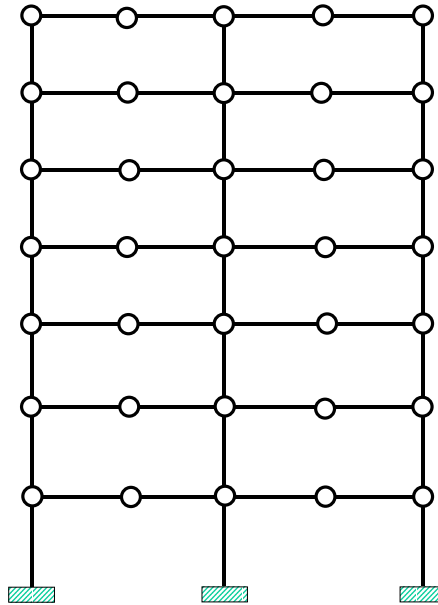
Figure 14.3 Frame Structure Subjected to Vertical Earthquake Motions

Table 14.6 Mass Participation Percentage Factors for Exact Eigenvalues

MODE	PERIOD (Seconds)	LATERAL MASS PARTICIPATION		VERTICAL MASS PARTICIPATION	
		EACH MODE	TOTAL	EACH MODE	TOTAL
1	1.273	79.957	79.957	0	0
2	0.421	11.336	91.295	0	0
3	0.242	4.172	95.467	0	0
4	0.162	1.436	96.903	0	0
5	0.158	0.650	97.554	0	0
6	0.148	0	97.554	60.551	60.551
7	0.141	0.031	97.584	0	60.551
8	0.137	0.015	97.584	0	60.551
9	0.129	0.037	97.639	0	60.551
10	0.127	0	97.639	2.775	63.326

The first 10 **L**oad **D**ependent **R**itz vectors are calculated and the mass participation percentages are summarized in Table 14.7. The two starting LDR vectors were generated using static loading proportional to the lateral and vertical mass distributions.

Table 14.7 Mass Participation Percentage Factors Using LDR Vectors

MODE	PERIOD (Seconds)	LATERAL MASS PARTICIPATION		VERTICAL MASS PARTICIPATION	
		EACH MODE	TOTAL	EACH MODE	TOTAL
1	1.273	79.957	79.957	0	0
2	0.421	11.336	91.295	0	0
3	0.242	4.176	95.471	0	0
4	0.158	2.388	97.859	0	0
5	0.149	0	97.859	60.567	60.567
6	0.123	0	97.859	4.971	65.538
7	0.104	2.102	99.961	0	65.538
8	0.103	0	99.961	13.243	78.781
9	0.064	0	99.961	9.696	88.477
10	0.041	0	99.961	8.463	96.940

The ten vectors produced by the LDR method more than satisfy the 90 percent code requirement. It would require the calculation of 34 eigenvectors for the exact eigenvalue approach to obtain the same mass participation percentage. This is just one additional example of why use of the LDR method is superior to the use of the exact eigenvectors for seismic loading.

The reason for the impressive accuracy of the LDR method compared to the exact eigenvector method is that only the mode shapes that are excited by the seismic loading are calculated.

14.13 SUMMARY

There are three different mathematical methods for the numerical solution of the eigenvalue problem. They all have advantages for certain types of problems.

First, the determinant search method, which is related to finding the roots of a polynomial, is a fundamental traditional method. It is not efficient for large structural problems. The Sturm sequence property of the diagonal elements of the factored matrix can be used to determine the number of frequencies of vibration within a specified range.

Second, the inverse and subspace iteration methods are subsets of a large number of power methods. The Stodola method is a power method. However, the use of a *sweeping matrix* to obtain higher modes is not practical because it eliminates the sparseness of the matrices. Gram-Schmidt orthogonalization is the most effective method to force iteration vectors to converge to higher modes.

Third, transformation methods are very effective for the calculation of all eigenvalues and eigenvectors of small dense matrices. Jacobi, Givens, Householder, Wilkinson and Rutishauser are all well-known transformation methods. The author prefers to use a modern version of the Jacobi method in the ETABS and SAP programs. It is not the fastest; however, we have found it to be accurate and robust. Because it is only used for problems equal to the size of the subspace, the computational time for this phase of the solution is very small compared to the time required to form the subspace eigenvalue problem. The derivation of the Jacobi method is given in Appendix D.

The use of Load Dependent Ritz vectors is the most efficient approach to solve for accurate node displacements and member forces within structures subjected to dynamic loads. The lower frequencies obtained from a Ritz vector analysis are always very close to the exact free vibration frequencies. If frequencies and mode shapes are missed, it is because the dynamic loading does not excite them; therefore, they are of no practical value. Another major advantage of using LDR vectors is that it is not necessary to be concerned about errors introduced by higher mode truncation of a set of exact eigenvectors.

All LDR mode shapes are linear combinations of the exact eigenvectors; therefore, the method always converges to the exact solution. Also, the computational time required to calculate the LDR vectors is significantly less than the time required to solve for eigenvectors.

14.14 REFERENCES

1.   Bathe, K. J., and E. L. Wilson. 1972. "Large Eigenvalue Problems in Dynamic Analysis," *Proceedings, American Society of Civil Engineers, Journal of the Engineering Mechanics Division*, EM6. December. pp. 1471-1485.

2.   Wilson, E. L., and T. Itoh. 1983. "An Eigensolution Strategy for Large Systems," in *J. Computers and Structures*. Vol. 16, No. 1-4. pp. 259-265.

3.   Wilson, E. L., M. Yuan and J. Dickens. 1982. "Dynamic Analysis by Direct Superposition of Ritz Vectors," *Earthquake Engineering and Structural Dynamics*. Vol. 10. pp. 813-823.

4.   Bayo, E. and E. L. Wilson. 1984. "Use of Ritz Vectors in Wave Propagation and Foundation Response," *Earthquake Engineering and Structural Dynamics*. Vol. 12. pp. 499-505.

15.

DYNAMIC ANALYSIS USING RESPONSE SPECTRUM SEISMIC LOADING

Before the Existence of Inexpensive Personal Computers,
the Response Spectrum Method was the Standard Approach
for Linear Seismic Analysis

15.1   INTRODUCTION

The basic mode superposition method, which is restricted to linearly elastic analysis, produces the complete time history response of joint displacements and member forces. In the past, there have been two major disadvantages in the use of this approach. First, the method produces a large amount of output information that can require a significant amount of computational effort to conduct all possible design checks as a function of time. Second, the analysis must be repeated for several different earthquake motions to ensure that all frequencies are excited because a response spectrum for one earthquake in a specified direction is not a smooth function.

There are computational advantages in using the response spectrum method of seismic analysis for prediction of displacements and member forces in structural systems. The method involves the calculation of only the maximum values of the displacements and member forces in each mode using smooth design spectra that are the average of several earthquake motions.

The purpose of this chapter is to summarize the fundamental equations used in the response spectrum method and to point out the many approximations and limitations of the method. For example, the response spectrum method cannot be used to approximate the nonlinear response of a complex three-dimensional structural system.

The recent increase in the speed of computers has made it practical to run many time history analyses in a short period of time. In addition, it is now possible to run design checks as a function of time, which produces superior results, because each member is not designed for maximum peak values as required by the response spectrum method.

15.2   DEFINITION OF A RESPONSE SPECTRUM

For three-dimensional seismic motion, the typical modal Equation (13.6) is rewritten as:

$$\ddot{y}(t)_n + 2\zeta_n \omega_n \dot{y}(t)_n + \omega_n^2 y(t)_n = p_{nx} \ddot{u}(t)_{gx} + p_{ny} \ddot{u}(t)_{gy} + p_{nz} \ddot{u}(t)_{gz} \qquad (15.1)$$

where the three *Mode Participation Factors* are defined by $p_{ni} = -\phi_n^T \mathbf{M}_i$ in which i is equal to x, y or z. Two major problems must be solved to obtain an approximate response spectrum solution to this equation. First, for each direction of ground motion, maximum peak forces and displacements must be estimated. Second, after the response for the three orthogonal directions has been solved, it is necessary to estimate the maximum response from the three components of earthquake motion acting at the same time. This section addresses the modal combination problem from one component of motion only. The separate problem of combining the results from motion in three orthogonal directions will be discussed later in this chapter.

For input in one direction only, Equation (15.1) is written as:

$$\ddot{y}(t)_n + 2\zeta_n \omega_n \dot{y}(t)_n + \omega_n^2 y(t)_n = p_{ni} \ddot{u}(t)_g \qquad (15.2)$$

Given a specified ground motion $\ddot{u}(t)_g$, damping value and assuming $p_{ni} = -1.0$, it is possible to solve Equation (15.2) at various values of ω and

plot a curve of the maximum peak response $y(\omega)_{MAX}$. For this acceleration input, the curve is by definition the ***displacement response spectrum*** for the earthquake motion. A different curve will exist for each different value of damping.

A plot of $\omega y(\omega)_{MAX}$ is defined as the ***pseudo-velocity spectrum*** and a plot of $\omega^2 y(\omega)_{MAX}$ is defined as the ***pseudo-acceleration spectrum***.

The three curves—displacement response spectrum, pseudo-velocity spectrum, and pseudo-acceleration spectrum—are normally plotted as one curve on special log paper. However, the pseudo-values have minimum physical significance and are not an essential part of a response spectrum analysis. The true values for maximum velocity and acceleration must be calculated from the solution of Equation (15.2).

There is a mathematical relationship, however, between the pseudo-acceleration spectrum and the total acceleration spectrum. The total acceleration of the unit mass, single degree-of-freedom system, governed by Equation (15.2), is given by:

$$\ddot{u}(t)_T = \ddot{y}(t) + \ddot{u}(t)_g \tag{15.3}$$

Equation (15.2) can be solved for $\ddot{y}(t)$ and substituted into Equation (15.3) to yield:

$$\ddot{u}(t)_T = -\omega^2 y(t) - 2\xi\omega\dot{y}(t) \tag{15.4}$$

Therefore, for the special case of zero damping, the total acceleration of the system is equal to $\omega^2 y(t)$. For this reason, the ***displacement response spectrum*** curve is normally not plotted as modal displacement $y(\omega)_{MAX}$ versus ω. It is standard to present the curve in terms of $S(\omega)$ versus a period T in seconds, where:

$$S(\omega)_a = \omega^2 y(\omega)_{MAX} \quad \text{and} \quad T = \frac{2\pi}{\omega} \tag{15.5a and 15.5b}$$

The pseudo-acceleration spectrum curve, $S(\omega)_a$, has the units of acceleration versus period that has some physical significance for zero damping only. It is apparent that all response spectrum curves represent the properties of the earthquake at a specific site and are not a function of the properties of the structural system. After an estimation is made of the linear viscous damping properties of the structure, a specific response spectrum curve is selected.

15.3 CALCULATION OF MODAL RESPONSE

The maximum modal displacement for a structural model can now be calculated for a typical mode n with period T_n and corresponding spectrum response value $S(\omega_n)$. The maximum modal response associated with period T_n is given by:

$$y(T_n)_{MAX} = \frac{S(\omega_n)}{\omega_n^2} \tag{15.6}$$

The maximum modal displacement response of the structural model is calculated from:

$$\mathbf{u}_n = y(T_n)_{MAX}\phi_n \tag{15.7}$$

The corresponding internal modal forces, f_{kn}, are calculated from standard matrix structural analysis using the same equations as required in static analysis.

15.4 TYPICAL RESPONSE SPECTRUM CURVES

A ten-second segment of the Loma Prieta earthquake motions recorded on a soft site in the San Francisco Bay Area is shown in Figure 15.1. The record has been corrected using an iterative algorithm for zero displacement, velocity and acceleration at the beginning and end of the ten-second record. For the earthquake motions given in Figure 15.1a, the response spectrum curves for displacement and pseudo-acceleration are summarized in Figure 15.2a and 15.2b

The velocity curves have been intentionally omitted because they are not an essential part of the response spectrum method. Furthermore, it would require

considerable space to clearly define terms such as peak ground velocity, pseudo velocity spectrum, relative velocity spectrum and absolute velocity spectrum.
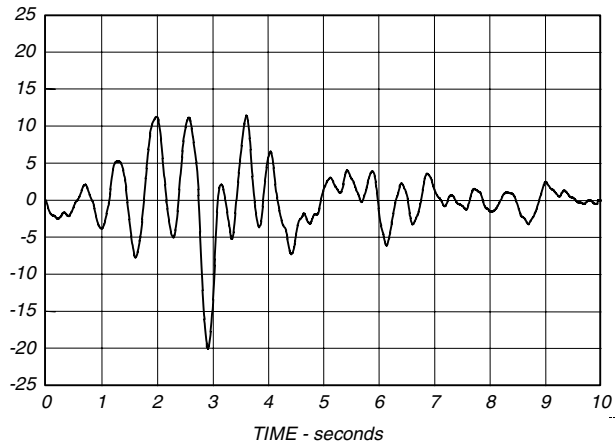
Figure 15.1a Typical Earthquake Ground Acceleration - Percent of Gravity
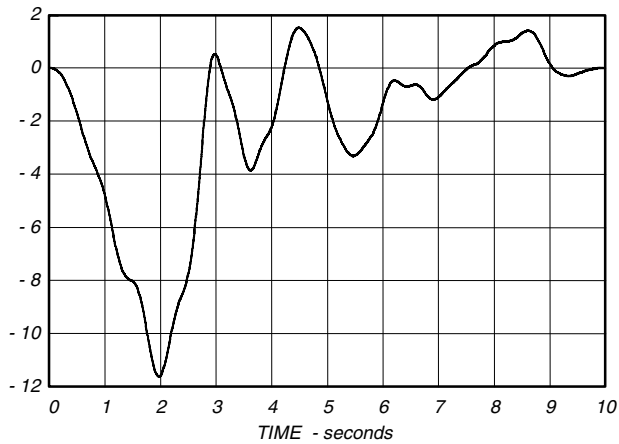
Figure 15.1b Typical Earthquake Ground Displacements - Inches
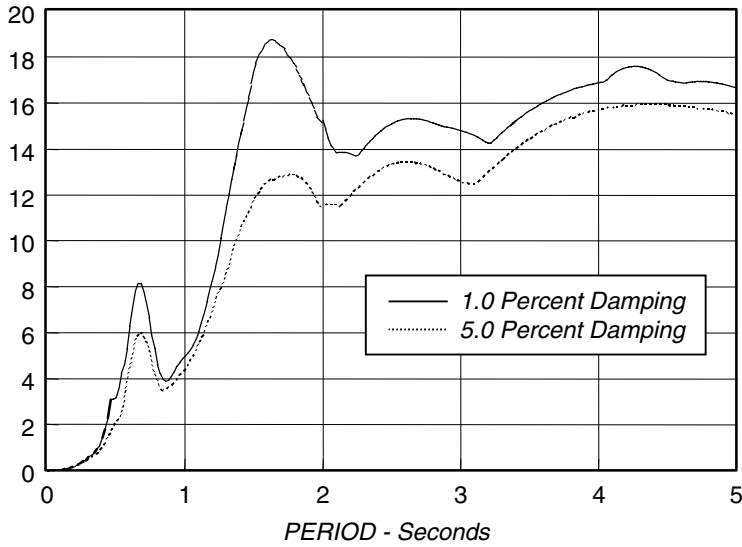
Figure 15.2a Relative Displacement Spectrum $y(\omega)_{MAX}$ - Inches
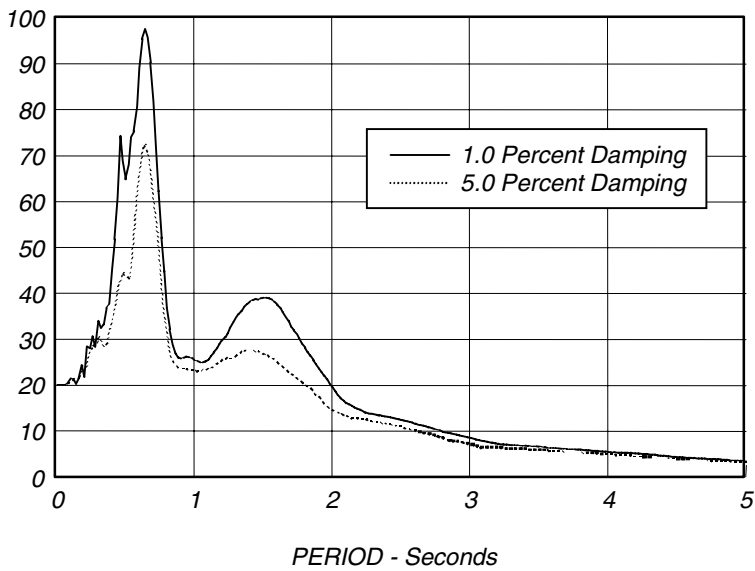
Figure 15.2b Pseudo-Acceleration Spectrum, $S_a = \omega^2 y(\omega)_{MAX}$ -

Percent of Gravity

The maximum ground acceleration for the earthquake defined by Figure 15.1a is 20.01 percent of gravity at 2.92 seconds. It is important to note that the pseudo-acceleration spectrum shown in Figure 15.2b has the same value for a very short period system. This is because of the physical fact that a very rigid structure moves as a rigid body and the relative displacements within the structure are equal to zero, as indicated by Figure 15.2a. Also, the behavior of a rigid structure is not a function of the viscous damping value.

The maximum ground displacement shown in Figure 15.1b is -11.62 inches at 1.97 seconds. For long period systems, the mass of the one-degree-of-freedom structure does not move significantly and has approximately zero absolute displacement. Therefore, the relative displacement spectrum curves shown in Figure 15.2a will converge to 11.62 inches for long periods and all values of damping. This type of real physical behavior is fundamental to the design of base isolated structures.

The relative displacement spectrum, Figure 15.2a, and the absolute acceleration spectrum, Figure 15.2b, have physical significance. However, the maximum relative displacement is directly proportional to the maximum forces developed in the structure. For that earthquake, the maximum relative displacement is 18.9 inches at a period of 1.6 seconds for 1 percent damping and 16.0 inches at a period of 4 seconds for 5 percent damping. It is important to note the significant difference between 1 and 5 percent damping for this typical soft site record.

Figure 15.2b, the absolute acceleration spectrum, indicates maximum values at a period of 0.64 seconds for both values of damping. Also, the multiplication by ω^2 tends to completely eliminate the information contained in the long period range. Because most structural failures during recent earthquakes have been associated with soft sites, perhaps we should consider using the relative displacement spectrum as the fundamental form for selecting a design earthquake. The high-frequency, short-period part of the curve should always be defined by:

$$y(\omega)_{MAX} = \ddot{u}_{gMAX} / \omega^2 \qquad \text{or} \qquad y(T)_{MAX} = \ddot{u}_{gMAX} \frac{T^2}{4\pi^2} \qquad\qquad (15.8)$$

where $\ddot{u}_{gMAX}$ is the peak ground acceleration.

15.5   THE CQC METHOD OF MODAL COMBINATION

The most conservative method that is used to estimate a peak value of displacement or force within a structure is to use the sum of the absolute of the modal response values. This approach assumes that the maximum modal values for all modes occur at the same point in time.

Another very common approach is to use the Square Root of the Sum of the Squares, SRSS, on the maximum modal values to estimate the values of displacement or forces. The SRSS method assumes that all of the maximum modal values are statistically independent. For three-dimensional structures in which a large number of frequencies are almost identical, this assumption is not justified.

The relatively new method of modal combination is the Complete Quadratic Combination, CQC, method [1] that was first published in 1981. It is based on random vibration theories and has found wide acceptance by most engineers and has been incorporated as an option in most modern computer programs for seismic analysis. Because many engineers and building codes are not requiring the use of the CQC method, one purpose of this chapter is to explain by example the advantages of using the CQC method and illustrate the potential problems in the use of the SRSS method of modal combination.

The peak value of a typical force can now be estimated from the maximum modal values using the CQC method with the application of the following double summation equation:

$$F = \sqrt{\sum_n \sum_m f_n \rho_{nm} f_m} \qquad\qquad (15.9)$$

where f_n is the modal force associated with mode n. The double summation is conducted over all modes. Similar equations can be applied to node displacements, relative displacements and base shears and overturning moments.

The cross-modal coefficients, ρ_{nm}, for the CQC method with constant damping are:

$$\rho_{nm} = \frac{8\zeta^2(1+r)r^{3/2}}{(1-r^2)^2 + 4\zeta^2 r(1+r)^2}$$

(15.10)

where $r = \omega_n / \omega_m$ and must be equal to or less than 1.0. It is important to note that the cross-modal coefficient array is symmetric and all terms are positive.

15.6   NUMERICAL EXAMPLE OF MODAL COMBINATION

The problems associated with using the absolute sum and the SRSS of modal combination can be illustrated by their application to the four-story building shown in Figure 15.3. The building is symmetrical; however, the center of mass of all floors is located 25 inches from the geometric center of the building.
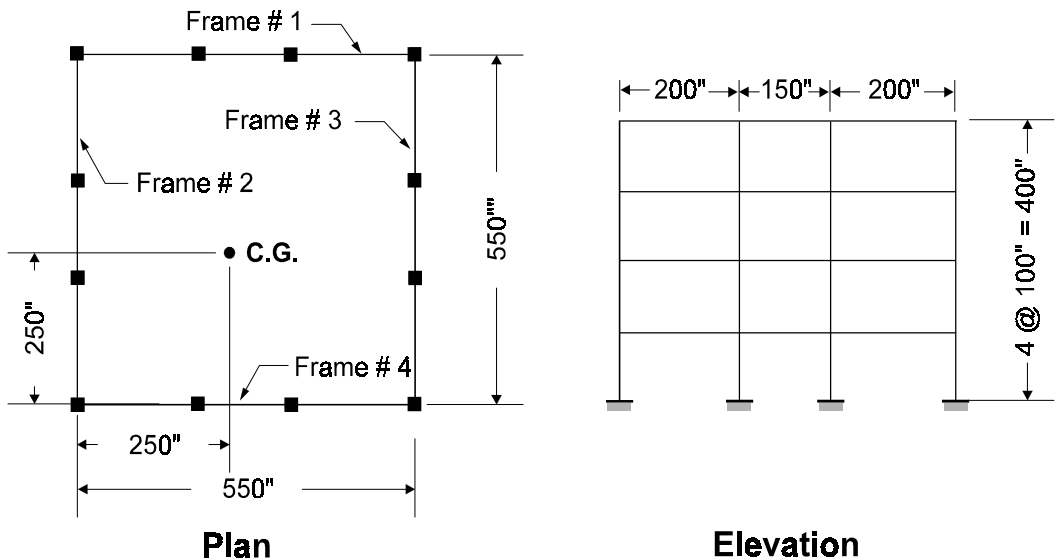
Figure 15.3 A Simple Three-Dimensional Building Example

The direction of the applied earthquake motion, a table of natural frequencies and the principal direction of the mode shape are summarized in Figure 15.4.

Mode	Frequencies (Radians/sec.)
1	13.869
2	13.931
3	43.995
4	44.189
5	54.418
6	77.686
7	78.029
8	108.32
9	108.80
10	172.613
11	304.80
12	425.00
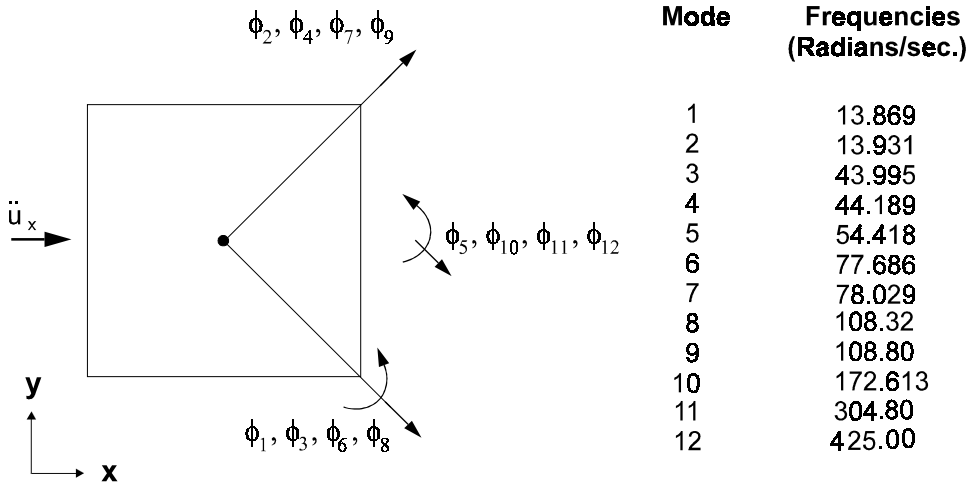
Figure 15.4 Frequencies and Approximate Directions of Mode Shapes

One notes the closeness of the frequencies that is typical of most three-dimensional building structures that are designed to resist earthquakes from both directions equally. Because of the small mass eccentricity, which is normal in real structures, the fundamental mode shape has x, y, as well as torsion components. Therefore, the model represents a very common three-dimensional building system. Also, note that there *is not a mode shape in a particular given direction,* as is implied in many building codes and some text books on elementary dynamics.

The building was subjected to one component of the Taft 1952 earthquake. An exact time history analysis using all 12 modes and a response spectrum analysis were conducted. The maximum modal base shears in the four frames for the first five modes are shown in Figure 15.5.

Figure 15.6 summarizes the maximum base shears in each of the four frames using different methods. The time history base shears, Figure 15.6a, are exact. The SRSS method, Figure 15.6b, produces base shears that under-estimate the exact values in the direction of the loads by approximately 30 percent and over-estimate the base shears normal to the loads by a factor of 10. The sum of the absolute values, Figure 15.6c, grossly over-estimates all results. The CQC

method, Figure 15.6d, produces very realistic values that are close to the exact time history solution.
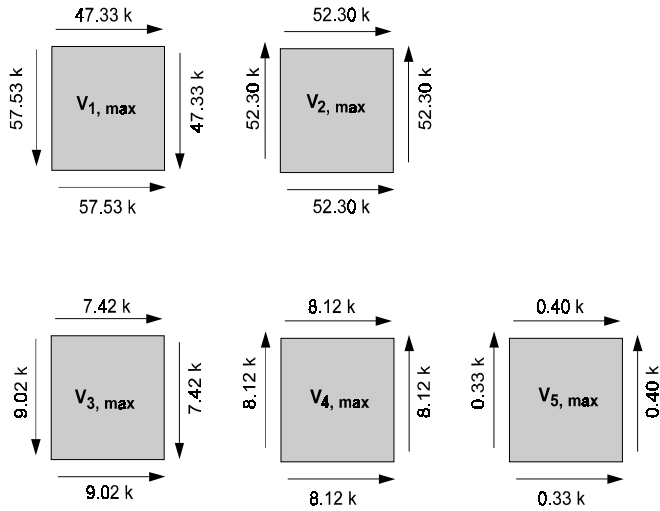
Figure 15.5 Base Shears in Each Frame for First Five Modes
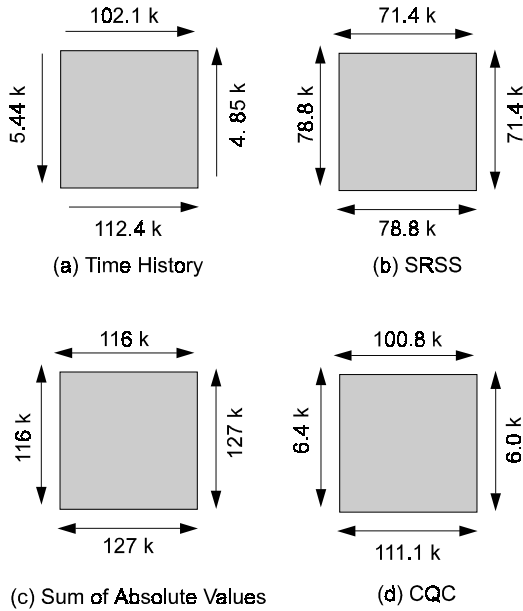
Figure 15.6 Comparison of Modal Combination Methods

The modal cross-correlation coefficients for this building are summarized in Table 15.1. It is of importance to note the existence of the relatively large off-diagonal terms that indicate which modes are coupled.

Table 15.1 Modal Cross-Correlation Coefficients - $\zeta = 0.05$

Mode	1	2	3	4	5	ω_n (rad/sec)
1	1.000	0.998	0.006	0.006	0.004	13.87
2	0.998	1.000	0.006	0.006	0.004	13.93
3	0.006	0.006	1.000	0.998	0.180	43.99
4	0.006	0.006	0.998	1.000	0.186	44.19
5	0.004	0.004	0.180	0.186	1.000	54.42

If one notes the signs of the modal base shears shown in Figure 15.3, it is apparent how the application of the CQC method allows the sum of the base shears in the direction of the external motion to be added directly. In addition, the sum of the base shears, normal to the external motion, tend to cancel. The ability of the CQC method to recognize the relative sign of the terms in the modal response is the key to the elimination of errors in the SRSS method.

15.7 DESIGN SPECTRA

Design spectra are not uneven curves as shown in Figure 15.2 because they are intended to be the average of many earthquakes. At the present time, many building codes specify design spectra in the form shown in Figure 15.7.
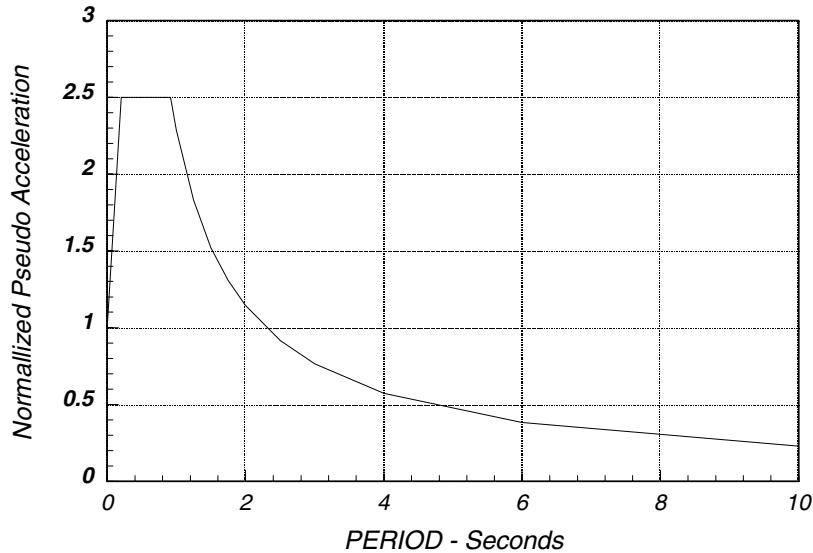
Figure 15.7 Typical Design Spectrum

The Uniform Building Code has defined specific equations for each range of the spectrum curve for four different soil types. For major structures, it is now common practice to develop a site-dependent design spectrum that includes the effect of local soil conditions and distance to the nearest faults.

15.8   ORTHOGONAL EFFECTS IN SPECTRAL ANALYSIS

A well-designed structure should be capable of equally resisting earthquake motions from all possible directions. One option in existing design codes for buildings and bridges requires that members be designed for "100 percent of the prescribed seismic forces in one direction plus 30 percent of the prescribed forces in the perpendicular direction." Other codes and organizations require the use of 40 percent rather than 30 percent. However, they give no indication on how the directions are to be determined for complex structures. For structures that are rectangular and have clearly defined principal directions, these "percentage" rules yield approximately the same results as the SRSS method.

For complex three-dimensional structures, such as non-rectangular buildings, curved bridges, arch dams or piping systems, the direction of the earthquake that

produces the maximum stresses in a particular member or at a specified point is not apparent. For time history input, it is possible to perform a large number of dynamic analyses at various angles of input to check all points for the critical earthquake directions. Such an elaborate study could conceivably produce a different critical input direction for each stress evaluated. However, the cost of such a study would be prohibitive.

It is reasonable to assume that motions that take place during an earthquake have one principal direction [2]. Or, during a finite period of time when maximum ground acceleration occurs, a principal direction exists. For most structures, this direction is not known and for most geographical locations cannot be estimated. Therefore, the only rational earthquake design criterion is that the structure must resist an earthquake of a given magnitude from any possible direction. In addition to the motion in the principal direction, a probability exists that motions normal to that direction will occur simultaneously. In addition, because of the complex nature of three-dimensional wave propagation, it is valid to assume that these normal motions are statistically independent.

Based on those assumptions, a statement of the design criterion is "a structure must resist a major earthquake motion of magnitude S_1 for all possible angles θ and at the same point in time resist earthquake motions of magnitude S_2 at 90° to the angle θ." These motions are shown schematically in Figure 15.1.

15.8.1 Basic Equations for Calculation of Spectral Forces

The stated design criterion implies that a large number of different analyses must be conducted to determine the maximum design forces and stresses. It will be shown in this section that maximum values for all members can be exactly evaluated from one computer run in which two global dynamic motions are applied. Furthermore, the maximum member forces calculated are invariant with respect to the selection system.
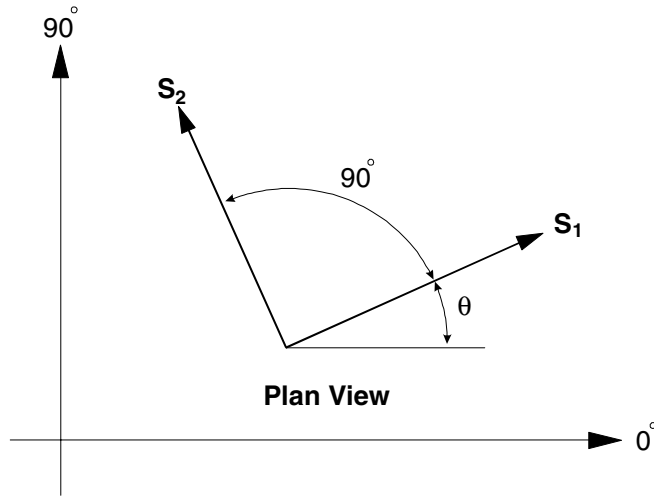
Figure 15.8 Definition of Earthquake Spectra Input

Figure 15.8 indicates that the basic input spectra S_1 and S_2 are applied at an arbitrary angle θ. At some typical point within the structure, a force, stress or displacement F is produced by this input. To simplify the analysis, it will be assumed that the minor input spectrum is some fraction of the major input spectrum. Or:

$$S_2 = a\,S_1 \tag{15.11}$$

where a is a number between 0 and 1.0.

Recently, Menun and Der Kiureghian [3] presented the CQC3 method for the combination of the effects of orthogonal spectrum.

The fundamental CQC3 equation for the estimation of a peak value is:

$$F = [F_0^2 + a^2 F_{90}^2 - (1-a^2)(F_0^2 - F_{90}^2)\sin^2\theta \\ + 2(1-a^2)F_{0-90}\sin\theta\cos\theta + F_z^2]^{\frac{1}{2}} \tag{15.12}$$

where,

$$F_0^2 = \sum_n \sum_m f_{0n} \rho_{nm} f_{0m} \tag{15.13}$$

$$F_{90}^2 = \sum_n \sum_m f_{90n} \rho_{nm} f_{90m} \tag{15.14}$$

$$F_{0-90} = \sum_n \sum_m f_{0n} \rho_{nm} f_{90m} \tag{15.15}$$

$$F_Z^2 = \sum_n \sum_m f_{zn} \rho_{nm} f_{zm} \tag{15.16}$$

in which f_{0n} and f_{90n} are the modal values produced by 100 percent of the lateral spectrum applied at 0 and 90 degrees respectively, and f_{zn} is the modal response from the vertical spectrum that can be different from the lateral spectrum.

It is important to note that for equal spectra $a = 1$, the value F is not a function of θ and the selection of the analysis reference system is arbitrary. Or:

$$F_{MAX} = \sqrt{F_0^2 + F_{90}^2 + F_z^2} \tag{15.17}$$

This indicates that it is possible to conduct only one analysis with any reference system, and the resulting structure will have all members that are designed to equally resist earthquake motions from all possible directions. This method is acceptable by most building codes.

15.8.2 The General CQC3 Method

For $a = 1$, the CQC3 method reduces to the SRSS method. However, this can be over conservative because real ground motions of equal value in all directions have not been recorded. Normally, the value of θ in Equation (15.12) is not known; therefore, it is necessary to calculate the critical angle that produces the maximum response. Differentiation of Equation (15.12) and setting the results to zero yields:

$$\theta_{cr} = \frac{1}{2} \tan^{-1} \left[\frac{2F_{0-90}}{F_0^2 - F_{90}^2} \right] \tag{15.18}$$

Two roots exist for Equation (15.17) that must be checked in order that the following equation is maximum:

$$F_{MAX} = [F_0^2 + a^2 F_{90}^2 - (1 - a^2)(F_0^2 - F_{90}^2)\sin^2 \theta_{cr}$$
$$- 2(1 - a^2)F_{0-90}\sin \theta_{cr} \cos \theta_{cr} + F_z^2]^{\frac{1}{2}} \tag{15.19}$$

At the present time, no specific guidelines have been suggested for the value of a. Reference [3] presented an example with values a between 0.50 and 0.85.

15.8.3 Examples of Three-Dimensional Spectra Analyses

The previously presented theory clearly indicates that the CQC3 combination rule, with a equal to 1.0, is identical to the SRSS method and produces results for all structural systems that are not a function of the reference system used by the engineer. One example will be presented to show the advantages of the method. Figure 15.9 illustrates a very simple one-story structure that was selected to compare the results of the 100/30 and 100/40 percentage rules with the SRSS rule.
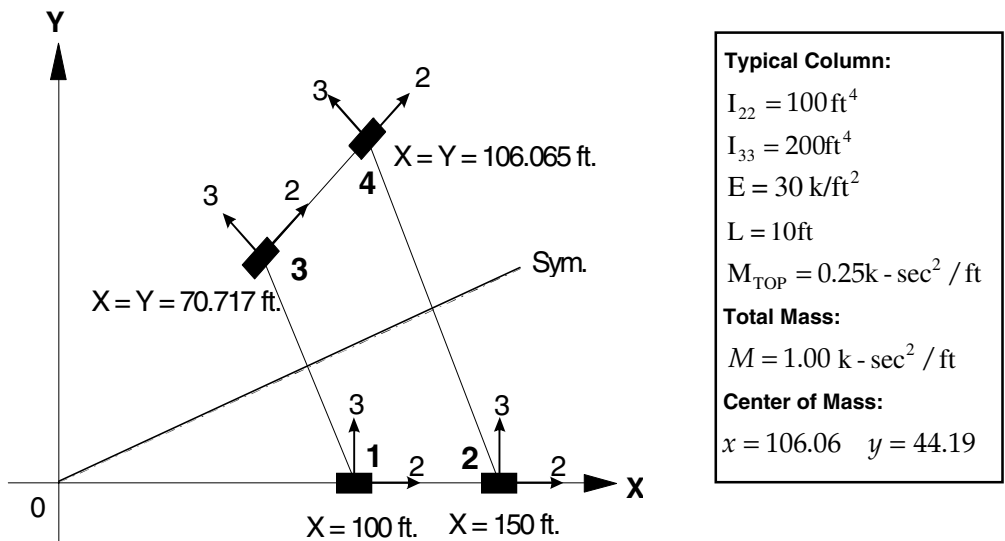
Figure 15.9 Three-Dimensional Structure

Note that the masses are not at the geometric center of the structure. The structure has two translations and one rotational degrees-of-freedom located at the center of mass. The columns, which are subjected to bending about the local 2 and 3 axes, are pinned at the top where they are connected to an in-plane rigid diaphragm.

The periods and normalized base shear forces associated with the mode shapes are summarized in Table 15.2. Because the structure has a plane of symmetry at 22.5 degrees, the second mode has no torsion and has a normalized base shear at 22.5 degrees with the x-axis. Because of this symmetry, it is apparent that columns 1 and 3 (or columns 2 and 4) should be designed for the same forces.

Table 15.2 Periods and Normalized Base Shear

Mode	Period (Seconds)	X-Force	Y-Force	Direction of-Base Shear-(Degrees)
1	1.047	0.383	-0.924	-67.5
2	0.777	-0.382	0.924	112.5
3	0.769	0.924	0.383	22.5

The definition of the mean displacement response spectrum used in the spectra analysis is given in Table 15.3.

Table 15.3 Participating Masses and Response Spectrum Used

Mode	Period (Seconds)	X-Mass	Y-Mass	Spectral Value Used for Analysis
1	1.047	12.02	70.05	1.00
2	0.777	2.62	15.31	1.00
3	0.769	85.36	14.64	1.00

The moments about the local 2 and 3 axes at the base of each of the four columns for the spectrum applied separately at 0.0 and 90 degrees are summarized in Tables 15.4 and 15.5 and are compared to the 100/30 rule.

Table 15.4 Moments About 2-Axes – SRSS vs. 100/30 Rule

Member	M_0	M_{90}	$M_{SRSS} = \sqrt{M_0^2 + M_{90}^2}$	$M_{100/30}$	Error(%)
1	0.742	1.750	1.901	1.973	3.8
2	1.113	2.463	2.703	2.797	3.5
3	0.940	1.652	1.901	1.934	1.8
4	1.131	2.455	2.703	2.794	3.4

Table 15.5 Moments About 3-Axes – SRSS vs. 100/30 Rule

Member	M_0	M_{90}	$M_{SRSS} = \sqrt{M_0^2 + M_{90}^2}$	$M_{100/30}$	Error(%)
1	2.702	0.137	2.705	2.743	1.4
2	2.702	0.137	2.705	2.743	1.4
3	1.904	1.922	2.705	2.493	-7.8
4	1.904	1.922	2.705	2.493	-7.8

For this example, the maximum forces do not vary significantly between the two methods. However, it does illustrate that the 100/30 combination method produces moments that are not symmetric, whereas the SRSS combination method produces logical and symmetric moments. For example, member 4 would be over-designed by 3.4 percent about the local 2-axis and under-designed by 7.8 percent about the local 3-axis using the 100/30 combination rule.

The SRSS and 100/40 design moments about the local 2 and 3 axes at the base of each of the four columns are summarized in Tables 15.6 and 15.7

Table 15.6 Moments About 2-Axes –SRSS vs. 100/40 Rule

Member	M_0	M_{90}	$M_{SRSS} = \sqrt{M_0^2 + M_{90}^2}$	$M_{100/40}$	Error(%)
1	0.742	1.750	1.901	2.047	7.7
2	1.113	2.463	2.703	2.908	7.6
3	0.940	1.652	1.901	2.028	1.2
4	1.131	2.455	2.703	2.907	7.5

Table 15.7 Moments About 3-Axes – SRSS vs. 100/40 Rule

Member	M_0	M_{90}	$M_{SRSS} = \sqrt{M_0^2 + M_{90}^2}$	$M_{100/40}$	Error(%)
1	2.702	0.137	2.705	2.757	1.9
2	2.702	0.137	2.705	2.757	1.9
3	1.904	1.922	2.705	2.684	-0.8
4	1.904	1.922	2.705	2.684	-0.8

The results presented in Tables 15.6 and 15.7 also illustrate that the 100/40 combination method produces results that are not reasonable. Because of symmetry, members 1 and 3 and members 2 and 4 should be designed for the same moments. Both the 100/30 and 100/40 rules fail this simple test.

If a structural engineer wants to be conservative, the results of the SRSS directional combination rule or the input spectra can be multiplied by an additional factor greater than one. One should not try to justify the use of the 100/40 percentage rule because it is conservative in "most cases." For complex three-dimensional structures, the use of the 100/40 or 100/30 percentage rule will produce member designs that are not equally resistant to earthquake motions from all possible directions.

15.8.4 Recommendations on Orthogonal Effects

For three-dimensional response spectra analyses, it has been shown that the "design of elements for 100 percent of the prescribed seismic forces in one direction plus 30 or 40 percent of the prescribed forces applied in the perpendicular direction" is dependent on the user's selection of the reference system. These commonly used "percentage combination rules" are empirical and can underestimate the design forces in certain members and produce a member design that is relatively weak in one direction. It has been shown that the alternate building code approved method, in which an SRSS combination of two 100 percent spectra analyses with respect to any user-defined orthogonal axes, will produce design forces that are not a function of the reference system. Therefore, the resulting structural design has equal resistance to seismic motions from all directions.

The CQC3 method should be used if a value of a less than 1.0 can be justified. It will produce realistic results that are not a function of the user-selected reference system.

15.9 LIMITATIONS OF THE RESPONSE SPECTRUM METHOD

It is apparent that use of the response spectrum method has limitations, some of which can be removed by additional development. However, it will never be accurate for nonlinear analysis of multi degree of freedom structures. The author believes that in the future more time history dynamic response analyses will be conducted and the many approximations associated with the use of the response spectrum method will be avoided. Some of these additional limitations will be discussed in this section.

15.9.1 Story Drift Calculations

All displacements produced by the response spectrum method are positive numbers. Therefore, a plot of a dynamic displaced shape has very little meaning because each displacement is an estimation of the maximum value. Inter-story displacements are used to estimate damage to nonstructural elements and cannot be calculated directly from the probable peak values of displacement. A simple

method to obtain a probable peak value of shear strain is to place a very thin panel element, with a shear modulus of unity, in the area where the deformation is to be calculated. The peak value of shear stress will be a good estimation of the damage index. The current code suggests a maximum value of 0.005 horizontal drift ratio, which is the same as panel shear strain if the vertical displacements are neglected.

15.9.2 Estimation of Spectra Stresses in Beams

The fundamental equation for the calculation of the stresses within the cross section of a beam is:

$$\sigma = \frac{P}{A} + \frac{M_y x}{I_y} + \frac{M_x y}{I_x} \tag{15.20}$$

This equation can be evaluated for a specified x and y point in the cross section and for the calculated maximum spectral axial force and moments that are all positive values. It is apparent that the resulting stress may be conservative because all forces will probably not obtain their peak values at the same time.

For response spectrum analysis, the correct and accurate approach for the evaluation of equation (15.20) is to evaluate the equation for each mode of vibration. This will take into consideration the relative signs of axial forces and moments in each mode. An accurate value of the maximum stress can then be calculated from the modal stresses using the CQC double sum method. It has been the author's experience with large three-dimensional structures that stresses calculated from modal stresses can be less than 50 percent of the value calculated using maximum peak values of moments and axial force.

15.9.3 Design Checks for Steel and Concrete Beams

Unfortunately, most design check equations for steel structures are written in terms of "design strength ratios" that are a nonlinear function of the axial force in the member; therefore, the ratios cannot be calculated in each mode. The author proposes a new approximate method to replace the state-of-the-art approach of calculating strength ratios based on maximum peak values of member forces. This would involve first calculating the maximum axial force.

The design ratios would then be evaluated mode by mode, assuming the maximum axial force reduction factor remains constant for all modes. The design ratio for the member would then be estimated using a double-sum modal combination method, such as the CQC3 method. This approach would improve accuracy and still be conservative.

For concrete structures, additional development work is required to develop a completely rational method for the use of maximum spectral forces in a design check equation because of the nonlinear behavior of concrete members. A time history analysis may be the only approach that will produce rational design forces.

15.9.4 Calculation of Shear Force in Bolts

With respect to the interesting problem of calculating the maximum shear force in a bolt, it is not correct to estimate the maximum shear force from a vector summation because the x and y shears do not obtain their peak values at the same time. A correct method of estimating the maximum shear in a bolt is to check the maximum bolt shear at several different angles about the bolt axis. This would be a tedious approach using hand calculations; however, if the approach is built into a post processor computer program, the computational time to calculate the maximum bolt force is trivial.

The same problem exists if principal stresses are to be calculated from a response spectrum analysis. One must check at several angles to estimate the maximum and minimum value of the stress at each point in the structure.

15.10 SUMMARY

In this chapter it has been illustrated that the response spectrum method of dynamic analysis must be used carefully. The CQC method should be used to combine modal maxima to minimize the introduction of avoidable errors. The increase in computational effort, as compared to the SRSS method, is small compared to the total computer time for a seismic analysis. The CQC method has a sound theoretical basis and has been accepted by most experts in earthquake engineering. The use of the absolute sum or the SRSS method for modal combination cannot be justified.

In order for a structure to have equal resistance to earthquake motions from all directions, the CQC3 method should be used to combine the effects of earthquake spectra applied in three dimensions. The percentage rule methods have no theoretical basis and are not invariant with respect to the reference system.

Engineers, however, should clearly understand that the response spectrum method is an ***approximate method*** used to estimate maximum peak values of displacements and forces and it has significant limitations. It is restricted to linear elastic analysis in which the damping properties can only be estimated with a low degree of confidence. The use of nonlinear spectra, which is common, has very little theoretical background, and this approach should not be applied in the analysis of complex three-dimensional structures. For such structures, true nonlinear time-history response should be used, as indicated in Chapter 19.

15.11 REFERENCES

1. Wilson, E. L., A. Der Kiureghian and E. R. Bayo. 1981. "A Replacement for the SRSS Method in Seismic Analysis," *Earthquake Engineering and Structural Dynamics*. Vol. 9. pp. l87-l92.

2. Penzien, J., and M. Watabe. 1975. "Characteristics of 3-D Earthquake Ground Motions," *Earthquake Engineering and Structural Dynamics*. Vol. 3. pp. 365-373.

3. Menun, C., and A. Der Kiureghian. 1998. "A Replacement for the 30 % Rule for Multicomponent Excitation," *Earthquake Spectra*. Vol. 13, Number 1. February.

16.

SOIL STRUCTURE INTERACTION

At a Finite Distance from a Structure,
the Absolute Displacements
Must Approach the Free-Field Displacements

16.1 INTRODUCTION

The estimation of earthquake motions at the site of a structure is the most important phase of the design or retrofit of a structure. Because of the large number of assumptions required, experts in the field often disagree, by more than a factor of two, about the magnitude of motions expected at the site without the structure present. This lack of accuracy about the basic input motions, however, does not justify the introduction of additional unnecessary approximations in the dynamic analysis of the structure and its interaction with the material under the structure. Therefore, it will be assumed that the free-field motions at the location of the structure, without the structure present, can be estimated and are specified in the form of earthquake acceleration records in three directions. It is now common practice, on major engineering projects, to investigate several different sets of ground motions to consider both near fault and far fault events.

If a lightweight flexible structure is built on a very stiff rock foundation, a valid assumption is that the input motion at the base of the structure is the same as the free-field earthquake motion. This assumption is valid for a large number of building systems because most building type structures are approximately 90 percent voids, and it is not unusual for the weight of the structure to be equal to

the weight of the soil excavated before the structure is built. However, if the structure is very massive and stiff, such as a concrete gravity dam, and the foundation is relatively soft, the motion at the base of the structure may be significantly different from the free-field surface motion. Even for this extreme case, however, it is apparent that the most significant interaction effects will be near the structure, and, at some finite distance from the base of the structure, the displacements will converge back to the free-field earthquake motion.

16.2   SITE RESPONSE ANALYSIS

The 1985 Mexico City and many other recent earthquakes clearly illustrate the importance of local soil properties on the earthquake response of structures. These earthquakes demonstrated that the rock motions could be amplified at the base of a structure by over a factor of five. Therefore, there is a strong engineering motivation for a site-dependent dynamic response analysis for many foundations to determine the free-field earthquake motions. The determination of a realistic site-dependent free-field surface motion at the base of a structure can be the most important step in the earthquake resistant design of any structure.

For most horizontally layered sites, a one-dimensional pure shear model can be used to calculate the free-field surface displacements given the earthquake motion at the base of a soil deposit. Many special purpose computer programs exist for this purpose. SHAKE [1] is a well-known program that is based on the frequency domain solution method. SHAKE iterates to estimate effective linear stiffness and damping properties to approximate the nonlinear behavior of a site. WAVES [2] is a new nonlinear program in which the nonlinear equations of motion are solved using a direct step-by-step integration method. If the soil material can be considered linear, the SAP2000 program, using the SOLID element, can calculate either the one-, two- or three-dimensional free-field motions at the base of a structure. In addition, a one-dimensional nonlinear site analysis can be accurately conducted using the FNA option in the SAP2000 program.

16.3 KINEMATIC OR SOIL STRUCTURE INTERACTION

The most common soil structure interaction (SSI) approach used for three-dimensional soil structure systems is based on the "added motion" formulation [3]. This formulation is mathematically simple, theoretically correct, and is easy to automate and use within a general linear structural analysis program. In addition, the formulation is valid for free-field motions caused by earthquake waves generated from all sources. The method requires that the free-field motions at the base of the structure be calculated before the soil structure interactive analysis.

To develop the fundamental SSI dynamic equilibrium equations, consider the three-dimensional soil structure system shown in Figure 16.1.
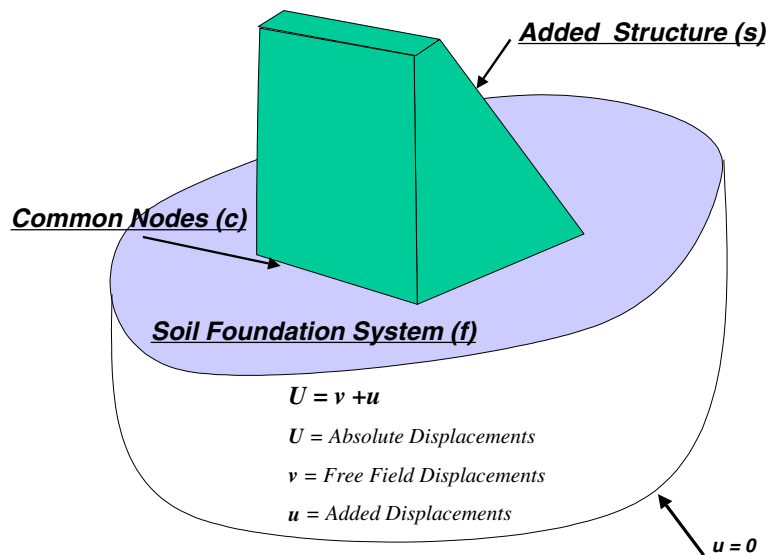

Figure 16.1 Soil structure Interaction Model

Consider the case where the SSI model is divided into three sets of node points. The common nodes at the interface of the structure and foundation are identified with *"c"*; the other nodes within the structure are *"s"* nodes; and the other nodes within the foundation are *"f"* nodes. From the direct stiffness approach in

structural analysis, the dynamic force equilibrium of the system is given in terms of the **absolute displacements**, $\mathbf{U}$, by the following sub-matrix equation:

$$\begin{bmatrix} \mathbf{M}_{ss} & 0 & 0 \\ 0 & \mathbf{M}_{cc} & 0 \\ 0 & 0 & \mathbf{M}_{ff} \end{bmatrix}\begin{bmatrix} \ddot{\mathbf{U}}_s \\ \ddot{\mathbf{U}}_c \\ \ddot{\mathbf{U}}_f \end{bmatrix} + \begin{bmatrix} \mathbf{K}_{ss} & \mathbf{K}_{sf} & 0 \\ \mathbf{K}_{cf} & \mathbf{K}_{cc} & \mathbf{K}_{cf} \\ 0 & \mathbf{K}_{fc} & \mathbf{K}_{ff} \end{bmatrix}\begin{bmatrix} \mathbf{U}_s \\ \mathbf{U}_c \\ \mathbf{U}_f \end{bmatrix} = \begin{bmatrix} 0 \\ 0 \\ 0 \end{bmatrix} \tag{16.1}$$

where the mass and the stiffness at the contact nodes are the sum of the contributions from the structure *(s)* and foundation *(f)*, and are given by:

$$\mathbf{M}_{cc} = \mathbf{M}_{cc}^{(s)} + \mathbf{M}_{cc}^{(f)} \quad \text{and} \quad \mathbf{K}_{cc} = \mathbf{K}_{cc}^{(s)} + \mathbf{K}_{cc}^{(f)} \tag{16.2}$$

In terms of absolute motion, there are no external forces acting on the system. However, the displacements at the boundary of the foundation must be known. To avoid solving this SSI problem directly, the dynamic response of the foundation without the structure is calculated. In many cases, this **free-field** solution can be obtained from a simple one-dimensional site model. The three-dimensional free-field solution is designated by the absolute displacements $\mathbf{v}$ and absolute accelerations $\ddot{\mathbf{v}}$. By a simple change of variables, it is now possible to express the absolute displacements $\mathbf{U}$ and accelerations $\ddot{\mathbf{U}}$ in terms of displacements $\mathbf{u}$ relative to the free-field displacements $\mathbf{v}$. Or:

$$\begin{bmatrix} \mathbf{U}_s \\ \mathbf{U}_c \\ \mathbf{U}_f \end{bmatrix} \equiv \begin{bmatrix} \mathbf{u}_s \\ \mathbf{u}_c \\ \mathbf{u}_f \end{bmatrix} + \begin{bmatrix} \mathbf{v}_s \\ \mathbf{v}_c \\ \mathbf{v}_f \end{bmatrix} \quad \text{and} \quad \begin{bmatrix} \ddot{\mathbf{U}}_s \\ \ddot{\mathbf{U}}_c \\ \ddot{\mathbf{U}}_f \end{bmatrix} \equiv \begin{bmatrix} \ddot{\mathbf{u}}_s \\ \ddot{\mathbf{u}}_c \\ \ddot{\mathbf{u}}_f \end{bmatrix} + \begin{bmatrix} \ddot{\mathbf{v}}_s \\ \ddot{\mathbf{v}}_c \\ \ddot{\mathbf{v}}_f \end{bmatrix} \tag{16.3}$$

Equation (16.1) can now be written as

$$\begin{bmatrix} \mathbf{M}_{ss} & 0 & 0 \\ 0 & \mathbf{M}_{cc} & 0 \\ 0 & 0 & \mathbf{M}_{ff} \end{bmatrix} \begin{bmatrix} \ddot{\mathbf{u}}_s \\ \ddot{\mathbf{u}}_c \\ \ddot{\mathbf{u}}_f \end{bmatrix} + \begin{bmatrix} \mathbf{K}_{ss} & \mathbf{K}_{sc} & 0 \\ \mathbf{K}_{cs} & \mathbf{K}_{cc} & \mathbf{K}_{cf} \\ 0 & \mathbf{K}_{fc} & \mathbf{K}_{ff} \end{bmatrix} \begin{bmatrix} \mathbf{u}_s \\ \mathbf{u}_c \\ \mathbf{u}_f \end{bmatrix} =$$

$$-\begin{bmatrix} \mathbf{M}_{ss} & 0 & 0 \\ 0 & \mathbf{M}_{cc} & 0 \\ 0 & 0 & \mathbf{M}_{ff} \end{bmatrix} \begin{bmatrix} \ddot{\mathbf{v}}_s \\ \ddot{\mathbf{v}}_c \\ \ddot{\mathbf{v}}_f \end{bmatrix} - \begin{bmatrix} \mathbf{K}_{ss} & \mathbf{K}_{sc} & 0 \\ \mathbf{K}_{cs} & \mathbf{K}_{cc} & \mathbf{K}_{cf} \\ 0 & \mathbf{K}_{fc} & \mathbf{K}_{ff} \end{bmatrix} \begin{bmatrix} \mathbf{v}_s \\ \mathbf{v}_c \\ \mathbf{v}_f \end{bmatrix} = \mathbf{R} \qquad (16.4)$$

If the free-field displacement $\mathbf{v}_c$ is constant over the base of the structure, the term $\mathbf{v}_s$ is the rigid body motion of the structure. Therefore, Equation (16.4) can be further simplified by the fact that the static rigid body motion of the structure is:

$$\begin{bmatrix} \mathbf{K}_{ss} & \mathbf{K}_{sc} \\ \mathbf{K}_{cs} & \mathbf{K}_{cc}^{(s)} \end{bmatrix} \begin{bmatrix} \mathbf{v}_s \\ \mathbf{v}_c \end{bmatrix} = \begin{bmatrix} 0 \\ 0 \end{bmatrix} \qquad (16.5)$$

Also, the dynamic free-field motion of the foundation requires that:

$$\begin{bmatrix} \mathbf{M}_{cc}^{(f)} & 0 \\ 0 & \mathbf{M}_{ff} \end{bmatrix} \begin{bmatrix} \ddot{\mathbf{v}}_c \\ \ddot{\mathbf{v}}_f \end{bmatrix} + \begin{bmatrix} \mathbf{K}_{cc}^{(f)} & \mathbf{K}_{cf} \\ \mathbf{K}_{cf} & \mathbf{K}_{ff} \end{bmatrix} \begin{bmatrix} \mathbf{v}_c \\ \mathbf{v}_f \end{bmatrix} = \begin{bmatrix} 0 \\ 0 \end{bmatrix} \qquad (16.6)$$

Therefore, the right-hand side of Equation (16.4) can be written as:

$$\mathbf{R} = \begin{bmatrix} \mathbf{M}_{ss} & 0 & 0 \\ 0 & \mathbf{M}_{cc}^{(s)} & 0 \\ 0 & 0 & 0 \end{bmatrix} \begin{bmatrix} \ddot{\mathbf{v}}_s \\ \ddot{\mathbf{v}}_c \\ 0 \end{bmatrix} \qquad (16.7)$$

Hence, the right-hand side of the Equation (16.4) does not contain the mass of the foundation. Therefore, three-dimensional dynamic equilibrium equations for the complete soil structure system with damping added are of the following form for a lumped mass system:

$$\mathbf{M}\ddot{\mathbf{u}} + \mathbf{C}\dot{\mathbf{u}} + \mathbf{K}\mathbf{u} = -\mathbf{m}_x \ddot{\mathbf{v}}_x(t) - \mathbf{m}_y \ddot{\mathbf{v}}_y(t) - \mathbf{m}_z \ddot{\mathbf{v}}_z(t) \qquad (16.8)$$

where $\mathbf{M}$, $\mathbf{C}$ and $\mathbf{K}$ are the mass, damping and stiffness matrices, respectively, of

the soil structure model. The added relative displacements, $\underline{\mathbf{u}}$, exist for the soil structure system and must be set to zero at the sides and bottom of the foundation. The terms $\ddot{\mathbf{v}}_x(t)$, $\ddot{\mathbf{v}}_y(t)$ and $\ddot{\mathbf{v}}_z(t)$ are the free-field components of the acceleration if the structure is not present. The column matrices, $\mathbf{m}_i$, are the directional masses for the added structure only.

Most structural analysis computer programs automatically apply the seismic loading to all mass degrees of freedom within the computer model and cannot solve the SSI problem. This lack of capability has motivated the development of the massless foundation model. This allows the correct seismic forces to be applied to the structure; however, the inertia forces within the foundation material are neglected. The results from a massless foundation analysis converge as the size of the foundation model is increased. However, the converged solutions may have avoidable errors in the mode shapes, frequencies and response of the system.

To activate the soil structure interaction within a computer program, it is only necessary to identify the foundation mass so that the loading is not applied to that part of the structure. The program then has the required information to form both the total mass and the mass of the added structure. The SAP2000 program has this option and is capable of solving the SSI problem correctly.

16.4   RESPONSE DUE TO MULTI-SUPPORT INPUT MOTIONS

The previous SSI analysis assumes that the free-field motion at the base of the structure is constant. For large structures such as bridges and arch dams, the free-field motion is not constant at all points where the structure is in contact with the foundation.

The approach normally used to solve this problem is to define a *quasi-static displacement* v_c that is calculated from the following equation:

$$\mathbf{K}_{ss}\mathbf{v}_s + \mathbf{K}_{sc}\mathbf{v}_c = \mathbf{0} \quad \text{or,} \quad \mathbf{v}_s = -\mathbf{K}_{ss}^{-1}\mathbf{K}_{sc}\mathbf{v}_c = \mathbf{T}_{sc}\mathbf{v}_c \qquad (16.9a)$$

The transformation matrix $\mathbf{T}_{sc}$ allows the corresponding quasi-static acceleration in the structure to be calculated from:

$$\ddot{\mathbf{v}}_s = \mathbf{T}_{sc}\ddot{\mathbf{v}}_c \tag{16.9b}$$

Equation (16.4) can be written as:

$$\mathbf{R} = -\begin{bmatrix} \mathbf{M}_{ss} & 0 & 0 \\ 0 & \mathbf{M}_{cc} & 0 \\ 0 & 0 & \mathbf{M}_{ff} \end{bmatrix}\begin{bmatrix} \ddot{\mathbf{v}}_s \\ \ddot{\mathbf{v}}_c \\ \ddot{\mathbf{v}}_f \end{bmatrix} - \begin{bmatrix} \mathbf{K}_{ss} & \mathbf{K}_{sc} & 0 \\ \mathbf{K}_{cs} & \mathbf{K}_{cc} & \mathbf{K}_{cf} \\ 0 & \mathbf{K}_{fc} & \mathbf{K}_{ff} \end{bmatrix}\begin{bmatrix} \mathbf{v}_s \\ \mathbf{v}_c \\ \mathbf{v}_f \end{bmatrix} \tag{16.10}$$

After substitution of Equations (16.6) and (16.9), Equation (16.10) can be written as:

$$\mathbf{R} = -\begin{bmatrix} 0 & \mathbf{M}_{ss}\mathbf{T}_{sc} & 0 \\ 0 & \mathbf{M}_{cc} & 0 \\ 0 & 0 & 0 \end{bmatrix}\begin{bmatrix} \ddot{\mathbf{v}}_s \\ \ddot{\mathbf{v}}_c \\ \ddot{\mathbf{v}}_f \end{bmatrix} - \begin{bmatrix} 0 & 0 & 0 \\ 0 & \overline{\mathbf{K}}_{cc} & 0 \\ 0 & 0 & 0 \end{bmatrix}\begin{bmatrix} \mathbf{v}_s \\ \mathbf{v}_c \\ \mathbf{v}_f \end{bmatrix} \tag{16.11}$$

The reduced structural stiffness at the contact surface $\overline{\mathbf{K}}_{cc}$ is given by:

$$\overline{\mathbf{K}}_{cc} = \mathbf{K}_{cc} + \mathbf{K}_{cs}\mathbf{T}_{sc} \tag{16.12}$$

Therefore, this approach requires a special program option to calculate the mass and stiffness matrices to be used on the right-hand side of the dynamic equilibrium equations. Note that the loads are a function of both the free-field displacements and accelerations at the soil structure contact. Also, to obtain the total stresses and displacements within the structure, the quasi-static solution must be added to the solution. At the present time, no general purpose structural analysis computer program is based on this "numerically cumbersome" approach.

An alternative approach is to formulate the solution directly in terms of the absolute displacements of the structure. This involves the introduction of the following change of variables:

$$\begin{bmatrix} \mathbf{U}_s \\ \mathbf{U}_c \\ \mathbf{U}_f \end{bmatrix} \equiv \begin{bmatrix} \mathbf{u}_s \\ \mathbf{u}_c \\ \mathbf{u}_f \end{bmatrix} + \begin{bmatrix} 0 \\ \mathbf{v}_c \\ \mathbf{v}_f \end{bmatrix} \quad \text{and} \quad \begin{bmatrix} \ddot{\mathbf{U}}_s \\ \ddot{\mathbf{U}}_c \\ \ddot{\mathbf{U}}_f \end{bmatrix} \equiv \begin{bmatrix} \ddot{\mathbf{u}}_s \\ \ddot{\mathbf{u}}_c \\ \ddot{\mathbf{u}}_f \end{bmatrix} + \begin{bmatrix} 0 \\ \ddot{\mathbf{v}}_c \\ \ddot{\mathbf{v}}_f \end{bmatrix} \tag{16.13}$$

Substitution of this change of variables into Equation (16.1) yields the following dynamic equilibrium equations in terms of the absolute displacement, $\mathbf{u}_s$, of the structure:

$$
\begin{bmatrix} \mathbf{M}_{ss} & 0 & 0 \\ 0 & \mathbf{M}_{cc} & 0 \\ 0 & 0 & \mathbf{M}_{ff} \end{bmatrix} \begin{bmatrix} \ddot{\mathbf{u}}_s \\ \ddot{\mathbf{u}}_c \\ \ddot{\mathbf{u}}_f \end{bmatrix} + \begin{bmatrix} \mathbf{K}_{ss} & \mathbf{K}_{sf} & 0 \\ \mathbf{K}_{cf} & \mathbf{K}_{cc} & \mathbf{K}_{cf} \\ 0 & \mathbf{K}_{fc} & \mathbf{K}_{ff} \end{bmatrix} \begin{bmatrix} \mathbf{u}_s \\ \mathbf{u}_c \\ \mathbf{u}_f \end{bmatrix} = \mathbf{R} \qquad (16.14)
$$

After the free-field response, Equation (16.6), has been removed, the dynamic loading is calculated from the following equation:

$$
\mathbf{R} = - \begin{bmatrix} \mathbf{K}_{ss} & \mathbf{K}_{sc} & 0 \\ \mathbf{K}_{cs} & \mathbf{K}_{cc}^{(s)} & 0 \\ 0 & 0 & 0 \end{bmatrix} \begin{bmatrix} 0 \\ \mathbf{v}_c \\ 0 \end{bmatrix} - \begin{bmatrix} \mathbf{M}_{ss} & 0 & 0 \\ 0 & \mathbf{M}_{cc}^{(s)} & 0 \\ 0 & 0 & 0 \end{bmatrix} \begin{bmatrix} 0 \\ \ddot{\mathbf{v}}_c \\ 0 \end{bmatrix} \qquad (16.15a)
$$

This equation can be further simplified by connecting the structure to the foundation with stiff massless springs that are considered as part of the structure. Therefore, the mass of the structure at the contact nodes is eliminated and Equation (16.15a) is reduced to:

$$
\mathbf{R} = - \begin{bmatrix} \mathbf{K}_{sc} \\ \mathbf{K}_{cc}^{(s)} \\ 0 \end{bmatrix} \begin{bmatrix} \mathbf{v}_c \end{bmatrix} \qquad (16.15b)
$$

It is apparent that the stiffness terms in Equation (16.15b) represent the stiffness of the contact springs only. Therefore, for a typical displacement component (n = x, y or z), the forces acting at point "i" on the structure and point "j" on the foundation are given by:

$$
\begin{bmatrix} R_i \\ R_j \end{bmatrix}_n = -k_n \begin{bmatrix} 1.0 & -1.0 \\ -1.0 & 1.0 \end{bmatrix} \begin{bmatrix} 0 \\ v_n \end{bmatrix} \qquad (16.16)
$$

where k_n is the massless spring stiffness in the nth direction and v_n is the free-field displacement. Hence, points "i" and "j" can be at the same location in space and the only loads acting are a series of time-dependent, concentrated point

loads that are equal and opposite forces between the structure and foundation. The spring stiffness selected must be approximately three orders-of-magnitude greater than the stiffness of the structure at the connecting nodes. The spring stiffness should be large enough so the fundamental periods of the system are not changed, and small enough not to cause numerical problems.

The dynamic equilibrium equations, with damping added, can be written in the following form:

$$\mathbf{M\ddot{u} + C\dot{u} + Ku = R} \tag{16.17}$$

It should be noted that concentrated dynamic loads generally require a large number of eigenvectors to capture the correct response of the system. However, if LDR vectors are used in a mode superposition analysis, the required number of vectors is reduced significantly. The SAP2000 program has the ability to solve the multi-support, soil structure interaction problems using this approach. At the same time, selective nonlinear behavior of the structure can be considered.

16.5   ANALYSIS OF GRAVITY DAM AND FOUNDATION

To illustrate the use of the soil structure interaction option, several earthquake response analyses of the Pine Flat Dam were conducted using different foundation models. The foundation properties were assumed to be the same properties as the dam. Damping was set at five percent. Ten Ritz vectors generated from loads on the dam only were used. However, the resulting approximate mode shapes used in the standard mode superposition analysis included the mass inertia effects of the foundation. The horizontal dynamic loading was the typical segment of the Loma Prieta earthquake defined in Figure 15.1a. A finite element model of the dam on a rigid foundation is shown in Figure 16.2.
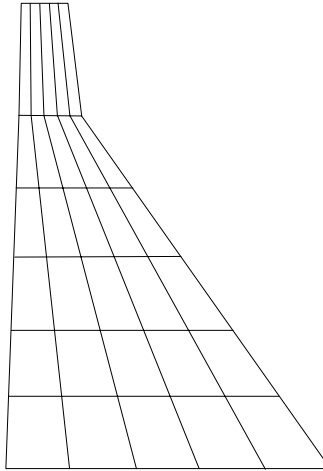
Figure 16.2 Finite Element Model of Dam Only

The two different foundation models used are shown in Figure 16.3.
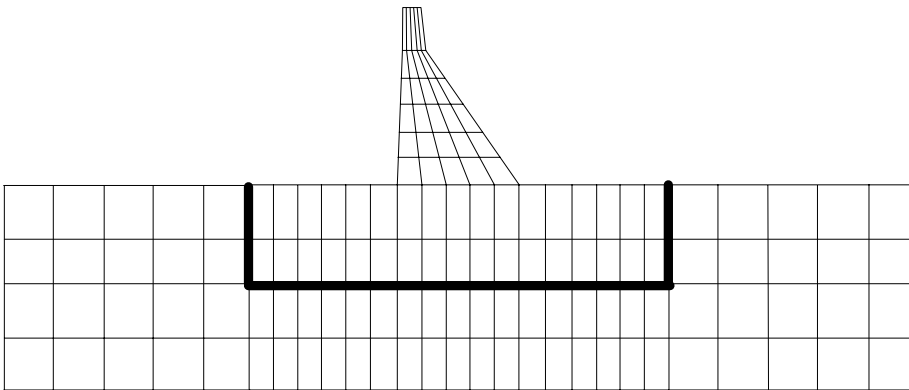
Figure 16.3 Models of Dam with Small and Large Foundation

Selective results are summarized in Table 16.1. For the purpose of comparison, it will be assumed that Ritz vector results for the large foundation mesh are the referenced values.

Table 16.1 Selective Results of Dam-Foundation Analyses

Dam Foundation	Total Mass (lb-sec²/in)	Periods (seconds)	Max. Displacement (inches)	Max. & Min. Stress (ksi)
None	1,870	0.335 0.158	0.65	-37 to +383
Small	13,250	0.404 0.210	1.28	-490 to +289
Large	77,360	0.455 0.371	1.31	-512 to +297

The differences between the results of the small and large foundation models are very close, which indicates that the solution of the large foundation model may be nearly converged. It is true that the radiation damping effects in a finite foundation model are neglected. However, as the foundation model becomes larger, the energy dissipation from normal modal damping within the massive foundation is significantly larger than the effects of radiation damping for transient earthquake-type loading.

16.6   THE MASSLESS FOUNDATION APPROXIMATION

Most general purpose programs for earthquake analysis of structures do not have the option of identifying the foundation mass as a separate type of mass on which the earthquake forces do not act. Therefore, an approximation that has commonly been used is to neglect the mass of the foundation completely in the analysis. Table 16.2 summarizes the results for an analysis of the same dam-foundation systems using a massless foundation. As expected, these results are similar. For this case the results are conservative; however, one cannot be assured of this for all cases.

Table 16.2 Selective Results of Dam With Massless Foundation Analyses

Dam Foundation	Total Mass (lb-sec^2/in)	Periods (seconds)	Max. Displacement (inches)	Max. & Min. Stress (ksi)
None	1,870	0.335 0.158	0.65	-37 to +383
Small	1,870	0.400 0.195	1.27	-480 to +289
Large	1,870	0.415 0.207	1.43	-550 to +330

16.7 APPROXIMATE RADIATION BOUNDARY CONDITIONS

If the foundation volume is large and the modal damping exists, it was demonstrated in the previous section that a finite foundation with fixed boundaries can produce converged results. However, the use of energy absorbing boundaries can further reduce the size of the foundation required to produce a converged solution.

To calculate the properties of this boundary condition, consider a plane wave propagating in the x-direction. The forces that cause wave propagation are shown acting on a unit cube in Figure 16.4.
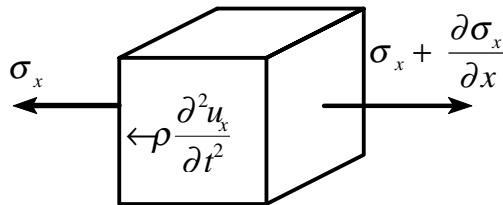
Figure 16.4 Forces Acting on Unit Cube

From Figure 16.4 the one dimensional equilibrium equation in the x-direction is:

$$\rho\frac{\partial^2 u}{\partial t^2} - \frac{\partial \sigma_x}{\partial x} = 0 \qquad\qquad (16.18)$$

Because $\sigma_x = \lambda\varepsilon_x = \lambda\dfrac{\partial u}{\partial x}$, the one-dimensional partial differential equation is written in the following classical wave propagation form:

$$\frac{\partial^2 u}{\partial t^2} - V_p^{\,2}\frac{\partial^2 u_x}{\partial x^2} = 0 \tag{16.19}$$

where V_p is the wave propagation velocity of the material and is given by:

$$V_p = \sqrt{\frac{\lambda}{\rho}} \tag{16.20}$$

in which ρ is the mass density and λ is the bulk modulus given by:

$$\lambda = \frac{1-\nu}{(1+\nu)(1-2\nu)} E \tag{16.21}$$

The solution of Equation (16.13) for harmonic wave propagation in the positive x-direction is a displacement of the following form:

$$u(t,x) = U\left[\sin(\omega t - \frac{\omega x}{V_p}) + \cos(\omega t - \frac{\omega x}{V_p})\right] \tag{16.22}$$

This equation can be easily verified by substitution into Equation (16.18). The arbitrary frequency of the harmonic motion is ω. The velocity, $\dfrac{\partial u}{\partial t}$, of a particle at location x is:

$$\dot{u}(t,x) = U\omega\left[\cos(\omega t - \frac{\omega x}{V_p}) - \sin(\omega t - \frac{\omega x}{V_p})\right] \tag{16.23}$$

The strain in the x-direction is:

$$\varepsilon(x,t) = \frac{\partial u}{\partial x} = -\frac{\dot{u}(x,t)}{V_p} \tag{16.24}$$

The corresponding stress can now be expressed in the following simplified form:

$$\sigma(x,t) = \lambda\varepsilon(x,t) = -V_p \rho \dot{u}(x,t) \qquad (16.25)$$

The compression stress is identical to the force in a simple viscous damper with constant damping value equal to $V_p\rho$ per unit area of the boundary. Therefore, a boundary condition can be created, at a cut boundary, which will allow the wave to pass without reflection and allow the strain energy to "radiate" away from the foundation.

Also, it can be easily shown that the shear wave "radiation" boundary condition, parallel to a free boundary, is satisfied if damping values are assigned to be $V_s\rho$ per unit of boundary area. The shear wave propagation velocity is given by:

$$V_s = \sqrt{\frac{G}{\rho}} \qquad (16.26)$$

where G is the shear modulus.

The FNA method can be used to solve structures in the time domain with these types of boundary conditions. In later editions of this book, the accuracy of those boundary condition approximations will be illustrated using numerical examples. Also, it will be used with a fluid boundary where only compression waves exist.

16.8   USE OF SPRINGS AT THE BASE OF A STRUCTURE

Another important structural modeling problem that must be solved is at the interface of the major structural elements within a structure and the foundation material. For example, the deformations at the base of a major shear wall in a building structure will significantly affect the displacement and force distribution in the upper stories of a building for both static and dynamic loads. Realistic spring stiffness can be selected from separate finite element studies or by using the classical half-space equations given in Table 16.3.

It is the opinion of the author that the use of appropriate site-dependent free-field earthquake motions and selection of realistic massless springs at the base of the structure are the only modeling assumptions required to include site and foundation properties in the earthquake analysis of most structural systems.

Table 16.3 also contains effective mass and damping factors that include the approximate effects of radiation damping. Those values can be used directly in a computer model without any difficulty. However, considerable care should be taken in using those equations at the base of a complete structure. For example, the effective earthquake forces must not be applied to the foundation mass.

Table 16.3 Properties of Rigid Circular Plate on Surface of Half-Space

DIRECTION	STIFFNESS	DAMPING	MASS
Vertical	$K = \dfrac{4Gr}{1-\nu}$	$1.79\sqrt{K\rho\, r^3}$	$1.50\rho\, r^3$
Horizontal	$18.2Gr\dfrac{(1-\nu^2)}{(2-\nu)^2}$	$1.08\sqrt{K\rho\, r^3}$	$0.28\rho\, r^3$
Rotation	$2.7Gr^3$	$0.47\sqrt{K\rho\, r^3}$	$0.49\rho\, r^5$
Torsion	$5.3Gr^3$	$1.11\sqrt{K\rho\, r^5}$	$0.70\rho\, r^5$

r = plate radius; G = shear modulus; ν = Poisson's ratio; ρ = mass density

Source: Adapted from "Fundamentals of Earthquake Engineering, by Newmark and Rosenblueth, Prentice-Hall, 1971.

16.9   SUMMARY

A large number of research papers and several books have been written on structure-foundation-soil analysis and site response from earthquake loading. However, the majority of those publications have been restricted to the linear behavior of soil structure systems. It is possible to use the numerical methods presented in this book to conduct accurate earthquake analysis of real soil structure systems in the time domain, including many realistic nonlinear properties. Also, it can be demonstrated that the solution obtained is converged to the correct soil structure interactive solution.

For major structures on soft soil, one-dimensional site response analyses should be conducted. Under major structural elements, such as the base of a shear wall, massless elastic springs should be used to estimate the foundation stiffness. For

massive structures, such as gravity dams, a part of the foundation should be modeled using three-dimensional SOLID elements in which SSI effects are included.

16.10 REFERENCES

1. Schnabel, P., J. Lysmer and H. Seed. 1970. "SHAKE - A Computer Program for the Earthquake Response for Horizontally Layered Sites," EERC Report No. 72-2. University of California, Berkeley. February.

2. Hart, J., and E. Wilson. "WAVES - An Efficient Microcomputer Program for Nonlinear Site Response Analysis," National Information Center for Earthquake Engineering. Davis Hall, University of California, Berkeley. Tel. # (415) 642-5113.

3. Clough, R., and J. Penzien. 1993. *Dynamics of Structures*, Second Edition. McGraw-Hill, Inc. ISBN 0-07-011394-7.

17.

SEISMIC ANALYSIS MODELING TO SATISFY BUILDING CODES

The Current Building Codes Use the Terminology: Principal Direction without a Unique Definition

17.1 INTRODUCTION

Currently a three-dimensional dynamic analysis is required for a large number of different types of structural systems that are constructed in Seismic Zones 2, 3 and 4 [1]. The lateral force requirements suggest several methods that can be used to determine the distribution of seismic forces within a structure. However, these guidelines are not unique and need further interpretations.

The major advantage of using the forces obtained from a dynamic analysis as the basis for a structural design is that the vertical distribution of forces may be significantly different from the forces obtained from an equivalent static load analysis. Consequently, the use of dynamic analysis will produce structural designs that are more earthquake resistant than structures designed using static loads.

For many years, approximate two-dimensional static load was acceptable as the basis for seismic design in many geographical areas and for most types of structural systems. Because of the increasing availability of modern digital computers during the past twenty years, most engineers have had experience with the static load analysis of three-dimensional structures. However, few

engineers and the writers of the current building code have had experience with the three-dimensional dynamic response analysis. Therefore, the interpretation of the dynamic analysis requirement of the current code represents a new challenge to most structural engineers.

The current code allows the results obtained from a dynamic analysis to be normalized so that the maximum dynamic base shear is equal to the base shear obtained from a simple two-dimensional static load analysis. Most members of the profession realize that there is no theoretical foundation for this approach. However, for the purpose of selecting the magnitude of the dynamic loading that will satisfy the code requirements, this approach can be accepted, in a modified form, until a more rational method is adopted.

The calculation of the "design base shears" is simple and the variables are defined in the code. It is of interest to note, however, that the basic magnitude of the seismic loads has not changed significantly from previous codes. The major change is that "dynamic methods of analysis" must be used in the "principal directions" of the structure. The present code does not state how to define the principal directions for a three-dimensional structure of arbitrary geometric shape. Because the design base shear can be different in each direction, this "scaled spectra" approach can produce a different input motion for each direction for both regular and irregular structures. Therefore, *the current code dynamic analysis approach can result in a structural design that is relatively "weak" in one direction*. The method of dynamic analysis proposed in this chapter results in a structural design that has equal resistance in all directions.

In addition, the maximum possible design base shear, which is defined by the present code, is approximately 35 percent of the weight of the structure. For many structures, it is less than 10 percent. It is generally recognized that this force level is small when compared to measured earthquake forces. Therefore, the use of this design base shear requires that substantial ductility be designed into the structure.

The definition of an irregular structure, the scaling of the dynamic base shears to the static base shears for each direction, the application of accidental torsional loads and the treatment of orthogonal loading effects are areas that are not clearly defined in the current building code. The purpose of this section is to

present one method of three-dimensional seismic analysis that will satisfy the Lateral Force Requirements of the code. The method is based on the response spectral shapes defined in the code and previously published and accepted computational procedures.

17.2   THREE-DIMENSIONAL COMPUTER MODEL

Real and accidental torsional effects must be considered for all structures. Therefore, all structures must be treated as three-dimensional systems. Structures with irregular plans, vertical setbacks or soft stories will cause no additional problems if a realistic three-dimensional computer model is created. This model should be developed in the very early stages of design because it can be used for static wind and vertical loads, as well as dynamic seismic loads.

Only structural elements with significant stiffness and ductility should be modeled. Non-structural brittle components can be neglected. However, shearing, axial deformations and non-center line dimensions can be considered in all members without a significant increase in computational effort by most modern computer programs. The rigid, in-plane approximation of floor systems has been shown to be acceptable for most buildings. For the purpose of elastic dynamic analysis, gross concrete sections are normally used, neglecting the stiffness of the steel. A cracked section mode should be used to check the final design.

The P-Delta effects should be included in all structural models. It has been shown in Chapter 11 that those second order effects can be considered, without iteration, for both static and dynamic loads. The effect of including P-Delta displacements in a dynamic analysis results in a small increase in the period of all modes. In addition to being more accurate, an additional advantage of automatically including P-Delta effects is that the moment magnification factor for all members can be taken as unity in all subsequent stress checks.

The mass of the structure can be estimated with a high degree of accuracy. The major assumption required is to estimate the amount of live load to be included as added mass. For certain types of structures, it may be necessary to conduct several analyses using different values of mass. The lumped mass approximation

has proven to be accurate. In the case of the rigid diaphragm approximation, the rotational mass moment of inertia must be calculated.

The stiffness of the foundation region of most structures can be modeled using massless structural elements. It is particularly important to model the stiffness of piles and the rotational stiffness at the base of shear walls.

The computer model for static loads only should be executed before conducting a dynamic analysis. Equilibrium can be checked and various modeling approximations can be verified using simple static load patterns. The results of a dynamic analysis are generally very complex and the forces obtained from a response spectra analysis are always positive. Therefore, dynamic equilibrium is almost impossible to check. However, it is relatively simple to check energy balances in both linear and nonlinear analysis.

17.3   THREE-DIMENSIONAL MODE SHAPES AND FREQUENCIES

The first step in the dynamic analysis of a structural model is the calculation of the three-dimensional mode shapes and natural frequencies of vibration. Within the past several years, very efficient computational methods have been developed that have greatly decreased the computational requirements associated with the calculation of orthogonal shape functions, as presented in Chapter 14. It has been demonstrated that load-dependent Ritz vectors, which can be generated with a minimum of numerical effort, produce more accurate results when used for a seismic dynamic analysis than if the exact free-vibration mode shapes are used.

Therefore, a dynamic response spectra analysis can be conducted with approximately twice the computer time requirements of a static load analysis. Given that systems with over 60,000 dynamic degrees of freedom can be solved within a few hours on personal computers, there is not a significant increase in cost between a static and a dynamic analysis. The major cost is the "man hours" required to produce the three-dimensional computer model used in a static or a dynamic analysis.

To illustrate the dynamic properties of the three-dimensional structure, the mode shapes and frequencies have been calculated for the irregular, eight-story, 80-foot-tall building shown in Figure 17.1. This building is a concrete structure with several hundred degrees of freedom. However, the three components of mass are lumped at each of the eight floor levels. Therefore, only 24 three-dimensional mode shapes are possible.
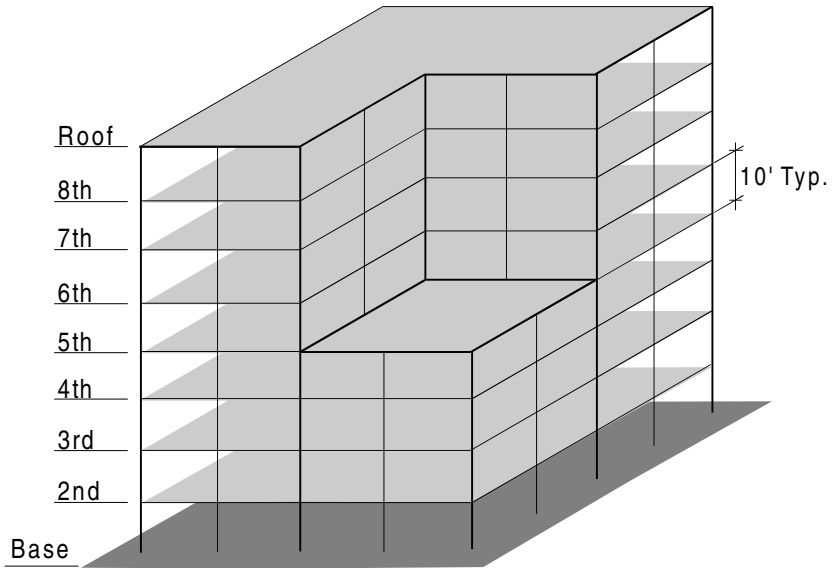
Figure 17.1 Example of Eight-Story Irregular Building

Each three-dimensional mode shape of a structure may have displacement components in all directions. For the special case of a symmetrical structure, the mode shapes are uncoupled and will have displacement in one direction only. Given that each mode can be considered to be a deflection because of a set of static loads, six base reaction forces can be calculated for each mode shape. For the structure shown in Figure 17.1, Table 17.1 summarizes the two base reactions and three overturning moments associated with each mode shape. Because vertical mass has been neglected, there is no vertical reaction. The magnitudes of the forces and moments have no meaning because the amplitude of a mode shape can be normalized to any value. However, the relative values of the different components of the shears and moments associated with each mode

are of considerable value. The modes with a large torsional component are highlighted in **bold**.

Table 17.1 Three-Dimensional Base Forces and Moments

MODE	PERIOD (Seconds)	MODAL BASE SHEAR REACTIONS			MODAL OVERTURNING MOMENTS		
		X-Dir.	Y-Dir.	Angle (Deg.)	X-Axis	Y-Axis	Z-Axis
1	.6315	.781	.624	38.64	-37.3	46.6	-18.9
2	.6034	-.624	.781	-51.37	-46.3	-37.0	38.3
3	**.3501**	**.785**	**.620**	**38.30**	**-31.9**	**40.2**	**85.6**
4	.1144	-.753	-.658	41.12	12.0	-13.7	7.2
5	.1135	.657	-.754	-48.89	13.6	11.9	-38.7
6	**.0706**	**.989**	**.147**	**8.43**	**-33.5**	**51.9**	**2,438.3**
7	.0394	-.191	.982	-79.01	-10.4	-2.0	29.4
8	.0394	-.983	-.185	10.67	1.9	-10.4	26.9
9	**.0242**	**.848**	**.530**	**32.01**	**-5.6**	**8.5**	**277.9**
10	.0210	.739	.673	42.32	-5.3	5.8	-3.8
11	.0209	.672	-.740	-47.76	5.8	5.2	-39.0
12	**.0130**	**-.579**	**.815**	**-54.63**	**-.8**	**-8.8**	**-1,391.9**
13	.0122	.683	.730	46.89	-4.4	4.1	-6.1
14	.0122	.730	-.683	-43.10	4.1	4.4	-40.2
15	.0087	-.132	-.991	82.40	5.2	-.7	-22.8
16	.0087	-.991	.135	-7.76	-.7	-5.2	30.8
17	**.0074**	**-.724**	**-.690**	**43.64**	**4.0**	**-4.2**	**-252.4**
18	.0063	-.745	-.667	41.86	3.1	-3.5	7.8
19	.0062	-.667	.745	-48.14	-3.5	-3.1	38.5
20	.0056	-.776	-.630	39.09	2.8	-3.4	54.1
21	.0055	-.630	.777	-50.96	-3.4	-2.8	38.6
22	.0052	.776	.631	39.15	-2.9	3.5	66.9
23	**.0038**	**-.766**	**-.643**	**40.02**	**3.0**	**-3.6**	**-323.4**
24	**.0034**	**-.771**	**-.637**	**39.58**	**2.9**	**-3.5**	**-436.7**

A careful examination of the directional properties of the three-dimensional mode shapes at the early stages of a preliminary design can give a structural engineer additional information that can be used to improve the earthquake resistant design of a structure. The current code defines an "irregular structure" as one that has a certain geometric shape or in which stiffness and mass discontinuities exist. A far more rational definition is that a "regular structure" is one in which there is a minimum coupling between the lateral displacements and the torsional rotations for the mode shapes associated with the lower frequencies of the system. Therefore, if the model is modified and "tuned" by studying the three-dimensional mode shapes during the preliminary design phase, it may be possible to convert a "geometrically irregular" structure to a "dynamically regular" structure from an earthquake-resistant design standpoint.

For this building, it is of interest to note that the mode shapes, which tend to have directions that are 90 degrees apart, have almost the same value for their period. This is typical of three-dimensional mode shapes for both regular and irregular buildings. For regular symmetric structures, which have equal stiffness in all directions, the periods associated with the lateral displacements will result in pairs of identical periods. However, the directions associated with the pair of three-dimensional mode shapes are not mathematically unique. For identical periods, most computer programs allow round-off errors to produce two mode shapes with directions that differ by 90 degrees. Therefore, the SRSS method should not be used to combine modal maximums in three-dimensional dynamic analysis. The CQC method eliminates problems associated with closely spaced periods.

For a response spectrum analysis, the current code states that "at least 90 percent of the participating mass of the structure must be included in the calculation of response for each principal direction." Therefore, the number of modes to be evaluated must satisfy this requirement. Most computer programs automatically calculate the participating mass in all directions using the equations presented in Chapter 13. This requirement can be easily satisfied using LDR vectors. For the structure shown in Figure 17.1, the participating mass for each mode and for each direction is shown in Table 17.2. For this building, only eight modes are required to satisfy the 90 percent specification in both the x and y directions.

Table 17.2 Three-Dimensional Participating Mass - (percentage)

MODE	X-Dir.	Y-Dir.	Z-Dir.	X-Sum	Y-Sum	Z-Sum
1	34.224	21.875	.000	34.224	21.875	.000
2	23.126	36.212	.000	57.350	58.087	.000
3	2.003	1.249	.000	59.354	59.336	.000
4	13.106	9.987	.000	72.460	69.323	.000
5	9.974	13.102	.000	82.434	82.425	.000
6	.002	.000	.000	82.436	82.425	.000
7	.293	17.770	.000	82.729	90.194	.000
8	7.726	.274	.000	90.455	90.469	.000
9	.039	.015	.000	90.494	90.484	.000
10	2.382	1.974	.000	92.876	92.458	.000
11	1.955	2.370	.000	94.831	94.828	.000
12	.000	.001	.000	94.831	94.829	.000
13	1.113	1.271	.000	95.945	96.100	.000
14	1.276	1.117	.000	97.220	97.217	.000
15	.028	1.556	.000	97.248	98.773	.000
16	1.555	.029	.000	98.803	98.802	.000
17	.011	.010	.000	98.814	98.812	.000
18	.503	.403	.000	99.316	99.215	.000
19	.405	.505	.000	99.722	99.720	.000
20	.102	.067	.000	99.824	99.787	.000
21	.111	.169	.000	99.935	99.957	.000
22	.062	.041	.000	99.997	99.998	.000
23	.003	.002	.000	100.000	100.000	.000
24	.001	.000	.000	100.000	100.000	.000

17.4   THREE-DIMENSIONAL DYNAMIC ANALYSIS

It is possible to conduct a dynamic, time-history response analysis using either the mode superposition or step-by-step methods of analysis. However, a standard time-history ground motion, for the purpose of design, has not been defined. Therefore, most engineers use the response spectrum method of analysis as the basic approach. The first step in a response spectrum analysis is the calculation

of the three-dimensional mode shapes and frequencies as indicated in the previous section.

17.4.1 Dynamic Design Base Shear

For dynamic analysis, the 1994 UBC requires that the "design base shear," **V**, be evaluated from the following formula:

$$V \;=\; [\, Z\,I\,C\,/\,R_w\,]\; W \tag{17.1}$$

Where

Z = Seismic zone factor given in Table 16-I of the UBC.

I = Importance factor given in Table 16-K of the UBC.

R_w = Numerical coefficient given in Table 16-N or 16-P of the UBC.

W = The total seismic weight of the structure.

C = Numerical coefficient (2.75 maximum value) determined from:

$$C \;=\; 1.25\,S/\,T^{2/3} \tag{17-2}$$

Where

S = Site coefficient for soil characteristics given in Table 16-J of the UBC.

T = Fundamental period of vibration (seconds).

The period, **T**, determined from the three-dimensional computer model can be used for most cases. This is essentially Method B of the code.

Because the computer model often neglects nonstructural stiffness, the code requires that Method A be used under certain conditions. Method A defines the period, **T**, as follows:

$$T \;=\; C_t\,h^{3/4} \tag{17-3}$$

where **h** is the height of the structure in feet and $\mathbf{C}_t$ is defined by the code for various types of structural systems.

The Period calculated by Method B cannot be taken as more than 30% longer than that computed using Method A in Seismic Zone 4 and more than 40% longer in Seismic Zones 1, 2 and 3.

For a structure that is defined by the code as "regular," the design base shear may be reduced by an additional 10 percent. However, it must not be less than 80 percent of the shear calculated using Method A. For an "irregular" structure, this reduction is not allowed.

17.4.2 Definition of Principal Directions

A weakness in the current code is the lack of definition of the "principal horizontal directions" for a general three-dimensional structure. If each engineer is allowed to select an arbitrary reference system, the "dynamic base shear" will not be unique and each reference system could result in a different design. One solution to this problem that will result in a unique design base shear is to use the direction of the base shear associated with the fundamental mode of vibration as the definition of the "major principal direction" for the structure. The "minor principal direction" will be, by definition, 90 degrees from the major axis. This approach has some rational basis because it is valid for regular structures. Therefore, this definition of the principal directions will be used for the method of analysis presented in this chapter.

17.4.3 Directional and Orthogonal Effects

The required design seismic forces may come from any horizontal direction and, for the purpose of design, they may be assumed to act non-concurrently in the direction of each principal axis of the structure. In addition, for the purpose of member design, the effects of seismic loading in two orthogonal directions may be combined on a square-root-of-the-sum-of-the-squares (SRSS) basis. (Also, it is allowable to design members for 100 percent of the seismic forces in one direction plus 30 percent of the forces produced by the loading in the other direction. We will not use this approach in the procedure suggested here for reasons presented in Chapter 15.)

17.4.4 Basic Method of Seismic Analysis

To satisfy the current requirements, it is necessary to conduct two separate spectrum analyses in the major and minor principal directions (as defined in the previous section). Within each of these analyses, the Complete Quadratic Combination (CQC) method is used to accurately account for modal interaction effects in the estimation of the maximum response values. The spectra used in both of these analyses can be obtained directly from the Normalized Response Spectra Shapes given by the Uniform Building Code.

17.4.5 Scaling of Results

Each of these analyses will produce a base shear in the major principal direction. A single value for the "dynamic base shear" is calculated using the SRSS method. Also, a "dynamic base shear" can be calculated in the minor principal direction. The next step is to scale the previously used spectra shapes by the ratio of "design base shear" to the minimum value of the "dynamic base shear." This approach is more conservative than proposed by the current requirements because only the scaling factor that produces the largest response is used. However, this approach is far more rational because it results in the same design earthquake in all directions.

17.4.6 Dynamic Displacements and Member Forces

The displacement and force distribution are calculated using the basic SRSS method to combine the results from 100 percent of the scaled spectra applied in each direction. If two analyses are conducted in any two orthogonal directions, in which the CQC method is used to combine the modal maximums for each analysis, and the results are combined using the SRSS method, exactly the same results will be obtained regardless of the orientation of the orthogonal reference system. Therefore, the direction of the base shear of the first mode defines a reference system for the building.

If site-specific spectra are given, for which scaling is not required, any orthogonal reference system can be used. In either case, only one computer run is necessary to calculate all member forces to be used for design.

17.4.7 Torsional Effects

Possible torsional ground motion, the unpredictable distribution of live load mass and the variations of structural properties are three reasons that both regular and irregular structures must be designed for accidental torsional loads. Also, for a regular structure, lateral loads do not excite torsional modes. One method suggested in the Code is to conduct several different dynamic analyses with the mass at different locations. This approach is not practical because the basic dynamic properties of the structure (and the dynamic base shears) would be different for each analysis. In addition, the selection of the maximum member design forces would be a monumental post-processing problem.

The current Code allows the use of pure static torsional loads to predict the additional design forces caused by accidental torsion. The basic vertical distribution of lateral static loads is given by the Code equations. The static torsional moment at any level is calculated by multiplying the static load at that level by 5 percent of the maximum dimension at that level. In this book it is recommended that those pure torsional static loads, applied at the center of mass at each level, be used as the basic approach to account for accidental torsional loads. This static torsional load is treated as a separate load condition so that it can be appropriately combined with the other static and dynamic loads.

17.5   NUMERICAL EXAMPLE

To illustrate the base-shear scaling method recommended here, a static seismic analysis has been conducted for the building illustrated in Figure 17.1. The eight-story building has 10-foot-story heights. The seismic dead load is 238.3 kips for the top four stories and 363.9 kips for the lower four stories. For I = 1, Z = 0.4, S = 1.0, and R_w = 6.0, the evaluation of Equation 17.1 yields the design base forces given in Table 17.3.

Table 17.3 Static Design Base Forces Using the Uniform Building Code

Period (Sec.)	Angle (Degree)	Base Shear	Overturning Moment
0.631	38.64	279.9	14,533
0.603	-51.36	281.2	14,979

The normalized response spectra shape for soil type 1, which is defined in the Uniform Building Code, is used as the basic loading for the three-dimensional dynamic analyses. Using eight modes only and the SRSS method of combining modal maxima, the base shears and overturning moments are summarized in Table 17.4 for various directions of loading.

Table 17.4 Dynamic Base Forces Using the SRSS Method

Angle (Degree)	BASE SHEARS		OVERTURNING MOMENTS	
	V_1	V_2	M_1	M_2
0	58.0	55.9	2,982	3,073
90	59.8	55.9	2,983	3,185
38.64	70.1	5.4	66	4,135
-51.36	83.9	5.4	66	4,500

The 1-axis is in the direction of the seismic input and the 2-axis is normal to the direction of the loading. This example clearly illustrates the major weakness of the SRSS method of modal combination. Unless the input is in the direction of the fundamental mode shapes, a large base shear is developed normal to the direction of the input and the dynamic base shear in the direction of the input is significantly underestimated, as illustrated in Chapter 15.

As indicated by Table 17.5, the CQC method of modal combination eliminates problems associated with the SRSS method. Also, it clearly illustrates that the directions of 38.64 and -51.36 degrees are a good definition of the principal directions for this structure. Note that the directions of the base shears of the first two modes differ by 90.00 degrees.

Table 17.5 Dynamic Base Forces Using the CQC Method

Angle (Degree)	BASE SHEARS		OVERTURNING MOMENTS	
	V_1	V_2	M_1	M_2
0	78.1	20.4	1,202	4,116
90	79.4	20.4	1,202	4,199
38.64	78.5	0.2	3.4	4,145
-51.36	84.2	0.2	3.4	4,503

Table 17.6 summarizes the scaled dynamic base forces to be used as the basis for design using two different methods.

Table 17.6 Normalized Base Forces in Principal Directions

	38.64 Degrees		-51.36 Degrees	
	V (kips)	M (ft-kips)	V (kips)	M (ft-kips)
Static Code Forces	279.9	14,533	281.2	14,979
Dynamic Design Forces Scaled by Base Shear 279.9/78.5 = 3.57	279.9	14,732	299.2	16,004

For this case, the input spectra scale factor of 3.57 should be used for all directions and is based on the fact that both the dynamic base shears and the dynamic overturning moments must not be less than the static code forces. This approach is clearly more conservative than the approach suggested by the current Uniform Building Code. It is apparent that the use of different scale factors for a design spectra in the two different directions, as allowed by the code, results in a design that has a weak direction relative to the other principle direction.

17.6   DYNAMIC ANALYSIS METHOD SUMMARY

In this section, a dynamic analysis method is summarized that produces unique design displacements and member forces that will satisfy the current Uniform Building Code. It can be used for both regular and irregular structures. The major steps in the approach are as follows:

1. A three-dimensional computer model must be created in which all significant structural elements are modeled. This model should be used in the early phases of design because it can be used for both static and dynamic loads.

2. The three-dimensional mode shapes should be repeatedly evaluated during the design of the structure. The directional and torsional properties of the mode shapes can be used to improve the design. A well-designed structure should have a minimum amount of torsion in the mode shapes associated with the lower frequencies of the structure.

3. The direction of the base reaction of the mode shape associated with the fundamental frequency of the system is used to define the principal directions of the three-dimensional structure.

4. The "design base shear" is based on the longest period obtained from the computer model, except when limited to 1.3 or 1.4 times the Method A calculated period.

5. Using the CQC method, the "dynamic base shears" are calculated in each principal direction subject to 100 percent of the Normalized Spectra Shapes. Use the minimum value of the base shear in the principal directions to produce one "scaled design spectra."

6. The dynamic displacements and member forces are calculated using the SRSS value of 100 percent of the scaled design spectra applied non-concurrently in any two orthogonal directions, as presented in Chapter 15.

7. A pure torsion static load condition is produced using the suggested vertical lateral load distribution defined in the code.

8. The member design forces are calculated using the following load
   combination rule:

$$\mathbf{F_{DESIGN} = F_{DEAD\ LOAD}\ \pm\ [\ F_{DYNAMIC}\ +\ |F_{TORSION}|\ ]\ +\ F_{OTHER}}$$

The dynamic forces are always positive and the accidental torsional forces must
always increase the value of force. If vertical dynamic loads are to be
considered, a dead load factor can be applied.

One can justify many other methods of analyses that will satisfy the current
code. The approach presented in this chapter can be used directly with the
computer programs ETABS and SAP2000 with their steel and concrete post-
processors. Because these programs have very large capacities and operate on
personal computers, it is possible for a structural engineer to investigate a large
number of different designs very rapidly with a minimum expenditure of
manpower and computer time.

17.7 SUMMARY

After being associated with the three-dimensional dynamic analysis and design
of a large number of structures during the past 40 years, the author would like to
take this opportunity to offer some constructive comments on the lateral load
requirements of the current code.

First, *the use of the "dynamic base shear" as a significant indication of the
response of a structure may not be conservative*. An examination of the modal
base shears and overturning moments in Tables 17.1 and 17.2 clearly indicates
that base shears associated with the shorter periods produce relatively small
overturning moments. Therefore, a dynamic analysis, which will contain higher
mode response, will always produce a larger dynamic base shear relative to the
dynamic overturning moment. Because the code allows all results to be scaled
by the ratio of dynamic base shear to the static design base shear, the dynamic
overturning moments can be significantly less than the results of a simple static
code analysis. A scale factor based on the ratio of the "static design overturning
moment" to the "dynamic overturning moment" would be far more logical. The

static overturning moment can be calculated using the static vertical distribution of the design base shear, which is currently suggested in the code.

Second, *for irregular structures, the use of the terminology "period (or mode shape) in the direction under consideration" must be discontinued.* The stiffness and mass properties of the structure define the directions of all three-dimensional mode shapes. The term "principal direction" should not be used unless it is clearly and uniquely defined.

Third, *the scaling of the results of a dynamic analysis should be re-examined.* The use of site-dependent spectra is encouraged.

Finally, *it is not necessary to distinguish between regular and irregular structures when a three-dimensional dynamic analysis is conducted.* If an accurate three-dimensional computer model is created, the vertical and horizontal irregularities and known eccentricities of stiffness and mass will cause the displacement and rotational components of the mode shapes to be coupled. A three-dimensional dynamic analysis based on those coupled mode shapes will produce a far more complex response with larger forces than the response of a regular structure. It is possible to predict the dynamic force distribution in a very irregular structure with the same degree of accuracy and reliability as the evaluation of the force distribution in a very regular structure. Consequently, if the design of an irregular structure is based on a realistic dynamic force distribution, there is no logical reason to expect that it will be any less earthquake resistant than a regular structure that was designed using the same dynamic loading. Many irregular structures have a documented record of poor performance during earthquakes because their designs were often based on approximate two-dimensional static analyses.

One major advantage of the modeling method presented in this chapter is that one set of dynamic design forces, including the effects of accidental torsion, is produced with one computer run. Of greater significance, the resulting structural design has equal resistance to seismic motions from all possible directions.

17.8   REFERENCES

1. Structural Engineers Association of California. 1996. *Recommended Lateral Force Requirements and Commentary*, *1996 Sixth Edition*. Seismology Committee. Tel. 916-427-3647.

<div align="right">

18.

</div>

FAST NONLINEAR ANALYSIS

The Dynamic Analysis of a Structure with a Small Number of Nonlinear Elements is Almost as Fast as a Linear Analysis

18.1 INTRODUCTION

The response of real structures when subjected to a large dynamic input often involves significant nonlinear behavior. In general, nonlinear behavior includes the effects of large displacements and/or nonlinear material properties.

The use of geometric stiffness and P-Delta analyses, as summarized in Chapter 11, includes the effects of first order large displacements. If the axial forces in the members remain relatively constant during the application of lateral dynamic displacements, many structures can be solved directly without iteration.

The more complicated problem associated with large displacements, which cause large strains in all members of the structure, requires a tremendous amount of computational effort and computer time to obtain a solution. Fortunately, large strains very seldom occur in typical civil engineering structures made from steel and concrete materials. Therefore, the solution methods associated with the large strain problem will not be discussed in detail in this chapter. However, certain types of large strains, such as those in rubber base isolators and gap elements, can be treated as a lumped nonlinear element using the Fast Nonlinear Analysis (FNA) method presented in this chapter.

The more common type of nonlinear behavior is when the material stress-strain, or force-deformation, relationship is nonlinear. This is because of the modern

design philosophy that "a well-designed structure should have a limited number of members which require ductility and that the failure mechanism be clearly defined." Such an approach minimizes the cost of repair after a major earthquake.

18.2   STRUCTURES WITH A LIMITED NUMBER OF NONLINEAR ELEMENTS

A large number of very practical structures have a limited number of points or members in which nonlinear behavior takes place when subjected to static or dynamic loading. Local buckling of diagonals, uplifting at the foundation, contact between different parts of the structures and yielding of a few elements are examples of structures with local nonlinear behavior. For dynamic loads, it is becoming common practice to add concentrated damping, base isolation and other energy dissipation elements. Figure 18.1 illustrates typical nonlinear problems. In many cases, those nonlinear elements are easily identified. For other structures, an initial elastic analysis is required to identify the nonlinear areas.

In this chapter the FNA method is applied to both the static and dynamic analysis of linear or nonlinear structural systems. A limited number of predefined nonlinear elements are assumed to exist. Stiffness and mass orthogonal Load Dependent Ritz Vectors of the elastic structural system are used to reduce the size of the nonlinear system to be solved. The forces in the nonlinear elements are calculated by iteration at the end of each time or load step. The uncoupled modal equations are solved exactly for each time increment.

Several examples are presented that illustrate the efficiency and accuracy of the method. The computational speed of the new FNA method is compared with the traditional "brute force" method of nonlinear analysis in which the complete equilibrium equations are formed and solved at each increment of load. For many problems, the new method is several magnitudes faster.
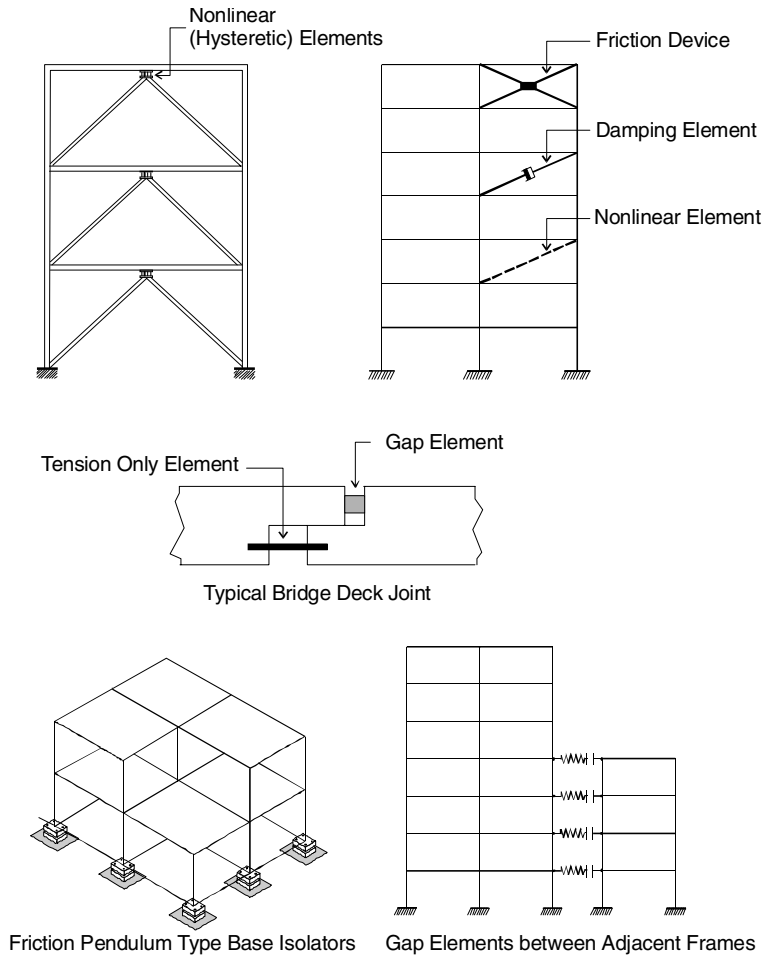
Figure 18.1 Examples of Nonlinear Elements

18.3   FUNDAMENTAL EQUILIBRIUM EQUATIONS

The FNA method is a simple approach in which the fundamental equations of mechanic (equilibrium, force-deformation and compatibility) are satisfied. The **exact** force equilibrium of the computer model of a structure at time t is expressed by the following matrix equation:

$$\mathbf{M\ddot{u}}(t) + \mathbf{C\dot{u}}(t) + \mathbf{Ku}(t) + \mathbf{R}(t)_{\mathrm{NL}} = \mathbf{R}(t) \tag{18.1}$$

where $\mathbf{M}, \mathbf{C}$ and $\mathbf{K}$ are the mass, proportional damping and stiffness matrices, respectively. The size of these three square matrices is equal to the total number of unknown node point displacements N_d. The elastic stiffness matrix $\mathbf{K}$ neglects the stiffness of the nonlinear elements. The time-dependent vectors $\ddot{\mathbf{u}}(t), \dot{\mathbf{u}}(t), \mathbf{u}(t)$ and $\mathbf{R}(t)$ are the node point acceleration, velocity, displacement and external applied load, respectively. And $\mathbf{R}(t)_{\mathrm{NL}}$ is the global node force vector from the sum of the forces in the nonlinear elements and is computed by iteration at each point in time.

If the computer model is unstable without the nonlinear elements, one can add "effective elastic elements" (at the location of the nonlinear elements) of arbitrary stiffness. If these effective forces, $\mathbf{K}_{\mathbf{e}}\mathbf{u}(t)$, are added to both sides of Equation (1), the exact equilibrium equations can be written as:

$$\mathbf{M}\ddot{\mathbf{u}}(t) + \mathbf{C}\dot{\mathbf{u}}(t) + (\mathbf{K} + \mathbf{K_e})\mathbf{u}(t) = \mathbf{R}(t) - \mathbf{R}(t)_{\mathrm{NL}} + \mathbf{K_e}\mathbf{u}(t) \qquad (18.2)$$

where $\mathbf{K_e}$ is the effective stiffness of arbitrary value. Therefore, the ***exact*** dynamic equilibrium equations for the nonlinear computer model can be written as:

$$\mathbf{M}\ddot{\mathbf{u}}(t) + \mathbf{C}\dot{\mathbf{u}}(t) + \overline{\mathbf{K}}\mathbf{u}(t) = \overline{\mathbf{R}}(t) \qquad (18.3)$$

The elastic stiffness matrix $\overline{\mathbf{K}}$ is equal to $\mathbf{K} + \mathbf{K_e}$ and is known. The effective external load $\overline{\mathbf{R}}(t)$ is equal to $\mathbf{R}(t) - \mathbf{R}(t)_{\mathrm{NL}} + \mathbf{K_e}\mathbf{u}(t)$, which must be evaluated by iteration. If a good estimate of the effective elastic stiffness can be made, the rate of convergence may be accelerated because the unknown load term $-\mathbf{R}(t)_{\mathrm{NL}} + \mathbf{K_e}\mathbf{u}(t)$ will be small.

18.4   CALCULATION OF NONLINEAR FORCES

At any time the *L* nonlinear deformations $\mathbf{d}(t)$ within the nonlinear elements are calculated from the following displacement transformation equation:

$$\mathbf{d}(t) = \mathbf{b}\mathbf{u}(t) \qquad (18.4)$$

Also, the rate of change with respect to time in the nonlinear deformations, $\dot{\mathbf{d}}(t)$, are given by:

$$\dot{\mathbf{d}}(t) = \mathbf{b}\dot{\mathbf{u}}(t) \tag{18.5}$$

Note that for small displacements, the displacement transformation matrix $\mathbf{b}$ is not a function of time and is *exact*. The displacement transformation matrix $\mathbf{b}$ for a truss element is given by Equation (2.11).

If the time-history deformations and velocities in all nonlinear elements are known, the nonlinear forces $\mathbf{f}(t)$ in the nonlinear elements can be calculated *exactly* at any time from the nonlinear material properties of each nonlinear element. It is apparent that this can only be accomplished by iteration at each point in time.

18.5 TRANSFORMATION TO MODAL COORDINATES

The first step in the solution of Equation (18.3) is to calculate a set of N orthogonal Load Dependent Ritz vectors, $\boldsymbol{\Phi}$, which satisfy the following equations:

$$\boldsymbol{\Phi}^{\mathrm{T}}\mathbf{M}\boldsymbol{\Phi} = \mathbf{II} \quad \text{and} \quad \boldsymbol{\Phi}^{\mathrm{T}}\overline{\mathbf{K}}\boldsymbol{\Phi} = \Omega^{2} \tag{18.6a) and (18.6b}$$

where $\mathbf{I}$ is a unit matrix and Ω^{2} is a diagonal matrix in which the diagonal terms are defined as $\omega^{2}{}_{n}$.

The response of the system can now be expressed in terms of those vectors by introducing the following matrix transformations:

$$\mathbf{u}(t) = \boldsymbol{\Phi}\mathbf{Y}(t) \qquad \dot{\mathbf{u}}(t) = \boldsymbol{\Phi}\dot{\mathbf{Y}}(t) \qquad \ddot{\mathbf{u}}(t) = \boldsymbol{\Phi}\ddot{\mathbf{Y}}(t) \tag{18.7}$$

The substitution of those equations into Equation (18.1) and the multiplication of both sides of the equation by $\boldsymbol{\Phi}^{\mathrm{T}}$ yield a set of N uncoupled equations expressed by the following matrix equation:

$$\mathbf{I}\ddot{\mathbf{Y}}(\mathrm{t}) + \Lambda\dot{\mathbf{Y}}(t) + \Omega^{2}\mathbf{Y}(t) = \mathbf{F}(t) \tag{18.8}$$

in which the linear and nonlinear modal forces are given by:

$$\mathbf{F}(t) = \boldsymbol{\Phi}^{\mathrm{T}}\overline{\mathbf{R}}(t) = \boldsymbol{\Phi}^{\mathrm{T}}\mathbf{R}(t) - \boldsymbol{\Phi}^{\mathrm{T}}\mathbf{R}(t)_{\mathrm{NL}} + \boldsymbol{\Phi}^{\mathrm{T}}\mathbf{K}_{\mathbf{e}}\mathbf{u}(t) \tag{18.9}$$

The assumption that the damping matrix can be diagonalized is consistent with the classical normal mode superposition method in which damping values are assigned, in terms of percent of critical damping, at the modal level. The diagonal terms of the Λ matrix are $2\xi_n\omega_n$ in which ξ_n is the damping ratio for mode n. It should be noted that the forces associated with concentrated dampers at any location in the structure can be included as part of the nonlinear force vector.

Also, if the number of LDR vectors used is equal to the total number of degrees of freedom N_d, Equation 18.8 is exact at time t. Therefore, if very small time steps are used and iteration is used within each time step, the method converges to the ***exact*** solution. The use of LDR vectors significantly reduces the number of modes required.

Because $\mathbf{u}(t) = \mathbf{\Phi Y}(t)$, the deformations in the nonlinear elements can be expressed directly in terms of the modal coordinate as:

$$\mathbf{d}(t) = \mathbf{BY}(t) \tag{18.10}$$

where the *element deformation - modal coordinate* transformation matrix is defined by:

$$\mathbf{B} = \mathbf{b\Phi} \tag{18.11}$$

It is very important to note that the L by N **B** matrix is not a function of time and is relatively small in size; also, it needs to be calculated only once before integration of the modal equations.

At any time, given the deformations and history of behavior in the nonlinear elements, the forces in the nonlinear elements $\mathbf{f}(t)$ can be evaluated from the basic nonlinear properties and deformation history of the element. From the basic principle of virtual work, the nonlinear modal forces are then calculated from:

$$\mathbf{F}(t)_{\mathrm{NL}} = \mathbf{B}^{\mathrm{T}}\mathbf{f}(t) \tag{18.12}$$

The effective elastic forces can also be rewritten as:

$$\mathbf{F}(t)_e = \mathbf{\Phi}^T \mathbf{K_e} \mathbf{u}(t) = \mathbf{\Phi}^T \mathbf{b}^T \mathbf{k}_e \mathbf{b} \mathbf{u}(t) = \mathbf{B}^T \mathbf{k}_e \mathbf{d}(t) \tag{18.13}$$

where $\mathbf{k}_e$ is the effective linear stiffness matrix in the local nonlinear element reference system.

18.6   SOLUTION OF NONLINEAR MODAL EQUATIONS

The calculation of the Load Dependent Vectors, without the nonlinear elements, is the first step before solving the modal equations. Also, the **B** deformation-modeshape transformation matrix needs to be calculated only once before start of the step-by-step solution phase. A typical modal equation is of the form:

$$\ddot{y}(t)_n + 2\xi_n \omega_n \dot{y}(t)_n + \omega_n^2 y(t)_n = \overline{f}(t)_n \tag{18.14}$$

where $\overline{f}(t)_n$ is the modal load and for nonlinear elements is a function of all other modal responses at the same point in time. Therefore, the modal equations must be integrated simultaneously and iteration is necessary to obtain the solution of all modal equations at time t. The exact solution of the modal equations for a linear or cubic variation of load within a time step is summarized by Equation (13.13) and is in terms of exponential, square root, sine and cosine functions. However, those computational intensive functions, given in Table 13.2, are pre-calculated for all modes and used as constants for the integration within each time step. In addition, the use of the exact piece-wise integration method allows the use of larger time steps.

The complete nonlinear solution algorithm, written in iterative form, is summarized in Table 18.1.

Table 18.1 Summary of Nonlinear Solution Algorithm

I INITIAL CALCULATION - BEFORE STEP-BY-STEP SOLUTION

1. Calculate N Load Dependent Ritz vectors Φ for the structure without the nonlinear elements. These vectors have N_d displacement DOF.

2. Calculate the L by N **B** matrix. Where L is the total number of DOF within all nonlinear elements.

3. Calculate integration constants $A_1 - - -$ for the piece-wise exact integration of the modal equations for each mode.

II NONLINEAR SOLUTION at times $\Delta t, 2\Delta t, 3\Delta t - - - - - - - -$

1. Use Taylor series to estimate solution at time t .

$$\mathbf{Y}(t) = \mathbf{Y}(t - \Delta t) + \Delta t \dot{\mathbf{Y}}(t - \Delta t) + \frac{\Delta t}{2} \ddot{\mathbf{Y}}(t - \Delta t)$$

$$\dot{\mathbf{Y}}(t) = \dot{\mathbf{Y}}(t - \Delta t) + \Delta t \ddot{\mathbf{Y}}(t - \Delta t)$$

2. For iteration i, calculate L nonlinear deformations and velocities.

$$\mathbf{d}(t)^i = \mathbf{B}\mathbf{Y}(t)^i \qquad \text{and} \qquad \dot{\mathbf{d}}(t)^i = \mathbf{B}\dot{\mathbf{Y}}(t)^i$$

3. Based on the deformation and velocity histories in nonlinear elements, calculate L nonlinear forces $\mathbf{f}(t)^i$.

4. Calculate new modal force vector $\bar{\mathbf{F}}(t)^i = \mathbf{F}(t) - \mathbf{B}^T[\mathbf{f}(t)^i - \mathbf{k}_e \mathbf{d}(t)]$

5. Use piece-wise exact method to solve modal equations for next iteration.

$$\mathbf{Y}(t)^i , \dot{\mathbf{Y}}(t)^i , \ddot{\mathbf{Y}}(t)^i$$

6. Calculate error norm: $\qquad Err = \dfrac{\sum\limits_{n=1}^{N} |\bar{f}(t)_n^i| - \sum\limits_{n=1}^{N} |\bar{f}(t)_n^{i-1}|}{\sum\limits_{n=1}^{N} |\bar{f}(t)_n^i|}$

7. Check Convergence – where the tolerance, Tol , is specified.

  If $Err > Tol$ go to step 2   with $i = i + 1$

  If $Err < Tol$ go to step 1 with $t = t + \Delta t$

18.7   STATIC NONLINEAR ANALYSIS OF FRAME STRUCTURE

The structure shown in Figure 18.2 is used to illustrate the use of the FNA algorithm for the solution of a structure subjected to both static and dynamic loads. It is assumed that the external columns of the seven-story frame structure cannot take axial tension or moment at the foundation level and the column can uplift. The axial foundation stiffness is 1,000 kips per inch at the external columns and 2,000 kips per inch at the center column. The dead load is 80 kips per story and is applied as concentrated vertical loads of 20 kips at the external columns and 40 kips at the center column. The static lateral load is specified as 50 percent of the dead load.

MEMBER PROPERTIES

BEAMS   I=80,000 IN⁴   A=300 IN²

CENTER COLUMN I=100,000 IN⁴   A=300 IN²

OUTER COLUMNS I= 50,000 IN⁴   A=200 IN²

MODULUS OF ELASTICITY   E=4,000 KSI

FOUNDATION STIFFNESS   k=1000 K/IN

WEIGHT PER STORY   w= 80 Kips
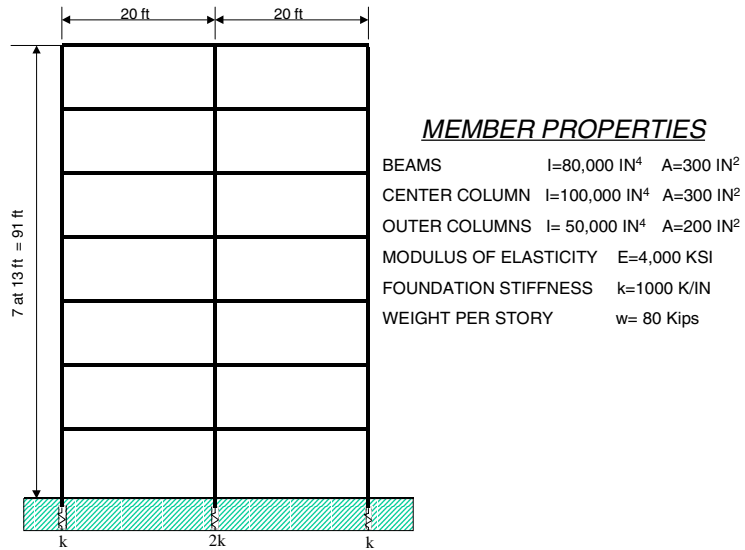
Figure 18.2 Properties of Frame Structure

For the purpose of calculating the dynamic response, the mass of the structure is calculated directly from the dead load. The fundamental period of the structure with the external columns not allowed to uplift is 0.708 seconds. The fundamental period of the structure allowing uplift is 1.691 seconds.

The static load patterns used to generate the series of LDR vectors are shown in Figure 18.3. The first load pattern represents the mass-proportional lateral

earthquake load. The second pattern represents the vertical dead load. The last two load patterns represent the possible contact forces that exist at the foundation of the external columns. It is very important that equal and opposite load patterns be applied at each point where a nonlinear element exists. These vectors allow for the accurate evaluation of member forces at the contact points. For this example, the vectors will not be activated in the solution when there is uplift at the base of the columns because the axial force must be zero. Also, the total number of Ritz vectors used should be a multiple of the number of static load patterns so that the solution is complete for all possible loadings. In addition, care should be taken to make sure that all vectors are linearly independent.
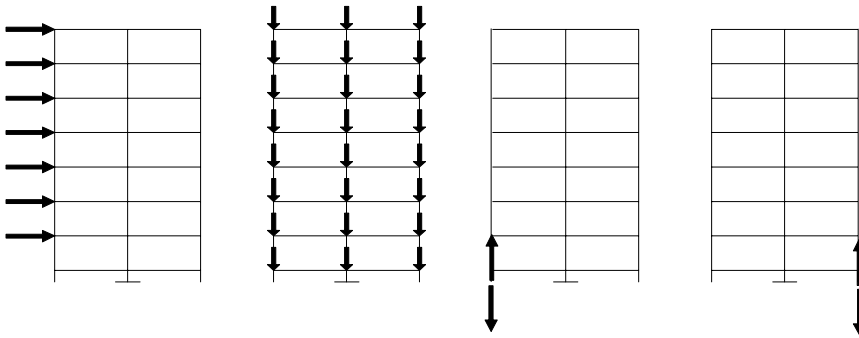
Figure 18.3 Four Static Load Vectors Used in Analysis

For this example, the dead load is applied at time zero and reaches its maximum value at one second, as shown in Figure 18.4. The time increment used is 0.10 second. The modal damping ratios are set to 0.999 for all modes; therefore, the dynamic solution converges to the static solution in less than one second. The lateral load is applied at two seconds and reaches a maximum value at three seconds. At four seconds after 40 load increments, a static equilibrium position is obtained.

It should be noted that the converged solution is the exact static solution for this problem because all possible combinations of the static vectors have been included in the analysis. The magnitude of the mass, damping and the size of the time step used will not affect the value of the converged static solution.
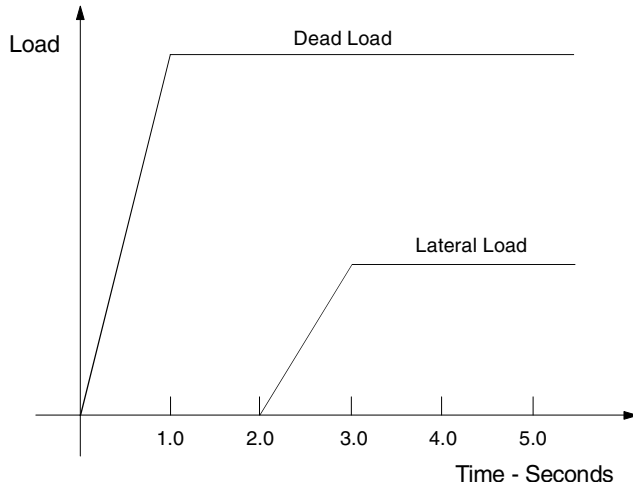
Figure 18.4 Application of Static Loads vs. Time

It is of interest to note that it is impossible for a real structure to fail under static loads only, because at the point of collapse, inertia forces must be present. Therefore, the application of static load increments with respect to time is a physically realistic approach. The approximate static load response of the frame is shown in Figure 18.5.
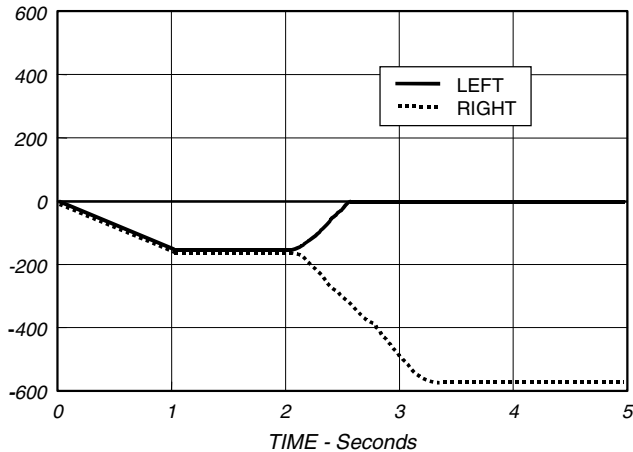

Figure 18.5 Column Axial Forces from "Static" Loads

18.8   DYNAMIC NONLINEAR ANALYSIS OF FRAME STRUCTURE

The same frame structure that is defined in Figure 18.2 is subjected to Loma Prieta Earthquake ground motions recorded on the east side of the San Francisco Bay at a maximum acceleration of 20.1 percent of gravity and a maximum ground displacement of 5.81 inches. The acceleration record used was corrected to zero acceleration, velocity and displacement at the end of the record and is shown in Figure 18.6.
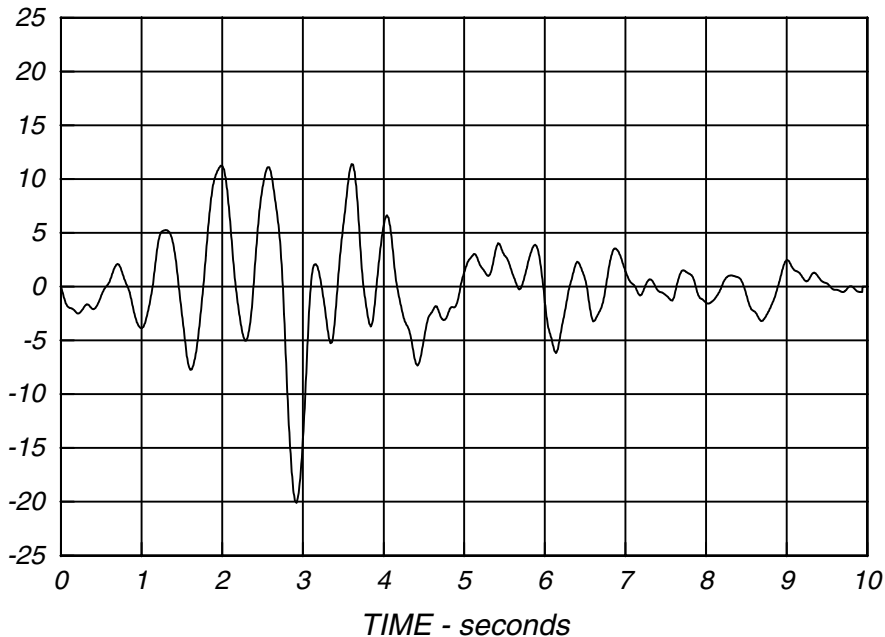
Figure 18.6 Segment of Loma Prieta Earthquake - Percent of Gravity

The dead load was applied as a ramp function in the time interval 0 to 1 second. The lateral earthquake load is applied starting at 2 seconds. Sixteen Ritz vectors and a modal damping value of 5 percent were used in the analysis. The column axial forces as a function of time are shown in Figure 18.7.
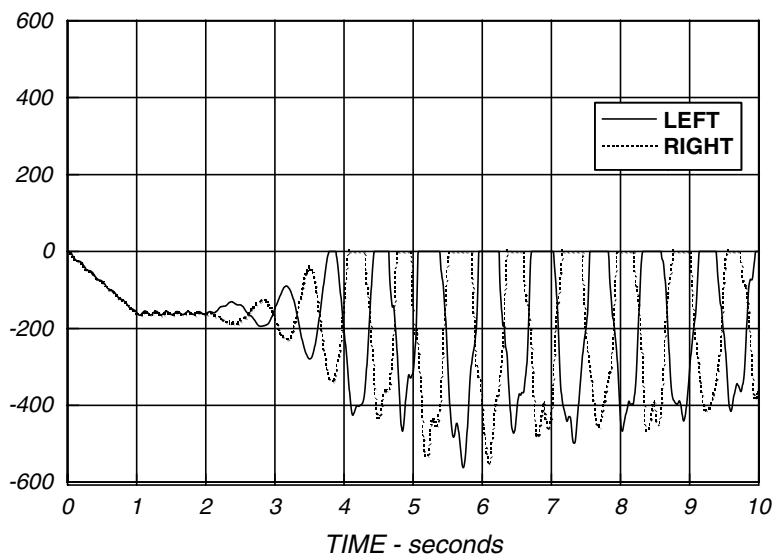
Figure 18.7 Column Axial Forces from Earthquake Loading

It is of considerable interest to compare the behavior of the building that is not allowed to uplift with the behavior of the same building that is allowed to uplift. These results are summarized in Table 18.2.

Table 18.2. Summary of Results for Building Uplifting Problem from the Loma Prieta Earthquake $\xi = 0.05$

Uplift	Max. Displace- ment (inches)	Max. Axial Force (kips)	Max. Base Shear (kips)	Max. Base Moment (k-in)	Max. Strain Energy (k-in)	Compu- tational Time (seconds)
Without	3.88	542	247	212,000	447	14.6
With	3.90	505	199	153,000	428	15
Percent Difference	+0.5 %	-6.8%	-19.4%	-27.8%	-4.2%	+3%

The lateral displacement at the top of the structure has not changed significantly by allowing the external columns to uplift. However, allowing column uplifting reduces significantly the base shear, overturning moment and strain energy

stored in the structure. It is apparent for this structure, that uplifting is a "natural" base isolation system. This reduction of forces in a structure from uplifting has also been observed in shaking table tests. However, it has not been used extensively for real structures because of the lack of precedent and the inability of the design engineer to easily compute the dynamic behavior of an uplifting structure.

For this small nonlinear example, there is a very small increase in computational time compared to a linear dynamic analysis. However, for a structural system with a large number of nonlinear elements, a large number of Ritz vectors may be required and the additional time to integrate the nonlinear modal equation can be significant.

Table 18.3 presents a summary of the results if the same structure is subjected to twice the ground accelerations of the Loma Prieta earthquake. One notes that all significant response parameters are reduced significantly.

Table 18.3 Summary of Results for Building Uplifting Problem from <u>Two Times</u> the Loma Prieta Earthquake - $\xi = 0.05$

Uplift	Max. Displace- ment (inches)	Max. Column Force (kips)	Max. Base Shear (kips)	Max. Base Moment (k-in)	Max. Strain Energy (k-in)	Max. Uplift (inches)
Without	7.76	924	494	424,000	1,547	
With	5.88	620	255	197,000	489	1.16
Percent Difference	-24%	-33%	-40%	-53%	-68%	

The maximum uplift at the base of the external columns is more than one inch; therefore, these may be ideal locations for the placement of additional energy dissipation devices such as viscous dampers.

18.9   SEISMIC ANALYSIS OF ELEVATED WATER TANK

A nonlinear earthquake response analysis of an elevated water tank was conducted using a well-known commercial computer program in which the

stiffness matrix for the complete structure was recalculated for each time step and equilibrium was obtained using iteration. The structural system and analysis had the following properties:

   92 nodes with 236 unknown displacements
  103 elastic frame elements
   56 nonlinear diagonal brace elements - tension only
 600 time steps at 0.02 seconds

The solution times on two different computers are listed below:

| Intel 486 | 3 days | 4,320 | minutes |
| Cray XMP-1 | 3 hours | 180 | minutes |

The same structure was solved using the FNA method presented in this chapter on an Intel 486 in less than 3 minutes. Thus, a structural engineer has the ability to investigate a large number of retrofit strategies within a few hours.

18.10 SUMMARY

It is common practice in engineering design to restrict the nonlinear behavior to a small number of predefined locations within a structure. In this chapter an efficient computational method has been presented to perform the static and dynamic analysis of these types of structural systems. The FNA method, using LDR vectors, is a completely different approach to structural dynamics. The nonlinear forces are treated as external loads and a set of LDR vectors is generated to accurately capture the effects of those forces. By iteration within each time step, *equilibrium*, *compatibility* and all element *force-deformation* equations within each nonlinear element are identically satisfied. The reduced set of modal equations is solved exactly for a linear variation of forces during a small time step. Numerical damping and integration errors from the use of large time steps are not introduced.

The computer model must be structurally stable without the nonlinear elements. All structures can be made stable if an element with an effective stiffness is placed parallel with the nonlinear element and its stiffness added to the basic computer model. The forces in this effective stiffness element are moved to the right side of the equilibrium equations and removed during the nonlinear

iterative solution phase. These dummy or effective stiffness elements will eliminate the introduction of long periods into the basic model and improve accuracy and rate of convergence for many nonlinear structures.

It has been demonstrated that structures subjected to static loads can also be solved using the FNA method. It is only necessary to apply the loads slowly to a constant value and add large modal damping values. Therefore, the final converged solution will be in static equilibrium and will not contain inertia forces. It should be noted that it is necessary to use Load Dependent Vectors associated with the nonlinear degrees of freedom, and not the exact eigenvectors, if static problems are to be solved using this approach.

The FNA method has been added to the commercial program ETABS for the analysis of building systems and the general purpose structural analysis program SAP2000. The ETABS program has special base isolation elements that are commonly used by the structural engineering profession. Those computer programs calculate and plot the total input energy, strain energy, kinetic energy and the dissipation of energy by modal damping and nonlinear elements as a function of time. In addition, an energy error is calculated that allows the user to evaluate the appropriate time step size. Therefore, the energy calculation option allows different structural designs to be compared. In many cases a good design for a specified dynamic loading is one that has a minimum amount of strain energy absorbed within the structural system.

As in the case of normal linear mode superposition analysis, it is the responsibility of the user to check, using multiple analyses, that a sufficiently small time step and the appropriate number of modes have been used. This approach will ensure that the method will converge to the exact solution.

Using the numerical methods presented in this chapter, the computational time required for a nonlinear dynamic analysis of a large structure, with a small number of nonlinear elements, can be only a small percentage more than the computational time required for a linear dynamic analysis of the same structure. This allows large nonlinear problems to be solved relatively quickly.

19.

LINEAR VISCOUS DAMPING

*Linear Viscous Damping
Is a Property of the Computational Model
And is not a Property of a Real Structure*

19.1 INTRODUCTION

In structural engineering, viscous velocity-dependent damping is very difficult to visualize for most real structural systems. Only a small number of structures have a finite number of damping elements where real viscous dynamic properties can be measured. In most cases modal damping ratios are used in the computer model to approximate unknown nonlinear energy dissipation within the structure.

Another form of damping, referred to as Rayleigh damping, is often used in the mathematical model for the simulation of the dynamic response of a structure; Rayleigh damping is proportional to the stiffness and mass of the structure. Both modal and Rayleigh damping are used to avoid the need to form a damping matrix based on the physical properties of the real structure.

In recent years, the addition of energy dissipation devices to the structure has forced the structural engineer to treat the energy dissipation in a more exact manner. However, the purpose of this chapter is to discuss the limitations of modal and Rayleigh damping.

19.2   ENERGY DISSIPATION IN REAL STRUCTURES

It is possible to estimate an "effective or approximate" viscous damping ratio directly from laboratory or field tests of structures. One method is to apply a static displacement by attaching a cable to the structure and then suddenly removing the load by cutting the cable. If the structure can be approximated by a single degree of freedom, the displacement response will be of the form shown in Figure 19.1. For multi degree of freedom structural systems, the response will contain more modes and the analysis method required to predict the damping ratios will be more complex.

It should be noted that the decay of the typical displacement response only indicates that energy dissipation is taking place. The cause of the energy dissipation may be from many different effects such as material damping, joint friction and radiation damping at the supports. However, if it is assumed that all energy dissipation is the result of linear viscous damping, the free vibration response is given by the following equation:

$$u(t) = u(0)e^{-\xi\omega t}\cos(\omega_D t) \tag{19.1}$$

where : $\omega_D = \omega\sqrt{1-\xi^2}$
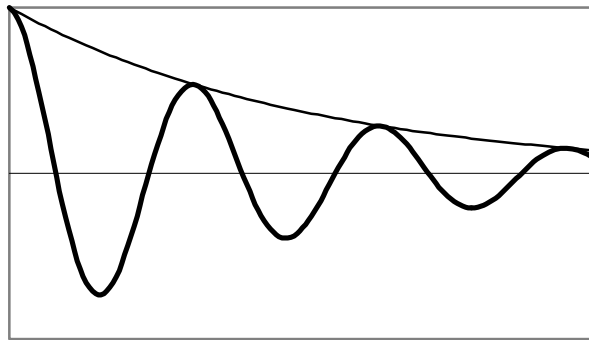
Figure 19.1 Free Vibration Test of Real Structures, Response vs. Time

Equation (19.1) can be evaluated at any two maximum points "m cycles" apart and the following two equations are produced:

$$u(2\pi n) = u_n = u(0)e^{-\xi\omega 2\pi n/\omega_D} \tag{19.2}$$

$$u(2\pi(n+m)) = u_{n+m} = u(0)e^{-\xi\omega 2\pi(n+m)/\omega_D} \tag{19.3}$$

The ratio of these two equations is:

$$\frac{u_{n+m}}{u_n} = e^{-\frac{2\pi m\xi}{\sqrt{1-\xi^2}}} = r_m \tag{19.4}$$

Taking the natural logarithm of this decay ratio, r_m, and rewriting produces the following equation:

$$\xi = \frac{-\ln(r_m)}{2\pi m}\sqrt{1-\xi^2} \tag{19.5a}$$

This equation can be written in iterative form as:

$$\xi_{(i)} = \xi_0\sqrt{1-\xi_{(i-1)}^2} \tag{19.5b}$$

If the decay ratio equals 0.730 between two adjacent maximums, three iterations yield the following damping ratio to three significant figures:

$$\xi \approx 0.0501 \approx 0.0500 = 0.0500$$

The damping value obtained by this approach is often referred to as **effective damping**. Linear modal damping is also referred to as **classical damping**. However, it must be remembered that it is an approximate value and is based on many assumptions.

Another type of energy dissipation that exists in real structures is radiation damping at the supports of the structure. The vibration of the structure strains the foundation material near the supports and causes stress waves to radiate into the infinite foundation. This can be significant if the foundation material is soft relative to the stiffness of the structure. The presence of a spring, damper and mass at each support often approximates this type of damping.

19.3   PHYSICAL INTERPRETATION OF VISCOUS DAMPING

The strain energy stored within a structure is proportional to the displacement squared. Hence, the amount of energy that is dissipated during each cycle of free vibration can be calculated for various damping ratios, as summarized in Table 19.1. In addition, Table 19.1 shows the number of cycles required to reduce the initial response by a factor of 10.

Table 19.1 Energy Loss Per Cycle for Different Damping Ratios

Damping Ratio Percentage	Decay Ratio $r = e^{-\frac{2\pi\xi}{\sqrt{1-\xi^2}}}$	Percentage Energy Loss Per Cycle $100\,(1-r^2)$	Number of Cycles to Damp Response by a Factor of 10 $n = \ln(0.10)/\ln(r)$
1	0.939	11.8	36.6
5	0.730	46.7	7.3
10	0.532	71.7	3.6
20	0.278	92.3	1.8
30	0.139	98.1	1.2

A 5 percent damping ratio indicates that 46.7 percent of the strain energy is dissipated during each cycle. If the period associated with the mode is 0.05 seconds, the energy is reduced by a factor of 10 in 0.365 second. Therefore, a 5 percent modal damping ratio produces a significant effect on the results of a dynamic response analysis.

Field testing of real structures subjected to small displacements indicates typical damping ratios are less than 2 percent. Also, for most structures, the damping is not linear and is not proportional to velocity. Consequently, values of modal damping over 5 percent are difficult to justify. However, it is often common practice for structural engineers to use values over 10 percent.

19.4   MODAL DAMPING VIOLATES DYNAMIC EQUILIBRIUM

For multi degree of freedom systems, the use of modal damping violates dynamic equilibrium and the fundamental laws of physics. For example, it is

possible to calculate the reactions as a function of time at the base of a structure using the following two methods:

First, the inertia forces at each mass point can be calculated in a specific direction by multiplying the absolute acceleration in that direction times the mass at the point. In the case of earthquake loading, the sum of all these forces must be equal to the sum of the base reaction forces in that direction because no other forces act on the structure.

Second, the member forces at the ends of all members attached to reaction points can be calculated as a function of time. The sum of the components of the member forces in the direction of the load is the base reaction force experienced by the structure.

In the case of zero modal damping, those reaction forces, as a function of time, are identical. However, for nonzero modal damping, those reaction forces are significantly different. These differences indicate that linear modal damping introduces external loads that are acting on the structure above the base and are physically impossible. This is clearly an area where the standard "state-of-the-art" assumption of modal damping needs to be re-examined and an alternative approach developed.

Energy dissipation exists in real structures. However, it must be in the form of equal and opposite forces between points within the structure. Therefore, a viscous damper, or any other type of energy dissipating device, connected between two points within the structure is physically possible and will not cause an error in the reaction forces. There must be zero base shear for all internal energy dissipation forces.

19.5 NUMERICAL EXAMPLE

To illustrate the errors involved in the use of modal damping, a simple seven-story building was subjected to a typical earthquake motion. Table 19.2 indicates the values of base shear calculated from the external inertia forces, which satisfy dynamic equilibrium, and the base shear calculated from the exact summation of the shears at the base of the three columns.

It is of interest to note that the maximum values of base shear calculated from two different methods are significantly different for the same computer run. The only logical explanation is that the external damping forces exist only in the mathematical model of the structure. Because this is physically impossible, the use of standard modal damping can produce a small error in the analysis.

Table 19.2 Comparison of Base Shear for Seven-Story Building

Damping Percentage	Dynamic Equilibrium Base Shear (kips)	Sum of Column Shears (kips)	Error Percentage
0	370.7 @ 5.355 Sec.	370.7 @ 5.355 Sec.	0.0
2	314.7 @ 4.690 Sec	318.6 @ 4.695 Sec	+1.2
5	253.7 @ 4.675 Sec	259.6 @ 4.690 Sec	+2.3
10	214.9 @ 3.745 Sec	195.4 @ 4.035 Sec	-9.1
20	182.3 @ 3.055 Sec	148.7 @ 3.365 Sec	-18.4

It is of interest to note that the use of only 5 percent damping reduces the base shear from 371 kips to 254 kips for this example. Because the measurement of damping in most real structures has been found to be less than 2 percent, the selection of 5 percent reduces the results significantly.

19.6   STIFFNESS AND MASS PROPORTIONAL DAMPING

A very common type of damping used in the nonlinear incremental analysis of structures is to assume that the damping matrix is proportional to the mass and stiffness matrices. Or:

$$\mathbf{C} = \eta\mathbf{M} + \delta\mathbf{K} \tag{19.6}$$

This type of damping is normally referred to as Rayleigh damping. In mode superposition analysis, the damping matrix must have the following properties in order for the modal equations to be uncoupled:

$$2\omega_n\zeta_n = \phi_n^T\mathbf{C}\phi_n = \eta\phi_n^T\mathbf{M}\phi_n + \delta\phi_n^T\mathbf{K}\phi_n$$
$$0 = \phi_n^T\mathbf{C}\phi_m \quad n \neq m \tag{19.7}$$

Because of the orthogonality properties of the mass and stiffness matrices, this equation can be rewritten as:

$$2\omega_n\zeta_n = \eta + \delta\omega_n^2 \qquad \text{or} \qquad \zeta_n = \frac{1}{2\omega_n}\eta + \frac{\omega_n}{2}\delta \qquad (19.8)$$

It is apparent that modal damping can be specified exactly at only two frequencies, i and j, to solve for η and δ in the following equation:

$$\begin{bmatrix} \xi_i \\ \xi_j \end{bmatrix} = \frac{1}{2}\begin{bmatrix} \dfrac{1}{\omega_i} & \omega_i \\ \dfrac{1}{\omega_j} & \omega_j \end{bmatrix}\begin{bmatrix} \eta \\ \delta \end{bmatrix} \quad \text{For } \xi_i = \xi_j = \xi \quad \begin{cases} \delta = \dfrac{2\xi}{\omega_i + \omega_j} \\ \eta = \omega_i\omega_j\delta \end{cases} \qquad (19.9)$$

For the typical case, the damping is set to be equal at the two frequencies; therefore $\xi_i = \xi_j = \xi$ and the proportionality factors are calculated from:

$$\delta = \frac{2\xi}{\omega_i + \omega_j} \quad \text{and} \quad \eta = \omega_i\omega_j\delta \qquad (19.10)$$

The assumption of mass proportional damping implies the existence of external supported dampers that are physically impossible for a base supported structure. The use of stiffness proportional damping has the effect of increasing the damping in the higher modes of the structure for which there is no physical justification. This form of damping can result in significant errors for impact-type problems and earthquake displacement input at the base of a structure. Therefore, the use of Rayleigh-type damping is difficult to justify for most structures. However, it continues to be used within many computer programs to obtain numerical results using large time integration steps.

19.7 CALCULATION OF ORTHOGONAL DAMPING MATRICES

In Chapter 13, the classical damping matrix was assumed to satisfy the following orthogonality relationship:

$$\Phi^T C \, \Phi = d \quad \text{where } d_{nn} = 2\xi_n \omega_n \text{ and } d_{nm} = 0 \quad \text{for } n \neq m \tag{19.11}$$

In addition, the mode shapes are normalized so that $\Phi^T M \Phi = I$. The following matrix can be defined:

$$\overline{\Phi} = \Phi M \quad \text{and} \quad \overline{\Phi}^T = M \Phi^T \tag{19.12}$$

Hence, if Equation 19.11 is pre-multiplied by $\overline{\Phi}$ and post-multiplied by $\overline{\Phi}^T$, the following damping matrix is obtained:

$$C = \overline{\Phi} d \overline{\Phi}^T = \sum_{n=1}^{N} C_n \tag{19.13}$$

Therefore, a classical damping matrix can be calculated for each mode that has a specified amount of damping in that mode and zero damping in all other modes:

$$C_n = 2\xi_n \omega_n \, M \phi_n \phi_n^T M \tag{19.14}$$

It must be noted that this modal damping matrix is a mathematical definition and that it is physically impossible for such damping properties to exist in a real multi degree of freedom structure.

The total damping matrix for all modes can be written as:

$$C = \sum_{n=1}^{N} C_n = \sum_{n=1}^{N} 2\xi_n \omega_n \, M \phi_n \phi_n^T M \tag{19.15}$$

It is apparent that given the mode shapes, a full damping matrix can be constructed from this mathematical equation. However, the resulting damping matrix may require that external dampers and negative damping elements be connected between nodes of the computer model.

The only reason to form such a damping matrix is to compare the results of a step-by-step integration solution with a mode superposition solution. A numerical example is given in reference [1].

19.8   STRUCTURES WITH NON-CLASSICAL DAMPING

It is possible to model structural systems with linear viscous dampers at arbitrary locations within a structural system. The exact solution involves the calculation of complex eigenvalues and eigenvectors and a large amount of computational effort. Because the basic nature of energy dissipation is not clearly defined in real structures and viscous damping is often used to approximate nonlinear behavior, this increase in computational effort is not justified given that we are not solving the real problem. A more efficient method to solve this problem is to move the damping force to the right-hand side of the dynamic equilibrium equation and solve the problem as a nonlinear problem using the FNA method. Also, nonlinear viscous damping can easily be considered by this new computational method.

19.9   NONLINEAR ENERGY DISSIPATION

Most physical energy dissipation in real structures is in phase with the displacements and is a nonlinear function of the magnitude of the displacements. Nevertheless, it is common practice to approximate the nonlinear behavior with an "equivalent linear damping" and not conduct a nonlinear analysis. The major reason for this approximation is that all linear programs for mode superposition or response spectrum analysis can consider linear viscous damping in an exact mathematical manner. This approximation is no longer necessary if the structural engineer can identify where and how the energy is dissipated within the structural system. The FNA method provides an alternative to the use of equivalent linear viscous damping.

Base isolators are one of the most common types of predefined nonlinear elements used in earthquake resistant designs. Mechanical dampers, friction devices and plastic hinges are other types of common nonlinear elements. In addition, gap elements are required to model contact between structural components and uplifting of structures. A special type of gap element, with the ability to crush and dissipate energy, is useful to model concrete and soil types of materials. Cables that can take tension only and dissipate energy in yielding are necessary to capture the behavior of many bridge type structures. However, when a nonlinear analysis is conducted where energy is dissipated within the

nonlinear devices, one cannot justify adding an additional 5 percent of linear modal damping

19.10 SUMMARY

The use of linear modal damping as a percentage of critical damping has been used to approximate the nonlinear behavior of structures. The energy dissipation in real structures is far more complicated and tends to be proportional to displacements rather than proportional to the velocity. The use of approximate "equivalent viscous damping" has little theoretical or experimental justification and produces a mathematical model that violates dynamic equilibrium.

One can mathematically create damping matrices to have different damping in each mode. In addition, one can use stiffness and mass proportional damping matrices. To justify these convenient mathematical assumptions, field experimental work must be conducted.

It is now possible to accurately simulate, using the FNA method, the behavior of structures with a finite number of discrete energy dissipation devices installed. The experimentally determined properties of the devices can be directly incorporated into the computer model.

19.11 REFERENCES

1. Wilson, E., and J. Penzien. 1972. "Evaluation of Orthogonal Matrices," *International Journal for Numerical Methods in Engineering*. Vol. 4. pp. 5-10.

DYNAMIC ANALYSIS USING NUMERICAL INTEGRATION

Normally, Direct Numerical Integration for Earthquake Loading is Very Slow

20.1 INTRODUCTION

The most general approach for solving the dynamic response of structural systems is the direct numerical integration of the dynamic equilibrium equations. This involves the attempt to satisfy dynamic equilibrium at discrete points in time after the solution has been defined at time zero. Most methods use equal time intervals at $\Delta t, 2\Delta t, 3\Delta t .... N\Delta t$. Many different numerical techniques have previously been presented; however, all approaches can fundamentally be classified as either *explicit* or *implicit* integration methods.

Explicit methods do not involve the solution of a set of linear equations at each step. Basically, those methods use the differential equation at time "t" to predict a solution at time "$t + \Delta t$". For most real structures, which contain stiff elements, a very small time step is required to obtain a stable solution. Therefore, all explicit methods are *conditionally stable* with respect to the size of the time step.

Implicit methods attempt to satisfy the differential equation at time "t" after the solution at time "$t - \Delta t$" has been found. Those methods require the solution of a set of linear equations at each time step; however, larger time steps may be used. Implicit methods can be *conditionally or unconditionally* stable.

A large number of accurate, higher-order, multi-step methods have been developed for the numerical solution of differential equations. Those multi-step methods assume that the solution is a smooth function in which the higher derivatives are continuous. The exact solution of many nonlinear structures requires that the accelerations, the second derivative of the displacements, are not smooth functions. This discontinuity of the acceleration is caused by the nonlinear hysteresis of most structural materials, contact between parts of the structure, and buckling of elements. Therefore, only single-step methods will be presented in this chapter. On the basis of a significant amount of experience, it is the conclusion of the author that only single-step, implicit, unconditional stable methods should be used for the step-by-step seismic analysis of practical structures.

20.2   NEWMARK FAMILY OF METHODS

In 1959 Newmark [1] presented a family of single-step integration methods for solving structural dynamic problems for both blast and seismic loading. During the past 40 years, Newmark's method has been applied to the dynamic analysis of many practical engineering structures. In addition, it has been modified and improved by many other researchers. To illustrate the use of this family of numerical integration methods, consider the solution of the linear dynamic equilibrium equations written in the following form:

$$\mathbf{M}\ddot{\mathbf{u}}_t + \mathbf{C}\dot{\mathbf{u}}_t + \mathbf{K}\mathbf{u}_t = \mathbf{F}_t \tag{20.1}$$

The direct use of Taylor's series provides a rigorous approach to obtain the following two additional equations:

$$\mathbf{u}_t = \mathbf{u}_{t\text{-}\Delta t} + \Delta t \dot{\mathbf{u}}_{t\text{-}\Delta t} + \frac{\Delta t^2}{2}\ddot{\mathbf{u}}_{t\text{-}\Delta t} + \frac{\Delta t^3}{6}\dddot{\mathbf{u}}_{t\text{-}\Delta t} + ...$$
$$\tag{20.2a}$$

$$\dot{\mathbf{u}}_t = \dot{\mathbf{u}}_{t\text{-}\Delta t} + \Delta t \ddot{\mathbf{u}}_{t\text{-}\Delta t} + \frac{\Delta t^2}{2}\dddot{\mathbf{u}}_{t\text{-}\Delta t} + ...$$
$$\tag{20.2b}$$

Newmark truncated those equations and expressed them in the following form:

$$\mathbf{u}_t = \mathbf{u}_{t\text{-}\Delta t} + \Delta t \dot{\mathbf{u}}_{t\text{-}\Delta t} + \frac{\Delta t^2}{2}\ddot{\mathbf{u}}_{t\text{-}\Delta t} + \beta \Delta t^3 \dddot{\mathbf{u}}$$
$$\tag{20.2c}$$

$$\dot{\mathbf{u}}_t = \dot{\mathbf{u}}_{t\text{-}\Delta t} + \Delta t \ddot{\mathbf{u}}_{t\text{-}\Delta t} + \gamma \Delta t^2 \ddot{\mathbf{u}} \qquad (20.2d)$$

If the acceleration is assumed to be linear within the time step, the following equation can be written:

$$\ddot{\mathbf{u}} = \frac{(\ddot{\mathbf{u}}_t - \ddot{\mathbf{u}}_{t-\Delta t})}{\Delta t} \qquad (20.3)$$

The substitution of Equation (20.3) into Equations (20.2c and 20.2d) produces Newmark's equations in standard form:

$$\mathbf{u}_t = \mathbf{u}_{t\text{-}\Delta t} + \Delta t \dot{\mathbf{u}}_{t\text{-}\Delta t} + (\frac{1}{2} - \beta)\Delta t^2 \ddot{\mathbf{u}}_{t\text{-}\Delta t} + \beta \Delta t^2 \ddot{\mathbf{u}}_t \qquad (20.4a)$$

$$\dot{\mathbf{u}}_t = \dot{\mathbf{u}}_{t\text{-}\Delta t} + (1-\gamma)\Delta t \ddot{\mathbf{u}}_{t\text{-}\Delta t} + \gamma \Delta t \ddot{\mathbf{u}}_t \qquad (20.4b)$$

Newmark solved Equations (20.4a, 20.4b and 20.1) by iteration for each time step for each displacement DOF of the structural system. The term $\ddot{u}_t$ was obtained from Equation (20.1) by dividing the equation by the mass associated with the DOF.

In 1962 Wilson [2] formulated Newmark's method in matrix notation, added stiffness and mass proportional damping, and eliminated the need for iteration by introducing the direct solution of equations at each time step. This requires that Equations (20.4a and 20.4b) be rewritten in the following form:

$$\ddot{\mathbf{u}}_t = b_1(\mathbf{u}_t - \mathbf{u}_{t-\Delta t}) + b_2 \dot{\mathbf{u}}_{t-\Delta t} + b_3 \ddot{\mathbf{u}}_{t-\Delta t} \qquad (20.5a)$$

$$\dot{\mathbf{u}}_t = b_4(\mathbf{u}_t - \mathbf{u}_{t-\Delta t}) + b_5 \dot{\mathbf{u}}_{t-\Delta t} + b_6 \ddot{\mathbf{u}}_{t-\Delta t} \qquad (20.5b)$$

where the constants b_1 to b_6 are defined in Table 20.1. The substitution of Equations (20.5a and 20.5b) into Equation (20.1) allows the dynamic equilibrium of the system at time " t "to be written in terms of the unknown node displacements $\mathbf{u}_t$. Or:

$$(b_1\mathbf{M} + b_4\mathbf{C} + \mathbf{K})\mathbf{u}_t = \mathbf{F}_t + \mathbf{M}(b_1\mathbf{u}_{t-\Delta t} - b_2\dot{\mathbf{u}}_{t-\Delta t} - b_3\ddot{\mathbf{u}}_{t-\Delta t})$$
$$+ \mathbf{C}(b_4\mathbf{u}_{t-\Delta t} - b_5\dot{\mathbf{u}}_{t-\Delta t} - b_6\ddot{\mathbf{u}}_{t-\Delta t}) \qquad (20.6)$$

The Newmark direct integration algorithm is summarized in Table 20.1. Note that the constants b_i need to be calculated only once. Also, for linear systems, the effective dynamic stiffness matrix $\overline{\mathbf{K}}$ is formed and triangularized only once.

Table 20.1 Summary of the Newmark Method of Direct Integration

---

I. INITIAL CALCULATION

  A. Form static stiffness matrix $\mathbf{K}$, mass matrix $\mathbf{M}$ and damping matrix $\mathbf{C}$

  B. Specify integration parameters β and γ

  C. Calculate integration constants

$$b_1 = \frac{1}{\beta \Delta t^2} \qquad b_2 = \frac{1}{\beta \Delta t} \qquad b_3 = \beta - \frac{1}{2} \qquad b_4 = \gamma \Delta t b_1$$

$$b_5 = 1 + \gamma \Delta t b_2 \quad b_6 = \Delta t (1 + \gamma b_3 - \gamma)$$

  D. Form effective stiffness matrix $\quad \overline{\mathbf{K}} = \mathbf{K} + b_1 \mathbf{M} + b_4 \mathbf{C}$

  E. Triangularize effective stiffness matrix $\quad \overline{\mathbf{K}} = \mathbf{L}\mathbf{D}\mathbf{L}^{\mathbf{T}}$

  F. Specify initial conditions $\quad \mathbf{u}_0 , \dot{\mathbf{u}}_0 , \ddot{\mathbf{u}}_0$

II. FOR EACH TIME STEP $\quad t = \Delta t, 2\Delta t, 3\Delta t \text{ - - - - - -}$

  A. Calculate effective load vector
$$\overline{\mathbf{F}}_t = \mathbf{F}_t + \mathbf{M}(b_1 \mathbf{u}_{t-\Delta t} - b_2 \dot{\mathbf{u}}_{t-\Delta t} - b_3 \ddot{\mathbf{u}}_{t-\Delta t}) + \mathbf{C}(b_4 \mathbf{u}_{t-\Delta t} - b_5 \dot{\mathbf{u}}_{t-\Delta t} - b_6 \ddot{\mathbf{u}}_{t-\Delta t})$$

  B. Solve for node displacement vector at time t
$$\mathbf{L}\mathbf{D}\mathbf{L}^{\mathbf{T}} \mathbf{u}_t = \overline{\mathbf{F}}_t \qquad \text{forward and back-substitution only}$$

  C. Calculate node velocities and accelerations at time t
$$\dot{\mathbf{u}}_t = b_4 (\mathbf{u}_t - \mathbf{u}_{t-\Delta t}) + b_5 \dot{\mathbf{u}}_{t-\Delta t} + b_6 \ddot{\mathbf{u}}_{t-\Delta t}$$
$$\ddot{\mathbf{u}}_t = b_1 (\mathbf{u}_t - \mathbf{u}_{t-\Delta t}) + b_2 \dot{\mathbf{u}}_{t-\Delta t} + b_3 \ddot{\mathbf{u}}_{t-\Delta t}$$

  D. Go to Step II.A with $\quad t = t + \Delta t$

20.3 STABILITY OF NEWMARK'S METHOD

For zero damping, Newmark's method is conditionally stable if:

$$\gamma \geq \frac{1}{2}, \beta \leq \frac{1}{2} \quad \text{and} \quad \Delta t \leq \frac{1}{\omega_{MAX}\sqrt{\frac{\gamma}{2}-\beta}} \tag{20.7}$$

where ω_{MAX} is the maximum frequency in the structural system [1]. Newmark's method is unconditionally stable if:

$$2\beta \geq \gamma \geq \frac{1}{2} \tag{20.8}$$

However, if γ is greater than ½, errors are introduced. Those errors are associated with "numerical damping" and "period elongation."

For large multi degree of freedom structural systems, the time step limit given by Equation (20.7) can be written in a more useable form as:

$$\frac{\Delta t}{T_{MIN}} \leq \frac{1}{2\pi\sqrt{\frac{\gamma}{2}-\beta}} \tag{20.9}$$

Computer models of large real structures normally contain a large number of periods that are smaller than the integration time step; therefore, it is essential that one **select** a numerical integration method that is unconditional for all time steps.

20.4 THE AVERAGE ACCELERATION METHOD

The average acceleration method is identical to the trapezoidal rule that has been used to numerically evaluate second order differential equations for approximately 100 years. It can easily be derived from the following truncated Taylor's series expansion:

$$\mathbf{u}_\tau = \mathbf{u}_{t-\Delta t} + \tau\dot{\mathbf{u}}_{t-\Delta t} + \frac{\tau^2}{2}\ddot{\mathbf{u}}_{t-\Delta t} + \frac{\tau^3}{6}\dddot{\mathbf{u}}_{t-\Delta t} + ...$$

$$\approx \mathbf{u}_{t-\Delta t} + \tau\dot{\mathbf{u}}_{t-\Delta t} + \frac{\tau^2}{2}(\frac{\ddot{\mathbf{u}}_{t-\Delta t} + \ddot{\mathbf{u}}_t}{2}) \tag{20.10}$$

where τ is a variable point within the time step. The consistent velocity can be obtained by differentiation of Equation (20.10). Or:

$$\dot{\mathbf{u}}_{\tau} = \dot{\mathbf{u}}_{t\text{-}\Delta t} + \tau \; (\frac{\ddot{\mathbf{u}}_{t\text{-}\Delta t} + \ddot{\mathbf{u}}_{t}}{2})$$

(20.11)

If $\tau = \Delta t$:

$$\mathbf{u}_{t} = \mathbf{u}_{t\text{-}\Delta t} + \Delta t \dot{\mathbf{u}}_{t\text{-}\Delta t} + \frac{\Delta t^2}{4} \ddot{\mathbf{u}}_{t\text{-}\Delta t} + \frac{\Delta t^2}{4} \ddot{\mathbf{u}}_{t}$$

(20.12a)

$$\dot{\mathbf{u}}_{t} = \dot{\mathbf{u}}_{t\text{-}\Delta t} + \frac{\Delta t}{2} \ddot{\mathbf{u}}_{t\text{-}\Delta t} + \frac{\Delta t}{2} \ddot{\mathbf{u}}_{t}$$

(20.12b)

These equations are identical to Newmark's Equations (20.4a and 20.4b) with $\gamma = 1/2$ and $\beta = 1/4$.

It can easily be shown that the average acceleration method conserves energy for the free vibration problem, $\mathbf{M}\ddot{\mathbf{u}} + \mathbf{K}\mathbf{u} = \mathbf{0}$, for all possible time steps [4]. Therefore, the sum of the kinetic and strain energy is constant. Or:

$$2E = \dot{\mathbf{u}}_{t}^{T}\mathbf{M}\dot{\mathbf{u}}_{t} + \mathbf{u}_{t}^{T}\mathbf{K}\mathbf{u}_{t} = \dot{\mathbf{u}}_{t\text{-}\Delta t}^{T}\mathbf{M}\dot{\mathbf{u}}_{t\text{-}\Delta t} + \mathbf{u}_{t\text{-}\Delta t}^{T}\mathbf{K}\mathbf{u}_{t\text{-}\Delta t}$$

(20.13)

20.5 WILSON'S θ FACTOR

In 1973, the general Newmark method was made unconditionally stable by the introduction of a θ factor [3]. The introduction of the θ factor is motivated by the observation that an unstable solution tends to oscillate about the true solution. Therefore, if the numerical solution is evaluated within the time increment, the spurious oscillations are minimized. This can be accomplished by a simple modification to the Newmark method using a time step defined by:

$$\Delta t' = \theta \Delta t$$

(20.14a)

and a load defined by:

$$R_{t'} = R_{t\text{-}\Delta t} + \theta \; (R_{t} - R_{t\text{-}\Delta t})$$

(20.14b)

where $\theta \geq 1.0$. After the acceleration $\ddot{u}_{t'}$ vector has been evaluated using Newmark's method at the integration time step $\theta \Delta t$, values of node accelerations, velocities and displacements are calculated from the following fundamental equations:

$$\ddot{u}_t = \ddot{u}_{t\text{-}\Delta t} + \frac{1}{\theta}(\ddot{u}_{t'} - \ddot{u}_{t\text{-}\Delta t}) \tag{20.15a}$$

$$\dot{u}_t = \dot{u}_{t\text{-}\Delta t} + (1 - \gamma)\Delta t \ddot{u}_{t\text{-}\Delta t} + \gamma \Delta t \ddot{u}_t \tag{20.15b}$$

$$u_t = u_{t\text{-}\Delta t} + \Delta t \dot{u}_{t\text{-}\Delta t} + \frac{\Delta t^2(1 - 2\beta)}{2}\ddot{u}_{t\text{-}\Delta t} + \beta\Delta t^2 \ddot{u}_t \tag{20.15c}$$

The use of the θ factor tends to numerically damp out the high modes of the system. If θ equals 1.0, Newmark's method is not modified. However, for problems where the higher mode response is important, the errors that are introduced can be large. In addition, the dynamic equilibrium equations are not exactly satisfied at time t. Therefore, the author no longer recommends the use of the θ factor. At the time of the introduction of the method, it solved all problems associated with stability of the Newmark family of methods. However, during the past twenty years, new and more accurate numerical methods have been developed.

20.6 THE USE OF STIFFNESS PROPORTIONAL DAMPING

Because of the unconditional stability of the average acceleration method, it is the most robust method to be used for the step-by-step dynamic analysis of large complex structural systems in which a large number of high frequencies—short periods—are present. The only problem with the method is that the short periods, which are smaller than the time step, oscillate indefinitely after they are excited. The higher mode oscillation can be reduced by the addition of stiffness proportional damping. The additional damping that is added to the system is of the form:

$$C_D = \delta K \tag{20.16}$$

where the modal damping ratio, given by Equation (13.5), is defined by:

$$\xi_n = \frac{1}{2}\delta\omega_n = \frac{\pi}{T_n}\delta \tag{20.17}$$

One notes that the damping is large for short periods and small for the long periods or low frequencies. It is apparent that when periods are greater than the time step, they cannot be integrated accurately by any direct integration method. Therefore, it is logical to damp those short periods to prevent them from oscillating during the solution procedure. For a time step equal to the period, Equation (20.17) can be rewritten as:

$$\delta = \xi_n \frac{\Delta T}{\pi} \tag{20.18}$$

Hence, if the integration time step is 0.02 second and we wish to assign a minimum of 1.0 to all periods shorter than the time step, a value of $\delta = 0.0064$ should be used. The damping ratio in all modes is now predictable for this example from Equation (20.17). Therefore, the damping ratio for a 1.0 second period is 0.02 and for a 0.10 second period, it is 0.2.

20.7   THE HILBER, HUGHES AND TAYLOR α METHOD

The α method [4] uses the Newmark method to solve the following modified equations of motion:

$$\begin{aligned}
\mathbf{M\ddot{u}}_t &+ (1+\alpha)\,\mathbf{C\dot{u}}_t + (1+\alpha)\ \mathbf{Ku}_t = (1+\alpha)\mathbf{F}_t \\
&- \alpha\,\mathbf{F}_t + \alpha\,\mathbf{C\dot{u}}_{t-\Delta t} + \alpha\,\mathbf{Ku}_{t-\Delta t}
\end{aligned} \tag{20.19}$$

When α equals zero, the method reduces to the constant acceleration method. It produces numerical energy dissipation in the higher modes; however, it cannot be predicted as a damping ratio as in the use of stiffness proportional damping. Also, it does not solve the fundamental equilibrium equation at time t. However, it is currently being used in many computer programs. The performance of the method appears to be very similar to the use of stiffness proportional damping.

20.8 SELECTION OF A DIRECT INTEGRATION METHOD

It is apparent that a large number of different direct numerical integration methods are possible by specifying different integration parameters. A few of the most commonly used methods are summarized in Table 20.2.

Table 20.2 Summary of Newmark Methods Modified by the δ Factor

METHOD	γ	β	δ	$\dfrac{\Delta t}{T_{MIN}}$	ACCURACY
Central Difference	1/2	0	0	0.3183	Excellent for small Δt Unstable for large Δt
Linear Acceleration	1/2	1/6	0	0.5513	Very good for small Δt Unstable for large Δt
Average Acceleration	1/2	1/4	0	∞	Good for small Δt No energy dissipation
Modified Average Acceleration	1/2	1/4	$\dfrac{\Delta T}{\pi}$	∞	Good for small Δt Energy dissipation for large Δt

For single degree of freedom systems, the central difference method is most accurate, and the linear acceleration method is more accurate than the average acceleration method. However, if only single degree of freedom systems are to be integrated, the piece-wise exact method previously presented should be used because there is no need to use an approximate method.

It appears that the modified average acceleration method, with a minimum addition of stiffness proportional damping, is a general procedure that can be used for the dynamic analysis of all structural systems. Using $\delta = \Delta T/\pi$ will damp out periods shorter than the time step and introduces a minimum error in the long period response.

20.9 NONLINEAR ANALYSIS

The basic Newmark constant acceleration method can be extended to nonlinear dynamic analysis. This requires that iteration be performed at each time step to

satisfy equilibrium. Also, the incremental stiffness matrix must be formed and triangularized before each iteration or at selective points in time. Many different numerical tricks, including element by element methods, have been developed to minimize the computational requirements. Also, the triangularization of the effective incremental stiffness matrix may be avoided by introducing iterative solution methods.

20.10 SUMMARY

For earthquake analysis of linear structures, it should be noted that the direct integration of the dynamic equilibrium equations is normally not numerically efficient as compared to the mode superposition method using LDR vectors. If the triangularized stiffness and mass matrices and other vectors cannot be stored in high-speed storage, the computer execution time can be long.

After using direct integration methods for approximately forty years, the author can no longer recommend the Wilson method for the direct integration of the dynamic equilibrium equations. The Newmark constant acceleration method, with the addition of very small amounts of stiffness proportional damping, is recommended for dynamic analysis nonlinear structural systems. For all methods of direct integration, great care should be taken to make certain that the stiffness proportional damping does not eliminate important high-frequency response. Mass proportional damping cannot be justified because it causes external forces to be applied to the structure that reduce the base shear for seismic loading.

In the area of nonlinear dynamic analysis, one cannot prove that any one method will always converge. One should always check the error in the conservation of energy for every solution obtained. In future editions of this book it is hoped that numerical examples will be presented so that the appropriate method can be recommended for different classes of problems in structural analysis.

20.11 REFERENCES

1. Newmark, N. M. 1959. "A Method of Computation for Structural Dynamics," ASCE Journal of the Engineering Mechanics Division. Vol. 85 No. EM3.

2. Wilson, E. L. 1962. "Dynamic Response by Step-By-Step Matrix Analysis," Proceedings, Symposium On The Use of Computers in Civil Engineering. Labortorio Nacional de Engenharia Civil. Lisbon, Portugal. October 1-5.

3. Wilson, E. L., I. Farhoomand and K. J. Bathe. 1973. "Nonlinear Dynamic Analysis of Complex Structures," *Earthquake Engineering and Structural Dynamics.* 1, 241-252.

4. Hughes, Thomas. 1987. *The Finite Element Method - Linear Static and Dynamic Finite Element Analysis.* Prentice Hall, Inc.

21.

NONLINEAR ELEMENTS

Earthquake Resistant Structures Should Have a Limited Number of Nonlinear Elements that can be Easily Inspected and Replaced after a Major Earthquake.

21.1 INTRODUCTION

Many different types of practical nonlinear elements can be used in conjunction with the application of the Fast Nonlinear Analysis method. The FNA method is very effective for the design or retrofit of structures to resist earthquake motions because it is designed to be computationally efficient for structures with a limited number of predefined nonlinear or energy dissipating elements. This is consistent with the modern philosophy of earthquake engineering that *energy dissipating elements should be able to be inspected and replaced after a major earthquake.*

Base isolators are one of the most common types of predefined nonlinear elements used in earthquake resistant designs. In addition, isolators, mechanical dampers, friction devices and plastic hinges are other types of common nonlinear elements. Also, gap elements are required to model contact between structural components and uplifting of structures. A special type of gap element with the ability to crush and dissipate energy is useful to model concrete and soil types of materials. Cables that can take tension only and dissipate energy in yielding are necessary to capture the behavior of many bridge type structures. In this chapter the behavior of several of those elements will be presented and detailed solution algorithms will be summarized.

21.2 GENERAL THREE-DIMENSIONAL TWO-NODE ELEMENT

The type of nonlinear element presented in this chapter is similar to the three-dimensional beam element. However, it can degenerate into an element with zero length where both ends are located at the same point in space. Therefore, it is possible to model sliding friction surfaces, contact problems and concentrated plastic hinges. Like the beam element, the user must define a local 1-2-3 reference system to define the local nonlinear element properties and to interpret the results. A typical element, connected between two points I and J, is shown in Figure 21.1.
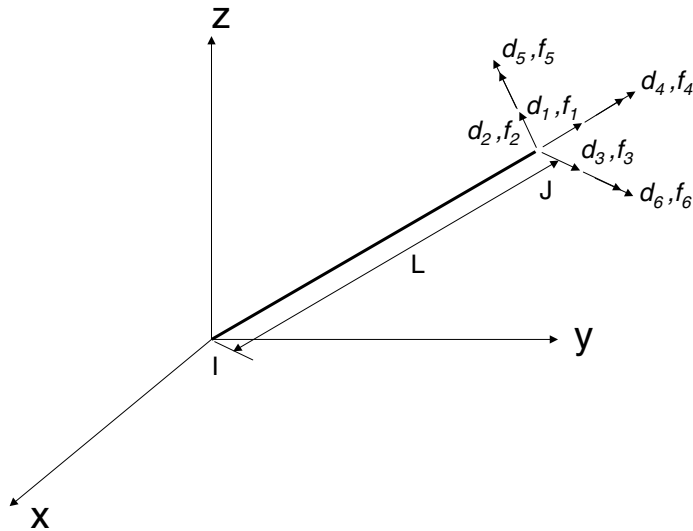
Figure 21.1 Relative Displacements - Three-Dimensional Nonlinear Element

It is important to note that three displacements and three rotations are possible at both points I and J and can be expressed in either the global X-Y-Z or local 1-2-3 reference system. The force and displacement transformation matrices for this nonlinear element are the same as for the beam element given in Chapter 4. For most element types, some of those displacements do not exist or are equal at I and J. Because each three-dimensional element has six rigid body displacements, the equilibrium of the element can be expressed in terms of the six relative displacements shown in Figure 21.1. Also, L can equal zero. For example, if a

concentrated plastic hinge with a relative rotation about the local 2-axis is placed between points I and J, only a relative rotation d_5 exists. The other five relative displacements must be set to zero. This can be accomplished by setting the absolute displacements at joints I and J equal.

21.3 GENERAL PLASTICITY ELEMENT

The general plasticity element can be used to model many different types of nonlinear material properties. The fundamental properties and behavior of the element are illustrated in Figure 21.2.
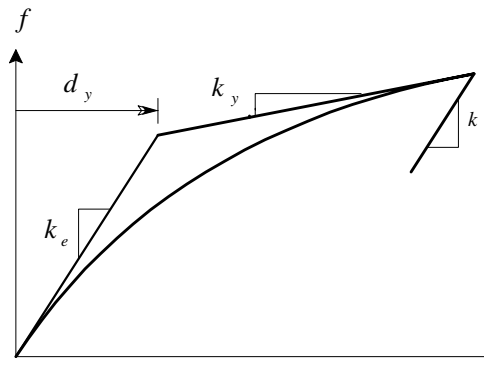
Figure 21.2 Fundamental Behavior of Plasticity Element

where k_e =   initial linear stiffness

k_y =   Yield stiffness

d_y =   Yield deformation

The force-deformation relationship is calculated from:

$$f = k_y\, d + (k_e - k_y)\, e \tag{21.1}$$

Where d is the total deformation and e is an elastic deformation term and has a range $\pm d_y$. It is calculated at each time step by the numerical integration of one of the following differential equations:

$$\text{If} \quad \dot{d}e \geq 0 \quad \dot{e} = (1 - |\frac{e}{d_y}|^n)\dot{d} \tag{21.2}$$

$$\text{If} \quad \dot{d}e < 0 \quad \dot{e} = \dot{d} \tag{21.3}$$

The following finite difference approximations for each time step can be made:

$$\dot{d} = \frac{d_t - d_{t-\Delta t}}{\Delta t} \qquad \text{and} \qquad \dot{e} = \frac{e_t - e_{t-\Delta t}}{\Delta t} \tag{21.4a and 21.4b}$$

The numerical solution algorithm (six computer program statements) can be summarized at the end of each time increment Δt, at time t for iteration i, in Table 21.1.

Table 21.1 Iterative Algorithm for Plasticity Element

1. Change in deformation for time step Δt at time t for iteration i

$$v = d_t^{(i)} - d_{t-\Delta t}$$

2. Calculate elastic deformation for iteration i

$$\text{if} \quad v e_t^{(i-1)} \leq 0 \qquad e_t^{(i)} = e_{t-\Delta t} + v$$

$$\text{if} \quad v e_t^{(i-1)} > 0 \qquad e_t^{(i)} = e_{t-\Delta t} + (1 - |\frac{e_{t-\Delta t}}{d_y}|^n) v$$

$$\text{if} \quad e_t^{(i)} > d_y \qquad e_t^{(i)} = d_y$$

$$\text{if} \quad e_t^{(i)} < -d_y \qquad e_t^{(i)} = -d_y$$

3. Calculate iterative force:

$$f_t^{(i)} = k_y d_t^{(i)} + (k_e - k_y) e_t^{(i)}$$

Note that the approximate term $\dfrac{e_{t-\Delta t}}{d_y}$ is used from the end of the last time increment rather than the iterative term $\dfrac{e_t^{(i)}}{d_y}$. This approximation eliminates all problems associated with convergence for large values of n. However, the approximation has insignificant effects on the numerical results for all values of

n. For all practical purposes, a value of n equal to 20 produces true bilinear behavior.

21.4 DIFFERENT POSITIVE AND NEGATIVE PROPERTIES

The previously presented plasticity element can be generalized to have different positive, d_p, and negative, d_n, yield properties. This will allow the same element to model many different types of energy dissipation devices, such as the double diagonal Pall friction element.

Table 21.2 Iterative Algorithm for Non-Symmetric Bilinear Element

1. Change in deformation for time step Δt at time t for iteration i

$\qquad v = d_t^{(i)} - d_{t-\Delta t}$

2. Calculate elastic deformation for iteration i

$\qquad$ if $v\,e_t^{(i-1)} \leq 0$ $\qquad\qquad\qquad\qquad$ $e_t^{(i)} = e_{t-\Delta t} + v$

$\qquad$ if $v\,e_t^{(i-1)} > 0$ and $e_{t-\Delta t} > 0$ $\qquad$ $e_t^{(i)} = e_{t-\Delta t} + (1 - |\frac{e_{t-\Delta t}}{d_p}|^n)\,v$

$\qquad$ if $v\,e_t^{(i-1)} > 0$ and $e_{t-\Delta t} < 0$ $\qquad$ $e_t^{(i)} = e_{t-\Delta t} + (1 - |\frac{e_{t-\Delta t}}{d_n}|^n)\,v$

$\qquad$ if $e_t^{(i)} > d_p$ $\qquad\qquad\qquad\qquad\qquad$ $e_t^{(i)} = d_p$

$\qquad$ if $e_t^{(i)} < -d_n$ $\qquad\qquad\qquad\qquad\qquad$ $e_t^{(i)} = -d_n$

3. Calculate iterative force at time t :

$\qquad f_t^{(i)} = k_y d_t^{(i)} + (k_e - k_y)e_t^{(i)}$

For constant friction, the double diagonal Pall element has $k_e = 0$ and $n \approx 20$. For small forces both diagonals remain elastic, one in tension and one in compression. At some deformation, d_n, the compressive element may reach a maximum possible value. Friction slipping will start at the deformation d_p after which both the tension and compression forces will remain constant until the maximum displacement for the load cycle is obtained.

This element can be used to model bending hinges in beams or columns with non-symmetric sections. The numerical solution algorithm for the general bilinear plasticity element is given in Table 21.2.

21.5   THE BILINEAR TENSION-GAP-YIELD ELEMENT

The bilinear tension-only element can be used to model cables connected to different parts of the structure. In the retrofit of bridges, this type of element is often used at expansion joints to limit the relative movement during earthquake motions. The fundamental behavior of the element is summarized in Figure 21.3. The positive number d_0 is the axial deformation associated with initial cable sag. A negative number indicates an initial pre-stress deformation. The permanent element yield deformation is d_p.
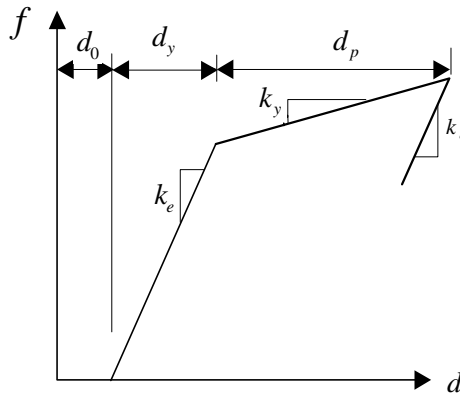
Figure 21.3 Tension-Gap-Yield Element

The numerical solution algorithm for this element is summarized in Table 21.3. Note that the permanent deformation calculation is based on the converged deformation at the end of the last time step. This avoids numerical solution problems.

Table 21.3 Iterative Algorithm for Tension-Gap-Yield Element

1. Update Tension Yield Deformation from Previous Converged Time Step
   $$y = d_{t-\Delta t} - d_0 - d_y$$
   if $y < d_p$ then $d_p = y$

2. Calculate Elastic Deformation for Iteration (i)
   $$d = d_t^{(i)} - d_0$$
   $$e_t^{(i)} = d - d_p$$
   if $e_t^{(i)} > d_y$ then $e_t^{(i)} = d_y$

3. Calculate Iterative Force:
   $$f_t^{(i)} = k_y(d_t^{(i)} - d_0) + (k_e - k_y)e_t^{(i)}$$
   if $f_t^{(i)} < 0$ then $f_t^{(i)} = 0$

21.6 NONLINEAR GAP-CRUSH ELEMENT

Perhaps the most common type of nonlinear behavior that occurs in real structural systems is the closing of a gap between different parts of the structure; or, the uplifting of the structure at its foundation. The element can be used at abutment-soil interfaces and for modeling soil-pile contact. The gap/crush element has the following physical properties:

1. The element cannot develop a force until the opening d_0 gap is closed. A negative value of d_0 indicates an initial compression force.

2. The element can only develop a negative compression force. The first yield deformation d_y is specified by a positive number.

3. The crush deformation d_c is always a monotonically decreasing negative number.

The numerical algorithm for the gap-crush element is summarized in Table 21.4.

Table 21.4 Iterative Algorithm for Gap-Crush Element

1. Update Crush Deformation from Previously Converged Time Step:

    $$y = d_{t-\Delta t} + d_0 + d_y$$

    if $y > d_c$ then $d_c = y$

2. Calculate Elastic Deformation:

    $$e_t^{(i)} = d_t^{(i)} + d_o - d_c$$

    if $e_t^{(i)} < -d_y$ then $\qquad e_t^{(i)} = -d_y$

3. Calculate Iterative Force:

    $$f_t^{(i)} = k_y (d_t^{(i)} + d_0) + (k_e - k_y) e_t^{(i)}$$

    if $f_t^{(i)} > 0$ then $f_t^{(i)} = 0$

The numerical convergence of the gap element can be very slow if a large elastic stiffness term k_e is used. The user must take great care in selecting a physically realistic number. To minimize numerical problems, the stiffness k_e should not be over 100 times the stiffness of the elements adjacent to the gap. The dynamic contact problem between real structural components often does not have a unique solution. Therefore, it is the responsibility of the design engineer to select materials at contact points and surfaces that have realistic material properties that can be predicted accurately.

21.7 VISCOUS DAMPING ELEMENTS

Linear velocity-dependent energy-dissipation forces exist in only a few special materials subjected to small displacements. In terms of equivalent modal damping, experiments indicate that they are a small fraction of one percent. Manufactured mechanical dampers cannot be made with linear viscous properties because all fluids have finite compressibility and nonlinear behavior is present in all manmade devices. In the past it has been common practice to approximate the behavior of those viscous nonlinear elements by a simple linear viscous force. More recently, vendors of those devices have claimed that the damping forces are proportional to a power of the velocity. Experimental

examination of a mechanical device indicates a far more complex behavior that cannot be represented by a simple one-element model.

The FNA method does not require that those damping devices be linearized or simplified to obtain a numerical solution. If the physical behavior is understood, it is possible for an iterative solution algorithm to be developed that will accurately simulate the behavior of almost any type of damping device. To illustrate the procedure, let us consider the device shown in Figure 21.4.

$$f_p^{(i)} = k_p d_t^{(i)}$$

$$f^{(i)} = f_p^{(i)} + f_s^{(i)}$$

$$f_s^{(i)} = k_s(d_t^{(i)} - e^{(i)}) = sign(\dot{e}^{(i)})\, \dot{e}^{(i)N} c$$
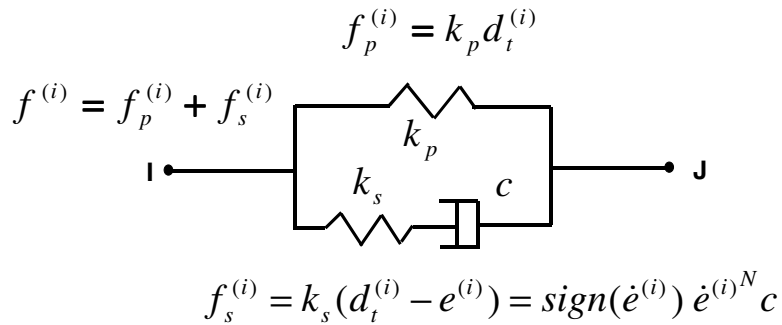
Figure 21.4 General Damping Element Connected Between Points I and J

It is apparent that the total deformation, $e_t^{(i)}$, across the damper must be accurately calculated to evaluate the equilibrium within the element at each time step. The finite difference equation used to estimate the damper deformation at time t is:

$$e_t^{(i)} = e_{t-\Delta t} + \int_{t-\Delta t}^{t} \dot{e}_\tau^{(i)} d\tau = e_{t-\Delta t} + \frac{\Delta t}{2}(\dot{e}_{t-\Delta t} + \dot{e}_t^{(i)}) \tag{21.5}$$

A summary of the numerical algorithm is summarized in Table 21.5.

Table 21.5 Iterative Algorithm for Nonlinear Viscous Element

1. Estimate damper force from last iteration:
    $$f_s^{(i)} = k_s(d_t^{(i)} - e_t^{(i-1)})$$

2. Estimate damper velocity:
    $$\dot{e}_t^{(i)} = (\frac{f_s^{(i)}}{c})^{\frac{1}{N}} sign(f_s^{(i)})$$

3. Estimate damper deformation:
    $$e_t^{(i)} = e_{t-\Delta t} + \frac{\Delta t}{2}(\dot{e}_{t-\Delta t)} + \dot{e}_t^{(i)})$$

4. Calculate total iterative force:
    $$f_t^{(i)} = k_p d_t^{(i)} + k_s(d_t^{(i)} - e_t^{(i)})$$

21.8   THREE-DIMENSIONAL FRICTION-GAP ELEMENT

Many structures have contact surfaces between components of the structures or between structure and foundation that can only take compression. During the time the surfaces are in contact, it is possible for tangential friction forces to develop between the surfaces. The maximum tangential surface forces, which can be developed at a particular time, are a function of the normal compressive force that exists at that time. If the surfaces are not in contact, the normal and the surface friction forces must be zero. Therefore, surface slip displacements will take place during the period of time when the allowable friction force is exceeded or when the surfaces are not in contact.

To develop the numerical algorithm to predict the dynamic behavior between surfaces, consider the contact surface element shown in Figure 21.5. The two surface nodes are located at the same point in space and are connected by the gap-friction element that has contact stiffness k in all three directions. The three directions are defined by a local n, s and $s+90^o$ reference system. The element deformations d_n, d_s and d_{s+90} are relative to the absolute displacements of the two surfaces.
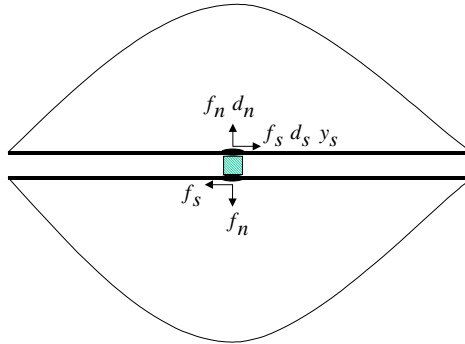
Figure 21.5 Three-Dimensional Nonlinear Friction-Gap Element

During the time of contact, the force-deformation relationships for the friction-gap element are:

Normal Force:
$$f_n = k d_n \qquad\qquad (21.6a)$$

Maximum Allowable Slip Force:
$$f_a = \mu \left| f_n \right| \qquad\qquad (21.6b)$$

Tangential Surface Forces:
$$f_s = k(d_s - y_s)$$
$$\text{or,} \qquad\qquad (21.6c)$$
$$\bar{f}_s = sign(f_s) f_a$$

The coefficient of sliding friction is designated by μ. The surface slip deformation in the s direction is y_s.

The iterative numerical algorithm for a typical time step is summarized in Table 21.6. To minimize numerical problems, the stiffness k should not be over 100 times the stiffness of the elements adjacent to the gap.

Table 21.6 Iterative Algorithm for Friction-Gap Element

---

1. If $i=1$, update slip deformations from previously converged time step at s and $s+90^0$

   $$y_s(t) = y_s(t - \Delta t)$$

2. Evaluate normal and allowable slip forces

   if $d_n^{(i)} > 0$ $f_n^{(i)} = 0$

   if $d_n^{(i)} \leq 0$ $f_n^{(i)} = kd_n^{(i)}$

   $$f_a^{(i)} = \mu \left| f_n^{(i)} \right|$$

3. Calculate surface forces at s and $s+90^0$

   if $d_n^{(i)} > 0$ $f_s^{(i)} = 0$

   if $d_n^{(i)} \leq 0$ $f_s^{(i)} = k(d_s^{(i)} - y_s)$

          if $\left| f_s^{(i)} \right| > f_a^{(i)}$ $\bar{f}_s^{(i)} = sign(f_s^{(i)}) f_a^{(i)}$

4. Calculate slip deformations at s and $s+90^0$

   if $d_n^{(i)} > 0$ $y_s^{(i)} = d_s^{(i)}$

   if $\left| f_s^{(i)} \right| = f_a^{(i)}$ $y_s^{(i)} = d_s^{(i)} - f_s^{(i)} / k$

21.9   SUMMARY

The use of approximate "equivalent linear viscous damping" has little theoretical or experimental justification and produces a mathematical model that violates dynamic equilibrium. It is now possible to accurately simulate the behavior of structures with a finite number of discrete gap, tension only, and energy dissipation devices installed. The experimentally determined properties of the devices can be directly incorporated into the computer model.

22.

SEISMIC ANALYSIS USING DISPLACEMENT LOADING

Direct use of Earthquake Ground Displacement in a Dynamic Analysis has Inherent Numerical Errors

22.1 INTRODUCTION

Most seismic structural analyses are based on the relative-displacements formulation where the base accelerations are used as the basic loading. Hence, experience with the direct use of absolute earthquake displacement loading acting at the base of the structure has been limited. Several new types of numerical errors associated with the use of absolute seismic displacement loading are identified. Those errors are inherent in all methods of dynamic analysis and are directly associated with the application of displacement loading.

It is possible for the majority of seismic analyses of structures to use the ground accelerations as the basic input, and the structural displacements produced are relative to the absolute ground displacements. In the case of multi-support input motions, it is necessary to formulate the problem in terms of the absolute ground motions at the different supports. However, the earthquake engineering profession has not established analysis guidelines to minimize the errors associated with that type of analysis. In this chapter, it will be shown that several new types of numerical errors can be easily introduced if absolute displacements are used as the basic loading.

A typical long-span bridge structure is shown in Figure 22.1. Different motions may exist at piers because of local site conditions or the time delay in the horizontal propagation of the earthquake motions in the rock. Therefore, several hundred different displacement records may be necessary to define the basic loading on the structure.

SOFT ROCK or SOIL

HARD ROCK
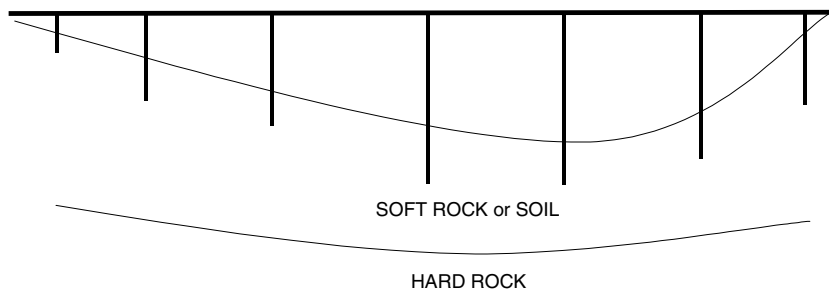
Figure 22.1 Long Bridge Structure With Multi-Support Input Displacements

The engineer/analyst must be aware that displacement loading is significantly different from acceleration loading with respect to the following possible errors:

1. The accelerations are linear functions within a time increment and an exact solution is normally used to solve the equilibrium equations. On the other hand, displacements derived from a linear acceleration function are a cubic function within each increment; therefore, a smaller time increment is required, or a higher order solution method must be used.

2. The spatial distribution of the loads in the relative displacement formulation is directly proportional to the mass; and the 90 percent modal mass-participation rule can be used to ensure that the results are accurate. In the case of base displacement input, however, the modal mass-participation factors cannot be used to estimate possible errors. For absolute displacement loading, concentrated forces are applied at the joints near the fixed base of the structure; therefore, a large number of high-frequency modes are excited. Hence, alternative error estimations must be introduced and a very large number of modes may be required.

3. If the same damping is used for acceleration and displacement analyses, different results are obtained. This is because, for the same damping ratio, the effective damping associated with the higher frequency response is larger when displacement input is specified (see Table 19.1). Also, if mass proportional damping is used, additional damping is introduced because of the rigid body motion of the structure.

The dynamic equilibrium equations for absolute seismic displacement type of loading are derived. The different types of errors that are commonly introduced are illustrated by an analysis of a simple shear-wall structure.

22.2   EQUILIBRIUM EQUATIONS FOR DISPLACEMENT INPUT

For a lumped-mass system, the dynamic equilibrium equations in terms of the unknown joint displacements $\mathbf{u}_s$ within the superstructure and the specified absolute displacements $\mathbf{u}_b$ at the base joints can be written as:

$$\begin{bmatrix} \mathbf{M}_{ss} & \mathbf{0} \\ \mathbf{0} & \mathbf{M}_{bb} \end{bmatrix} \begin{bmatrix} \ddot{\mathbf{u}}_s \\ \ddot{\mathbf{u}}_b \end{bmatrix} + \begin{bmatrix} \mathbf{C}_{ss} & \mathbf{C}_{sb} \\ \mathbf{C}_{bs} & \mathbf{C}_{bb} \end{bmatrix} \begin{bmatrix} \dot{\mathbf{u}}_s \\ \dot{\mathbf{u}}_b \end{bmatrix} + \begin{bmatrix} \mathbf{K}_{ss} & \mathbf{K}_{sb} \\ \mathbf{K}_{bs} & \mathbf{K}_{bb} \end{bmatrix} \begin{bmatrix} \mathbf{u}_s \\ \mathbf{u}_b \end{bmatrix} = \begin{bmatrix} \mathbf{0} \\ \mathbf{R}_b \end{bmatrix} \quad (22.1)$$

The mass, damping and stiffness matrices associated with those displacements are specified by $\mathbf{M}_{ij}$, $\mathbf{C}_{ij}$, and $\mathbf{K}_{ij}$. Note that the forces $\mathbf{R}_b$ associated with the specified displacements are unknown and can be calculated after $\mathbf{u}_s$ has been evaluated.

Therefore, from Equation (22.1) the equilibrium equations for the superstructure only, with specified absolute displacements at the base joints, can be written as:

$$\mathbf{M}_{ss}\ddot{\mathbf{u}}_s + \mathbf{C}_{ss}\dot{\mathbf{u}}_s + \mathbf{K}_{ss}\mathbf{u}_s = -\mathbf{K}_{sb}\mathbf{u}_b - \mathbf{C}_{sb}\dot{\mathbf{u}}_b \quad (22.2)$$

The damping loads $\mathbf{C}_{sb}\dot{\mathbf{u}}_b$ can be numerically evaluated if the damping matrix is specified. However, the damping matrix is normally not defined. Therefore, those damping forces are normally neglected and the absolute equilibrium equations are written in the following form:

$$\mathbf{M}_{ss}\ddot{\mathbf{u}}_s + \mathbf{C}_{ss}\dot{\mathbf{u}}_s + \mathbf{K}_{ss}\mathbf{u}_s = -\mathbf{K}_{sb}\mathbf{u}_b = \sum_{j=1}^{J}\mathbf{f}_j u_j(t)$$

$$(22.3)$$

Each independent displacement record $u_j(t)$ is associated with the space function $\mathbf{f}_j$ that is the negative value of the j th column in the stiffness matrix $\mathbf{K}_{sb}$. The total number of displacement records is J, each associated with a specific displacement degree of freedom.

For the special case of a rigid-base structure, a group of joints at the base are subjected to the following three components of displacements, velocities and accelerations.

$$\mathbf{u}_b = \begin{bmatrix} u_x(t) \\ u_y(t) \\ u_z(t) \end{bmatrix}, \quad \dot{\mathbf{u}}_b = \begin{bmatrix} \dot{u}_x(t) \\ \dot{u}_y(t) \\ \dot{u}_z(t) \end{bmatrix}, \quad \text{and} \quad \ddot{\mathbf{u}}_b = \begin{bmatrix} \ddot{u}_x(t) \\ \ddot{u}_y(t) \\ \ddot{u}_z(t) \end{bmatrix}$$

$$(22.4)$$

The exact relationship between displacements, velocities and acceleration is presented in Appendix J.

The following change of variables is now possible:

$$\mathbf{u}_s = \mathbf{u}_r + \mathbf{I}_{xyz}\mathbf{u}_b, \quad \dot{\mathbf{u}}_s = \dot{\mathbf{u}}_r + \mathbf{I}_{xyz}\dot{\mathbf{u}}_b, \quad \text{and} \quad \ddot{\mathbf{u}}_s = \ddot{\mathbf{u}}_r + \mathbf{I}_{xyz}\ddot{\mathbf{u}}_b$$

$$(22.5)$$

The matrix $\mathbf{I}_{xyz} = [\mathbf{I}_x \mathbf{I}_y \mathbf{I}_z]$ and has three columns. The first column has unit values associated with the x displacements, the second column has unit values associated with the y displacements, and the third column has unit values associated with the z displacements. Therefore, the new displacements $\mathbf{u}_r$ are relative to the specified absolute base displacements. Equation (22.2) can now be rewritten in terms of the relative displacements and the specified base displacements:

$$\mathbf{M}_{ss}\ddot{\mathbf{u}}_r + \mathbf{C}_{ss}\dot{\mathbf{u}}_r + \mathbf{K}_{ss}\mathbf{u}_r =$$
$$- \mathbf{M}_{ss}\mathbf{I}_{xyz}\ddot{\mathbf{u}}_b - [\mathbf{C}_{ss}\mathbf{I}_{xyz} + \mathbf{C}_{sb}]\dot{\mathbf{u}}_b - [\mathbf{K}_{ss}\mathbf{I}_{xyz} + \mathbf{K}_{sb}]\mathbf{u}_b$$

$$(22.6)$$

The forces $[\mathbf{K}_{ss}\mathbf{I}_{xyz} + \mathbf{K}_{sb}]\mathbf{u}_b$ associated with the rigid body displacement of the structure are zero. Because the physical damping matrix is almost impossible to

define, the damping forces on the right-hand side of the equation are normally neglected. Hence, the three-dimensional dynamic equilibrium equations, in terms of relative displacements, are normally written in the following approximate form:

$$\mathbf{M}_{ss}\ddot{\mathbf{u}}_r + \mathbf{C}_{ss}\dot{\mathbf{u}}_r + \mathbf{K}_{ss}\mathbf{u}_r = -\mathbf{M}_{ss}\mathbf{I}_{xyz}\ddot{\mathbf{u}}_b$$
$$= -\mathbf{M}_{ss}\mathbf{I}_x\ddot{u}_x(t) - \mathbf{M}_{ss}\mathbf{I}_y\ddot{u}_y(t) - \mathbf{M}_{ss}\mathbf{I}_z\ddot{u}_z(t) \qquad (22.7)$$

Note that the spatial distribution of the loading in the relative formulations is proportional to the directional masses.

It must be noted that in the absolute displacement formulation, the stiffness matrix $\mathbf{K}_{sb}$ only has terms associated with the joints adjacent to the base nodes where the displacements are applied. Therefore, the only loads, $\mathbf{f}_j$, acting on the structure are point loads acting at a limited number of joints. This type of spatial distribution of point loads excites the high frequency modes of the system as the displacements are propagated within the structure. Hence, the physical behavior of the analysis model is very different if displacements are applied rather than if the mass times the acceleration is used as the loading. Therefore, the computer program user must understand that both approaches are approximate for non-zero damping.

If the complete damping matrix is specified and the damping terms on the right-hand sides of Equations (22.2 and 22.6) are included, an exact solution of both the absolute and relative formulations will produce identical solutions.

22.3   USE OF PSEUDO-STATIC DISPLACEMENTS

An alternate formulations, which is restricted to linear problems, is possible for multi support displacement loading that involves the use of pseudo-static displacements, which are defined as:

$$\mathbf{u}_p = -\mathbf{K}_{ss}^{-1}\mathbf{K}_{sb}\mathbf{u}_b = \mathbf{T}\mathbf{u}_b \qquad (22.8)$$

The following change of variable is now introduced:

$$\mathbf{u}_s = \mathbf{u} + \mathbf{u}_p = \mathbf{u} + \mathbf{T}\mathbf{u}_b \,, \; \dot{\mathbf{u}}_s = \dot{\mathbf{u}} + \mathbf{T}\dot{\mathbf{u}}_b \text{ and } \ddot{\mathbf{u}}_s = \ddot{\mathbf{u}} + \mathbf{T}\ddot{\mathbf{u}}_b \qquad (22.9)$$

The substitution of Equations (9) into Equation (2) yields the following set of equilibrium equations:

$$\mathbf{M}_{ss}\ddot{\mathbf{u}} + \mathbf{C}_{ss}\dot{\mathbf{u}} + \mathbf{K}_{ss}\mathbf{u} = -\mathbf{K}_{sb}\mathbf{u}_b - \mathbf{C}_{sb}\dot{\mathbf{u}}_b - \mathbf{M}_{ss}\mathbf{T}\ddot{\mathbf{u}}_b$$
$$- \mathbf{C}_{ss}\mathbf{T}\dot{\mathbf{u}}_b - \mathbf{K}_{ss}\mathbf{T}\mathbf{u}_b \qquad (22.10)$$

Hence Equation (22.10) can be written in the following simplified form:

$$\mathbf{M}_{ss}\ddot{\mathbf{u}} + \mathbf{C}_{ss}\dot{\mathbf{u}} + \mathbf{K}_{ss}\mathbf{u} = -\mathbf{M}_{ss}\mathbf{T}\ddot{\mathbf{u}}_b - [\mathbf{C}_{sb} + \mathbf{C}_{ss}\mathbf{T}]\dot{\mathbf{u}}_b \qquad (22.11)$$

Equation (22.11) is exact if the damping terms are included on the right-hand side of the equation. However, these damping terms are normally not defined and are neglected. Hence, different results will be obtained from this formulation when compared to the absolute displacement formulation. The pseudo-static displacements cannot be extended to nonlinear problems; therefore, it cannot be considered a general method that can be used for all structural systems.

22.4 SOLUTION OF DYNAMIC EQUILIBRIUM EQUATIONS

The absolute displacement formulation, Equation (22.3), and the relative formulation, Equation (22.7), can be written in the following generic form:

$$\mathbf{M}\ddot{\mathbf{u}}(t) + \mathbf{C}\dot{\mathbf{u}}(t) + \mathbf{K}\mathbf{u}(t) = \sum_{j=1}^{J} \mathbf{f}_j g_j(t) \qquad (22.12)$$

Many different methods can be used to solve the dynamic equilibrium equations formulated in terms of absolute or relative displacements. The direct incremental numerical integration can be used to solve these equations. However, because of stability problems, large damping is often introduced in the higher modes, and only an approximate solution that is a function of the size of the time step used is obtained. The frequency domain solution using the **F**ast-**F**ourier-**T**ransform, FFT, method also produces an approximate solution. Therefore, the errors identified in this paper exist for all methods of dynamic response analysis. Only the mode superposition method, for both linear acceleration and cubic

displacement loads, can be used to produce an exact solution. This approach is presented in Chapter 13.

22.5 NUMERICAL EXAMPLE

22.5.1 Example Structure

The problems associated with the use of absolute displacement as direct input to a dynamic analysis problem can be illustrated by the numerical example shown in Figure 22.2.

Properties:

Thickness = 2.0 ft
Width =20.0 ft
I = 27,648,000 in⁴
E = 4,000 ksi
W = 20 kips /story
M_x = 20/g
*   = 0.05176 kip-sec² /in*
M_{yy} = 517.6 kip-sec² -in
Total Mass = 400 /g
Typical Story Height
* h = 15 ft = 180 in.*

Typical Story Load

$$M\ddot{u}_b(t)$$

First Story Load

$$\frac{12EI}{h^3}u_b(t)$$

First Story Moment

$$\frac{6EI}{h^2}u_b(t)$$

A. 20 Story Shear Wall
   With Story Mass

B. Base Acceleration Loads
   Relative Formulation

C. Displacement Loads
   Absolute Formulation

Figure 22.2 Comparison of Relative and Absolute Displacement Seismic Analysis

Neglecting shear and axial deformations, the model of the structure has forty displacement degrees of freedom, one translation and one rotation at each joint. The rotational masses at the nodes have been included; therefore, forty modes of vibration exist. Note that loads associated with the specification of the absolute base displacements are concentrated forces at the joint near the base of the structure. The exact periods of vibration for these simple cantilever structures are summarized in Table 22.1 in addition to the mass, static and dynamic load-

participation factors. The derivations of mass-participation factor, static-participation factors, and dynamic-participation factors are given in Chapter 13.

Table 22.1 Periods and Participation Factors for Exact Eigenvectors

Mode Number	Period (Seconds)	Cumulative Sum of Mass Participation Factors X-Direction (Percentage)	Cumulative Sum of Load Participation Factors Base Displacement Loading (Percentage)	
			Static	Dynamic
1	1.242178	62.645	0.007	0.000
2	0.199956	81.823	0.093	0.000
3	0.072474	88.312	0.315	0.000
4	0.037783	91.565	0.725	0.002
5	0.023480	93.484	1.350	0.007
6	0.016227	94.730	2.200	0.023
7	0.012045	95.592	3.267	0.060
8	0.009414	96.215	4.529	0.130
9	0.007652	96.679	5.952	0.251
10	0.006414	97.032	7.492	0.437
11	0.005513	97.304	9.099	0.699
12	0.004838	97.515	10.718	1.042
13	0.004324	97.678	12.290	1.459
14	0.003925	97.804	13.753	1.930
15	0.003615	97.898	15.046	2.421
16	0.003374	97.966	16.114	2.886
17	0.003189	98.011	16.913	3.276
18	0.003052	98.038	17.429	3.551
19	0.002958	98.050	17.683	3.695
20	0.002902	98.053	17.752	3.736
21	0.002066	99.988	99.181	98.387
30	0.001538	99.999	99.922	99.832
40	0.001493	100.000	100.000	100.000

It is important to note that only four modes are required to capture over 90 percent of the mass in the x-direction. However, for displacement loading, 21 eigenvectors are required to capture the static response of the structure and the kinetic energy under rigid-body motion. Note that the period of the 21th mode is 0.002066 seconds, or approximately 50 cycles per second. However, this high frequency response is essential so that the absolute base displacement is accurately propagated into the structure.

22.5.2 Earthquake Loading

The acceleration, velocity and displacement base motions associated with an idealized near-field earthquake are shown in Figure 22.3. The motions have been selected to be simple and realistic so that this problem can be easily solved using different dynamic analysis programs.
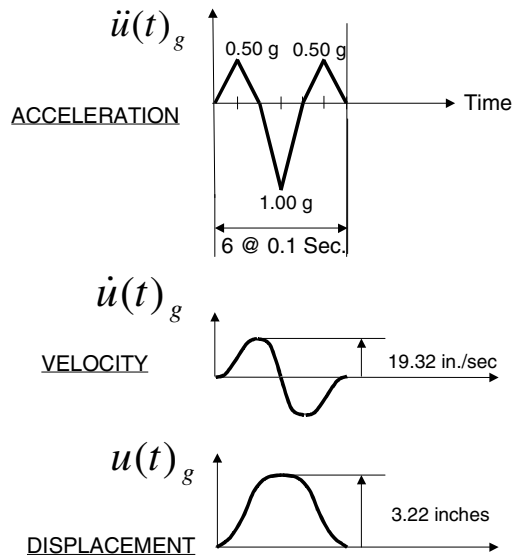
Figure 22.3 Idealized Near-Field Earthquake Motions

22.5.3 Effect of Time Step Size for Zero Damping

To illustrate the significant differences between acceleration and displacement loading, this problem will be solved using all forty eigenvectors, zero damping and three different integration time steps. The absolute top displacement, base

shears and moments at the second level are summarized in Table 22.2. In addition, the maximum input energy and kinetic energy in the model are summarized.

Table 22.2   Comparison of Acceleration and Displacement Loads (40 Eigenvalues – 0.0 Damping Ratio)

	Linear Acceleration Loads			Linear Displacement Loads		
	$\Delta t = 0.01$	$\Delta t = 0.005$	$\Delta t = 0.001$	$\Delta t = 0.01$	$\Delta t = 0.005$	$\Delta t = 0.001$
u_{20} (Inches)	5.306 @ 0.610	5.306 @0.610	5.306 @0.610	5.306 @0.610	5.307 @0.610	5.307 @0.610
V_2 (Kips)	-94.35 @0.310	-94.35 @0.310	-94.58 @0.308	-90.83 @0.660	-74.74 @0.310	94.91 @0.308
M_2 (K - In.)	-149,500 @0.610	-149,500 @0.610	-149,500 @0.610	-152,000 @0.610	-148,100 @0.605	-149,500 @0.610
ENERGY (Input To Model)	339.9 @0.410	339.9 @0.405	340.0 @0.401	1,212,000 @0.310	1,183,000 @0.305	1,180,000 @0.301
K-ENERGY (Within Model)	339.9 @0.410	339.9 @0.405	339.9 @0.402	166.2 @0.410	164.1 @0.405	163.9 @0.402

For linear acceleration load, all results are exact regardless of the size of the time step because the integration algorithm is based on the exact solution for a linear function. The minor difference in results is because some maximum values occur within the larger time step results. However, using the same linear integration algorithm for displacement loads produces errors because displacements are cubic function within each time step (Appendix J). Therefore, the larger the time step, the larger the error.

For linear displacement loads, the maximum displacement at the top of the structure and the moment t at the second level appear to be insensitive to the size of the time step. However, the forces near the top of the structure and the shear at the second level can have significant errors because of large integration time steps. For a time step of 0.01 seconds, the maximum shear of -90.83 kips occurs at 0.660 seconds; whereas, the exact value for the same time step is –94.35 kips

and occurs at 0.310 seconds. A time-history plot of both shears forces is shows in Figure 22.4.
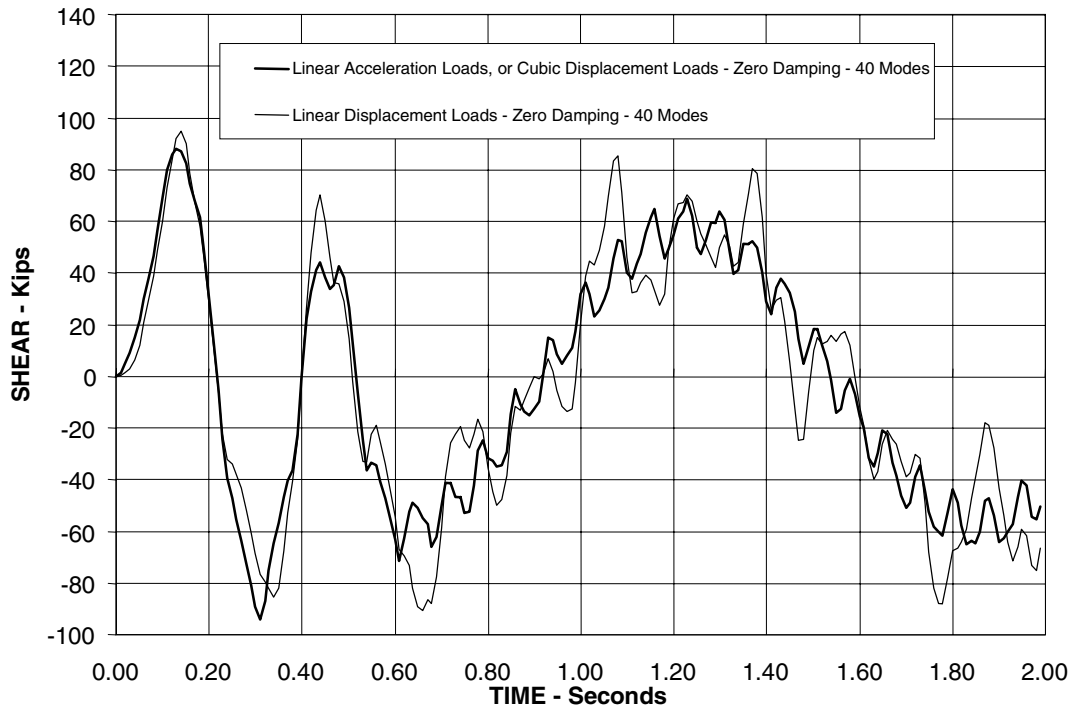
Figure 22.4 Shear at Second Level Vs.
Time With $\Delta t = 0.01$ ***-Seconds and Zero Damping***

The errors resulting from the use of large time steps are not large in this example because the loading is a simple function that does not contain high frequencies. However, the author has had experience with other structures, using real earthquake displacement loading, where the errors are over 100 percent using a time step of 0.01 seconds. The errors associated with the use of large time steps in a mode superposition analysis can be eliminated for linear elastic structures using the new exact integration algorithm presented in Chapter 13.

An examination of the input and kinetic energy clearly indicates that there is a major ***mathematical*** differences between acceleration loads (relative displacement formulation) and displacement loads (absolute displacement formulation). In the relative displacement formulation, a relatively small amount

of energy, 340 k-in, is supplied to the mathematical model; whereas the point loads associated with the absolute formulation applied near the base of the structure imparts over 1,000,000 k-in of energy to the model. Also, the maximum kinetic energy (proportional to the sum of mass times velocity squared) within the model is 340 k-in for the relative formulation compared to 164 kip-in for the absolute formulation.

The results clearly indicate that errors are introduced if large time steps are used with the linear displacement approximation within each time step. The spatial load distribution is significantly different between the relative and displacement formulations. For linear acceleration loads, large time steps can be used. However, very small time steps, 0.001 second, are required for absolute displacement loading to obtain accurate results. However, if modal superposition is used, the new cubic displacement load approximation produces results identical to those obtained using linear acceleration loads for zero damping.

22.5.4 Earthquake Analysis with Finite Damping

It is very important to understand that the results produced from a mathematical computer model may be significantly different from the behavior of the real physical structure. The behavior of a real structure will satisfy the basic laws of physics, whereas the computer model will satisfy the laws of mathematics after certain assumption have been made. The introduction of classical linear viscous damping will illustrate this problem.

Table 22.3 summarizes selective results of an analysis of the structure shown in Figure 22.2 for both zero and five percent damping for all frequencies. The time step used for this study is 0.005 second; hence, for linear acceleration loads and cubic displacement loads, exact results (within three significant figures) are produced.

The results clearly indicate that 5 percent damping produces different results for acceleration and displacement loading. The top displacements and the moments near the base are very close. However, the shear at the second level and the moment at the tenth level are significantly different. The shears at the second level vs. time for displacement loading are plotted in Figure 22.5 for 5 percent damping.

Table 22.3. Comparison of Acceleration and Displacement Loads for Different Damping (40 Eigenvalues, 0.005 Second Time Step)

	Linear Acceleration Loads		Cubic Displacement Loads	
	$\xi = 0.00$	$\xi = 0.05$	$\xi = 0.00$	$\xi = 0.05$
u_{20} (Inch)	5.306 @ 0.610 -5.305 @ 1.230	4.939 @ 0.580 -4.217 @ 1.205	5.307 @ 0.610 -5.304 @ 1.230	4.913 @ 0.600 -4.198 @ 1.230
V_2 (Kips)	88.31 @ 0.130 -94.35 @ 0.310	84.30 @ 0.130 -95.78 @ 0.310	88.28 @ 0.135 -94.53 @ 0.310	135.1 @ 0.150 -117.1 @ 0.340
M_2 (K-in.)	148,900 @1.230 -149,500 @ 0.605	116,100 @1.200 -136,300 @ 0.610	148,900 @1.230 -149,500 @ 0.605	115,300 @1.230 -136,700 @ 0.605
M_{10} (K-in.)	81,720 @ 0.290 -63,470 @ 0.495	77,530 @ 0.300 -64,790 @ 0.485	81,720 @ 0.290 -63,470 @ 0.495	80,480 @ 0.320 -59,840 @ 0.495
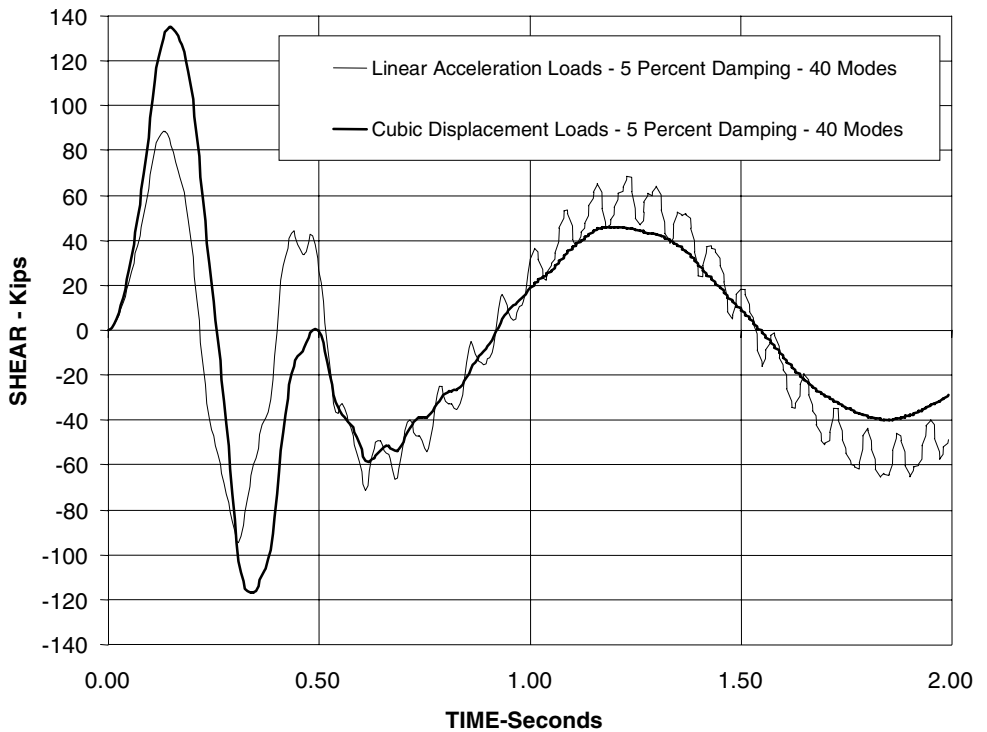
Figure 22.5 Shear at Second Level Vs. Time Due To Cubic Displacement Loading. (40 Eigenvalues – $\Delta t = 0.005$ Seconds)

The results shown in Figure 22.5 are physically impossible for a real structure because the addition of 5 percent damping to an undamped structure should not increase the maximum shear from 88.28 kips to 135.10 kips. The reason for this violation of the fundamental laws of physics is the invalid assumption of an orthogonal damping matrix required to produce *classical damping*.

Classical damping always has a mass-proportional damping component, as physically illustrated in Figure 22.6, which causes external velocity-dependent forces to act on the structure. For the relative displacement formulation, the forces are proportional to the relative velocities. Whereas for the case of the application of base displacement, the external force is proportional to the absolute velocity. Hence, for a rigid structure, large external damping forces can be developed because of rigid body displacements at the base of the structure. This is the reason that the shear forces increase as the damping is increased, as shown in Figure 22.6. For the case of a very flexible (or base isolated) structure, the relative displacement formulation will produce large errors in the shear forces because the external forces at a level will be carried direct by the dash-pot at that level. Therefore, neither formulation is physically correct.

In the left diagram (relative displacement formulation):
$$m\,\ddot{u}_x$$
$$\mathbf{C}_{ss}\mathbf{I}_x\dot{u}_x = 0$$
$$u_s = u_x + u_r$$

In the right diagram (absolute displacement formulation):
$$\mathbf{C}_{ss}\mathbf{I}_x\dot{u}_x \neq 0$$

RELATIVE DISPLACEMENT FORMULATION   ABSOLUTE DISPLACEMENT FORMULATION
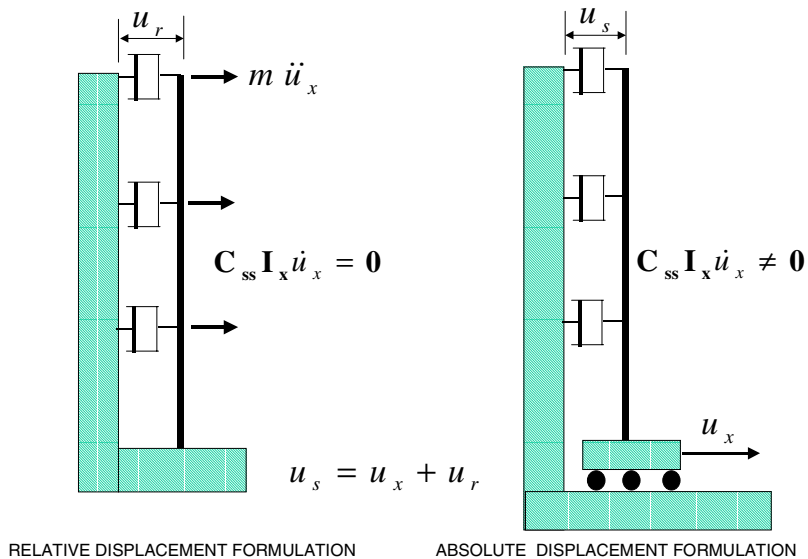
Figure 22.6 Example to Illustrate Mass-Proportional Component
in Classical Damping.

These inconsistent damping assumptions are inherent in ***all methods*** of linear and nonlinear dynamic analysis that use classical damping or mass-proportional damping. For most applications, this damping-induced error may be small; however, the engineer/analyst has the responsibility to evaluate, using simple linear models, the magnitude of those errors for each different structure and earthquake loading.

22.5.5 The Effect of Mode Truncation

The most important difference between the use of relative and absolute displacement formulations is that higher frequencies are excited by base displacement loading. Solving the same structure using a different number of modes can identify this error. If zero damping is used, the equations of motions can be evaluated exactly for both relative and absolute displacement formulations and the errors associated with mode-truncation only can be isolated.

Selective displacements and member forces for both formulations are summarized in Table 22.4.

Table 22.4   Mode-Truncation Results - Exact Integration for 0.005 Second Time Steps – Zero Damping

Number of Modes	Linear Acceleration Loads				Cubic Displacement Loads			
	u_{20}	V_2	M_2	M_{10}	u_{20}	V_2	M_2	M_{10}
4	5.306	83.10	-149,400	81,320	5.307	-51,580	-1,441,000	346,800
10	5.306	-94.58	-149,500	81,760	5.307	-33,510	-286,100	642,100
21	5.306	-94.73	-149,500	81,720	5.307	-55,180	-4,576,000	78,840
30	5.306	-94.42	149,500	81,720	5.307	-11,060	-967,200	182,400
35	5.306	94,35	149,500	81,720	5.307	-71,320	-149,500	106,100
40	5.306	-94.35	-149,500	81,720	5.307	-94.53	-149,500	81,720

The results shown in Table 22.4 clearly indicate that only a few modes are required to obtain a converged solution using the relative displacement formulation. However, the results using the absolute displacement formulation are almost unbelievable. The reason for this is that the computational model and the real structure are required to propagate the high frequencies excited by the

base displacement loading into the structure. The displacement at the top of the structure, which is dominated by the first mode, is insensitive to the high frequency wave propagation effects. However, the shear and moment forces within the structure will have significant errors if all the frequencies are not present in the analysis. Table 22.5 summarizes selective displacements and member forces for both formulations for 5 percent damping.

Table 22.5   Mode-Truncation Errors - Exact Integration for 0.005 Second Time Steps – 5 % Damping

Number of Modes	Linear Acceleration Loads				Cubic Displacement Loads			
	u_{20}	V_2	M_2	M_{10}	u_{20}	V_2	M_2	M_{10}
4	4.934	-82.51	-136,300	77,110	4.913	-5,153	1,439,000	374,600
10	4.939	-96.01	-136,300	-64,810	4.913	-33,500	-290,000	640,900
21	4.939	-96.16	-136,300	-64,790	4.913	-55,170	-4,573,000	77,650
30	"	"	"	"	4.913	-11,050	-966,000	180,800
35	"	"	"	"	4.913	-342.7	-136,800	104,500
40	"	"	"	"	4.913	-135.1	-136,800	80,480

The results shown in Table 22.5 indicate that the addition of modal damping does not significantly change the fundamental behavior of the computational model. It is apparent that a large number of high frequencies must be included in the analysis if the computational model is to accurately predict forces in the real structure. It is of considerable interest, however, that mode truncation for this problem produces erroneously large forces that are difficult to interpret. To explain those errors, it is necessary to examine the individual mode shapes. For example, the 21st mode is a lateral displacement at the second level only, with all other mode displacement near zero. This is a very important mode because a concentrated force associated with the base displacement loading is applied at the second level. Hence, the addition of that mode to the analysis increases the bending moment at the second level to 4,573,000 and decreases the moment at the 10th level to 77,650. Additional modes are then required to reduce the internal forces at the second level.

22.6   USE OF LOAD DEPENDENT RITZ VECTORS

In Table 22.6 the results of an analysis using different numbers of Load Dependent Ritz vectors is summarized. In addition, mass, static and dynamic participation factors are presented.

Table 22.6   Results Using LDR Vectors- $\Delta t = 0.005$ Cubic Displacement Loading – Damping = 5 %

Number of Vectors	u_{20}	V_2	M_2	M_{10}	Mass, Static and Dynamic Load-Participation
4	4.913	111.4	-136,100	80,200	100. 100. 29.5
7	4.913	132.6	-136,700	80,480	100. 100. 75.9
10	4.913	134.5	-136,800	80,490	100. 100. 98.0
21	4.913	135.1	-136,800	80.480	100. 100. 100.
30	4.913	135.1	-136,800	80,480	100. 100. 100.

The use of LDR vectors virtually eliminates all problem associated with the use of the exact eigenvectors. The reason for this improved accuracy is that each set of LDR vectors contains the static response of the system. To illustrate this, the fundamental properties of a set of seven LDR vectors are summarized in Table 22.7.

Table 22.7   Periods and Participation Factors for LDR Vectors

Vector Number	Approximate Period (Seconds)	Cumulative Sum of Mass Participation Factors X-Direction (Percentage)	Cumulative Sum of Load Participation Factors Base Displacement Loading (Percentage)	
			Static	Dynamic
1	1.242178	62.645	0.007	0.000
2	0.199956	81.823	0.093	0.000
3	0.072474	88.312	0.315	0.000
4	0.037780	91.568	0.725	0.002
5	0.023067	93.779	1.471	0.009
6	0.012211	96.701	5.001	0.126
7	0.002494	100.000	100.00	75.882

The first six LDR vectors are almost identical to the exact eigenvectors summarized in Table 22.1. However, the seventh vector, which is a linear combination of the remaining eigenvectors, contains the high frequency response of the system. The period associated with this vector is over 400 cycles per second; however, it is the most important vector in the analysis of a structure subjected to base displacement loading.

22.7 SOLUTION USING STEP-BY-STEP INTEGRATION

The same problem is solved using direct integration by the trapezoidal rule, which has no numerical damping and theoretically conserves energy. However, to solve the structure with zero damping, a very small time step would be required. It is almost impossible to specify constant modal damping using direct integration methods. A standard method to add energy dissipation to a direct integration method is to add Rayleigh damping, in which only damping ratios can be specified at two frequencies. For this example 5 percent damping can be specified for the lowest frequency and at 30 cycles per second. Selective results are summarized in Table 22.8 for both acceleration and displacement loading.

Table 22.8   Comparison of Results Using Constant Modal Damping and the Trapezoidal Rule and Rayleigh Damping (0.005 Second Time Step)

	Acceleration Loading		Displacement Loading	
	Trapezoidal Rule Using Rayleigh Damping	Exact Solution Using Constant, Modal Damping $\xi = 0.05$	Trapezoidal Rule Using Rayleigh Damping	Exact Solution Using Constant, Modal Damping $\xi = 0.05$
u_{20} (Inch)	4.924 @ 0.580 -4.217 @ 1.200	4.939 @ 0.580 -4.217 @ 1.205	4.912 @ 0.600 -4.182 @ 1.220	4.913 @ 0.600 -4.198 @ 1.230
V_2 (Kips)	86.61 @ 0.125 -95.953 @ 0.305	84.30 @ 0.130 -95.78 @ 0.310	89.3 @ 0.130 -93.9 @ 0.305	135.1 @ 0.150 -117.1 @ 0.340
M_2 (k–in.)	115,600 @ 1.185 -136,400 @ 0.605	116,100 @1.200 -136,300 @ 0.610	107.300 @ 1.225 -126,300 @ 0.610	115,300 @1.230 -136,700 @ 0.605
M_{10} (K-in.)	78,700 @ 0.285 -64,500 @ 0.485	77,530 @ 0.300 -64,790 @ 0.485	81.,30 @ 0.280 61,210@ 0.480	80,480 @ 0.320 -59,840 @ 0.495

It is apparent that the use of Rayleigh damping for acceleration loading produces a very good approximation of the exact solution using constant modal damping. However, for displacement loading, the use of Rayleigh damping, in which the high frequencies are highly damped and some lower frequencies are under damped, produces larger errors. A plot of the shears at the second level using the different methods is shown in Figure 22.7. It is not clear if the errors are caused by the Rayleigh damping approximation or by the use of a large time step.

It is apparent that errors associated with the unrealistic damping of the high frequencies excited by displacement loading are present in all step-by-step integration methods. It is a property of the mathematical model and is not associated with the method of solution of the equilibrium equations.
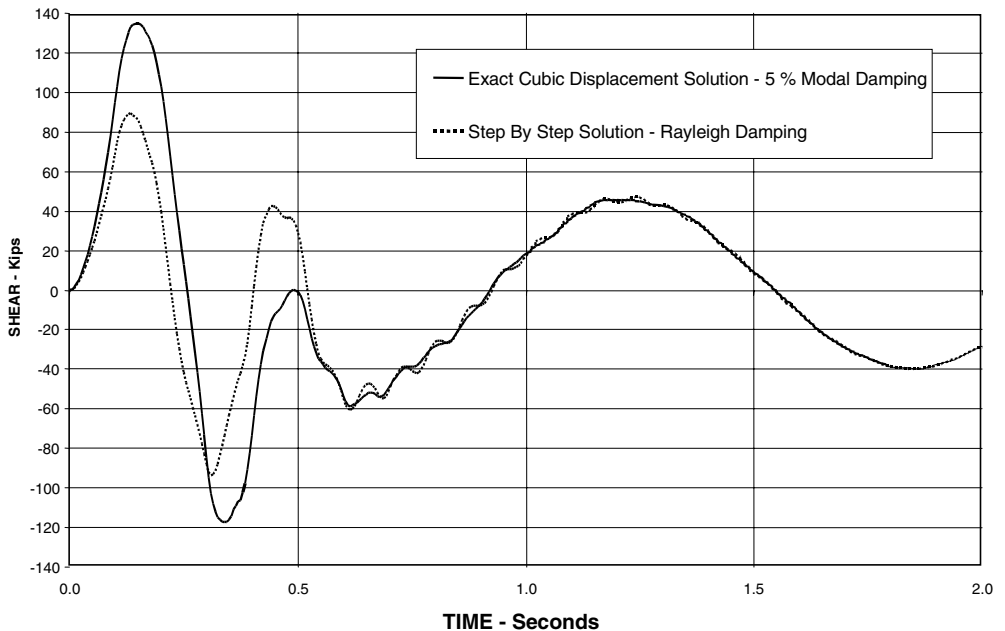
*Figure 22.7 Comparison of Step-By-Step Solution Using the Trapezoidal Rule
and Rayleigh Damping with Exact Solution
(0.005 second time-step and 5% damping)*

The effective damping in the high frequencies, using displacement loading and Rayleigh damping, can be so large that the use of large numerical integration time steps produces almost the same results as using small time steps. However,

the accuracy of the results cannot be justified using this argument, because the form of the Rayleigh damping used in the computer model is physically impossible within a real structure. In addition, the use of a numerical integration method that produces numerical energy dissipation in the higher modes may produce unrealistic result when compared to an exact solution using displacement loading.

22.8 SUMMARY

Several new sources of numerical errors associated with the direct application of earthquake displacement loading have been identified. Those problems are summarized as follows:

1. Displacement loading is fundamentally different from acceleration loading because a larger number of modes are excited. Hence, a very small time step is required to define the displacement record and to integrate the dynamic equilibrium equations. A large time step, such as 0.01 second, can cause significant unpredictable errors.

2. The effective damping associated with displacement loading is larger than that for acceleration loading. The use of mass proportional damping, inherent in Rayleigh and classical modal damping, cannot be physically justified.

3. Small errors in maximum displacements do not guarantee small errors in member forces.

4. The 90 percent mass participation rule, which is used to estimate errors for acceleration loading, does not apply to displacement loading. A larger number of modes are required to accurately predict member forces for absolute displacement loading.

5. For displacement loading, mode truncation in the mode superposition method may cause large errors in the internal member forces.

The following numerical methods can be used to minimize those errors:

1. A new integration algorithm based on cubic displacements within each time step allows the use of larger time steps.

2. To obtain accurate results, the static load-participation factors must be very close to 100 percent.

3. The use of LDR vectors will significantly reduce the number of vectors required to produce accurate results for displacement loading.

4. The example problem illustrates that the errors can be significant if displacement loading is applied based on the same rules used for acceleration loading. However, additional studies on different types of structures, such as bridge towers, must be conducted. Also, more research is required to eliminate or justify the differences in results produced by the relative and absolute displacement formulations for non-zero modal damping.

Finally, the state-of-the-art use of classical modal damping and Rayleigh damping contains mass proportional damping that is physically impossible. Therefore, the development of a new mathematical energy dissipation model is required if modern computer programs are to be used to accurately simulate the true dynamic behavior of real structures subjected to displacement loading.

APPENDIX A

VECTOR NOTATION

*Vector Notation is Based on
The Physical Laws of Statics*

A.1   INTRODUCTION

To define member properties, skew boundary conditions and other information required to specify the input data for three-dimensional structures, the computer program user must have a working knowledge of vector notation. Because forces and moments are vectors in three-dimensional space, this appendix reviews, from a physical standpoint, vector notation and vector operations that are required to use a structural analysis program intelligently. Any force acting in three-dimensional space has a magnitude and direction or line of action, as shown in Figure A.1.
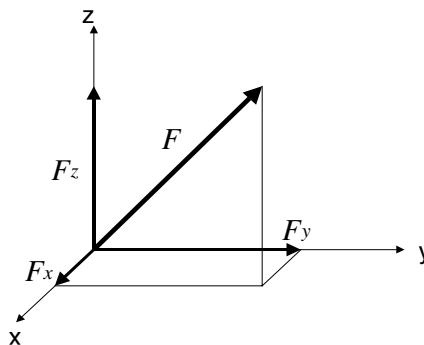
Figure A.1 Typical Force Vector

The point of application of the force on the structure is on this line of action. Also, a force can be expressed in terms of its components in the global x, y and z axes. In vector notation, the force is written in terms of its components as:

$$F = F_x\,\hat{x} + F_y\,\hat{y} + F_y\,\hat{z} \tag{A.1}$$

where $\hat{x}, \hat{y}$ and $\hat{z}$ are by definition the unit vectors along the x, y, and z axes respectively. Note that a **vector equation always has three components**.

It is apparent that the absolute value of the magnitude of the force vector is given by:

$$|F| = \sqrt{F_x^2 + F_y^2 + F_z^2} \tag{A.2}$$

We can now define the following dimensionless ratios:

$$V_{xf} = \frac{F_x}{|F|}, \quad V_{yf} = \frac{F_y}{|F|}, \quad \text{and} \quad V_{zf} = \frac{F_z}{|F|} \tag{A.3}$$

In vector notation, these ratios are termed the direction cosines of the vector. Hence, the unit vector in the direction of the vector is:

$$\hat{f} = V_{xf}\,\hat{x} + V_{yf}\,\hat{y} + V_{zf}\,\hat{z} \tag{A.4}$$

Therefore, the direction cosines are not independent because:

$$1 = V_{xf}\,\hat{x} + V_{yf}\,\hat{y} + V_{zf}\,\hat{z} \tag{A.5}$$

A.2   VECTOR CROSS PRODUCT

The vector cross product can be defined using traditional, abstract mathematical notation. Or, the physical laws of statics can be applied to develop and explain the use of the cross product operation in defining the geometry of three-dimensional structural systems. The definition of a positive moment vector is defined by the right-hand rule, illustrated in Figure A.2.
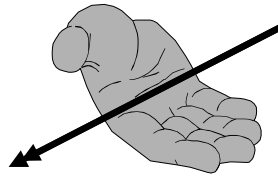
Figure A.2 Definition of Positive Moment (rotation)
using the Right Hand Rule

Figure A.3 shows two vectors, a distance vector ***d*** and a force vector ***F***. Point 2
is on the line of action of the force vector ***F***.
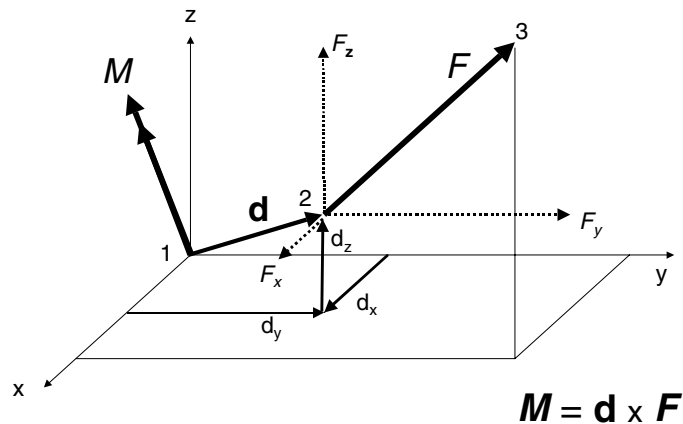
Figure A.3 Cross Product of Two Vectors

To calculate the moment acting at point 1, one can use the three components of
the force vectors and the three components of the distance vector to calculate the
three components of the resulting moment. Or:

$$M_x = d_y F_z - d_z F_y, \quad M_y = d_z F_x - d_x F_z \quad \text{and} \quad M_z = d_x F_y - d_y F_x \qquad \text{(A.6)}$$

The resulting moment at point 1 is written in vector notation as:

$$M = M_x \hat{x} + M_y \hat{y} + M_z \hat{z} \qquad \text{(A.7)}$$

Therefore, this physical procedure defined as the cross, or vector, product of two vectors is defined as:

$$M = d \times F \tag{A.8}$$

Because all of these calculations are performed within computer programs, it is not necessary to remember this cross product equation. The important physical fact to remember is that the resultant rotational vector is normal to the plane defined by points 1, 2 and 3.

A.3   VECTORS TO DEFINE A LOCAL REFERENCE SYSTEM

A local 1, 2, 3 reference system can be defined by the specification of three points in space, as shown in Figure A.4.
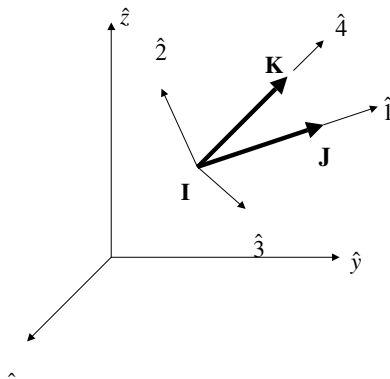
Figure A.4 Definition of Local Reference System from Points I, J and K

Unit vectors $\hat{1}$ and $\hat{4}$ can be defined from the vectors I to J and I to K respectively. Now, if we form the cross product vectors 1 with 4, we can define a vector $\hat{3}$ normal to the plane I-J-K. The unit vector $\hat{2}$ is now defined by the cross product of the vectors $\hat{3}$ with $\hat{1}$. The resulting local 1,2,3 right-hand reference system is related to the global x,y,z system by the following matrix equations of direction cosines:

$$\begin{bmatrix} \hat{1} \\ \hat{2} \\ \hat{3} \end{bmatrix} = \begin{bmatrix} V_{1x} & V_{1y} & V_{1z} \\ V_{2x} & V_{2y} & V_{2z} \\ V_{3x} & V_{3y} & V_{3z} \end{bmatrix} \begin{bmatrix} \hat{x} \\ \hat{y} \\ \hat{z} \end{bmatrix} \qquad (A.9)$$

The 3 by 3 **V** matrix can now be used to transform displacements, rotations, forces and moments from one reference system to another reference system. For example, the displacement transformation equations are:

$$\begin{bmatrix} u_1 \\ u_2 \\ u_3 \end{bmatrix} = \mathbf{V} \begin{bmatrix} u_x \\ u_y \\ u_z \end{bmatrix} \quad \text{and} \quad \begin{bmatrix} u_x \\ u_y \\ u_x \end{bmatrix} = \mathbf{V}^\mathsf{T} \begin{bmatrix} u_1 \\ u_2 \\ u_2 \end{bmatrix} \qquad (A.10a \text{ and } A.10b)$$

This allows element stiffness and load matrices to be formed in a local element reference system and then transformed to a global reference system to form the global equilibrium equations.

A.4   FORTRAN SUBROUTINES FOR VECTOR OPERATIONS

Within a structural analysis program, only two vector operations are required. To define a vector, the coordinates of the starting point "I" and ending point "J" must be given. The FORTRAN subroutine given in Table A.1 illustrates how the three direction cosines are calculated and how the length of the vector is calculated. The results are stored in the "V" array.

Table A.1 FORTRAN Subroutine to Define Vector

```
      SUBROUTINE VECTOR (V,XI,YI,ZI,XJ,YJ,ZJ)
      IMPLICIT REAL*8 (A-H,O-Z)
      DIMENSION V(4)
C---- GIVEN TWO POINTS DEFINE VECTOR IN I-J DIRECTION -
      X = XJ - XI                       ! X PROJECTION
      Y = YJ - YI                       ! Y PROJECTION
      Z = ZJ - ZI                       ! Z PROJECTION
      V(4) = DSQRT( X*X + Y*Y + Z*Z )  ! VECTOR LENGTH
C---- ERROR CHECK ------------------------------------
      IF (V(4).LE.0.0D0) THEN
      WRITE (*,*) '*ERROR* ZERO LENGTH MEMBER OR VECTOR'
      PAUSE       'CORRECT ERROR AND RERUN PROGRAM'
      STOP ' '
      ENDIF
C---- COMPUTER DIRECTION COSINES ----------------------
      V(3) = Z/V(4)
      V(2) = Y/V(4)
      V(1) = X/V(4)
C
      RETURN
      END
```

The subroutine given in Table A.2 produces the cross product vector "C," given vectors "A" and "B."

Table A.2 FORTRAN Subroutine to Perform Vector Cross Product

```
      SUBROUTINE CROSS(A,B,C)
      IMPLICIT REAL*8 (A-H,O-Z)
      DIMENSION A(4),B(4),C(4)
C---- CROSS PRODUCT OF VECTORS "A" x "B" = VECTOR "C"-
      X = A(2)*B(3) - A(3)*B(2)        ! X COMPONENT
      Y = A(3)*B(1) - A(1)*B(3)        ! Y COMPONENT
      Z = A(1)*B(2) - A(2)*B(1)        ! Z COMPONENT
      C(4) = DSQRT( X*X + Y*Y + Z*Z) ! VECTOR LENGTH
C---- CHECK FOR ERROR --------------------------------
      IF(C(4).LE.0.0D0) THEN
      WRITE (*,*) '*ERROR* VECTORS ARE IN SAME DIRECTION'
      PAUSE 'CORRECT ERROR AND RERUN PROGRAM'
      STOP ' '
      ENDIF
C---- COMPUTE DIRECTION COSINES ----------------------
      C(3) = Z/C(4)
      C(2) = Y/C(4)
      C(1) = X/C(4)
C
      RETURN
      END
```

APPENDIX B

MATRIX NOTATION

The Definition of Matrix Notation is the
Definition of Matrix Multiplication

B.1   INTRODUCTION

The use of matrix notations is not necessary to solve problems in the static and dynamic analysis of complex structural systems. However, it does allow engineers to write the fundamental equation of mechanics in a compact form. In addition, it produces equations in a form that can be easily programmed for digital computers. Also, it allows the properties of the structure to be separated from the loading. Therefore, dynamic analysis of structures is a simple extension of static analysis.

To understand and use matrix notation, it is not necessary to remember mathematical laws and theorems. Every term in a matrix has a physical meaning, such as *force per unit of displacement*. Many structural analysis textbooks present the traditional techniques of structural analysis without the use of matrix notation; then, near the end of the book *MATRIX METHODS* are presented as a different method of structural analysis. The fundamental equations of equilibrium, compatibility and material properties, when written using matrix notation, are not different from those used in traditional structural analysis. Therefore, in my opinion, the terminology *matrix methods of structural analysis* should never be used.

B.2   DEFINITION OF MATRIX NOTATION

To clearly illustrate the application of matrix notation, let us consider the joint equilibrium of the simple truss structure shown in Figure B.1.
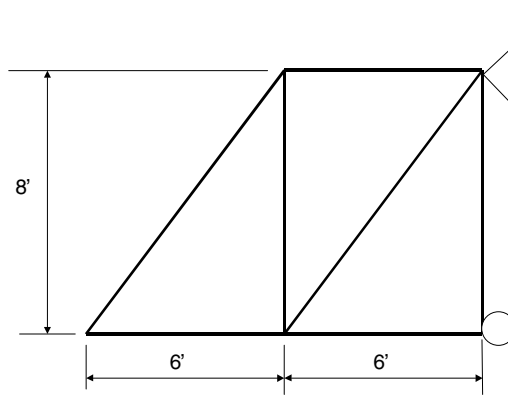
Figure B.1 Simple Truss Structure

Positive external node loads and node displacements, shown in Figure B.2, are in the direction of the x and y reference axes. Axial forces f_i and deformations d_i are positive if tension is produced in the member.
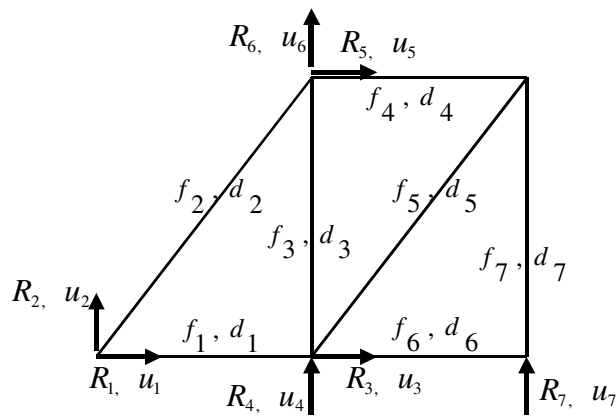
Figure B.2 Definition of Positive Joint Forces and Node Displacements

For the truss structure shown in Figure B.1, the joint equilibrium equations for the sign convention shown are:

$$R_1 = -f_1 - 0.6f_2 \tag{B.1a}$$

$$R_2 = -0.8f_2 \tag{B.1b}$$

$$R_3 = f_1 - 0.6f_5 - f_6 \tag{B.1c}$$

$$R_4 = -f_3 - 0.8f_5 \tag{B.1d}$$

$$R_5 = 0.6f_2 - f_4 \tag{B.1e}$$

$$R_6 = 0.8f_2 + f_3 \tag{B1.f}$$

$$R_7 = -f_7 \tag{B.1g}$$

We can write these seven equilibrium equations in matrix form where each row is one joint equilibrium equation. The resulting matrix equation is

$$
\begin{bmatrix} R_1 \\ R_2 \\ R_3 \\ R_4 \\ R_5 \\ R_6 \\ R_7 \end{bmatrix}
=
\begin{bmatrix}
-1.0 & -0.6 & 0 & 0 & 0 & 0 & 0 \\
0 & -0.8 & 0 & 0 & -0.6 & 1.0 & 0 \\
1.0 & 0 & 0 & 0 & 0 & 0 & 0 \\
0 & 0 & -1.0 & 0 & -0.8 & 0 & 0 \\
0 & 0.6 & 0 & 1.0 & 0 & 0 & 0 \\
0 & 0.8 & 1.0 & 0 & 0 & 0 & 0 \\
0 & 0 & 0 & 0 & 0 & 0 & -1.0
\end{bmatrix}
\begin{bmatrix} f_1 \\ f_2 \\ f_3 \\ f_4 \\ f_5 \\ f_6 \\ f_7 \end{bmatrix}
\tag{B.2}
$$

Or, symbolically

$$\mathbf{R} = \mathbf{A}\mathbf{f} \tag{B.3}$$

Now, if two load conditions exist, the 14 equilibrium equations can be wrtten as one matrix equation in the following form:

$$
\begin{bmatrix}
R_{11} & R_{12} \\
R_{21} & R_{22} \\
R_{31} & R_{32} \\
R_{41} & R_{42} \\
R_{51} & R_{52} \\
R_{61} & R_{62} \\
R_{71} & R_{72}
\end{bmatrix}
=
\begin{bmatrix}
-1.0 & -0.6 & 0 & 0 & 0 & 0 & 0 \\
0 & -0.8 & 0 & 0 & -0.6 & 1.0 & 0 \\
1.0 & 0 & 0 & 0 & 0 & 0 & 0 \\
0 & 0 & -1.0 & 0 & -0.8 & 0 & 0 \\
0 & 0.6 & 0 & 1.0 & 0 & 0 & 0 \\
0 & 0.8 & 1.0 & 0 & 0 & 0 & 0 \\
0 & 0 & 0 & 0 & 0 & 0 & -1.0
\end{bmatrix}
\begin{bmatrix}
f_{11} & f_{12} \\
f_{21} & f_{22} \\
f_{31} & f_{32} \\
f_{41} & f_{42} \\
f_{51} & f_{52} \\
f_{61} & f_{62} \\
f_{71} & f_{72}
\end{bmatrix}
\quad \text{(B.4)}
$$

It is evident that one can extract the 14 equilibrium equations from the one matrix equation. Also, it is apparent that the definition of matrix notation can be written as:

$$
f_{il} = \sum_{k=1,7} A_{ik} R_{kl}
\tag{B.5}
$$

Equation (B.5) is also the definition of matrix multiplication. Note that we have defined that each load is factored to the right and stored as a column in the load matrix. Therefore, there is no need to state the matrix analysis theorem that:

$$
\mathbf{Af} \neq \mathbf{fA}
\tag{B.6}
$$

Interchanging the order of matrix multiplication indicates that one does not understand the basic definition of matrix notation.

B.3 MATRIX TRANSPOSE AND SCALAR MULTIPLICATION

Referring to Figure B.1, the energy, or work, supplied to the structure is given by:

$$
W = \frac{1}{2} \sum_{i=1,7} R_i u_i
\tag{B.7}
$$

We have defined:

$$\mathbf{R} = \begin{bmatrix} R_1 \\ R_2 \\ R_3 \\ R_4 \\ R_5 \\ R_6 \\ R_7 \end{bmatrix} \quad \text{and} \quad \mathbf{u} = \begin{bmatrix} u_1 \\ u_2 \\ u_3 \\ u_4 \\ u_5 \\ u_6 \\ u_7 \end{bmatrix} \qquad \text{(B.8a and B.8b)}$$

The definition of the transpose of a matrix is "the columns of the original matrix are stored as rows in the transposed matrix." Therefore:

$$\mathbf{R}^\mathsf{T} = \begin{bmatrix} R_1 & R_2 & R_3 & R_4 & R_5 & R_6 & R_7 \end{bmatrix} \qquad \text{(B.9a)}$$

$$\mathbf{u}^\mathsf{T} = \begin{bmatrix} u_1 & u_2 & u_3 & u_4 & u_5 & u_6 & u_7 \end{bmatrix} \qquad \text{(B.9b)}$$

It is now possible to express the external work, Equation (B.7), as the following matrix equation:

$$W = \frac{1}{2}\mathbf{R}^\mathsf{T}\mathbf{u} \text{ or } W = \frac{1}{2}\mathbf{u}^\mathsf{T}\mathbf{R} \qquad \text{(B.10)}$$

Also, the internal strain energy Ω, stored in the truss members, is defined by the following:

$$\Omega = \frac{1}{2}\mathbf{f}^\mathsf{T}\mathbf{d} \text{ or } \Omega = \frac{1}{2}\mathbf{d}^\mathsf{T}\mathbf{f} \qquad \text{(B.11)}$$

Therefore, the purpose of the transpose notation is to use a matrix that has been defined column-wise as a matrix that has been defined row-wise. The major use of the notation, in structural analysis, is to define work and energy. Note that the scalar 1/2 has been factored out of the equations and is applied to each term in the transposed matrix.

From the above example, it is apparent that if:

$$\mathbf{A} = \mathbf{BC} \text{ then } \mathbf{A}^\mathsf{T} = \mathbf{C}^\mathsf{T}\mathbf{B}^\mathsf{T} \qquad \text{(B.12)}$$

It important to point out that within a computer program, it is not necessary to create a new transformed matrix within the computer storage. One can use the data from the original matrix by interchanging the subscripts.

B.4   DEFINITION OF A NUMERICAL OPERATION

One of the most significant advantages of using a digital computer is that one can predict the time that is required to perform various numerical operations. It requires computer time to move and store numbers and perform floating-point arithmetic, such as addition and multiplication. Within a structural analysis program, a typically arithmetic statement is of the following form:

$$A = B + C \times D \tag{B.13}$$

The execution of this statement involves removing three numbers from storage, one multiplication, one addition, and then moving the results back in high-speed storage. Rather than obtaining the time required for each phase of the execution of the statement, it has been found to be convenient and accurate to simply define the evaluation of this statement as *one numerical operation*. In general, the number of operations per second a computer can perform is directly proportional to the clock-speed of the computer. For example, for a 150 MHz Pentium, using Microsoft Power FORTRAN, it is possible to perform approximately *6,000,000 numerical operations each second*.

B.5   PROGRAMMING MATRIX MULTIPLICATION

Programming matrix operations is very simple. For example, the FORTRAN-90 statements required to multiply the N-by-M-matrix-**A** by the M-by-L-matrix-**B** to form the N-by-L-matrix-**C** are given by:

```
     C = 0.0
     DO   I=1,N
      DO   J=1,L
        DO K=1,M
       C(I,J) =  C(I,J) + A(I,K)*B(K,L)
        ENDDO      ! end K do loop
       ENDDO        ! end J  do loop
```

ENDDO   ! end I do loop

Note that the number of times the basic arithmetic statement is executed is the product of the limits of the DO LOOPS. Therefore, the number of numerical operations required to multiply two matrices is:

$$Nop = NML, \text{ or, if } M = L = N, \text{ then } Nop = N^3 \tag{B.14}$$

It will later be shown that this is a large number of numerical operations compared to the solution of a set of N linear equations.

B.6   ORDER OF MATRIX MULTIPLICATION

Consider the case of a statically determinate structure where the joint displacements can be calculated using the following matrix equation:

$$\mathbf{u} = \mathbf{A}^T \mathbf{C} \mathbf{A} \mathbf{R} = [[\mathbf{A}^T \mathbf{C}]\mathbf{A}]\mathbf{R} = \mathbf{A}^T [\mathbf{C}[\mathbf{A}\mathbf{R}]] \tag{B.15}$$

If A and B are N by N matrices and R is an N by 1 matrix, the order in which the matrix multiplication is conducted is very important. If the evaluation is conducted from left to right, the total number of numerical operations is $2N^3 + N^2$. On the other hand, if the matrix equation is evaluated from right to left, the total number of numerical operations is $3N^2$. This is very important for large matrices such as those encountered in the dynamic response of structural systems.

B.7   SUMMARY

Matrix notation, as used in structural analysis, is very logical and simple. There is no need to remember abstract mathematical theorems to use the notation. The mathematical properties of matrices are of academic interest; however, it is far more important to understand the physical significance of each term within every matrix equation used in structural analysis.

There is no need to create a transpose of a matrix within a computer program. Because no new information is created, it is only necessary to interchange the

subscripts to access the information in transposed form. There are a large number of computational techniques that exploit symmetry, sparseness and compact storage and eliminate the direct storage of large rectangular matrices.

Different methods of structural analysis can be evaluated by comparing the number of numerical operations. However, very few modern research papers on structural analysis use this approach. There is a tendency of many researchers to make outrageous claims of numerical efficiency without an accurate scientific evaluation of computer effort required by their proposed *new* method.

APPENDIX C

SOLUTION OR INVERSION OF LINEAR EQUATIONS

*The Computer Time Required to Solve a
Symmetric Set of "N " Linear Equations
Is Approximately 1/6th the Computer Time
Required to Multiply Two "N By N" Matrices*

C.1 INTRODUCTION

The solution of a large set of equations by hand calculations is a tenuous and time-consuming process. Therefore, before 1960 the majority of structural analysis techniques were based on *approximations and computational tricks*. Many of those methods, such as moment distribution, allowed the engineer to gain physical insight into the behavior of structures and were forgiving with respect to human computational errors. It was very common for an experienced structural engineering *human-computer* to predict the answer to within two significant figures before performing any calculations. At the present time, however, with the assistance of an inexpensive personal computer and efficient computational methods, the structural engineer can solve over 1,000 equations in a few seconds.

The fundamental method currently used to directly solve sets of equilibrium equations is the Gauss elimination that was first used in 1826. Gauss also worked with approximate approaches that resulted in the Gauss-Seidel iterative method in 1860. Most of the methods presented in the last 150 years, such as

Cholesky (1916) and Grout (1938), are numerically equivalent to the Gauss elimination method; however, they were easier to use for hand calculations. A modified form of the Gauss elimination method can also be used for matrix inversion.

Cramer's rule and the theory of determinates, which are presented by many mathematicians as fundamental to matrix analysis, are abstract theorems and are not necessary to understand matrix notation. It is easily shown that the use of Cramer's rule to solve equations is very numerically inefficient (approximately $N!$ numerical operations) and should never be used to solve practical problems in all fields of engineering.

The author's "hobby" has been the writing of numerically efficient computer programs for the solution of equations. This "pastime" has resulted in the publication of several papers on this topic[1, 2, 3, 4]. Most of this development is summarized in this appendix; therefore, it is not necessary to read the references to fully understand the numerical algorithms presented in this section.

C.2   NUMERICAL EXAMPLE

To illustrate the detailed numerical operations required to solve a set of linear equations by the Gauss elimination method, consider the solution of the following three equations:

$$5.0\,x_1 + 4.0\,x_2 + 3.0\,x_3 = 2.0 \qquad\qquad (C.1)$$

$$4.0\,x_1 + 7.0\,x_2 + 4.0\,x_3 = -1.0 \qquad\qquad (C.2)$$

$$3.0\,x_1 + 4.0\,x_2 + 4.0\,x_3 = 3.0 \qquad\qquad (C.3)$$

First, solve Equation (C.1) for x_1:

$$x_1 = 0.40 - 0.80\,x_2 - 0.60\,x_3 \qquad\qquad (C.4)$$

Second, substitute Equation (C.4) into Equations (C.2) and (C.3) to eliminate x_1 and the following two equations are obtained:

$$3.80\,x_2 + 1.60\,x_3 = -2.60 \qquad\qquad (C.5)$$

$$1.60x_2 + 2.20x_3 = 1.80 \tag{C.6}$$

Third, solve Equation (C.5) for x_2:

$$x_2 = -0.68421 - 0.42105x_3 \tag{C.7}$$

Fourth, substitute Equation (C.7) into Equation (C.6) to eliminate x_2, and the following equation is obtained:

$$x_3 = 1.8865 \tag{C.8a}$$

Back-substitute Equation (C.8a) into Equations (C.7) to obtain:

$$x_2 = -1.4829 \tag{C.8b}$$

Back-substitute Equations (C.8a) and (C8.b) into (C.4) to obtain:

$$x_1 = 0.44828 \tag{C.8c}$$

Therefore, matrix notation is not necessary to solve a set of linear equations. However, the Gauss elimination algorithm can be summarized in a general subscript notation that can be programmed for the computer for an arbitrary number of equations.

It is important to point out that the back-substitution Equations (C.4), (C.7) and (C.8) can be written as the following matrix equation:

$$\begin{bmatrix} 1.00 & 0.80 & 0.60000 \\ 0 & 1.00 & 0.42105 \\ 0 & 0 & 1.00000 \end{bmatrix} \begin{bmatrix} x_1 \\ x_2 \\ x_3 \end{bmatrix} = \begin{bmatrix} 0.40000 \\ -0.68421 \\ 1.8865 \end{bmatrix} = \mathbf{L}^T \mathbf{y} \tag{C.9}$$

It will be later shown that Equation (C.9) is identical to the equation used in the matrix factorization solution method.

C.3   THE GAUSS ELIMINATION ALGORITHM

To develop a computer program for the solution of equations, it is first necessary to uniquely define the numerical procedure, *or algorithm*, by a finite number of

clearly defined steps. For Gauss elimination, the initial set of N equations can be written as:

$$\sum_{j=1}^{N} a_{nj}x_j = b_n \qquad n = 1......N \tag{C.10}$$

Starting with the first equation, $n = 1$, we can solve for x_n by dividing all terms in equation n by a_{nn}. Or:

$$x_n = \frac{b_n}{a_{nn}} - \sum_{j=n+1}^{N} \frac{a_{nj}}{a_{nn}} x_j = \bar{b}_n - \sum_{j=n+1}^{N} \bar{a}_{nj} x_j \tag{C.11}$$

Substitution of Equation (C.11) into a typical remaining equation i yields:

$$\sum_{j=n+1}^{N} (a_{ij} - a_{in}\bar{a}_{nj})x_j = b_i - \bar{a}_{nj}b_n \text{ or, } \sum_{j=n+1}^{N} \bar{a}_{ij} x_j = \bar{b}_i \quad i = n+1...Neq \tag{C.12}$$

This simple Gauss elimination algorithm is summarized in a FORTRAN subroutine shown in Table C.1. Note that within a computer subroutine, the modified terms $\bar{a}_{ij}$ and $\bar{b}_i$ can be stored in the same locations as the original terms a_{ij} and b_i. Therefore, after Equations (C.11) and (C.12) have been applied N times, the unknown x_N is evaluated and stored in the same location as b_N. All other unknowns are evaluated using the back-substitution Equation (C.11). The FORTRAN subroutine allows for an arbitrary number of load vectors. Therefore, for large systems, additional load vectors do not increase the number of numerical operations significantly.

An examination of the subroutine clearly indicates the approximate number of numerical operations for L load conditions is given by :

$$Nop = \frac{1}{3}N^3 + NL \tag{C.13}$$

Note that the FORTRAN program statements very closely resemble the equations given by the Gauss elimination algorithm. As one notes, the major restriction on this subroutine is that it cannot solve systems that have zero terms on the diagonal of the matrix. However, it can be proven that non-singular stiffness and flexibility matrices will not have zero terms on the diagonal if the displacement u_n and associated force R_n have the same sign convention.

Table C.1 FORTRAN Subroutine to Solve Equations by Gauss Elimination

```
      SUBROUTINE GAUSSEL(A,B,NEQ,LL)
      IMPLICIT REAL*8 (A-H,O-Z)
C---- POSITIVE DEFINITE EQUATION SOLVER ---
      DIMENSION A(NEQ,NEQ),B(NEQ,LL)
C---- FORWARD REDUCTION  -----------------
      DO 500 N=1,NEQ
C---- CHECK FOR POSITIVE-DEFINITE MATRIX -
      IF (A(N,N).LE.0.0D0) THEN
      WRITE (*,*) 'MATRIX NOT POSSITIVE DEFINITE'
      STOP
      ENDIF
C---- DIVIDE B(N,L) BY A(N,N) ------------------------
      DO 100 L=1,LL
  100 B(N,L) = B(N,L)/A(N,N)
C---- DIVIDE A(N,J) BY A(N,N) ------------------------
      IF (N.EQ.NEQ) GO TO 500 ! CHECK FOR LAST EQUATION
      DO 200 J=N+1,NEQ
  200 A(N,J) = A(N,J)/A(N,N)
C---- MODIFY REMAINING EQUATIONS ---------------------
      DO 500 I=N+1,NEQ
      DO 300 J=N+1,NEQ
  300 A(I,J) = A(I,J) - A(I,N)*A(N,J)
      DO 400 L=1,LL
  400 B(I,N) = B(I,L) - A(I,N)*B(N,L)
C
  500 CONTINUE                   ! ELIMINATE NEXT UNKNOWN
C---- BACK-SUBSTITUTIONS ----------------------------
  600 N = N - 1
      IF (N.EQ.0) RETURN
      DO 700 L=1,LL
      DO 700 J=N+1,NEQ
  700 B(N,L) = B(N,L) - A(N,J)*B(N,L)
      GO TO 600
      END
```

Therefore, the subroutine as presented can be used to solve many small structural systems.

C.4   SOLUTION OF A GENERAL SET OF LINEAR EQUATIONS

It is very easy to modify the subroutine presented in Table C.1 to solve any non-singular sets of linear equations that have zero terms on the diagonal of the **A** matrix during the elimination process. The same Gauss elimination algorithm is

used to solve the general set of equations with a very minor modification. The FORTRAN subroutine for this general Gauss elimination algorithm is given in Table C.2.

Before eliminating the next unknown, it is only necessary to search for the largest term that exists in the remaining equations. The largest term is then moved to the a_{nn} position by the interchange of the order of the equations (row interchange) and the interchange of the order of the unknowns (column interchange). The column interchange must be recorded to recover the unknowns in their original order.

If after r equations have been eliminated and all the remaining terms in the $\mathbf{A}$ matrix are zero (or near zero compared to their initial values), the matrix is singular and the equations cannot be solved. For this case, the matrix is said to have a rank of r. If the set of equations represents force-equilibrium, it simply means that the stiffness matrix has $N - r$ unstable modes or zero energy modes. This is an excellent physical illustration of a ***rank deficient matrix***.

C.5   ALTERNATIVE TO PIVOTING

An alternative method to pivoting can be used to solve a non-positive definite set of equations. Any set of equations can be made symmetrical and positive-definite by the multiplication of both sides of the equation by the transpose of the nonsymmetrical matrix. Or, Equation (C.10) can be written as

$$\overline{\mathbf{A}}x = \overline{\mathbf{B}} \tag{C.14}$$

where, $\overline{\mathbf{A}} = \mathbf{A}^\mathsf{T}\mathbf{A}$ is symmetric; and, the effective load is $\overline{\mathbf{B}} = \mathbf{A}^\mathsf{T}\mathbf{B}$. The additional numerical effort involved in the matrix multiplication is recovered by the reduction in numerical effort required to solve a symmetrical set of equations. In addition, the interchange of rows and columns, or pivoting, is eliminated.

Table C.2 FORTRAN Subroutine for Solution of a General Set of Equations

```fortran
      SUBROUTINE SOLVE(A,B,IEQ,NEQ,NLV)
C---- SOLUTION OF GENERAL SET OF LINEAR
EQUATIONS
C     WHERE
C     A = NEQ x NEQ NON-SYMMETRIX, NON-POSITIVE
C         DEFINITE MATRIX
C     B = NEQ x NLV LOAD MATRIX TO BE REPLACED
C         BY SOLUTION
C     IEQ = TEMPORARY STORAGE ARRAY OF NEQ
C           INTERGERS
C-----------------------------------------------
      REAL*8     A(NEQ,NEQ),B(NEQ,NLV),D,BIG
      INTEGER*4  IEQ(NEQ),NEQ,NLV,II,JJ,I,J,L,N
C---- SET INITIAL UNKNOWN NUMBERS -------------
      DO 100 N=1,NEQ
 100  IEQ(N) = N
C---- ELIMINATE UNKNOWNS N=1,2....NEQ  --------
      DO 1000 N=1,NEQ
C---- (1) LOCATE LARGEST TERM REMAINING -------
      IF (N.NE.NEQ) THEN
      BIG = ABS(A(N,N))
      II = N
      JJ = N
      DO 200 I=N,NEQ
      DO 200 J=N,NEQ
       IF (ABS(A(I,J)).GT.BIG) THEN
       BIG = ABS(A(I,J))
       II = I
       JJ = J
       ENDIF
 200  CONTINUE
C---- (2) CHECK FOR SINGULAR MATRIX -----------
      IF (BIG.EQ.0.0) THEN
      WRITE (*,*) ' MATRIX IS SINGULAR '
      PAUSE 'CORRECT DATA AND RERUN'
      STOP
      ENDIF
C---- (3) INTERCHANGE COLUMNS -----------------
      DO 300 I=1,NEQ
      D = A(I,JJ)
      A(I,JJ) = A(I,N)
 300  A(I,N)  = D
C---- (4) KEEP TRACK OF EQUATION NUMBERS ------
      J =  IEQ(N)
      IEQ(N) = IEQ(JJ)
      IEQ(JJ)= J
C---- (5) INTERCHANGE ROW "N" AND ROW "II" ----
      DO 400 J=N,NEQ
      D = A(N,J)
      A(N,J) = A(II,J)
 400  A(II,J)= D
C---- (6)INTERCHANGE LOADS --------------------
      D = B(N,L)
      B(N,L) = B(II,L)
 500  B(II,L)= D
      ENDIF
C---- (6)INTERCHANGE LOADS ------------
      DO 500 L=1,NLV
      D = B(N,L)
      B(N,L) = B(II,L)
 500  B(II,L)= D
      ENDIF
C---- (7) DIVIDE LOADS BY DIAGONAL TERM
 550  DO 600 L=1,NLV
 600  B(N,L) =B(N,L)/A(N,N)
C---- (8) DIVIDE ROW BY DIAGONAL TERM -
      IF (N.NE.NEQ) THEN
      DO 700 J=N+1,NEQ
 700  A(N,J) = A(N,J)/A(N,N)
C---- (9) SUBSTITUTE IN REMAINING Eq.--
      DO 900 I=N+1,NEQ
      DO 800 J=N+1,NEQ
 800  A(I,J) = A(I,J) - A(I,N)*A(N,J)
      DO 900 L=1,NLV
 900  B(I,L) = B(I,L) - A(I,N)*B(N,L)
      ENDIFC
1000 CONTINUE
C---- BACK-SUBSTITUTION ---------------
      IF (NEQ.EQ.1) GO TO 1700
      DO 1300 N=NEQ-1,1,-1
       DO 1200 L=1,NLV
        IF (N.NE.NEQ) THEN
        DO 1100 J=N+1,NEQ
1100   B(N,L) = B(N,L) - A(N,J)*B(J,L)
        ENDIF
1200  CONTINUE
1300 CONTINUE
C---- RETURN UNKNOWNS IN ORIGINAL ORDER
      DO 1600 N=1,NEQ
       DO 1500 I=N,NEQ
        II = IEQ(I)
         IF(II.EQ.N) THEN
          DO 1400 L=1,NLV
          D = B(N,L)
          B(N,L) = B(I,L)
1400      B(I,L)= D
          IEQ(I) = IEQ(N)
          GO TO 1600 !CHECK NEXT UNKNOWN
         ENDIF
1500  CONTINUE
1600 CONTINUE
C---- RETURN TO CALLING PROGRAM -------
1700 RETURN
      END
```

```
DO 500 L=1,NLV
```

Mathematicians do not recommend this approach because it increases the "condition number" and the theoretical error. However, for small, well-conditioned systems, it has been the author's experience that this approach works very well. It also can be proven that this approach will minimize the sum of the square of the error terms.

C.6   MATRIX INVERSION

The inverse of a matrix can be obtained by setting the matrix **B** to a unit matrix, **I,** and then solving the following equation for the N by N x matrix (the inverse of **A**):

$$\mathbf{A}x = \mathbf{B} \text{ or } \mathbf{A}\mathbf{A}^{-1} = \mathbf{I} \tag{C.15}$$

The major problem with this approach is that it requires more numerical operations and computer storage than the direct application of the modified Gauss algorithm. It is only necessary to write an algorithm to interchange x_n with b_n and then apply it with $n = 1.....N$. A typical equation is:

$$\sum_{j=1}^{Neq} a_{ij} x_j = b_i \qquad i = 1......N \tag{C.16}$$

By dividing the *n th* equation by a_{nn}, it can be written as:

$$-\sum_{j=1}^{n-1} \overline{a}_{nj} x_j + \frac{b_n}{a_{nn}} - \sum_{j=n+1}^{N} \overline{a}_{nj} x_j = x_n \tag{C.17}$$

Now, x_n can be eliminated from all equations before and after equation *n*. It is then moved to the right-hand side of the equation, and b_n is moved to the left-hand side of the equation. Or:

$$\sum_{j=1}^{n-1} (a_{ij} - a_{in} \overline{a}_{nj}) x_j - \frac{a_{jn}}{a_{nn}} b_n + \sum_{j=n+1}^{N} (a_{ij} - a_{in} \overline{a}_{nj}) x_j = b_i \tag{C.18}$$

$$\text{for } i = 1..n, \ n + 1..N$$

Hence, the new set of Equations can be written, after n transformations, in matrix form as:

$$\mathbf{A}^{(n)}\mathbf{x}^{(n)} = \mathbf{b}^{(n)} \tag{C.19}$$

After N transformations:

$$\mathbf{A}^{(N)} = \mathbf{A}^{-1}, \quad \mathbf{x}^{(N)} = -\mathbf{b} \quad \text{and} \quad \mathbf{b}^{(N)} = -\mathbf{x} \tag{C.20}$$

Using this modified Gauss inversion algorithm, it can easily be shown that a closed form solution for a 2 by 2 system is

$$\begin{bmatrix} x_1 \\ x_2 \end{bmatrix} = \frac{1}{a_{11}a_{22} - a_{12}a_{21}} \begin{bmatrix} a_{22} & -a_{12} \\ -a_{21} & a_{11} \end{bmatrix} \begin{bmatrix} b_1 \\ b_2 \end{bmatrix} \tag{C.21}$$

A FORTRAN subroutine that summarizes the matrix inversion algorithm is given in Table C.3. Note that the inverse can be stored in the same locations as the original matrix and no new computer storage is required.

Table C.3 Subroutine to Invert a Matrix by Modified Gauss Elimination

```
      SUBROUTINE INVERT(A,NMAX)
      IMPLICIT REAL*8 (A-H,O-Z)
      DIMENSION A(NMAX,NMAX)
C---- MATRIX INVERSION BY MODIFIED GAUSS ELIMINATION
      DO 200 N=1,NMAX
      D = A(N,N)        ! SAVE DIAGONAL TERM
C---- DIVIDE ROW BY DIAGONAL TERM ------------------
      DO 100 J=1,NMAX
  100 A(N,J) = -A(N,J)/D
C---- MODIFY OTHER EQUATIONS ----------------------
      DO 150 I=1,NMAX
      IF(N.EQ.I) GO TO 150
       DO 140 J=1,NMAX
       IF(N.EQ.J) GO TO 140
       A(I,J) = A(I,J) + A(I,N)*A(N,J)
  140  CONTINUE
C---- MODIFY COLUMN -------------------------------
  150 A(I,N) = A(I,N)/D
C---- INVERT DIAGONAL TERM ------------------------
      A(N,N) = 1.0/D
  200 CONTINUE          ! REDUCE NEXT EQUATION
      RETURN            ! INVERSION COMPLETE
      END
```

It should be emphasized that matrix inversion is almost never required in structural analysis. The only exception is the inversion of the 6 by 6 strain-stress

matrix. Many textbooks imply that if a large number of load vectors exists, the additional numerical effort associated with matrix inversion is justifiable—not true.

An examination of the matrix inversion subroutine indicates that the approximate number of numerical operations, as previously defined, to invert an N by N matrix is approximately N^3. If there are L load vectors, the total number of numerical operations to invert the matrix and multiply by the load matrix will be:

$$n.o. = N^3 + N^2 L \tag{C.22}$$

If the set of equations is solved directly by Gauss elimination, the total number of numerical operations is:

$$n.o. = \frac{1}{3} N^3 + N^2 L \tag{C.23}$$

Therefore, matrix inversion is always inefficient compared to the direct solution of equations by Gauss elimination. In addition, if a sparse or banded matrix is inverted, a full matrix may be produced that would require a significant increase in computer storage and execution time.

C.7   PHYSICAL INTERPRETATION OF MATRIX INVERSION

To illustrate the physical interpretation of the matrix inversion algorithm, consider the force-deformation relationship for the simple beam shown in Figure C.1.
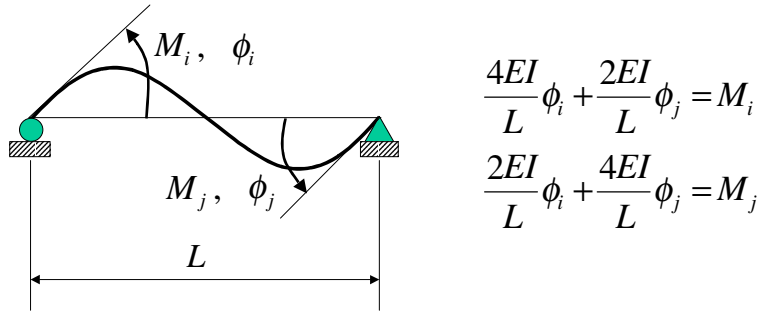
$$\frac{4EI}{L}\phi_i + \frac{2EI}{L}\phi_j = M_i$$

$$\frac{2EI}{L}\phi_i + \frac{4EI}{L}\phi_j = M_j$$

Figure C.1 Force-Deformation Behavior of Simple Supported Beam

The force-deformation equations written in matrix form are:

$$\begin{bmatrix} \dfrac{4EI}{L} & \dfrac{2EI}{L} \\ \dfrac{2EI}{L} & \dfrac{4EI}{L} \end{bmatrix} \begin{bmatrix} \phi_i \\ \phi_j \end{bmatrix} = \begin{bmatrix} M_i \\ M_j \end{bmatrix} \tag{C.24}$$

Note the first column of the stiffness matrix represents the moments developed at the ends as a result of a unit rotation at *i*. The second column of the stiffness matrix represents the moments developed at the ends as a result of a unit rotation at *j*. By applying the inversion algorithm for *n=1,* the following equation is obtained:

$$\begin{bmatrix} \dfrac{L}{4EI} & -\dfrac{1}{2} \\ \dfrac{1}{2} & \dfrac{3EI}{L} \end{bmatrix} \begin{bmatrix} M_i \\ \phi_j \end{bmatrix} = \begin{bmatrix} \phi_i \\ M_j \end{bmatrix} \tag{C.25}$$

Each term in the modified matrix has a physical meaning. The first column, with $\phi_j = 0$, a unit moment applied at *i* produces a rotation of $L/4EI$ at *i* and a moment of $1/2$ at *j*. The second column, with $M_j = 0$, a unit rotation applied at *j* produces a rotation of $-1/2$ at *i* and a moment of $3EI/L$ at *j*.

After application of the inversion algorithm for *n=2,* the following flexibility equation is obtained:

$$\frac{L}{12EI}\begin{bmatrix} 4 & -2 \\ -2 & 4 \end{bmatrix}\begin{bmatrix} M_i \\ M_j \end{bmatrix} = \begin{bmatrix} \phi_i \\ \phi_j \end{bmatrix} \tag{C.26}$$

Therefore, the abstract mathematical procedure of matrix inversions has a very physical interpretation. Each term in the matrix, after an interchange of x_n and b_n, represents a displacement or force per unit of displacement or forces. It also indicates, using the displacement method of structural analysis for the solution of joint equilibrium equations, that the diagonal term has the units of stiffness and cannot be negative or zero for a stable structural system; therefore, there is no need to pivot during the solution algorithm.

C.8   PARTIAL GAUSS ELIMINATION, STATIC CONDENSATION AND SUBSTRUCTURE ANALYSIS

In the displacement method of structural analysis the stiffness matrix times the joint displacements are equal to the external joint loads. The application of the Gauss elimination algorithm to the solution of these equilibrium equations has a very important physical interpretation. The initial terms on the diagonal of the stiffness matrix are in the units of force per unit of deformation with all other degrees of freedom in the structure fixed. The elimination of an unknown displacement is equivalent to releasing the displacement, and the loads are carried over to the other degrees of freedom in the structure. The stiffness terms at the adjacent degrees of freedom are modified to reflect that movement is allowed at the degrees of freedom eliminated. Therefore, the solutions of the equilibrium equations by applying the Gauss elimination algorithm to all degrees of freedom can be interpreted, *by a structural engineer over the age of fifty*, as one giant cycle of moment distribution in which iteration is not required.

What is of greater significance, however, is if the algorithm is stopped at any point, the remaining equations represent the stiffness matrix with respect to the degrees of freedom not eliminated. This substructure stiffness can be extracted and used as a super element in another structural model. Also, the loads associated with the eliminated displacements are carried over to the substructure joints and must be applied to the new structural model. After the displacements associated with the substructure joints have been found, the eliminated displacements can be calculated by back-substitution.

This partial Gauss elimination algorithm is also called the static condensation method. The algorithm and a FORTRAN subroutine are summarized in Table C.4. Note that the stiffness matrix is still stored in square form; however, the number of numerical operations is reduced by recognition of the symmetry of the stiffness matrix, and some of the operations on zero terms are skipped.

Table C.4 Partial Gauss Elimination Algorithm and Subroutine

```
      SUBROUTINE SUBSOL(K,R,NEQ,LEQ,LL,MOP)
      REAL*8 K(NEQ,NEQ),R(NEQ,LL),T,ZERO
C---- SUBSTRUCTURE EQUATION SOLVER - WHERE -------------------
C     K   = STIFFNESS MATRIX TO BE REDUCED
C     R   = LOAD VECTORS - REPLACED BY DISPLACEMENTS
C     NEQ = TOTAL NUMBER OF EQUATIONS
C     LEQ = NUMBER OF MASSLESS D.O.F. TO BE ELIMINATED
C     LL  = NUMBER OF LOAD VECTORS
C     MOP = 0 TRIANGULARIZATION AND COMPLETE SOLUTION
C     MOP = 1 TRIANGULARIZATION ONLY
C     MOP = 2 LOAD REDUCTION ONLY
C     MOP = 3 DISPLACEMENT RECOVERY ONLY
      DATA ZERO /0.0D0/
C-------------------------------------------------------------
      IF(MOP.EQ.3) GO TO 800   ! DISPLACEMENT RECOVERY ONLY
      IF(MOP.EQ.2) GO TO 500   ! LOAD REDUCTION ONLY
C---- TRIANGULARIZATION ---------------------------------------
      DO 400 N=1,LEQ
      IF(K(N,N).LE.ZERO) STOP ' STRUCTURE UNSTABLE '
      IF (N.EQ.NEQ) GO TO 400  ! CHECK FOR LAST EQUATION
      DO 300 J=N+1,NEQ
       IF(K(N,J).NE.ZERO) THEN ! OPERATE ONLY ON NONZERO TERMS
        T = K(N,J)/K(N,N)
        DO 200 I=J,NEQ          ! MODIFY OTHER EQUATIONS
  200   K(J,I) = K(J,I) - K(N,I)*T
        K(N,J) = T
       ENDIF
  300 CONTINUE                 ! END OF J LOOP
  400 CONTINUE                 ! END OF N LOOP
      IF(MOP.EQ.1) RETURN      ! TRIAGULARIZE  ONLY
C---- FORWARD REDUCTION OF LOAD VECTORS ---------------------
  500 DO 700 N=1,LEQ
      DO 650 L=1,LL            ! REDUCE ALL LOAD VECTORS
      IF (N.EQ.NEQ) GO TO 650
      DO 600 J=N+1,NEQ
  600 R(J,L) = R(J,L) - K(N,J)*R(N,L)
  650 R(N,L) = R(N,L)/K(N,N)
  700 CONTINUE                 ! END OF N LOOP
      IF(MOP.EQ.2) RETURN      ! RETURN TO CALLING PROGRAM
C---- RECOVERY OF DISPLACEMENTS -----------------------------
  800 DO 1000 NN=1,LEQ,1
      N = LEQ - NN + 1
      IF (N.EQ.NEQ) GO TO 1000 ! LAST EQUATION HAS BEEN SOLVED
```

```
       DO 900 L=1,LL              ! RECOVER ALL LOAD CONDITIONS
       DO 900 J=N+1,NEQ
  900  R(N,L) = R(N,L) - K(N,J)*R(J,L)
 1000 CONTINUE                    ! END OF N LOOP
      RETURN                      ! RETURN  TO CALLING PROGRAM
C-------------------------------------------------------------
      END
```

This subroutine can be used to solve a full set of equations. For this case, it is apparent that the number of numerical operations required for a solution of a complete set of equations is:

$$n.o. = \frac{1}{6}N^3 + N^2 L \tag{C.27}$$

C.9   EQUATIONS STORED IN BANDED OR PROFILE FORM

A careful examination of the Gauss elimination algorithm as applied to the global stiffness matrix indicates that new terms in the stiffness matrix are only generated below the first non-zero term in each column. Also, only the terms above the diagonal need to be stored during the solution procedure. Therefore, the symmetric stiffness matrix can be stored in banded or profile form, as indicated in Figure C.2.
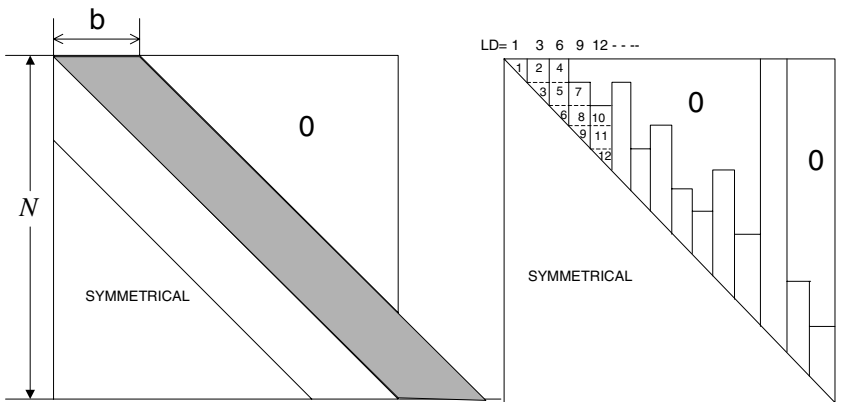
Figure C.2 Methods of Storage for Symmetric Stiffness Matrices

The banded form of storage for the stiffness matrix was used in the early years of the development of structural analysis programs. For example, SAP-IV used a blocked-banded approach. However, the banded storage method initially required that the user number the nodes in an order that would minimize the bandwidth. Later, bandwidth minimization algorithms were developed; however, a large number of zero terms still existed within the band for most structural systems.

The profile method of storage reduces the computer storage requirements and reduces the operation on zero terms. For this method, the stiffness matrix is stored in one dimensional form, from the first non-zero term in a column to the diagonal term, as shown in Figure C.2.B. In addition, a one-dimensional integer array, LD, indicates the location of the diagonal term for each column. The profile storage method is used in most modern structural analysis programs. Many different algorithms have been developed to reduce the number of numerical operations and computer storage requirements for stiffness matrices. Within the SAP90 and SAP2000 programs, three different algorithms are tried, and the one that requires the minimum computer storage is used.

From the fundamental Gauss elimination equations, it is apparent that the banded storage method requires the following number of numerical operations:

$$Nop = \frac{1}{2}Nb^2 - \frac{1}{3}b^2 + NbL \qquad (C.28)$$

Note that for a small half-bandwidth b, the number of numerical operations to solve a set of equations can be very small, compared to the formation of element matrices and the calculation of member forces and stresses.

In the case of profile storage, the number of numerical operations to solve the set of equations can be estimated from:

$$Nop = \sum_{n=1}^{N}\frac{1}{2}h_n^2 + 2h_nL \qquad (C.29)$$

The column height is given by $h_n = LD(n) - LD(n-1)$. Note that both Equations (C.28) and (C.29) reduce to Equation (C.27) for a full stiffness matrix.

C.10 LDL FACTORIZATION

In books on numerical analysis, the most common approach proposed to solve a set of symmetric equations is the **LDL**^{T} factorization, or decomposition, method. This approach involves the identical number of numerical operations, computer storage and accuracy as the Gauss elimination method; however, it lacks the physical analogy that exists with the partial Gauss elimination method. On the other hand, the factorization approach has advantages in that the operations on the stiffness and load matrices are separated. Also, error estimations can be obtained from the method, and it can be directly extended to the solution of eigenvector or Ritz vector analysis. In any case, we can use the advantages of both approaches without being forced to use one or the other.

The set of linear equations to be solved is written in the following matrix form:

$$\mathbf{Ax=b} \quad \text{or,} \quad \mathbf{LDL}^T\mathbf{x}=\mathbf{b} \quad \text{or,} \quad \mathbf{LDy}=\mathbf{b} \quad \text{where,} \quad \mathbf{L}^T\mathbf{x}=\mathbf{y} \qquad (C.30)$$

where **A** is an N by N symmetric matrix that contains a large number of zero terms. The N by M **x** displacement and **b** load matrices indicate that more than one load condition can be solved at the same time. The solution of equations is divided into the following three steps:

C10.1 Triangularization or Factorization of the A Matrix

The first step in the solution of the set of linear equations is to factor the **A** matrix into the product of a lower triangular matrix **L,** with all diagonal terms equal to 1.0, times an upper triangular matrix **U**. Or, in the case of a symmetric matrix:

$$\mathbf{A = LU = LDL}^T \qquad (C.31)$$

From the basic definition of matrix multiplication, the following equation can be written:

$$A_{ij} = \sum_{k=1}^{N} L_{ik} U_{kj} = \sum_{k=1}^{i} L_{ik} U_{kj} \qquad (C.32)$$

From Equation (C.32) a careful examination of the limits of the summation indicates that the $n\,th$ column of the **U** matrix and the $n\,th$ row of the **L** matrix

can be calculated, in the order shown in Figure C.3, from the following equations:

$$U_{in} = A_{in} - \sum_{k=1}^{i-1} L_{ik} U_{kn} \qquad\qquad (C.33)$$

$$L_{nj} = \frac{U_{nj}}{D_{jj}} \qquad\qquad (C.34)$$

From Equation (C.34) the diagonal term is:

$$D_{nn} = U_{nn} = A_{nn} - \overline{A}_{nn} \quad \text{where} \quad \overline{A}_{nn} = \sum_{k=1}^{n-1} L_{nk} U_{kn} \qquad\qquad (C.35)$$

If these equations are evaluated in the appropriate order, it is possible to store the $\mathbf{L}^{\mathrm{T}}$ matrix in the same locations as the original $\mathbf{A}$ matrix. Because the L_{nn} are always equal to one, the diagonal terms D_{nn} can be stored on the diagonal of the original matrix. Hence, it is possible to factor the matrix without additional storage requirements. Note that the lower limit of the "k" summation can be changed to the location of the first non-zero term in the column or row.
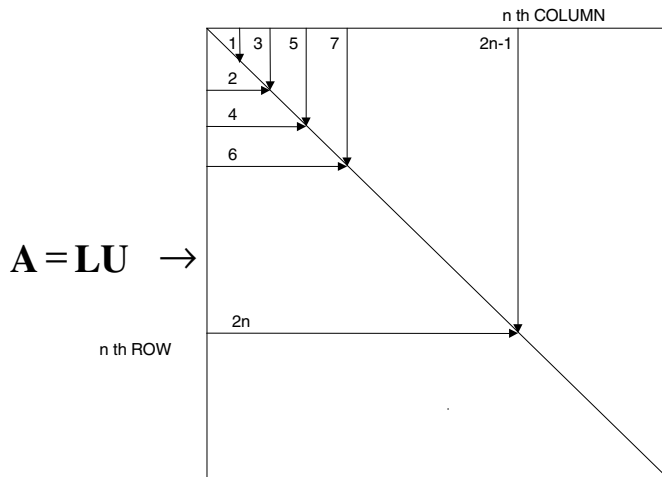
Figure C.3 Order of Calculation of the Rows and Columns in Factored Matrix

C10.2 Forward Reduction of the b Matrix

The next step in the solution of linear equations is to conduct a forward reduction of the load vector by solving the following set of equations where $\mathbf{y} = \mathbf{L}^T \mathbf{x}$:

$$\mathbf{LDy} = \mathbf{b} \qquad\qquad (C.36)$$

The solution is given by:

$$y_{nm} = \frac{b_{nm}}{D_{nn}} - \sum_{k=1}^{n-1} L_{nk}\, y_{km} \quad n = 1 \ldots\, N \qquad\qquad (C.37)$$

C10.3 Calculation of x by Backsubstitution

It is apparent that the unknowns $\mathbf{x}$ can now be calculated from:

$$x_{nm} = y_{nm} - \sum_{k=1}^{n-1} L_{kn}\, y_{km} \qquad n = N \ldots\, 1 \qquad\qquad (C.38)$$

The forward reduction and back substitution is conducted for all load vectors from m = 1 to the total number of load vectors. The fact that the factorization phase is completely separate from the solution phase allows the factorized matrix to be used for both the static and dynamic phase of the solution. FORTRAN subroutines, using profile storage, are given in reference [3].

The determinant of $\mathbf{LDL}^T$ is the product of the determinant of each matrix. Hence, the product of the diagonal terms of the $\mathbf{D}$ matrix is the determinant of the matrix. The determinant of a matrix is of little physical value. However, the mathematical properties of the sequence of diagonal terms D_{nn} are very significant.

The three equation given by Equations (C.1), (C.2) and (C.3) can be factored as:

$$\mathbf{L}^T \mathbf{DL} = \begin{bmatrix} 1.0 & 0.0 & 0.0 \\ 0.8 & 1.0 & 0.0 \\ 0.6 & .421 & 1.0 \end{bmatrix} \begin{bmatrix} 5.0 & 0 & 0 \\ 0 & 3.8 & 0 \\ 0 & 0 & 1.527 \end{bmatrix} \begin{bmatrix} 1.00 & 0.80 & 0.600 \\ 0 & 1.00 & 0.421 \\ 0 & 0 & 1.000 \end{bmatrix} \qquad (C.39)$$

Note that the $\mathbf{L}$ matrix is identical to the Gauss elimination back-substitution matrix shown in Equation (C.9). Also,

$$\mathbf{y} = \begin{bmatrix} 0.40000 \\ -0.68421 \\ 1.8865 \end{bmatrix} \quad \text{and} \quad \mathbf{x} = \begin{bmatrix} 0.44828 \\ -1.4829 \\ 1.8865 \end{bmatrix} \qquad \text{(C.40a and C.40b)}$$

Therefore, there is very little difference between the factorization approach and the Gauss elimination method.

C.11 DIAGONAL CANCELLATION AND NUMERICAL ACCURACY

The numerical accuracy of the solution of a set of linear equations can be estimated by the examination of the expression for the diagonal terms, Equation (C.35). Or, in simplified form:

$$D_{nn} = A_{nn} - \overline{A}_{nn} \qquad \text{(C.41)}$$

Where A_{nn} is the original unmodified term in the matrix and $\overline{A}_{nn}$ is the modification to the term to produce the new diagonal term D_{nn}. We know that if D_{nn} is zero, or very near zero, the matrix is singular and the solution algorithm must be terminated. Within modern computer systems, numbers have a range of approximately 10^{-300} to 10^{300}; therefore, an exact zero number is almost impossible to detect because of round off errors. What is really important, however, is the size of the original diagonal term compared to the reduced diagonal term. Therefore, the number of significant decimal *figures lost* can be estimated from:

$$f.l. = \log_{10}(A_{nn}) - \log_{10}(\overline{A}) \qquad \text{(C.42)}$$

Because all normal engineering calculations are completed within the computer using approximately 15 significant figures, a loss of over 12 figures indicates that significant errors may exist; hence, the structural engineer should be warned, and the computer model of the structure examined. This problem exists if the model lacks appropriate boundary conditions, a collapse mechanism exists or if members with large relative stiffness are used.

C.12 SUMMARY

The most general approach for the solution, inversion and condensation of equilibrium equations is Gauss elimination. In programming this method for use in structural analysis programs, sparse storage and profile minimization [4] is required to minimize the numerical effort. Diagonal cancellation must be checked to detect numerical problems.

For the solution of structural equilibrium equations, pivoting should not be used. Before eliminating a degree of freedom, the diagonal term always represents the stiffness associated with the degree of freedom. Hence, a zero or near zero diagonal term indicates that the computational model of the structure is unstable.

Given the speed of a computer system, number of operations per second, it is possible to accurately predict the computer time to solve a set of equations. Whereas the computer time required by an iterative solver, which can be faster for certain large systems, cannot be accurately predicted. In addition, the triangularized stiffness matrix can be used directly to generate mode shapes required for a dynamic analysis.

C.13 REFERENCES

1   Wilson, E. 1974. "The Static Condensation Algorithm," *International Journal for Numerical Methods in Engineering*. Vol. 8. January. pp. 198-203.

2. Wilson, E.L., K. J. Bathe and W. P. Doherty. 1974. "Direct Solution of Large Systems of Linear Equations," *Computers and Structures.* Vol. 4. January. pp. 363-372.

3. Wilson E.L., and H. H. Dovey. 1979. "Solution or Reduction of Equilibrium Equations for Large Complex Structural Systems," *Advances in Engineering Software.* Vol. 1, No. 1. pp. 19-25.

4. Hoit M. and E. L. Wilson. 1983. "An Equation Numbering Algorithm Based on a Minimum Front Criterion," *J. Computers and Structures.* Vol. 16, No. 1-4. pp. 225-239.

APPENDIX D

THE EIGENVALUE PROBLEM

Eigenvalues and Eigenvectors are Properties of the Equations that Simulate the Behavior of a Real Structure

D.1 INTRODUCTION

The classical mathematical eigenvalue problem is defined as the solution of the following equation:

$$\mathbf{A}\mathbf{v}_n = \lambda_n \mathbf{v}_n \quad n = 1......N \tag{D.1}$$

The N by N **A** matrix is real and symmetric; however, it may be singular and have zero eigenvalues λ_n. A typical eigenvector $\mathbf{v}_n$ has the following orthogonality properties:

$$\mathbf{v}_n^T \mathbf{v}_n = 1 \quad \text{and} \quad \mathbf{v}_n^T \mathbf{v}_m = 0 \quad \text{if } n \neq m, \text{ therefore}$$
$$\mathbf{v}_n^T \mathbf{A}\mathbf{v}_n = \lambda_n \text{ and} \quad \mathbf{v}_n^T \mathbf{A}\mathbf{v}_m = 0 \quad \text{if } n \neq m \tag{D.2}$$

If all eigenvectors **V** are considered, the problem can be written as:

$$\mathbf{A}\mathbf{V} = \Omega\mathbf{V}\Omega \quad \text{or} \quad \mathbf{V}^T\mathbf{A}\mathbf{V} = \Omega\Omega \tag{D.3}$$

There are many different numerical methods to solve Equation (D.3) for eigenvectors **V** and the diagonal matrix of eigenvalues Ω. In structural analysis, in general, it is only necessary to solve for the exact eigenvalues of small matrices. Therefore, the most reliable and robust will be selected because the computational time will always be relatively small. For the determination of the dynamic mode shapes and frequencies of large structural systems, subspace

iteration or Load Dependent Ritz, LDR, vectors are the most efficient approaches.

D.2   THE JACOBI METHOD

One of the oldest and most general approaches for the solution of the classical eigenvalue problem is the Jacobi method that was first presented in 1846. This is a simple iterative algorithm in which the eigenvectors are calculated from the following series of matrix multiplications:

$$\mathbf{V} = \mathbf{T}^{(0)}\mathbf{T}^{(1)}.....\mathbf{T}^{(k)}.........\mathbf{T}^{(n-1)}\mathbf{T}^{(n)} \tag{D.4}$$

The starting transformation matrix $\mathbf{T}^{(0)}$ is set to a unit matrix. The iterative orthogonal transformation matrix $\mathbf{T}^{(k)}$, with four non-zero terms in the i and j rows and columns, is of the following orthogonal form:

$$\mathbf{T}^{(k)} = \begin{bmatrix} - & - & - & - & - & - & - & - \\ - & - & - & - & - & - & - & - \\ - & - & T_{ii} & - & - & T_{ij} & - & - \\ - & - & - & - & - & - & - & - \\ - & - & - & - & - & - & - & - \\ - & - & T_{ji} & - & - & T_{jj} & - & - \\ - & - & - & - & - & - & - & - \\ - & - & - & - & - & - & - & - \end{bmatrix} \tag{D.5}$$

The four non-zero terms are functions of an unknown rotation angle θ and are defined by:

$$T_{ii} = T_{jj} = \cos\theta \quad \text{and} \quad T_{ji} = -T_{ij} = \sin\theta \tag{D.6}$$

Therefore, $\mathbf{T}^{(k)T}\mathbf{T}^{(k)} = \mathbf{I}$, which is independent of the angle θ. The typical iteration involves the following matrix operation:

$$\mathbf{A}^{(k)} = \mathbf{T}^{(k)T}\mathbf{A}^{(k-1)}\mathbf{T}^{(k)} \tag{D.7}$$

The angle is selected to force the terms *i,j* and *j,i* in the matrix $\mathbf{A}^{(k)}$ to be zero. This is satisfied if the angle is calculated from:

$$\tan 2\theta = \frac{2A_{ij}^{(k-1)}}{A_{ii}^{(k-1)} - A_{jj}^{(k-1)}} \tag{D.8}$$

The classical Jacobi eigenvalue algorithm is summarized within the computer subroutine given in Table D.1.

Table D.1 Subroutine to Solve the Symmetric Eigenvalue Problem

```
      SUBROUTINE JACOBI(A,V,NEQ,TL)
      IMPLICIT REAL*8 (A-H,O-Z)
      DIMENSION A(NEQ,NEQ),V(NEQ,NEQ)
C     EIGENVALUE SOLUTION BY JACOBI METHOD
C     WRITTEN BY ED WILSON DEC. 25, 1990
C     A - MATRIX (ANY RANK) TO BE SOLVED -
C         EIGENVALUES ON DIAGONAL
C     V - MATRIX OF EIGENVECTORS PRODUCED
C     TL- NUMBER OF SIGNIFICANT FIGURES
C---- INITIALIZATION --------------------
      ZERO = 0.0D0
      SUM = ZERO
      TOL = DABS(TL)
C---- SET INITIAL EIGENVECTORS -----------
      DO 200 I=1,NEQ
      DO 190 J=1,NEQ
      IF (TL.GT.ZERO) V(I,J) = ZERO
  190 SUM = SUM + DABS(A(I,J))
      IF (TL.GT.ZERO) V(I,I) = 1.0
  200 CONTINUE
C---- CHECK FOR TRIVIAL PROBLEM  ---------
      IF (NEQ.EQ.1)    RETURN
      IF (SUM.LE.ZERO) RETURN
      SUM = SUM/DFLOAT(NEQ*NEQ)
C----------------------------------------
C---- REDUCE MATRIX TO DIAGONAL ----------
C----------------------------------------
  400 SSUM = ZERO
      AMAX = ZERO
      DO 700 J=2,NEQ
      IH = J - 1
      DO 700 I=1,IH
C---- CHECK IF A(I,J) IS TO BE REDUCED ---
      AA = DABS(A(I,J))
      IF (AA.GT.AMAX) AMAX = AA
      SSUM = SSUM + AA
      IF (AA.LT.0.1*AMAX) GO TO 700
```

```
C---- CALCULATE ROTATION ANGLE ----------
      AA=ATAN2(2.0*A(I,J),A(I,I)-(J,J))/2.0
      SI = DSIN(AA)
      CO = DCOS(AA)
C---- MODIFY "I" AND "J" COLUMNS --------
      DO 500 K=1,NEQ
      TT = A(K,I)
      A(K,I) =  CO*TT + SI*A(K,J)
      A(K,J) = -SI*TT + CO*A(K,J)
      TT = V(K,I)
      V(K,I) =  CO*TT + SI*V(K,J)
  500 V(K,J) = -SI*TT + CO*V(K,J)
C---- MODIFY DIAGONAL TERMS -------------
      A(I,I) = CO*A(I,I) + SI*A(J,I)
      A(J,J) =-SI*A(I,J) + CO*A(J,J)
      A(I,J) = ZERO
C---- MAKE "A" MATRIX SYMMETRICAL -------
      DO 600 K=1,NEQ
      A(I,K) =  A(K,I)
      A(J,K) =  A(K,J)
  600 CONTINUE
C---- A(I,J) MADE ZERO BY ROTATION ------
  700 CONTINUE
C---- CHECK FOR CONVERGENCE -------------
      IF(DABS(SSUM)/SUM .GT.TOL)GO TO 400
      RETURN
      END
```

One notes that the subroutine for the solution of the symmetric eigenvalue problem by the classical Jacobi method does not contain a division by any number. Also, it can be proved that after each iteration cycle, the absolute sum of the off-diagonal terms is always reduced. Hence, the method will always converge and yield an accurate solution for positive, zero or negative eigenvalues.

The Jacobi algorithm can be directly applied to all off-diagonal terms, in sequence, until all terms are reduced to a small number compared to the absolute value of all terms in the matrix. However, the subroutine presented uses a "threshold" approach in which it skips the relatively small off-diagonal terms and operates only on the large off-diagonal terms.

To reduce one off-diagonal term to zero requires approximately 8N numerical operations. Clearly, one cannot precisely predict the total number of numerical operation because it is an iterative method; however, experience has indicated that the total number of numerical operations to obtain convergence is the order of $10N^3$. Assuming a modern (1998) personal computer can perform over 6,000,000 operations per second, it would require approximately one second of computer time to calculate the eigenvalues and eigenvectors of a full 100 by 100 matrix.

D.3   CALCULATION OF 3D PRINCIPAL STRESSES

The calculation of the principal stresses for a three-dimensional solid can be numerically evaluated from the stresses in the x-y-z system by solving a cubic equation. However, the definition of the directions of the principal stresses is not a simple procedure. An alternative approach to this problem is to write the basic stress transformation equation in terms of the unknown directions of the principal stresses in the 1-2-3 reference system. Or:

$$\begin{bmatrix} \sigma_1 & 0 & 0 \\ 0 & \sigma_2 & 0 \\ 0 & 0 & \sigma_3 \end{bmatrix} = \begin{bmatrix} V_{x1} & V_{y1} & V_{z1} \\ V_{x2} & V_{y2} & V_{z2} \\ V_{x3} & V_{y3} & V_{z3} \end{bmatrix} \begin{bmatrix} \sigma_x & \tau_{xy} & \tau_{xz} \\ \tau_{yx} & \sigma_y & \tau_{yz} \\ \tau_{zx} & \tau_{zy} & \sigma_z \end{bmatrix} \begin{bmatrix} V_{x1} & V_{x2} & V_{x3} \\ V_{y1} & V_{y2} & V_{y3} \\ V_{z1} & V_{z2} & V_{z3} \end{bmatrix} \quad \text{(D.9)}$$

Or, in symbolic form:

$$\Omega\Omega = V^T S V \tag{D.10}$$

in which V is the standard direction cosine matrix. Because $V V^T$ is a unit matrix, Equation (D.3) can be written as the following eigenvalue problem:

$$SV = V\Omega \tag{D.11}$$

where Ω is an unknown diagonal matrix of the principal stresses (eigenvalues) and V is the unknown direction cosine matrix (eigenvectors) that uniquely define the directions of the principal stresses. To illustrate the practical application of the classical Jacobi method, consider the following state of stress:

$$S = \begin{bmatrix} \sigma_x & \tau_{xy} & \tau_{xz} \\ \tau_{yx} & \sigma_y & \tau_{yz} \\ \tau_{zx} & \tau_{zy} & \sigma_z \end{bmatrix} = \begin{bmatrix} 120 & -55 & -75 \\ -55 & -55 & 33 \\ -75 & 33 & -85 \end{bmatrix} \tag{D.12}$$

The eigenvalues, principal stresses, and eigenvectors (direction cosines) are:

$$\begin{bmatrix} \sigma_1 \\ \sigma_2 \\ \sigma_3 \end{bmatrix} = \begin{bmatrix} 162.54 \\ -68.40 \\ -114.14 \end{bmatrix} \quad \text{and} \quad V = \begin{bmatrix} .224 & .352 & .909 \\ -.308 & .910 & -.277 \\ .925 & .217 & -.312 \end{bmatrix} \tag{D.13}$$

The solution of a 3 by 3 eigenvalue problem can be considered as a trivial numerical problem. Several hundred of those problems can be solved by the classical Jacobi method in one second of computer time. Note that negative eigenvalues are possible.

D.4   SOLUTION OF THE GENERAL EIGENVALUE PROBLEM

The general eigenvalue problem is written as:

$$AV = \Omega B V\Omega \tag{D.14}$$

where both $\mathbf{A}$ and $\mathbf{B}$ are symmetrical matrices. The first step is to calculate the eigenvectors $\mathbf{V}_B$ of the $\mathbf{B}$ matrix. We can now let the eigenvectors $\mathbf{V}$ be a linear combination or the eigenvectors of the $\mathbf{B}$ matrix. Or:

$$\mathbf{V} = \Omega\mathbf{V}_B\overline{\mathbf{V}} \tag{D.15}$$

Substitution of Equation (D.15) into Equation (D.14) and the pre-multiplication of both sides by $\mathbf{V}_B^T$ yields:

$$\mathbf{V}_B^T\mathbf{A}\mathbf{V}_B\overline{\mathbf{V}} = \Omega\mathbf{V}_B^T\mathbf{B}\mathbf{V}_B\overline{\mathbf{V}}\Omega \tag{D.16}$$

If all eigenvalues of the $\mathbf{B}$ matrix are non-zero, the eigenvectors can be normalized so that $\mathbf{V}_B^T\mathbf{B}\mathbf{V}_B = \mathbf{I}$. Hence, Equation (D.16) can be written in the following classical form:

$$\overline{\mathbf{A}}\,\overline{\mathbf{V}} = \overline{\mathbf{V}}\Omega \tag{D.17}$$

where $\overline{\mathbf{A}} = \mathbf{V}_B^T\mathbf{A}\mathbf{V}_B$. Therefore, the general eigenvalue problem can be solved by applying the Jacobi algorithm to both matrices. If the $\mathbf{B}$ matrix is diagonal, the eigenvectors $\mathbf{V}_B$ matrix will be diagonal, with the diagonal terms equal to $1/\sqrt{B_{nn}}$. This is the case for a lumped mass matrix. Also, mass must be associated with all degrees of freedom and all eigenvectors and values must be calculated.

D.5   SUMMARY

Only the Jacobi method has been presented in detail in this section. It is restricted to small full matrices in which all eigenvalues are required. For this problem, the method is very robust and simple to program. For the dynamic modal analysis of large structural systems or for the stability analysis of structural systems, other more numerically efficient methods are recommended.

APPENDIX E

TRANSFORMATION OF MATERIAL PROPERTIES

Many of the New Materials used in Structural Engineering Have Orthotropic Material Properties

E.1   INTRODUCTION

Orthotropic material properties are defined in a local 1-2-3 coordinate system and are defined by the following equation:

$$
\begin{bmatrix} \varepsilon_1 \\ \varepsilon_2 \\ \varepsilon_3 \\ \gamma_{21} \\ \gamma_{31} \\ \gamma_{23} \end{bmatrix} =
\begin{bmatrix}
\dfrac{1}{E_1} & -\dfrac{\nu_{12}}{E_2} & -\dfrac{\nu_{13}}{E_3} & -\dfrac{\nu_{14}}{E_4} & -\dfrac{\nu_{15}}{E_5} & -\dfrac{\nu_{16}}{E_6} \\[2mm]
-\dfrac{\nu_{21}}{E_1} & \dfrac{1}{E_2} & -\dfrac{\nu_{23}}{E_3} & -\dfrac{\nu_{24}}{E_4} & -\dfrac{\nu_{25}}{E_5} & -\dfrac{\nu_{26}}{E_6} \\[2mm]
-\dfrac{\nu_{31}}{E_1} & -\dfrac{\nu_{32}}{E_2} & \dfrac{1}{E_3} & -\dfrac{\nu_{34}}{E_4} & -\dfrac{\nu_{35}}{E_5} & -\dfrac{\nu_{36}}{E_6} \\[2mm]
-\dfrac{\nu_{41}}{E_1} & -\dfrac{\nu_{42}}{E_2} & -\dfrac{\nu_{43}}{E_3} & \dfrac{1}{E_4} & -\dfrac{\nu_{45}}{E_5} & -\dfrac{\nu_{46}}{E_6} \\[2mm]
-\dfrac{\nu_{51}}{E_1} & -\dfrac{\nu_{52}}{E_2} & -\dfrac{\nu_{53}}{E_3} & -\dfrac{\nu_{54}}{E_4} & \dfrac{1}{E_5} & -\dfrac{\nu_{56}}{E_6} \\[2mm]
-\dfrac{\nu_{61}}{E_1} & -\dfrac{\nu_{62}}{E_2} & -\dfrac{\nu_{63}}{E_3} & -\dfrac{\nu_{64}}{E_4} & -\dfrac{\nu_{65}}{E_5} & \dfrac{1}{E_6}
\end{bmatrix}
\begin{bmatrix} \sigma_1 \\ \sigma_2 \\ \sigma_3 \\ \tau_{21} \\ \tau_{31} \\ \tau_{23} \end{bmatrix}
+ \Delta T \begin{bmatrix} \alpha_1 \\ \alpha_2 \\ \alpha_3 \\ \alpha_{21} \\ \alpha_{31} \\ \alpha_{23} \end{bmatrix} \quad (E.1)
$$

Or in matrix notation:

$$\mathbf{d} = \mathbf{Cf} + \Delta T \mathbf{a} \qquad\qquad\qquad\qquad (E.2)$$

However, it is necessary to write equilibrium equations and other equations in a common "global" x-y-z coordinate system. Therefore, it is necessary for Equation (E.2) to be converted, or rotated, to the x-y-z system.

The classical equation for three-dimensional stress transformation can be written, by considering the equilibrium of a three-dimensional element, as the following matrix equation:

$$\begin{bmatrix} \sigma_1 & \tau_{12} & \tau_{13} \\ \tau_{21} & \sigma_2 & \tau_{23} \\ \tau_{31} & \tau_{32} & \sigma_3 \end{bmatrix} = \begin{bmatrix} V_{x1} & V_{y1} & V_{z1} \\ V_{x2} & V_{y2} & V_{z2} \\ V_{x3} & V_{y3} & V_{z3} \end{bmatrix} \begin{bmatrix} \sigma_x & \tau_{xy} & \tau_{xz} \\ \tau_{yx} & \sigma_y & \tau_{yz} \\ \tau_{zx} & \tau_{zy} & \sigma_z \end{bmatrix} \begin{bmatrix} V_{x1} & V_{x2} & V_{x3} \\ V_{y1} & V_{y2} & V_{y3} \\ V_{z1} & V_{z2} & V_{z3} \end{bmatrix} \qquad (E.3)$$

where V_{xi}, V_{yi}, and V_{zi} are the direction cosines of axis "i" with respect to the global x-y-z system. Equation (E.3) can be expanded to nine scalar equations. However, because of equilibrium, only six independent stresses exist in each system. Therefore, the 6 stresses in the local system can be written in terms of 6 global stresses in the following form:

$$\sigma = a \ \sigma_g \qquad\qquad\qquad\qquad (E.4)$$

where " a " is a 6 by 6 stress transformation matrix that must be numerically formed for each different element within a structural system. One approach would be to form analytical expressions, in terms of the products of the direction cosines, for each of the 36 terms in the matrix. An alternative to this traditional algebraic approach is to numerically evaluate, within the computer program, the 6 by 6 matrix directly from the 3 by 3 direction cosine matrix. This simple approach is best illustrated by the FORTRAN subroutine given in Table E.1.

One notes that a 3 by 3 integer array "IJ" is used to map the 3 by 3 stress to a 6 by 1 column matrix.

Table E.1 Formation of the "a" Matrix

```
       SUBROUTINE CALA(A,V)
       DIMENSION A(6,6),V(4,3),IJ(3,3)
       DATA IJ/1,4,5,  4,2,6,  5,6,3/
C---- ZERO 6 by 6 STRESS TRANSFORMATION MATRIX ----
       DO 100 I=1,6
       DO 100 J=1,6
 100  A(I,J) = 0.0
C---- FORM "A" ARRAY -----------------------------
       DO 400 II=1,3
       DO 400 JJ=II,3
       I = IJ(II,JJ)
        DO 300 K=1,3
        DO 300 L=1,3
        J = IJ(K,L)
 300   A(I,J) = A(I,J) + V(K,II)*V(L,JJ)
 400   CONTINUE
C---- MATRIX FORMED ------------------------------
       RETURN
       END
```

Also, the classical equations for strain transformation can be written as:

$$\varepsilon_g = a^T \, \varepsilon \tag{E.5}$$

Equation (E.1) can now be written in the global x-y-z system as:

$$\varepsilon_g = C_g \, \varepsilon + \varepsilon_{og} \tag{E.6}$$

where:

$$C_g = a^T \, C \, a \tag{E.7}$$

$$\varepsilon_{og} = \Delta T \, a^T \alpha \tag{E.8}$$

Because each member of a complex structural system may have different orthotropic material properties, the matrix multiplication required to calculate

Equations (E.7) and (E.8) are numerically evaluated within the computer program before inversion of C_g.

E.2   SUMMARY

Many material properties are orthotropic. In the past the structural engineer has often neglected to use those properties because of the increase in hand computational requirements. However, material properties can be easily incorporated into modern computer programs without a significant increase in computational time. The necessary equations to transform those local properties within each element to a common global reference system have been presented in this appendix.

APPENDIX F

A DISPLACEMENT-BASED BEAM ELEMENT WITH SHEAR DEFORMATIONS

Never use a Cubic Function
Approximation for a Non-Prismatic Beam

F.1 INTRODUCTION

In this appendix a unique development of a displacement-based beam element with transverse shearing deformations is presented. The purpose of this formulation is to develop constraint equations that can be used in the development of a plate bending element with shearing deformations. The equations developed, which are based on a cubic displacement, apply to a beam with constant cross-section subjected to end loading only. For this problem both the force and displacement methods yield identical results.

To include shearing deformation in plate bending elements, it is necessary to constrain the shearing deformations to be constant along each edge of the element. A simple approach to explain this fundamental assumption is to consider a typical edge of a plate element as a deep beam, as shown in Figure F.1.
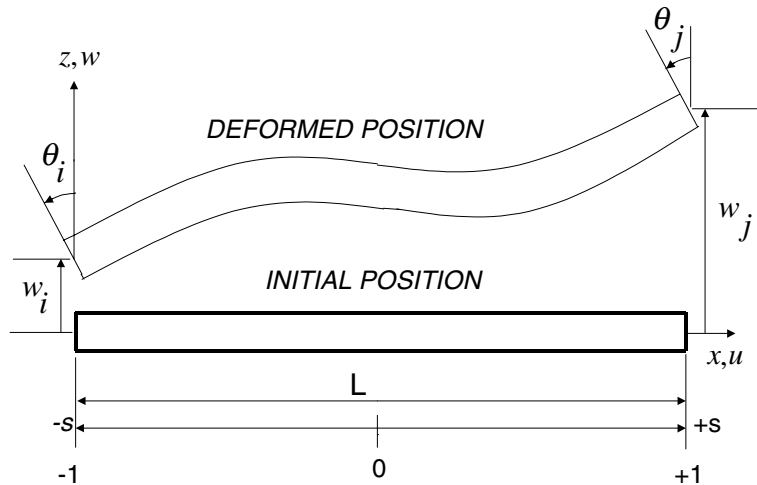
Figure F.1 Typical Beam Element with Shear Deformations

F.2   BASIC ASSUMPTIONS

In reference to Figure F.1, the following assumptions on the displacement fields are made:

First, the horizontal displacement caused by bending can be expressed in terms of the average rotation, θ, of the section of the beam using the following equation:

$$u = - z\,\theta \tag{F.1}$$

where z is the distance from the neutral axis.

Second, the consistent assumption for cubic normal displacement is that the average rotation of the section is given by:

$$\theta = N_1\theta_i + N_2\theta_j + N_3\Delta\theta \tag{F.2}$$

The cubic equation for the vertical displacement w is given by:

$$w = N_1 w_i + N_2 w_j + N_3 \beta_1 + N_4 \beta_2 \tag{F.3a}$$

where:

$$N_1 = \frac{1-s}{2}, \quad N_2 = \frac{1+s}{2}, \quad N_3 = 1 - s^2 \quad \text{and} \quad N_4 = s(1 - s^2) \tag{F.3b}$$

Note that the term $(1 - s^2)\Delta\theta$ is the relative rotation with respect to a linear function; therefore, it is a hierarchical rotation with respect to the displacement at the center of the element. One notes the simple form of the equations when the natural coordinate system is used.

It is apparent that the global variable x is related to the natural coordinate s by the equation $x = \frac{L}{2} s$. Therefore:

$$\partial x = \frac{L}{2} \partial s \tag{F.4}$$

Third, the elasticity definition of the "effective" shear strain is:

$$\gamma_{xz} = \frac{\partial w}{\partial x} + \frac{\partial u}{\partial z}; \quad \text{hence,} \quad \gamma_{xz} = \frac{\partial w}{\partial x} - \theta \tag{F.5}$$

Because $\dfrac{\partial w}{\partial x} = \dfrac{2}{L} \dfrac{\partial w}{\partial s}$, the evaluation of the shear strain, Equation (F.5), produces an expression in terms of constants, a linear equation in terms of s and a parabolic equation in terms of s^2. Or:

$$\gamma_{xz} = \frac{1}{L}(w_j - w_i) - \frac{4}{L} s \beta_1 - \frac{2}{L}(1 - 3s^2) \beta_2$$
$$- \frac{1-s}{2}\theta_i - \frac{1+s}{2}\theta_j - (1 - s^2)\alpha \tag{F.6}$$

If the linear and parabolic expressions are equated to zero, the following constraint equations are determined:

$$\beta_1 = \frac{L}{8}(\theta_i - \theta_j) \tag{F.7a}$$

$$\beta_2 = \frac{L}{6}\Delta\theta \tag{F.7b}$$

The normal displacements, Equation (F.2), can now be written as:

$$w = N_1 w_i + N_2 w_j + N_3 \frac{L}{8}(\theta_i - \theta_j) + N_4 \frac{L}{6}\alpha \tag{F.8}$$

Also, the effective shear strain is constant along the length of the beam and is given by:

$$\gamma_{xz} = \frac{1}{L}(w_j - w_i) - \frac{1}{2}(\theta_i + \theta_j) - \frac{2}{3}\Delta\theta \tag{F.9}$$

Now, the normal bending strains for a beam element can be calculated directly from Equation (2.1) from the following equation:

$$\varepsilon_x = \frac{\partial u}{\partial x} = -\frac{2z}{L}\frac{\partial\theta}{\partial s} = \frac{z}{L}[\theta_i - \theta_j + 4s\Delta\theta] \tag{F.10}$$

In addition, the bending strain ε_x can be written in terms of the beam curvature term ψ, which is associated with the section moment M. Or:

$$\varepsilon_x = z\psi \tag{F.11}$$

The deformation-displacement relationship for the bending element, including shear deformations, can be written in the following matrix form:

$$\begin{bmatrix} \psi \\ \gamma_{xz} \end{bmatrix} = \frac{1}{L} \begin{bmatrix} 1 & -1 & 0 & 0 & 4s \\ -L/2 & -L/2 & -1 & 1 & -2L/3 \end{bmatrix} \begin{bmatrix} \theta_i \\ \theta_j \\ w_i \\ w_j \\ \Delta\theta \end{bmatrix} \quad \text{or, } \mathbf{d} = \mathbf{B}\,\mathbf{u} \qquad (F.12)$$

The force-deformation relationship for a bending element is given by:

$$\begin{bmatrix} M \\ V \end{bmatrix} = \begin{bmatrix} \int z^2 E\, dA & 0 \\ 0 & \int \alpha\, G\, dA \end{bmatrix} \begin{bmatrix} \psi \\ \gamma_{xz} \end{bmatrix} \quad \text{or, } \sigma f = \mathbf{C}\, d\Delta \qquad (F.13)$$

where E is Young's modulus, $\alpha\,G$ is the effective shear modulus and V is the total shear acting on the section.

The application of the theory of minimum potential energy produces a 5 by 5 element stiffness matrix of the following form:

$$\mathbf{K} = \frac{L}{2} \int \mathbf{B}^{\mathrm{T}} \mathbf{C} \mathbf{B}\, ds \qquad (F.14)$$

Static condensation is used to eliminate $\Delta\theta$ to produce the 4 by 4 element stiffness matrix.

F.3   EFFECTIVE SHEAR AREA

For a homogeneous rectangular beam of width "b" and depth "d," the shear distribution over the cross section from elementary strength of materials is given by:

$$\tau = [1 - \left(\frac{2z}{d}\right)^2]\,\tau_0 \qquad (F.15)$$

where, τ_0 is the maximum shear stress at the neutral axis of the beam. The integration of the shear stress over the cross section results in the following equilibrium equation:

$$\tau_0 = \frac{3}{bd} V \tag{F.16}$$

The shear strain is given by:

$$\gamma = \frac{1}{G}[1 - \left(\frac{2z}{d}\right)^2] \tau_0 \tag{F.17}$$

The internal strain energy per unit length of the beam is:

$$E_I = \frac{1}{2}\int \gamma \, \tau \, dA \quad = \quad \frac{3}{5bdG} V^2 \tag{F.18}$$

The external work per unit length of beam is:

$$E_E = \frac{1}{2} V \, \gamma_{xz} \tag{F.19}$$

Equating external to internal energy we obtain:

$$V = \frac{5}{6} G bd \gamma_{xz} \tag{F.20}$$

Therefore, the area reduction factor for a rectangular beam is:

$$\alpha = \frac{5}{6} \tag{F.21}$$

For non-homogeneous beams and plates, the same general method can be used to calculate the shear area factor.

APPENDIX G

NUMERICAL INTEGRATION

Exact Integration of Approximate Solutions
May Not Produce the Most Realistic Results

G.1 INTRODUCTION

Traditional mathematics education implies that exact integration should be used whenever possible. In fact, approximate numerical integration is only recommended in cases where exact integration is not possible. However, in the development of finite element stiffness matrices, which are based on approximate displacement functions that do not satisfy equilibrium, it has been found that approximate numerical integration methods can produce more accurate results, and converge faster, than exact integration.

In this appendix, one-, two- and three-dimensional numerical integration formulas will be developed and summarized. These formulas are often referred to as **numerical quadrature rules**. The term **reduced integration** implies that a lower order integration formula is used and certain functions are intentionally neglected. In order that the integration rules are general, the functions to be integrated must be in the range –1.0 to +1.0. A simple change of variable can be introduced to transform any integral to this natural reference system. For example, consider the following one-dimensional integral:

$$I = \int_{x_1}^{x_2} f(x)\, dx \qquad\qquad (G.1)$$

The introduction of the change of variable $x = \frac{1}{2}(1-r)x_1 + \frac{1}{2}(1+r)x_2$ allows the integral to be written as:

$$I = J \int\limits_{-1}^{-1} f(r)\, dr = J\, I_r \tag{G.2}$$

It is apparent that:

$$dx = (x_2 - x_1)\, dr = J\, dr \tag{G.3}$$

The mathematical term J is defined as the **Jacobian of the transformation**. For two- and three-dimensional integrals, the Jacobian is more complicated and is proportional to the area and volume of the element respectively. Normally the displacement approximation is written directly in the three-dimensional isoparametric reference system r, s and t. Therefore, no change of variable is required for the function to be integrated.

G.2   ONE-DIMENSIONAL GAUSS QUADRATURE

The integration of a one-dimensional function requires that the integral be written in the following form:

$$I_r = \int\limits_{-1}^{-1} f(r)\, dr = \sum_{i=1}^{N} w_i\, f(r_i) = w_1 f(r_1) + w_2 f(r_2) + ...w_N f(r_N) \tag{G.4}$$

The integral is evaluated at the Gauss points r_i and the corresponding Gauss weighting factors are w_i. To preserve symmetry, the Gauss points are located at the center or in pairs at equal location from the center with equal weights.

Let us consider the case where the function to be integrated is a polynomial of the form $f(r) = a_0 + a_1 r + a_2 r^2 + a_3 r^3 + ...a_n r^n$. Or, at a typical numerical integration point:

$$f(r_i) = a_0 + a_1 r_i + a_2 r_i^2 + a_3 r_i^3 + ...a_n r_i^n \tag{G.5}$$

It is apparent that the integrals of the odd powers of the polynomial are zero. The exact integration of the even powers of the polynomial produce the following equation:

$$I_r = \int_{-1}^{-1} f(r)\, dr = \sum_n \int_{-1}^{1} a_n r^n dr = \sum_n \frac{2a_n}{n+1} = 2a_0 + \frac{2}{3}a_2 + \frac{2}{5}a_4 + \dots \tag{G.6}$$

A one to three point rule is written as:

$$I_r = w_\alpha f(-\alpha) + w_0 f(0) + w_\alpha f(\alpha) \tag{G.7}$$

Hence, from Equations (G.5) and (G.7), a one point integration rule at $r = 0$ is:

$$I_r = w_0 a_0 = 2a_0 \quad \text{or,} \quad w_0 = 2 \tag{G.8}$$

Similarly, a two-point integration rule at $r = \pm\alpha$ produces:

$$I_r = w_\alpha(a_0 + a_1\alpha + a_2\alpha^2) + w_\alpha(a_0 - a_1\alpha + a_2\alpha^2) = 2a_0 + \frac{2}{3}a_2 \tag{G.9}$$

Equating the coefficients of a_0 and a_2 produces the following equations:

$$2w_\alpha a_0 = 2a_0 \qquad \text{or,} \quad w_\alpha = 1$$
$$2w_\alpha a_2\alpha^2 = \frac{2}{3}a_2 \quad \text{or,} \quad \alpha = \sqrt{\frac{1}{3}} \tag{G.10}$$

A three-point integration rule requires that:

$$I_r = w_\alpha(a_0 + a_1\alpha + a_2\alpha^2 + a_3\alpha^3 + a_4\alpha^4) + w_0 a_0$$
$$+ w_\alpha(a_0 - a_1\alpha + a_2\alpha^2 - a_3\alpha^3 + a_4\alpha^4) = 2a_0 + \frac{2}{3}a_2 + \frac{2}{5}a_4 \tag{G.11}$$

Equating the coefficients of a_0 and a_2 produces the following equations:

$$2w_\alpha a_0 + w_0 a_0 = 2a_0 \qquad \text{or,} \quad 2w_\alpha + w_0 = 2$$

$$2w_\alpha a_2 \alpha^2 = \frac{2}{3} a_2 \qquad \text{or,} \quad \alpha^2 = \frac{1}{3w_\alpha} \tag{G.12}$$

$$2w_\alpha a_4 \alpha^4 = \frac{2}{5} a_4 \qquad \text{or,} \quad \alpha^4 = \frac{1}{5w_\alpha}$$

The solution of these three equations requires that:

$$w_\alpha = \frac{5}{9}, \quad w_0 = \frac{8}{9} \quad \text{and} \quad \alpha = \sqrt{\frac{3}{5}} \tag{G.13}$$

Note that the sum of the weighting functions for all one-dimensional integration rules are equal to 2.0, or the length of the integration interval from –1 to +1. Clearly one can develop higher order integration rules using the same approach with more integration points. It is apparent that the Gauss method using N points will exactly integrate polynomials of order 2N-1 or less. However, finite element functions are not polynomials in the global reference system if the element is not a rectangle. Therefore, for arbitrary isoparametric elements, all functions are approximately evaluated.

G.3   NUMERICAL INTEGRATION IN TWO DIMENSIONS

The one-dimensional Gauss approach can be extended to the evaluation of two-dimensional integrals of the following form:

$$I_{rs} = \int_{-1}^{1}\int_{-1}^{1} f(r,s)\,dr\,ds = \sum_{i=1}^{N}\sum_{j=1}^{N} w_i w_j f(r_i s_j) \tag{G.14}$$

Using one-dimensional Gauss rules in both the r and s directions, Equation (G.14) can be evaluated directly. Two by two integration will require four points and three by three integration requires nine points. For two dimensions, the sum of the weighting factors $w_i w_j$ will be 4.0 or, the area of the element in the natural reference system.

G.4 AN EIGHT-POINT TWO-DIMENSIONAL RULE

It is possible to develop integration rules for two-dimensional elements that produce the same accuracy as the one-dimensional Gauss rules using fewer points. A general, two-dimensional polynomial is of the following form:

$$f(r,s) = \sum_{n,m} a_{nm} r^n s^m \tag{G.15}$$

A typical term in Equation (G.15) may be integrated exactly. Or:

$$\int_{-1}^{1}\int_{-1}^{1} a_{nm} r^n s^m \, dr \, ds = \frac{4\, a_{nm}}{(n+1)(m+1)} \quad \text{if } n \text{ and } m \text{ are both even.} \tag{G.16}$$

A two-dimensional N point integration rule can be written as:

$$I = \sum_{i=1}^{N} w_i \, f(r_i, s_i) = a_{00} \sum_i w_i + a_{10} \sum_i w_i r_i + a_{01} \sum_i w_i s_i$$
$$+ a_{11} \sum_i w_i s_i r_i + a_{20} \sum_i w_i r_i^2 + \dots\dots a_{nm} \sum_i w_i r_i^n s_i^m \tag{G.17}$$

The eight integration points, shown in Figure G.1, produce a two-dimensional rule that can be summarized as:

$$I = w_\alpha \, f(\pm\alpha, \pm\alpha) + w_\beta \, [f(\pm\beta, 0) + f(0, \pm\beta)] \tag{G.18}$$

Equating all non-zero terms in the integrated polynomial of the fifth order produces the following four equations in terms of four unknowns:

$$
\begin{aligned}
a_{00}: \quad & 4w_\alpha + 4w_\beta = 4 \\
a_{02} \; a_{20}: \quad & 4w_\alpha \alpha^2 + 2w_\beta \beta^2 = 4/3 \\
a_{22}: \quad & 4w_\alpha \alpha^4 = 4/9 \\
a_{40} \; a_{04}: \quad & 4w_\alpha \alpha^4 + 2w_\beta \beta^4 = 4/5
\end{aligned}
\tag{G.19}
$$
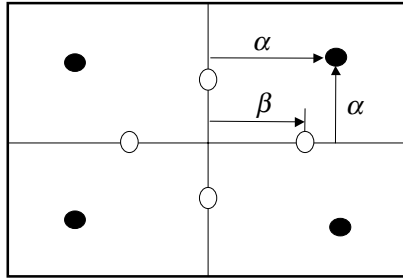
$$W_\beta = \frac{40}{49} = ?$$

$$W_\alpha = 1.0 - W_\beta$$

$$\alpha = \sqrt{\frac{1.0}{3\sqrt{W_\alpha}}}$$

$$\beta = \sqrt{\frac{2 - 2\sqrt{W_\alpha}}{3W_\beta}}$$

Figure G.1 Two-Dimensional Eight-Point Integration Rule

The solution of these equations produces the following locations of the eight points and their weighting factors:

$$\alpha = \sqrt{\frac{7}{9}} \qquad \beta = \sqrt{\frac{7}{15}} \qquad w_\alpha = \frac{9}{49} \qquad w_\beta = \frac{40}{49} \tag{G.20}$$

It is apparent that the eight-point two-dimensional rule has the same accuracy as the 3 by 3 Gauss rule. Note that the sum of the eight weighting factors is 4.0, the area of the element.

G.5   AN EIGHT-POINT LOWER ORDER RULE

A lower order, or reduced, integration rule can be produced by not satisfying the equation associated with a_{40} in Equation G.19. This allows the weighting factor w_β to be arbitrarily specified. Or:

$$w_\beta = ? \quad w_\alpha = 1.0 - w_\beta \quad \alpha = \frac{1}{3\sqrt{w_\alpha}} \quad \beta = \sqrt{\frac{2 - 2\sqrt{w_\alpha}}{3w_\alpha}} \tag{G.21}$$

Therefore, if $w_\beta = 0$ the rule reduces to the 2 by 2 Gauss rule. If w_β is set to 40/49, the accuracy is the same as the 3 by 3 Gauss rule.

G.6 A FIVE-POINT INTEGRATION RULE

Using the same approach, a five-point integration rule, shown in Figure G.2, can be produced.
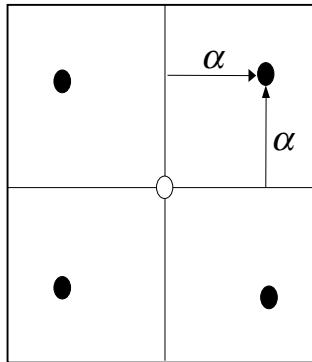
$$W_0 = ?$$
$$W_\alpha = 1.0 - W_0/4$$
$$\alpha = \sqrt{\frac{1.0}{3W_\alpha}}$$

Figure G.2 Five-Point Integration Rule

The two-dimensional five-point rule can be written as:

$$I = w_\alpha \, f(\pm\alpha,\pm\alpha) + w_0 \, f(0,0) \tag{G.22}$$

Equating all non-zero terms in the integrated polynomial of the third order produces the following two equations in terms of three unknowns:

$$
\begin{aligned}
a_{00} : &\quad 4w_\alpha + 4w_\beta = 4 \\
a_{20} \, a_{02} : &\quad 4w_\alpha \alpha^2 = 4/3
\end{aligned}
\tag{G.23}
$$

This has the same, or greater, accuracy as the 2 by 2 Gauss rule for any value of the center node weighting value. The two-dimensional five-point numerical integration rule is summarized as:

$$w_0 = ? \quad w_\alpha = (4 - w_0)/4 \quad \text{and} \quad \alpha = \sqrt{\frac{1}{3w_\alpha}} \tag{G.24}$$

This equation is often used to add stability to an element that has rank deficiency when 2 by 2 integration is used. For example, the following rule has been used for this purpose:

$$w_0 = .004 \quad w_\alpha = 0.999 \quad \text{and} \quad \alpha = 0.5776391 \tag{G.25}$$

Because the five-point integration rule has a minimum of third order accuracy for any value of the center weighting value, the following rule is possible:

$$w_0 = 8/3 \quad w_\alpha = 1/3 \quad \text{and} \quad \alpha = 1.00 \tag{G.26}$$

Therefore, the integration points are at the center node and at the four node points of the two-dimensional element. Hence, for this rule it is not necessary to project integration point stresses to estimate node point stresses.

G.7   THREE-DIMENSIONAL INTEGRATION RULES

The one dimensional Gauss rules can be directly extended to numerical integration within three dimensional elements in the r, s and t reference system. However, the 3 by 3 by 3 rule requires 27 integration points and the 2 by 2 by 2 rule requires 8 points. In addition, one cannot derive the benefits of reduced integration from the direct application of the Gauss rules. Similar to the case of two-dimensional elements, one can produce more accurate and useful elements by using fewer points.

First, consider a three-dimensional, 14-point, numerical integration rule that is written in the following form:

$$I = w_\alpha \, f(\pm\alpha,\pm\alpha,\pm\alpha) + w_\beta \, [f(\pm\beta,0,0) + f(0,\pm\beta,0) + f(0,0,\pm\beta)] \tag{G.27}$$

A general, three-dimensional polynomial is of the following form:

$$f(r,s,t) = \sum_{n,m,l} a_{nml} r^n s^m t^l \tag{G.28}$$

A typical term in Equation (G.27) may be integrated exactly. Or:

$$\int_{-1}^{1}\int_{-1}^{1}\int_{-1}^{1} a_{nml} r^n s^m t^l \, dr \, ds \, dt = \frac{8 a_{nml}}{(n+1)(m+1)(l+1)} \tag{G.29}$$

If n, m and l are all even numbers, Equation (G.29) is non-zero; however, for all other cases, the integral is zero. As in the case of two dimensions, equating all non-zero terms of the fifth order produces the following set of four equations in terms of four unknowns:

$$
\begin{aligned}
a_{000} : & \quad 8w_\alpha + 6w_\beta = 8 \\
a_{200} \; a_{020} \; a_{002} : & \quad 8w_\alpha \alpha^2 + 2w_\beta \beta^2 = 8/3 \\
a_{220} \; a_{022} \; a_{202} : & \quad 8w_\alpha \alpha^4 = 8/9 \\
a_{400} \; a_{040} \; a_{004} : & \quad 8w_\alpha \alpha^4 + 2w_\beta \beta^4 = 8/5
\end{aligned} \tag{G.30}
$$

The exact solution of these equations produces the following locations and numerical weighting values:

$$\alpha = \sqrt{\frac{19}{33}} \qquad \beta = \sqrt{\frac{19}{30}} \qquad w_\alpha = \frac{121}{361} \qquad w_\beta = \frac{320}{361} \tag{G.31}$$

Note that the sum of the weighting values is equal to 8.0, the volume of the element.

A nine-point numerical integration rule, with a center point, can be derived that has the following form:

$$I = w_\alpha \, f(\pm\alpha,\pm\alpha,\pm\alpha) + w_0 \, f(0,0,0) \tag{G.32}$$

The nine-point rule requires that the following equations be satisfied:

$$
\begin{aligned}
a_{000} : & \quad 8w_\alpha + w_0 = 8 \\
a_{200} \; a_{020} \; a_{002} : & \quad 8w_\alpha \alpha^2 = 8/3
\end{aligned} \tag{G.33}
$$

This is a third order rule, where the weight at the center point is arbitrary, that can be summarized as

$$w_0 = ? \qquad w_\alpha = 1.0 - w_0 / 8 \qquad \alpha = \sqrt{\frac{1}{3w_\alpha}} \qquad \text{(G.34)}$$

A small value of the center point weighting function can be selected when the standard 2 by 2 by 2 integration rule produces a rank deficient stiffness matrix.

In addition, the following nine-point three-dimensional rule is possible:

$$w_0 = 16/3 \qquad w_\alpha = 1/3 \qquad \alpha = 1.0 \qquad \text{(G.35)}$$

For this third order accuracy rule, the eight integration points are located at the eight nodes of the element.

A six-point three-dimensional integration rule can be developed that has the six integration points at the center of each face of the hexahedral element. The form of this rule is:

$$I = w_\alpha \left[f(\pm\beta,0,0) + f(0,\pm\beta,0) + f(0,0,\pm\beta) \right] \qquad \text{(G.36)}$$

Equating all non-zero terms up to the third order produces the following two equations:

$$\begin{aligned} a_{000}: \quad & 6w_\beta = 8 \\ a_{200} \; a_{020} \; a_{002}: \quad & 2w_\beta\beta^2 = 8/3 \end{aligned} \qquad \text{(G.37)}$$

Therefore, the location of the integration points and weighting values for the six point rule is:

$$\beta = 1.0 \qquad w_\beta = 4/3 \qquad \text{(G.38)}$$

The author has had no experience with this rule. However, it appears to have some problems in the subsequent calculation of node point stresses.

G.8   SELECTIVE INTEGRATION

One of the first uses of *selective integration* was to solve the problem of shear locking in the four-node plane element. To eliminate the shear locking, a one-

point integration rule was used to integrate the shear energy only. A 2 by 2 integration rule was used for the normal stress. This selected integration approach produced significantly improved results. Since the introduction of corrected incompatible elements, however, selective integration is no longer used to solve this problem.

For many coupled field problems, which involve both displacements and pressure as unknowns, the use of different order integration on the pressure and displacement field may be required to obtain accurate results. In addition, for fluid-like elements, a different order integration of the volume change function has produced more accurate results than the use of the same order of integration for all variables.

G.9   SUMMARY

In this appendix, the fundamentals of numerical integration in one, two and three dimensions are presented. By using the principles presented in this appendix, many different rules can be easily derived

The selection of a specific integration method requires experimentation and a physical understanding of the approximation used in the formulation of the finite element model. The use of reduced integration (lower order) and selective integration has proven to be effective for many problems. Therefore, one should not automatically select the most accurate rule. Table G.1 presents a summary of the rules derived in this appendix.

Table G.1 Summary of Numerical Integration Rules

RULE	Number of Points	Location of Points			Weighting Values		
		α	β	0	w_α	w_β	w_0
One Dimensional-Gauss $I = \int\limits_{-1}^{1} f(r)\,dr$	1	-	-	0	-	-	2
	2	$\pm\dfrac{1}{\sqrt{3}}$	-	-	1.0	-	-
	3	$\pm\sqrt{\dfrac{3}{5}}$	-	0	$\dfrac{5}{9}$	-	$\dfrac{8}{9}$
Two Dimensional $I = \int\limits_{-1}^{1}\int\limits_{-1}^{1} f(r,s)\,dr\,ds$	5	$\pm\dfrac{1}{\sqrt{3w_\alpha}}$	-	0	$w_\alpha = 1 - w_0/4$	-	$w_0 = ?$
	5	± 1	-	0	$\dfrac{1}{3}$	-	$\dfrac{8}{3}$
	8	$\pm\sqrt{\dfrac{7}{9}}$	$\pm\sqrt{\dfrac{7}{15}}$	-	$\dfrac{9}{49}$	$\dfrac{40}{49}$	-
Three Dimensional $I = \int\limits_{-1}^{1}\int\limits_{-1}^{1}\int\limits_{-1}^{1} f(r,s,t)\,dr\,ds\,dt$	9	$\pm\dfrac{1}{\sqrt{3w_\alpha}}$	-	0	$w_\alpha = 1 - w_{0/8}$	-	$w_0 = ?$
	14	$\pm\sqrt{\dfrac{19}{33}}$	$\pm\sqrt{\dfrac{19}{30}}$	-	$\dfrac{121}{361}$	$\dfrac{320}{361}$	-

APPENDIX H

SPEED OF COMPUTER SYSTEMS

*The Current Speed of a $2,000 Personal Computer is
Faster than the $10,000,000 Cray Computer of 1975*

H.1   INTRODUCTION

The calculation of element stiffness matrices, solution of equations and
evaluation of mode shapes and frequencies are all computationally intensive.
Furthermore, it is necessary to use double-precision floating-point arithmetic to
avoid numerical errors. Therefore, all numbers must occupy 64 bits of computer
storage. The author started developing structural analysis and design programs
on the IBM-701 in 1957 and since that time has been exposed to a large number
of different computer systems. In this appendix the approximate double-
precision floating-point performances of some of those computer systems are
summarized. Because different FORTRAN compilers and operating systems
were used, the speeds presented can only be considered accurate to within 50
percent.

H.2   DEFINITION OF ONE NUMERICAL OPERATION

For the purpose of comparing floating-point speeds, the evaluation of the
following equation is defined as one operation:

$$A = B + C * D \qquad \text{Definition of one numerical operation}$$

Using double precision arithmetic, the definition involves the sum of one
multiplication, one addition, extracting three numbers from high-speed storage,
and transferring the results to storage. In most cases, this type of operation is

within the inner DO LOOP for the solution of linear equations and the evaluation of mode shapes and frequencies.

H.3   SPEED OF DIFFERENT COMPUTER SYSTEMS

Table H.1 indicates the speed of different computers used by the author.

Table H.1 Floating-Point Speeds of Computer Systems

Year	Computer or CPU	Operations Per Second	Relative Speed
1963	CDC-6400	50,000	1
1967	CDC-6600	100,000	2
1974	CRAY-1	3,000,000	60
1980	VAX-780	60,000	1.2
1981	IBM-3090	20,000,000	400
1981	CRAY-XMP	40,000,000	800
1990	DEC-5000	3,500,000	70
1994	Pentium-90	3,500,000	70
1995	Pentium-133	5,200,000	104
1995	DEC-5000 upgrade	14,000,000	280
1998	Pentium II - 333	37,500,000	750
1999	Pentium III - 450	69,000,000	1,380

If one considers the initial cost and maintenance of the various computer systems, it is apparent that the overall cost of engineering calculations has reduced significantly during the past several years. The most cost effective computer system at the present time is the INTEL Pentium III type of personal computer system. At the present time, a very powerful personal computer system that is 25 times faster than the first CRAY computer, the fastest computer made in 1974, can be purchased for approximately $1,500.

H.4   SPEED OF PERSONAL COMPUTER SYSTEMS

Many engineers do not realize the computational power of the present day inexpensive personal computer. Table H.2 indicates the increased speed of personal computers that has occurred during the past 18 years.

Table H.2 Floating-Point Speeds of Personal Computer Systems

YEAR	INTEL CPU	Speed MHz	Operations Per Second	Relative Speed	COST
1980	8080	4	200	1	$6,000
1984	8087	10	13,000	65	$2,500
1988	80387	20	93,000	465	$8,000
1991	80486	33	605,000	3,025	$10,000
1994	80486	66	1,210,000	6,050	$5,000
1995	Pentium	90	4,000,000	26,000	$5,000
1996	Pentium	233	10,300,000	52,000	$4,000
1997	Pentium II	233	11,500,000	58,000	$3,000
1998	Pentium II	333	37,500,000	198,000	$2,500
1999	Pentium III	450	69,000,000	345,000	$1,500

One notes that the floating-point speed of the Pentium III is significantly different from the Pentium II chip. The increase in clock speed, from 333 to 450 MHz, does not account for the increase in speed.

H.5   PAGING OPERATING SYSTEMS

The above computer speeds assume all numbers are in high-speed memory. For the analysis of large structural systems, it is not possible to store all information within high-speed storage. If data needs to be obtained from low-speed disk storage, the effective speed of a computer can be reduced significantly. Within the SAP and ETABS programs, the transfer of data to and from disk storage is conducted in large blocks to minimize disk access time. That programming

philosophy was used before introduction of the paging option used in the modern Windows operating systems.

In a paging operating system, if the data requested is not stored in high-speed memory, the computer automatically reads the data from disk storage in relatively small blocks of information. Therefore, the modern programmer need not be concerned with data management. However, there is a danger in the application of this approach. The classical example that illustrates the problem with paging is adding two large matrices together. The FORTRAN statement can be one of the following forms:

```
    DO 100 J=1,NCOL              DO 100 I=1,NROW
    DO 100 I=1,NROW              DO 100 J=1,NCOL
100 A(I,J)=B(I,J)+C(I,J)  100 A(I,J)=B(I,J)+C(I,J)
```

Because all arrays are stored row-wise, the data will be paged to and from disk storage in the same order as needed by the program statements on the left. However, if the program statements on the right are used, the computer may be required to read and write blocks of data to the disk for each term in the matrix. Hence, the computer time required for this simple operation can be very large if paging is automatically used.

H.6   SUMMARY

Personal computers will continue to increase in speed and decrease in price. It is the opinion of many experts in the field that the only way significant increases in speed will occur is by the addition of multi-processors to personal computer systems. The NT operating system supports the use of multi-processors. However, the *free* LINUX operating system has proven faster for many functions.

APPENDIX I

METHOD OF LEAST SQUARE

*The Method of Least Square can be used to Approximately Solve a Set of **N** Equations with **M** Unknowns*

I.1 SIMPLE EXAMPLE

In experimental mechanics, it is very common to obtain a large amount of data that cannot be exactly defined by a simple analytical function. For example, consider the following four (N) data points:

Table I.1 Four Data Points

x	y
0.00	1.0
0.75	0.6
1.50	0.3
2.00	0.0

Now let us approximate the data with the following linear function with two *(M)* unknown constants:

$$c_1 + c_2 x = y(x) \tag{I.1}$$

If this equation is evaluated at the four data points, the following ***observational equations*** are obtained:

$$c_1 = 1.0$$
$$c_1 + 0.75c_2 = 0.6$$
$$c_1 + 1.50c_2 = 0.3$$
$$c_1 + 2.00c_2 = 0.0$$

(I.2)

These four equations can be written as the following matrix equation:

$$\begin{bmatrix} 1.0 & 0.00 \\ 1.0 & 0.75 \\ 1.0 & 1.50 \\ 1.0 & 2.00 \end{bmatrix} \begin{bmatrix} c_1 \\ c_2 \end{bmatrix} = \begin{bmatrix} 1.0 \\ 0.6 \\ 0.3 \\ 0.0 \end{bmatrix} \qquad \text{Or, symbolically as} \quad \mathbf{Ac = b}$$

(I.3)

Equation I.3 cannot be solved exactly because the four equations have two unknowns. However, both sides of the equation can be multiplied by $\mathbf{A^T}$ and the following two equations in terms of two unknowns are produced:

$$\mathbf{A^T Ac = A^T b} \qquad \text{Or,} \quad \begin{bmatrix} 4.00 & 4.25 \\ 4.25 & 6.81 \end{bmatrix} \begin{bmatrix} c_1 \\ c_2 \end{bmatrix} = \begin{bmatrix} 1.9 \\ 0.9 \end{bmatrix}$$

(I.4)

The solution of this symmetric set of equations is:

$$\begin{bmatrix} c_1 \\ c_2 \end{bmatrix} = \begin{bmatrix} 0.992 \\ -0.487 \end{bmatrix}$$

(I.5)

It is apparent that the error, which is the difference between the values at the data points and the values produced by the approximate equation, can be calculated from:

$$\mathbf{e = Ac - b} \quad = \begin{bmatrix} -.008 \\ +.035 \\ -.030 \\ -.018 \end{bmatrix}$$

(I.6)

I.2   GENERAL FORMULATION

It will be shown in this section that the ad hoc approach, presented in the previous section, produces results in which **the sum of the square of the errors at the data points** is a minimum. The error vector can be written as:

$$\mathbf{e} = \mathbf{A}\mathbf{c} - \mathbf{b} \quad \text{or,} \quad \mathbf{e}^{\mathrm{T}} = \mathbf{c}^{\mathrm{T}}\mathbf{A}^{\mathrm{T}} - \mathbf{b}^{\mathrm{T}} \tag{I.7}$$

It is now possible to calculate the sum of the square of the errors, a scalar value S, from the following matrix equation:

$$S = \mathbf{e}^{\mathrm{T}}\mathbf{e} = \mathbf{c}^{\mathrm{T}}\mathbf{A}^{\mathrm{T}}\mathbf{A}\mathbf{c} - \mathbf{b}^{\mathrm{T}}\mathbf{A}\mathbf{c} - \mathbf{c}^{\mathrm{T}}\mathbf{A}^{\mathrm{T}}\mathbf{b} + \mathbf{b}^{\mathrm{T}}\mathbf{b} = \mathbf{c}^{\mathrm{T}}\mathbf{H}\mathbf{c} - 2\mathbf{c}^{\mathrm{T}}\mathbf{B}^{\mathrm{T}} + \mathbf{b}^{\mathrm{T}}\mathbf{b} \tag{I.8}$$

From basic mathematical theory, the minimum value S must satisfy the following M equations:

$$\frac{\partial S}{\partial c_m} = 0 \quad \text{where } m = 1 ---- M \tag{I.9}$$

Application of Equation (I.9) to Equation (I.8) yields the following typical matrix equation in which each term is a scalar:

$$\frac{\partial S}{\partial c_m} = \begin{bmatrix} 0 & 0 & - & 1 & - & 0 \end{bmatrix} \mathbf{H}\mathbf{c} + \mathbf{c}^{\mathrm{T}}\mathbf{H}^{\mathrm{T}} \begin{bmatrix} 0 \\ 0 \\ - \\ 1 \\ - \\ 0 \end{bmatrix} + \tag{I.10}$$

$$2\begin{bmatrix} 0 & 0 & - & 1 & - & 0 \end{bmatrix}\mathbf{B} = 2\begin{bmatrix} 0 & 0 & - & 1 & - & 0 \end{bmatrix}[\mathbf{H}\mathbf{c} - \mathbf{B}] = 0$$

Hence, all M equations can be written as the following matrix equation:

$$
\begin{bmatrix}
\dfrac{\partial S\Omega}{\partial c_1} \\[6pt]
\dfrac{\partial S\Omega}{\partial c_2} \\[6pt]
\overline{} \\[2pt]
\dfrac{\partial \overline{S\Omega}}{\partial c_m} \\[6pt]
\overline{} \\[2pt]
\dfrac{\partial \overline{S\Omega}}{\partial c_M}
\end{bmatrix}
=
\begin{bmatrix}
1 & 0 & - & 0 & - & 0 \\
0 & 1 & - & 0 & - & 0 \\
- & - & - & - & - & - \\
0 & 0 & - & 1 & - & 0 \\
- & - & - & - & - & - \\
0 & 0 & - & 0 & - & 1
\end{bmatrix}
[2\mathbf{Hc}-2\mathbf{B}] = 2\mathbf{I}[\mathbf{Hc}-\mathbf{B}] = [0] \qquad (I.11)
$$

Therefore, the vector of constants $\mathbf{c}$ can be determined from the solution of the following matrix equation:

$$\mathbf{Hc} = \mathbf{B} \qquad\qquad\qquad (I.12)$$

Because the positive-definite symmetric matrix $\mathbf{H} = \mathbf{A}^{\mathrm{T}}\mathbf{A}$ and $\mathbf{B} = \mathbf{A}^{\mathrm{T}}\mathbf{b}$, the multiplication of the observational equations by $\mathbf{A}^{\mathrm{T}}$ produces the same set of equations. Therefore, it is not necessary to perform the formal minimization procedure each time one uses the least square method.

I.3   CALCULATION OF STRESSES WITHIN FINITE ELEMENTS

The basic equilibrium equation of a finite element system, as produced by the application of the principle of minimum potential energy, can be written as a summation of element contributions in the following form:

$$\mathbf{R} = \sum_{i=1}^{\#elements} \mathbf{k}_i\mathbf{u} = \sum_{i=1}^{\#elements} \mathbf{f}_i \qquad\qquad (I.13)$$

where $\mathbf{k}_i$ is a typical element stiffness, $\mathbf{u}$ is the element node displacements and $\mathbf{f}_i$ is the element nodal forces, or stress resultants. The external node loads $\mathbf{R}$ are the specified point loads, the body forces that are integrated over the element volume, the consistent nodal loads associated with surface tractions and thermal loads. Those external nodal loads are in exact equilibrium with the sum of the forces acting on the elements.

The original development of the finite element method was presented as an extension of structural analysis in which node point equilibrium was the fundamental starting point. Therefore, the accuracy of the element nodal forces was apparent. Unfortunately, the use of abstract variational methods in modern computational mechanics has tended to make this very important equilibrium property obscure. Hence, using virtual work and the method of least square, one can calculate element stresses directly from nodal forces.

The consistent stresses within a finite element, developed using displacement functions, normally do not satisfy the fundamental equilibrium equations. From Equation (2.1), the three-dimensional equilibrium equations, written in a global x, y, and z reference system, are:

$$\frac{\partial \sigma_x}{\partial x} + \frac{\partial \tau_{xy}}{\partial y} + \frac{\partial \tau_{xz}}{\partial z} = 0$$

$$\frac{\partial \tau_{yx}}{\partial x} + \frac{\partial \sigma_y}{\partial y} + \frac{\partial \tau_{yz}}{\partial z} = 0 \tag{I.14}$$

$$\frac{\partial \tau_{zx}}{\partial x} + \frac{\partial \tau_{zy}}{\partial y} + \frac{\partial \sigma_z}{\partial z} = 0$$

Those equations, which are fundamental laws of physics, are always exactly satisfied within a real structure; therefore, it is very important that the stress distribution calculated within elements of a finite element system satisfy those equations. To accomplish that objective for three-dimensional solids, the assumed stress distribution satisfies those equations and is of the following form:

$$\begin{aligned}
\sigma_x &= c_1 - (c_{12} + c_{17})x + c_3 y + c_3 z \\
\sigma_y &= c_4 + c_5 x - (c_{11} + c_{21})y + c_3 y + c_6 z \\
\sigma_x &= c_7 + c_8 x + c_9 y - (c_{15} + c_{20})z \\
\tau_{xy} &= c_{10} + c_{11} x + c_{12} y + c_{13} z \\
\tau_{xz} &= c_{14} + c_{15} x + c_{16} y + c_{17} z \\
\tau_{yz} &= c_{18} + c_{19} x + c_{20} y + c_{21} z
\end{aligned}$$
$$\text{or, } \mathbf{s} = \mathbf{Pc} \tag{I.15}$$

where $\mathbf{P}$ is a 6 by 21 array that is a function of the global x, y and z reference system.

The element node forces can be expressed in terms of the assumed stress distribution by the direct application of the principle of virtual work in which the virtual displacements $\overline{\mathbf{d}}$ are of the same form as the basic displacement approximation. Or, from Equation (6.3), the virtual displacements, including incompatible modes, are:

$$\overline{\mathbf{d}} = \begin{bmatrix} \mathbf{B_C} & \mathbf{B_I} \end{bmatrix} \begin{bmatrix} \overline{\mathbf{u}} \\ \alpha \end{bmatrix} \tag{I.16}$$

If the virtual and incompatible displacements are all set to one, the following equation can be used to calculate node forces for an eight-node solid element:

$$\mathbf{f} = \begin{bmatrix} \mathbf{f_i} \\ 0 \end{bmatrix} = \int_{Vol} \overline{\mathbf{d}}^T \mathbf{s} \, dV = \left[\int_{Vol} \begin{bmatrix} \mathbf{B_C^T} \\ \mathbf{B_I^T} \end{bmatrix} \mathbf{P} \, dV \right] \mathbf{c} = \mathbf{Qc} \tag{I.17}$$

The 33 by 21 matrix $\mathbf{Q}$ is calculated using standard numerical integration. The forces associated with the nine incompatible modes are zero.

The system of equations is approximately solved by the least square method, which involves the solution of:

$$\mathbf{Q}^T \mathbf{Q} \mathbf{c} = \mathbf{Q}^T \mathbf{f} \quad \text{or} \quad \mathbf{Hc} = \mathbf{B} \tag{I.18}$$

After $\mathbf{c}$ is evaluated for each load condition, the six components of stress at any point (x,y,z) within the element can be evaluated from Equation (I.15).

APPENDIX J

CONSISTENT EARTHQUAKE ACCELERATION AND DISPLACEMENT RECORDS

Earthquake Accelerations can be Measured. However, Structures are Subjected to Earthquake Displacements

J.1 INTRODUCTION

At the present time most earthquake motions are approximately recorded by accelerometers at equal time intervals. After correcting the acceleration record, as a result of the dynamic properties of the instrument, the record may still contain recording errors. Assuming a linear acceleration within each time interval, a direct integration of the accelerations generally produces a velocity record with a non-zero velocity at the end of the record that should be zero. And an exact integration of the velocity record does not produce a zero displacement at the end of the record. One method currently used to mathematically produce a zero displacement at the end of the record is to introduce a small initial velocity so that the displacement at the end of the record is zero. However, this initial condition is not taken into account in the dynamic analysis of the computer model of the structure. In addition, those displacement records cannot be used directly in multi-support earthquake response analysis.

The purpose of this appendix is to summarize the fundamental equations associated with time history records. It will be demonstrated that the recovery of accelerations from displacements is an unstable numerical operation. A new

numerical method is presented for the modification of an acceleration record, or part of an acceleration record, so that it satisfies the fundamental laws of physics in which the displacement, velocity and acceleration records are consistent.

J.2   GROUND ACCELERATION RECORDS

Normally, 200 points per second are used to define an acceleration record, and it is assumed that the acceleration function is linear within each time increment, as shown in Figure J.1.
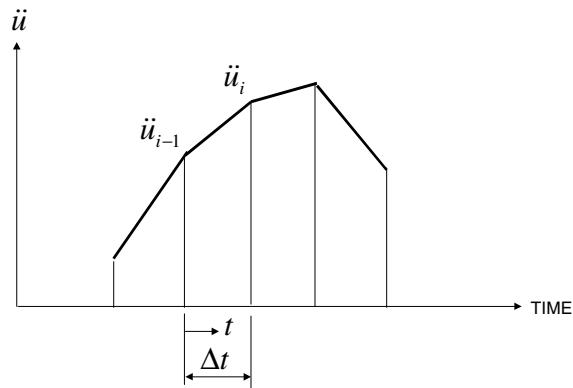
Figure J.1 Typical Earthquake Acceleration Record

Ground velocities and displacements can then be calculated from the integration of the accelerations and velocities within each time step. Or:

$$\dddot{u} = \frac{1}{\Delta t}(\ddot{u}_i - \ddot{u}_{i-1})$$
$$\ddot{u}(t) = \ddot{u}_{i-1} + t\,\dddot{u}$$
$$\dot{u}(t) = \dot{u}_{i-1} + t\,\ddot{u}_{i-1} + \frac{t^2}{2}\dddot{u} \qquad\qquad\text{(J.1)}$$
$$u(t) = u_{i-1} + t\,\dot{u}_{i-1} + \frac{t^2}{2}\ddot{u}_{i-1} + \frac{t^3}{6}\dddot{u}$$

The evaluation of those equations at $t = \Delta t$ produces the following set of recursive equations:

$$\ddot{u} = \frac{1}{\Delta t}(\ddot{u}_i - \ddot{u}_{i-1})$$

$$\ddot{u}_i = \ddot{u}_{i-1} + \Delta t\,\ddot{u}$$

$$\dot{u}_i = \dot{u}_{i-1} + \Delta t\,\ddot{u}_{i-1} + \frac{\Delta t^2}{2}\ddot{u} \qquad\qquad i=1,2,3 \text{ --------} \qquad\qquad (J.2)$$

$$u_i = u_{i-1} + \Delta t\,\dot{u}_{i-1} + \frac{\Delta t^2}{2}\ddot{u}_{i-1} + \frac{\Delta t^3}{6}\ddot{u}$$

The integration of ground acceleration records should produce zero velocity at the end of the record. In addition, except for near fault earthquake records, zero displacements should be obtained at the end of the record. Real earthquake accelerations are normally corrected to satisfy those requirements.

Note that the displacements are cubic functions within each time increment. Therefore, if displacements are used as the specified seismic loading, smaller time steps or a higher order solution method, based on cubic displacements, must be used for the dynamic structural analysis. On the other hand, if accelerations are used as the basic loading, a lower order solution method, based on linear functions, may be used to solve the dynamic response problem.

J.3   CALCULATION OF ACCELERATION RECORD FROM DISPLACEMENT RECORD

Rewriting Equation (J.2), it should be possible, given the displacement record, to calculate the velocity and acceleration records from the following equations:

$$\ddot{u} = \frac{6}{\Delta t^3}[u_i - u_{i-1} - \Delta t\,\dot{u}_{i-1} - \frac{\Delta t^2}{2}\ddot{u}_{i-1}]$$

$$\dot{u}_i = \dot{u}_{i-1} + \Delta t\,\ddot{u}_{i-1} + \frac{\Delta t^2}{2}\ddot{u} \qquad\qquad\qquad (J.3)$$

$$\ddot{u}_i = \ddot{u}_{i-1} + \Delta t\,\ddot{u}$$

On the basis of linear acceleration within each time step, Equations (J.2) and (J.3) are theoretically exact, given the same initial conditions. However, computer round off introduces errors in the velocities and accelerations and the recurrence Equation (J.3) is unstable and cannot be used to recover the input acceleration

record. This instability can be illustrated by rewriting the equations in the following form:

$$\dot{u}_i = -2\,\dot{u}_{i-1} - \frac{\Delta t}{2}\ddot{u}_{i-1} + \frac{3}{\Delta t}(u_i - u_{i-1})$$

$$\ddot{u}_i = -\frac{6}{\Delta t}\dot{u}_{i-1} - 2\ddot{u}_{i-1} + \frac{6}{\Delta t^2}(u_i - u_{i-1})$$

(J.4)

If the displacements are constant, the recurrence equation written in matrix form is:

$$\begin{bmatrix} \dot{u} \\ \ddot{u} \end{bmatrix}_i = -\begin{bmatrix} 2 & \dfrac{\Delta t}{2} \\ \dfrac{6}{\Delta t} & 2 \end{bmatrix}\begin{bmatrix} \dot{u} \\ \ddot{u} \end{bmatrix}_{i-1}$$

(J.5)

Or, if a small round-off error, ε, is introduced as an initial condition, the following results are produced:

$$\mathbf{u}_0 = \begin{bmatrix} \dot{u} \\ \ddot{u} \end{bmatrix}_0 = \begin{bmatrix} \varepsilon \\ 0 \end{bmatrix}, \qquad \mathbf{u}_1 = -\varepsilon\begin{bmatrix} 2 \\ 6/\Delta t \end{bmatrix}, \qquad \mathbf{u}_2 = \varepsilon\begin{bmatrix} 7 \\ 24/\Delta t \end{bmatrix}$$

(J.6)

It is apparent from Equation (J.6) that the introduction of a small round-off error in the velocity or acceleration at any step will have an opposite sign and be amplified in subsequent time steps. Therefore, it is necessary to use an alternate approach to calculate the velocities and accelerations directly from the displacement record.

It is possible to use cubic spline functions to fit the displacement data and to recover the velocity and acceleration data. The application of Taylor's series at point i produces the following equations for the displacement and velocity:

$$u(t) = u_i + t\,\dot{u}_i + \frac{t^2}{2}\ddot{u}_i + \frac{t^3}{6}\dddot{u}$$

$$\dot{u}(t) = \dot{u}_i + t\,\ddot{u}_i + \frac{t^2}{2}\dddot{u}$$

(J.7)

Elimination of $\dddot{u}$ from these equations produces an equation for the acceleration at time t_i. Or:

$$\ddot{u}_i = \frac{6}{t^2}(u_i - u(t)) + \frac{2}{t}(\dot{u}(t) + 2\dot{u}_i) \tag{J.8}$$

Evaluation of Equation (22.10) at $t = \pm \Delta t$ (at $i+1$ and i-1) produces the following equations:

$$\ddot{u}_i = \frac{6}{\Delta t^2}(u_i - u_{i+1}) + \frac{2}{\Delta t}(\dot{u}_{i+1} + 2\dot{u}_i) = \frac{6}{\Delta t^2}(u_i - u_{i-1}) - \frac{2}{\Delta t}(\dot{u}_{i-1} + 2\dot{u}_i) \tag{J.9}$$

Requiring that $\ddot{u}$ be continuous, the following equation must be satisfied at each point:

$$\dot{u}_{i-1} + 4\dot{u}_i + \dot{u}_{i+1} = \frac{3}{\Delta t}(u_{i+1} - u_{i-1}) \tag{J.10}$$

Therefore, there is one unknown velocity per point. This well-conditioned tridiagonal set of equations can be solved directly or by iteration. Those equations are identical to the moment equilibrium equations for a continuous beam that is subjected to normal displacements. After velocities (slopes) are calculated, accelerations (curvatures) and derivatives (shears) are calculated from:

$$\ddot{u}_i = \frac{6}{\Delta t^2}(u_i - u_{i+1}) + \frac{2}{\Delta t}(\dot{u}_i + 2\dot{u}_i)$$
$$\dddot{u} = \frac{\ddot{u}_i - \ddot{u}_{i-1}}{\Delta t} \tag{J.11}$$

This "spline function" approach eliminates the numerical instability problems associated with the direct application of Equations (J.4). However, it is difficult to physically justify how the displacements at a future time point $i+1$ can affect the velocities and accelerations at time point i.

J.4   CREATING CONSISTENT ACCELERATION RECORD

Earthquake compression, shear and surface waves propagate from a fault rupture at different speeds with the small amplitude compression waves arriving first. For example, acceleration records recorded near the San Francisco-Oakland Bay Bridge from the 1989 Loma Prieta earthquake indicate high frequency, small acceleration motions for the first ten seconds. The large acceleration phase of the

record is between 10 and 15 seconds only. However, the official record released covers approximately a 40-second time span. Such a long record is not suitable for a nonlinear, time-history response analysis of a structural model because of the large computer storage and execution time required.

It is possible to select the "large acceleration part of the record" and use it as the basic input for the computer model. To satisfy the fundamental laws of physics, the truncated acceleration record must produce zero velocity and displacement at the beginning and end of the earthquake. This can be accomplished by applying a correction to the truncated acceleration record that is based on the fact that any earthquake acceleration record is a sum of acceleration pluses, as shown in Figure J.2.
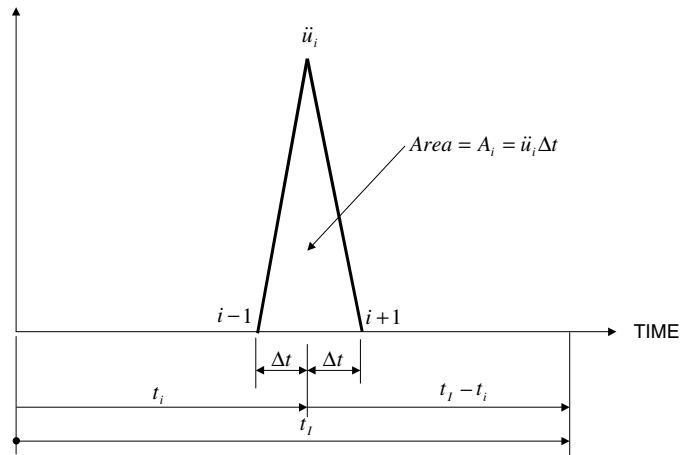
Figure J.2 Typical Earthquake Acceleration Pulse

From spline theory, the exact displacement at the end of the record is given by the following equation:

$$u_I = \sum_{i=1}^{I}(t_I - t_i)\ddot{u}_i \Delta t = \Delta U \tag{J.12}$$

A correction to the acceleration record may now be calculated so that the displacement at the end of the record, Equation (J.12), is identically equal to zero. Rather then apply an initial velocity, the first second or two of the acceleration record can be modified to obtain zero displacement at the end of the

record. Let us assume that all of the correction is to be applied to the first "L" values of the acceleration record. To avoid a discontinuity in the acceleration record, the correction will be weighted by a linear function, from α at time zero to zero at time t_L. Therefore, the displacement resulting from the correction function at the end of the record is of the following form:

$$\sum_{i=1}^{L} \alpha \frac{L-i}{L}(t_I - t_i)\ddot{u}_i \Delta t = \alpha_p U_{pos} + \alpha_n U_{neg} = -\Delta U \qquad (J.13)$$

For Equation (J.13) the positive and negative terms are calculated separately. If it is assumed that the correction is equal for the positive and negative terms, the amplitudes of the correction constants are given by:

$$\alpha_p = -\frac{2U_{pos}}{\Delta U} \quad \text{and } \alpha_n = -\frac{2U_{neg}}{\Delta U} \qquad (J.14a \text{ and } J.14b)$$

Therefore, the correction function can be added to the first "L" values of the acceleration record to obtain zero displacement at the end of the record. This simple correction algorithm is summarized in Table J.1.

If the correction period is less that one second, this very simple algorithm, presented in Table J.1, produces almost identical maximum and minimum displacements and velocities as the mathematical method of selecting an initial velocity. However, this simple one-step method produces physically consistent displacement, velocity and acceleration records. This method does not filter important frequencies from the record and the maximum peak acceleration is maintained.

The velocity at the end of the record can be set to zero if a similar correction is applied to the final few seconds of the acceleration record. Iteration would be required to satisfy both the zero displacement and velocity at the end of the record.

Table J.1 Algorithm to Set Displacement at End of Records to Zero

1. GIVEN UNCORRECTED ACCELERATION RECORD

    $0, \ddot{u}_1, \ddot{u}_2, \ddot{u}_3, \ddot{u}_4, \text{.................................} \ddot{u}_{I-1}, 0 \text{ and } L$

2. COMPUTE CORRECTION FUNCTION

    $$\Delta U = \sum_{i=1}^{I} (t_I - t_i) \ddot{u}_i \Delta t$$

    $$\sum_{i=0}^{L} \frac{L-i}{L} (t_I - t_i) \ddot{u}_i \Delta t = U_{pos} + U_{neg}$$

    $$\alpha_p = -\frac{\Delta U}{2U_{pos}} \quad \text{and} \quad \alpha_n = -\frac{\Delta U}{2U_{neg}}$$

3. CORRECT ACCELERATION RECORD

    if $\ddot{u}_i > 0$ then $\ddot{u}_i = (1 + \alpha_p \frac{L-i}{L}) \ddot{u}_i$

    if $\ddot{u}_i < 0$ then $\ddot{u}_i = (1 + \alpha_n \frac{L-i}{L}) \ddot{u}_i \qquad i = 1,2....L$

J.5   SUMMARY

Acceleration records can be accurately defined by 200 points per second and with the assumption that the acceleration is a linear function within each time step. However, the resulting displacements are cubic functions within each time step and smaller time steps must be user-define displacement records. The direct calculation of an acceleration record from a displacement record is a numerically unstable problem, and special numerical procedures must be used to solve this problem.

The mathematical method of using an initial velocity to force the displacement at the end of the record to zero produces an inconsistent displacement record that should not be directly used in a dynamic analysis. A simple algorithm for the correction of the acceleration record has been proposed that produces physically acceptable displacement, velocity and acceleration records.

INDEX

N

O

P